THE UNIVERSITY
of EDINBURGH

The evolution and function of variable NK cell receptors and their HLA class I ligands

Hugo G. Hilton, BVM&S

A critical review submitted in partial fulfillment of the requirements of the degree of Doctor of Philosophy in the School of Medicine and Veterinary Medicine at the University of Edinburgh

December 2015

The University of Edinburgh

Thesis Advisor: Ivan Morrison, PhD

Declaration statement

I declare that I designed and performed the experimental work described in this thesis. I was the major contributing author to each of the published works except where indicated. I have clearly referenced and listed all sources as appropriate and given the source of all data that is not my own. I have not made use of the work of other students either past or present and have not sought the help of professional academic agencies for the work. I understand that any false claim for this work will be penalized in accordance with the University of Edinburgh regulations.

Signature: ……

Hugo G. Hilton, BVM&S

Date: May 6Th 2016

Abstract

In combating variable pathogens, mammalian immune systems have evolved diverse families of ligands and receptors. Epitomizing this strategy are the polymorphic *major histocompatibility complex class I* genes (termed *HLA class I* in humans) that encode ligands for highly variable natural killer (NK) cell receptors (in humans, the killer cell immunoglobulin-like receptors or KIR). Technological advances are poised to allow sequencing of these polymorphic genes, the most variable in the human genome, at the highest possible accuracy and resolution. However, studies that correlate immunogenetic polymorphisms with functional changes are in their infancy and often limited to those variants that combine high ligand avidity and high frequency in Caucasians. As a result, there is a paucity of information regarding the true scope of functional human immunogenetic diversity. This not only restricts our understanding of the evolution and function of the human immune system, but also underserves non-Caucasian populations with respect to disease association studies and therapeutic advances. The work presented in this thesis details original research and methodological advances that begin to address these functional shortfalls, the goal being to improve our understanding of the relationship between immunogenetic diversity, protein structure and immune function.

Lay Summary

The genes that control the response of the human immune system vary enormously between people. Understanding the evolution of these genetic differences and how they individualize immune responses is central to understanding how the immune system works in health and disease. This thesis specifically investigates the genes that control the function of natural-killer cells. These cells act as the body's first line of defense against viruses and other pathogens. They are also able detect cancerous cells and eliminate them before they take hold. Because natural-killer cells are so vital to maintaining human health, the genes that control them have evolved rapidly to match the unique set of pathogens that are present amongst different global populations. Thus, populations from around the world all have slightly different gene variants that control their natural-killer cells. We have studied the extent of this genetic diversity and how specifically it has shaped natural-killer cell function in these populations. Our results have informed our understanding of the evolution of these genes, their function and how natural-killer cells may be used in treating human diseases in the future.

Acknowledgements

I would like to express my sincere thanks to my post-doctoral advisor *Peter Parham, PhD, FRS* for giving me the opportunity to work in his group and his guidance during my career at Stanford University. All of the members of the Parham lab have been exceptional friends and mentors and I would particularly like to thank *Paul Norman, PhD* and *Lisbeth Guethlein, PhD*, both of whom provided invaluable advice and support over a number of years. I particularly appreciate their patience and constant generosity in sharing their own data to further my research.

I also acknowledge the support of *John Hammond, PhD*. His thoughtful advice and guidance were critical to my pursuing this PhD. I am grateful for his honesty and candor, not only recently, in making the decision to pursue this degree but also throughout our professional relationship.

Jorge Nieto DVM, PhD and *Monica Aleman, DVM, PhD* were utterly steadfast in their belief that I would be able to pursue a successful career in research, even when I was not certain of that myself and I thank them for their support and for providing me with my first research position at UC Davis.

Lastly, I would like to thank my PhD advisor *Ivan Morrison, PhD* for his advice, guidance and engagement during the final phases of this degree.

Contents

Introduction

Killer-cell immunoglobulin-like receptors regulate human NK cell function

Natural killer (NK) cells are versatile lymphocytes that function in human immunity and reproduction [1, 2]. First described in 1975, NK cells were initially identified as a distinct sub-population of lymphocytes by their capacity to lyse tumor cells without prior sensitization [3-6]. As such, they are functionally distinct from the B and T-lymphocyte cells that derive from the same lymphoid progenitor lineage but function in the adaptive immune response. NK cells are now accepted to play an important role in innate and adaptive immune responses that govern infection, autoimmunity, tumor immune-surveillance and placental formation [7, 8].

NK cells are cytotoxic cells that release perforin when in close proximity to a cell slated for killing. Perforin forms pores in the cell membrane of the target cell, creating a channel through which intracellular granzymes can enter, inducing apoptosis [9, 10]. NK cells are also responsible for production of immunoregulatory cytokines including interferon-γ, tumor necrosis factor, granulocyte macrophage colony stimulating factor and IL-10 [11, 12]. Uterine NK cells form a distinct subset of lymphocytes that are potent cytokine secretors but have reduced cytotoxic function. These specialized cells form the dominant leucocyte in the uterus during early pregnancy and mediate the formation of the placenta through interaction with fetal trophoblast cells [13].

NK cells are controlled by a wide array of activating and inhibitory cell-surface receptors that distinguish healthy cells from diseased cells to allow targeted effector function. A common mechanism by which this occurs involves inhibitory NK cell receptors that engage MHC class I or MHC class I-like molecules [14]. By their level of expression and diverse repertoire of peptides, MHC class I molecules provide NK cell receptors with a sensitive read-out of cellular health.

Humans have two broad, complimentary types of germline-encoded inhibitory NK cell receptor that recognize human MHC (HLA) class I molecules. Recognition of HLA-E by CD94:NKG2A involves both a highly conserved ligand and a highly conserved receptor, and is thus a constant feature of human immune systems [15]. At the opposite end of the spectrum are the extraordinarily diverse interactions between polymorphic HLA-A, -B and –C molecules and the family of variable killer-cell immunoglobulin-like receptors (KIR). The interactions between KIR and HLA class I direct NK cells to kill virus-infected cells and tumor cells; they also induce the secretion of cytokines that activate other leucocytes or guide fetal trophoblast cells to invade the uterus during early pregnancy [2, 16]. In human populations, both *KIR* and *HLA class I* are highly polymorphic. Their combinatorial diversity contributes to the resistance and susceptibility of individuals to a range of infections [17-19], autoimmune diseases [20-22] and pregnancy disorders [23, 24], as well as to the success or failure of hematopoietic stem cell transplantation [25, 26].

NK cells require education to become functional

Unlike CD8+ T-cells, which respond to foreign peptides bound to HLA class I, NK cells attack cells that lack HLA class I [27]. During their maturation in the bone marrow, NK cells undergo an education process that ensures they are tolerant to healthy peripheral tissues. Immature NK cells begin to express inhibitory KIR early in development; this initiates an education process whereby inhibitory KIR engagement of autologous HLA class I results in the generation of functional effector NK cells in the periphery. Failure to engage inhibitory receptors during development, due to lack of inhibitory receptor expression on the NK cell or lack of interaction with HLA class I results in the generation of a subset of hyporesponsive peripheral NK cells [28-30]. In this manner, interactions between inhibitory KIR and HLA class I are critical to NK cell reactivity.

NK cell education is also influenced by signals received through activating receptors. In a process analogous to negative selection of developing T-

cells, ligation of activating receptors on developing NK cells by ubiquitously expressed cognate viral or self-ligands leads to both a repression of cellular function through that particular receptor and a partial deletion of the subset repertoire [31-33]. Together these mechanisms ensure that mature NK cells do not attack healthy self-tissues.

HLA-C is the dominant ligand for KIR

KIRs recognize four mutually exclusive epitopes of HLA-A, -B and -C. These are defined by polymorphisms at positions 76-83 in the helix of the α1 domain [2]. The A3/11 epitope is carried by HLA-A*03 and A*11 and the Bw4 epitope by around 33% of HLA-A and HLA-B allotypes. The C1 epitope is carried by HLA-C allotypes having asparagine 80 and by two exceptional HLA-B allotypes (HLA-B*46:01 and HLA-B*73:01). The C2 epitope is carried by HLA-C allotypes having lysine 80. Data from functional immunology, clinical correlations and species comparisons are consistent with a model in which HLA-C evolved under natural selection to be a more specialized ligand for KIR than either HLA-A or HLA-B [16, 34]. Thus, the interactions of C1 and C2 with their cognate KIR dominate human NK-cell regulation. For this reason, KIRs that recognize HLA-C are the focus of the work in this thesis.

Approximately half of the >1900 known HLA-C allotypes have asparagine at position 80 that defines the C1 epitope [35]. Recognition of HLA-C1 is mediated by the inhibitory receptors KIR2DL2 and KIR2DL3, both of which have lysine at position 44 in the D1 protein domain [36]. Genomic characterization and population studies of the *KIR* gene family are consistent with the genes encoding KIR2DL2 and KIR2DL3 segregating as alleles of a single genetic locus, which is referred to as *KIR2DL2/3* [37]. The inhibitory receptor that recognizes the HLA-C2 epitope is KIR2DL1, although KIR2DL2 does display some cross-reactivity with HLA-C2 also. In addition to the inhibitory receptors, both KIR2DL1 and KIR2DL2/3 have short-tailed, activating counterparts, KIR2DS1 and KIR2DS2 respectively, whose extracellular Ig-like domains are highly homologous to

those of their inhibitory partners. Like its homologous inhibitory partner, KIR2DS1 recognizes the HLA-C2 epitope [38]. By contrast, KIR2DS2, does not have a well-characterized HLA class I ligand, although a recent study has raised the possibility that it binds to A*11:02 with a restricted peptide repertoire [39].

Humans have four phylogenetic lineages of KIR that have different structures and specificities for HLA class I. Human lineage II KIR recognize the Bw4 and A3/11 epitopes carried by HLA-A and HLA-B. In contrast, all KIR that recognize HLA-C, and it orthologs in other hominoid species, belong to the lineage III KIR. Old world monkeys have counterparts to HLA-A and –B, but not to HLA-C [40]. Consistent with this distribution, Old world monkeys have diverse lineage II *KIR* genes, but limited lineage III *KIR* diversity [41-43]. Only hominoid species with a counterpart to HLA-C – chimpanzee, bonobo, gorilla and orangutan – have diverse lineage III *KIR* evolved to recognize HLA-C [44, 45].

Lineage III KIRs are characterized by having two extracellular binding domains, D1 and D2. Crystal structures of the KIR alone, or in combination with their cognate HLA class I ligands, provide great insight into the molecular mechanisms that govern KIR interactions with HLA class I and determine the C1 and C2 specificities [46, 47]. Lysine at position 44 of KIR2DL2 forms a hydrogen bond with the C1-determining asparagine-80 of HLA-C*03 whereas methionine 44 of KIR2DL1 forms part of a charge pocket that accommodates the lysine-80 of HLA-C*04.

KIR are diversified by gene content and allelic polymorphism

KIRs are encoded by a compact cluster of genes that forms part of the *leukocyte receptor complex* (LRC) on chromosome *19q13.4* [48, 49]. An important component of *KIR* variation is that the *KIR* haplotypes vary in gene content [49, 50]. Conserved genes are present at the centromeric (*KIR3DL3*) and telomeric (*KIR3DL2*) ends of the haplotype, as well as in the central part (*KIR3DP1* and *KIR2DL4*) of the locus [51]. These

framework genes define two regions of gene-content variation, one in the centromeric part of the locus, the other in the telomeric part. Found in both parts of the locus are two types of alternative gene-content motifs that are qualitatively different called *Cen-A*, *Cen-B*, *Tel-A* and *Tel-B*. The combination of the *Cen-A* and *Tel-A* form the group A *KIR* haplotype, a relatively short haplotype with a predominance of inhibitory receptors that recognize HLA class I. The three other combinations *Cen-B* with *Tel-B*, *Cen-B* with *Tel-A* and *Cen-A* with *Tel-B* are collectively called the group *B KIR* haplotypes. Characterizing the *Cen-B* and *Tel-B* motifs are activating *KIR* and *KIR* that have reduced or lost recognition of HLA class I. Gene content variation of *KIR* haplotypes has evolved through asymmetric recombination, which is facilitated by the short intergenic regions with high sequence similarity. Complementing this mechanism is homologous recombination at the center of the locus, which assorts the difference *Cen* and *Tel* motifs [49, 51].

KIR are further diversified by allelic variation, which is a common feature of all HLA-C reactive KIR. A systematic evaluation of the functional consequences of this allelic variation is lacking. However, two broad allotypic groups of KIR2DL1 have been identified on the basis of a dimorphism at position 245 in the transmembrane domain. KIR2DL1 encoding C245 form weaker receptors than those that encode R245 [52]. In an analogous fashion, two broad and functionally distinct allotypic groups have been identified for KIR2DL2/3. KIR2DL3 encodes weak C1-specific receptors whereas KIR2DL2 encodes a stronger C1 receptor that also cross-reacts with C2.

Objectives of the studies described in the publications

The work presented in this thesis builds upon the observations presented in the introduction with the overall goal being to better describe the genetics and functional interactions between the polymorphic *lineage III KIR* and their *HLA-C* ligands. The specific aims can be summarized as follows:

1. Identify and characterize key functional residues in *lineage III KIR*
2. Determine the true genetic diversity of naturally occurring *lineage III KIR*
3. Determine the functional range of lineage III KIR and HLA-C interactions
4. Refine the Luminex multiplex platform for the investigation of KIR-Fc fusion proteins and monoclonal antibodies for MHC class I

Chapter 1 describes an investigation of amino acid residues that have been subject to positive selection during hominoid evolution [53]. Central to our mission of correlating genetic variation with functional immune variation, this approach not only yielded specific information regarding the nature of the interactions between lineage III KIR and HLA-C, but also provided an evolutionary context for the development of a bipartite receptor-ligand system and how that might be beneficial for the control of human NK cells.

Expanding on this study, Chapter 2 examines how natural polymorphism of *lineage III KIR* and *HLA-C* influences the avidity and specificity of their interactions. My study of the KhoeSan, a genetically diverse hunter-gatherer population from Southern Africa discovered two new *KIR2DL1* alleles that encode receptors with highly divergent function. Examination of the function of these novel receptors and those found in 5 other global populations with different demographic histories and genetic backgrounds shed light on the selective pressures that have shaped the evolution of the human immune system [54]. This topic is explored in greater detail in Chapter 3 that focuses on the functional variation between the *KIR A* and *B* haplotypes [55] .

One methodological advance that forms the backbone of each of these three studies was our development of a multiplex binding assay in which a specific KIR can be tested for reactivity against a panel of around 100 HLA class I allotypes. It is examination of this methodological advance and its further adaptation for investigation of monoclonal antibody reactivity that is the subject of Chapters 4 and 5. The specific KIR of interest is first solubilized by replacing its cytoplasmic tail with that of a human IgG1 antibody (Fc). The resultant KIR-Fc, produced in recombinant form in insect cells, can then be incubated with microbeads, each coated with a specific HLA class I allotype to determine its reactivity. This method was developed in the Parham lab and I have refined the production of these proteins and the multiplex immunoassay to allow reliable recombinant protein production and reduce inter-assay variability [56]. I have also adapted this platform to investigate the reactivity of monoclonal antibodies that recognize polymorphic epitopes of HLA class I [57]. This work refined the epitopes of these antibodies thereby allowing more accurate interpretation of flow-cytometry results. This platform was adapted to investigate the reactivity of antibodies directed against Patr-AL, a non-classical MHC class I molecule found in chimpanzees [58].

Chapter 1

Functional significance of positively selected residues in *lineage III KIR* ligand-binding domains

Interaction of KIR with HLA-C is sensitive to single amino acid substitutions in the KIR that can change its epitope specificity [36] or abrogate recognition entirely [36, 59, 60]. In the context of KIR2DL1 and KIR2DL3, mutagenesis at position 44 was sufficient to "swap" the C1 and C2 specificities. Thus, the KIR2DL1 mutant with lysine-44 acquired C1 specificity, whilst the KIR2DL3 mutant with methionine acquired C2 specificity [36]. On this basis, position 44 has been described as the specificity-determining position of the lineage III KIR [61].

Comparing the binding of inhibitory KIR2DL1 to its closely related activating counterpart KIR2DS1 revealed a second residue in lineage III KIR that modified ligand recognition. Although both receptors recognize the HLA-C2 epitope, the avidity of KIR2DS1 for C2 was lower than that of KIR2DL1 [59, 62]. Mutational analysis showed that lysine at position 70, naturally present in KIR2DS1, reduced affinity for HLA-C*04 to approximately half that of KIR2DL1 which encodes threonine at position 70. Consistent with their effect on receptor-ligand interaction, examination of the crystallographic structures of KIR2DL1 and KIR2DL3 showed that both position 44 and position 70 are found in the HLA class I binding footprint [46, 47].

To identify additional functionally important residues in the KIR molecule *Abi-Rached et al* [44] performed maximum-likelihood analysis on the aligned sequences of 110 *lineage III KIR* from humans and apes (including hominoid species chimpanzee, gorilla, orangutan and gibbon). This analysis, which uses the ratio of the number of non-synonymous substitutions per non-synonymous site to the number of synonymous substitutions per synonymous site as an indicator of selective pressure acting on a protein-coding gene, identified 16 sites in the extracellular,

ligand-binding domains and 3 sites in the signaling domains that had been subject to positive selection.

Ten of these positions (6, 13, 16, 44, 50, 68, 70, 71, 84 and 90) mapped to the D1 protein domain with the remaining 6 residues found in the D2 protein domain (119, 123, 131, 148, 182 and 190). Consistent with their previously documented effect on HLA-C recognition both positions 44 and 70 were amongst those identified as having been subject to positive selection. Just six of these residues (44, 68, 70 and 71 in the D1 domain and 131 and 182 in the D2 domain) are found in the HLA class I binding footprint (Figure 1). For these six positions, sequence variability is notably higher in the D1 domain than in the D2 domain, both in the number of positively selected positions and the number of alternative residues at each position. Nonetheless, there is a variety of residues with distinctive chemistry and functional potential at all six positions. Lysine 44, proline 68, arginine 131 and arginine 182 are the only residues present in all five hominoid species examined, consistent with them having been present in a common hominoid ancestor. Greater variability and species specificity are observed for positions 70 and 71. Position 70 stands out for its diversification in humans but relative conservation in other species, whereas position 71 is more variable in chimpanzees and gorillas than in humans. These suggested that variation at these six positions had been selected for their direct effect on the functional interactions of hominoid lineage III KIR with MHC class I. To test this hypothesis, we introduced all naturally occurring variations at the six positions into human C2 specific KIR2DL1 and C1-specific KIR2DL3 and then determined the effects of these mutations on KIR specificity and avidity for HLA-C [53]. The results of these experiments have informed not only our understanding of the detailed molecular architecture of the KIR-HLA-C interface, but have also informed our understanding of the evolution and function of the C2 specific receptor KIR2DL1 and the C1-sepcific receptor KIR2DL3.

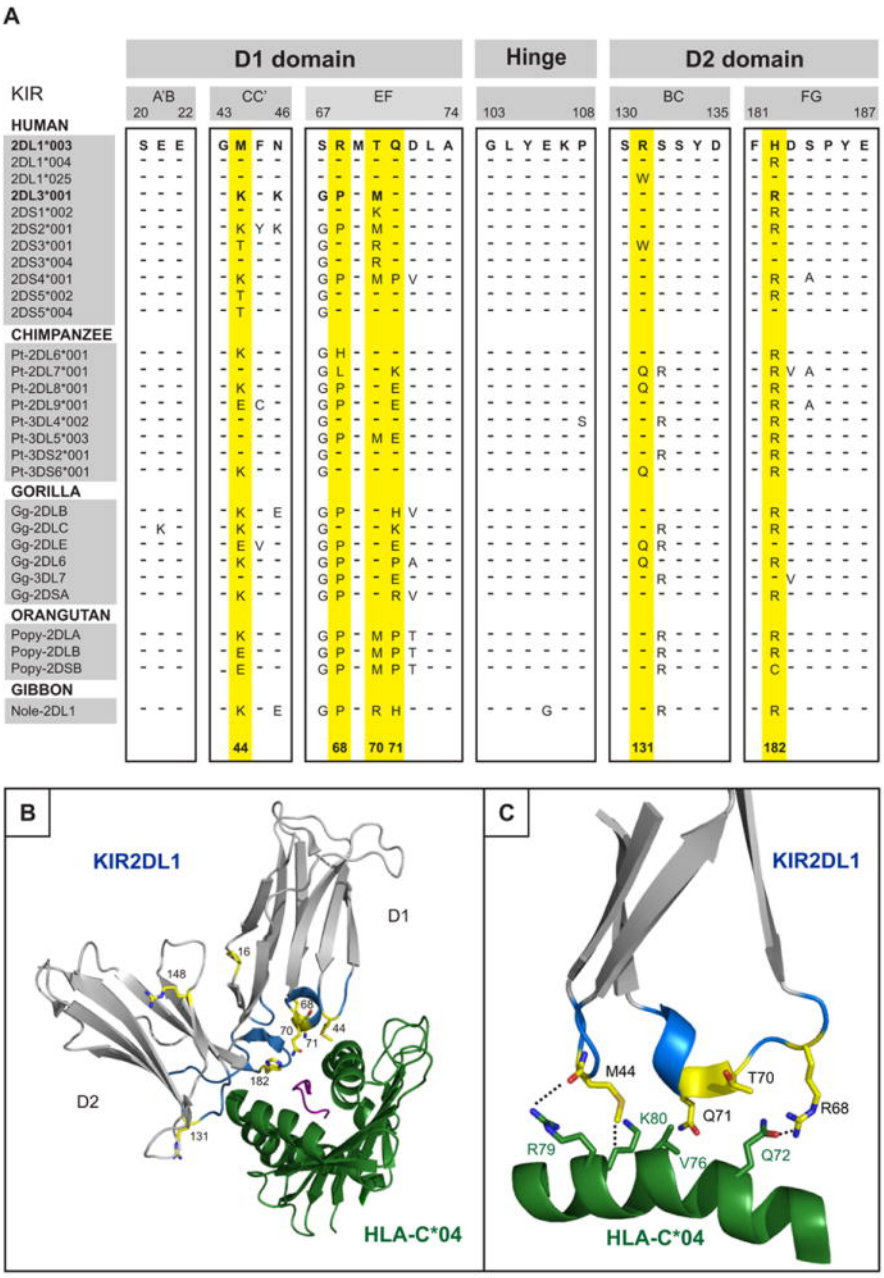

Figure 1: *Six positively selected residues in the binding site of hominoid lineage III KIR*

(A) Alignment of partial amino acid sequences of hominoid lineage III KIR showing the loops of the D1 and D2 domains that contact HLA-C. Sequences were aligned to 2DL1*003, identities being indicated by dashes (–). The six positively selected residues in the binding site for HLA class I are colored yellow, as is also the case for panels B and C. (B) Ribbon diagram of KIR2DL1 (grey) bound to HLA-C*04:01 (green) (PDB1IM9) (56). The loops of the KIR molecule are colored blue and positively selected residues are colored yellow. (C) Details of the binding between the D1 domain contact loop of KIR2DL1*003 (in blue with positively selected residues in yellow) and the α_1 domain helix of HLA-C*04:01 (green).

Summary of results

Evolution of a switch and a rheostat: position 44 controls KIR specificity and position 70 controls avidity for HLA class I

Consistent with previous studies, swapping the position 44 residues of KIR2DL1 and KIR2DL3 was sufficient to swap their HLA class I specificities. Thus, the 2DL3-44M mutant has C2 specificity like KIR2DL1 and the 2DL1-44K mutant has C1 specificity like KIR2DL3. On average, the binding of KIR2DL1 to C2 was approximately twice that of KIR2DL3 to C1, indicating that KIR2DL1 is a stronger receptor than KIR2DL3. That mutant 2DL1-44K bound to C1 at a much higher level (180%) than KIR2DL3 confirms that 2DL1 is an inherently stronger receptor, as well as demonstrating that substitutions other than the lysine-methionine dimorphism at position 44 contribute to the avidity difference. [Note: in the context of describing the differences in binding between naturally occurring and mutant KIR-Fc I have used the term "avidity". Although the differences in binding are likely to depend in large part on the specific avidity of binding between the two protein moieties, there are likely to be other factors that contribute to the binding differences. Thus, this term represents a short-hand. I have also used this term to correspond to the language used in the published papers that describe this work and that are included in this thesis.] However, the observation that mutant 2DL3-44M binds C2 almost as well (85%) as KIR2DL1 shows clearly that methionine 44 must also contribute to KIR2DL1 having higher avidity than KIR2DL3.

Threonine 44 is naturally present in KIR2DS3 and KIR2DS5, activating receptors exhibiting no detectable avidity for any HLA class I allotype when tested in the same binding assay as that used in this study [62]. In contrast, KIR2DL1 and KIR2DL3 mutants with 44T recognize some HLA-C allotypes. KIR2DL3-44T abrogated binding to C1, with the exception of C*16:01, which retained ~50% of binding. Accompanying the loss of C1 reactivity was acquisition of C2 specificity, but with much lower avidity than 2DL1 or 2DL3-44M. The 2DL1-44T mutant retained the C2 specificity of 2DL1 but with avidity reduced by ~50% (binding avidity comparable to

2DL3 for C1 and therefore well within the functional range). Thus human lineage III KIR with threonine 44 have the potential to be C2-specific receptors, suggesting that KIR2DS3 and KIR2DS5, for which ligands have yet to be determined, likely evolved from C2 receptors that lost the capacity to bind HLA class I through selected substitutions at positions other than position 44. That threonine 44 is present only in human lineage III KIR suggests that these receptors both arose and became attenuated during the course of human evolution. Interestingly, since the publication of the paper on which this chapter is based, both epidemiological [24] and direct experimental evidence (Blokhuis *et al* unpublished) point to a subset of *KIR2DS5* alleles (commonly found in African populations) that encode weak HLA-C2 specific receptors.

Although orangutan, gorilla and chimpanzee have KIR with glutamate 44, such KIR were lost during human evolution. Mutant 2DL1-44E retained the C2 specificity of KIR2DL1 but with 36% loss of avidity, properties similar to those of chimpanzee KIR2DL9 that has glutamate 44 [63]. By contrast, 2DL3-44E acquired reactivity with C2, while retaining 87% of the avidity for C1. Consequently, 2DL3-44E binds with comparable avidity to C1 and C2, thus having pan specificity for HLA-C. This C1+C2 specificity of 2DL3-44E is very similar to that of Popy-2DLB and Popy-2DSB, paired inhibitory and activating orangutan KIR that have glutamate 44 [34].

Substitutions at position 70 had no effect on either the C2 specificity of KIR2DL1 or the C1 specificity of KIR2DL3, but did have a profound effect on the avidity of the interactions. Substitution of threonine 70 in KIR2DL1 to lysine, methionine or arginine reduced the avidity by 43-66%, with the greatest effect seen with methionine, the residue present at position 70 in KIR2DL3. In contrast, substitution of methionine 70 in KIR2DL3 with arginine or threonine (the residue present in KIR2DL1) gave a modest increase (16-38%) in the avidity for C1, whereas the lysine substitution reduced the avidity by 48%. The results obtained for the position 70 swap mutants indicate that the threonine-methionine difference at position 70 is a

major factor contributing to the higher avidity of KIR2DL1 and lower avidity of KIR2DL3.

Thus, like a switch, mutation at position 44 can turn on or turn off reactivity of KIR2DL1 and KIR2DL3 for C1 or C2. By contrast, like a rheostat, position 70 controls the subsequent avidity of binding between receptor and ligand.

*Mutation at position 71 and 131 introduce binding to HLA-A*11:02 in KIR2DL3 but not KIR2DL1*

The introduction of proline at position 71 in 2DL3 broadened the specificity of mutant 2DL3-71P to include HLA-A*11:02. KIR2DS4 is an activating lineage III KIR that naturally has proline 71 and exhibits similar reactivity [64]. However, proline 71 is not necessary for recognition of HLA-A*11:02, as became apparent from analysis of the position 131 mutants. Substitution of arginine 131 in KIR2DL3 with glutamine introduced reactivity with HLA-A*11:02 while preserving avidity for C1-bearing HLA-C. In contrast, substitution of arginine 131 for tryptophan caused 86% loss of avidity for C1 but no binding to HLA-A*11:02. For KIR2DL1, replacement of arginine 131 by glutamine preserved the avidity and specificity for C2 with no acquisition of reactivity for HLA-A*11:02, whereas replacement with tryptophan preserved a pure C2 specificity but reduced avidity by 40%.

Of the four HLA class I epitopes (A3/11, Bw4, C1 and C2) recognized by KIR, the functional significance of A3/11 remains uncertain. Carried by HLA-A*03 and HLA-A*11 allotypes, the A3/11 epitope was first shown to engage the lineage II KIR KIR3DL2 [65, 66]. Although Bw4, C1 and C2 mediate robust inhibition and education of NK cells on binding their cognate KIR, the interaction of the A3/11 epitope with KIR3DL2 provides weak inhibition [67], and no detectable education [68]. Previous studies of lineage III KIR2DS4 [64] and orangutan lineage III KIR [34], demonstrated their recognition of HLA-A allotypes carrying the A3/11 epitope, with the strength of binding A*11:02>A*11:01>A*0301. This same hierarchy is seen

again for mutant 2DL3-71P, which binds significantly to A*11:02 but not to A*11:01 or A*03:01. With this background and context, we tested whether the recognition of HLA-A*11:02 by 2DL3-71P could influence NK cell function.

In cytotoxic assays G4-NKL (that lack the potentially confounding inhibitory receptor LILRB1) cells expressing KIR2DL3 killed 221-A*11:02 cells showing that A*11:02 is not a ligand for wild-type KIR2DL3. In contrast, killing of 221-A*11:02 was strongly inhibited when G4-NKL cells expressed the 2DL3-71P mutant, showing that binding of A*11:02 to 2DL3-71P is a functional ligand–receptor interaction that leads to the transduction of an inhibitory signal.

Major conclusions

Overall, mutation had a wider range of effects on KIR2DL3 than on KIR2DL1. The C1 specificity of KIR2DL3 was changed in two ways: a major broadening to give a pan HLA-C receptor with C1 plus specificity and a minor broadening to give reactivity with HLA-A*11:02, as well as C1. The avidity of KIR2DL3 was also changed in two ways: 2 of the mutations increased avidity for C1 by 10%, 13 decreased the avidity by >10%, and 3 had little effect. In comparison, the ligand binding properties of KIR2DL1 were more resistant to mutation: none of the 18 mutations altered the C2 specificity, and none of them increased the avidity for C2. Ten mutations in KIR2DL1 reduced C2 avidity by >10% and eight had little effect. Consideration of all the mutants, with the exception of those at position 44, shows that all KIR2DL1 mutants retained a minimum of 32% of the wild-type binding, whereas the binding of KIR2DL3 mutants ranged from 0-138% of wild-type binding. Exemplifying the variety of effects that mutation had on KIR2DL3 and their limited effect on KIR2DL1 are the avidities and specificities of the mutants containing glutamate 44, proline 71 and glutamate 131. Thus KIR2DL3 is seen as the weaker and less selective receptor, which, by being less refined, retains greater potential for change.

By contrast, having acquired specificity for C2, KIR2DL1 is now more specialized and comparatively inflexible.

These contrasting and complimentary properties fit well with an evolutionary model in which the C1 epitope and their cognate C1-specific KIR evolved first and subsequently underwent mutation and selection to give rise to the C2 epitope and C2-speififc KIR [34]. The crucial feature of this model is the flexibility of the C1 receptor and its cross-reactivity with C2, which, while maintaining function as a C1 receptor, provides a potential C2 receptor prior to formation of the C2 epitope. Thus, the inherent flexibility of the C1 receptor allows C2 and C2-specific KIR to evolve by stepwise point mutation through a series of intermediate forms that all have biological function and could be maintained by natural selection.

Critical appraisal of results and conclusions

This study investigated the effect of mutation on six amino acids found in the HLA class I binding site of lineage III KIR. These residues were hypothesized to have been subject to positive selection because they influence KIR-HLA interactions and therefore influence the downstream function of NK cells. My experimental approach used single amino acid mutations to investigate the specific functions of these residues, identifying changes that informed both the function and evolution of the C2 receptor KIR2DL1 and the C1 receptor KIR2DL3.

One major drawback of determining the effect of single amino acid substitutions is that the effect of these mutations is seen in isolation. Although clearly informative and a practical experimental approach to cover as many positions as possible, this approach will not reveal any synergy between positions. Synergy describes the process by which mutation at two residues has an effect greater than single mutations at either position.

There is clear precedent for this mechanism having occurred in *KIR* evolution. Positions 16 in the D1 domain and 148 in the D2 domain are

found in the hinge region of the KIR molecule. These residues, both of which have been subject to positive selection, account for the differences in specificity and avidity between KIR2DL2 and its allelic counterpart KIR2DL3 [69]. KIR2DL3 is a C1 specific receptor that displays relatively minimal binding to C2 targets whereas KIR2DL2 has higher avidity for C1 and significant cross-reactivity with C2. Single mutations at either position 16 or position 148 do not result in receptors with these properties, but mutating both residues is sufficient to change the binding properties consistent with there being synergy between these two positions. The changes in specificity were hypothesized to occur as a result of a shift in the relative orientation of the D1 and D2 domains. Another study subsequently showed that this synergy in the hinge region was not restricted to positions 16 and 148, but may be a more widespread feature of residues in the hinge region of the molecule [70]. A more detailed analysis of the effect of mutation at positions 16 and 148 is presented in chapter 3.

Traditionally, the specificity of primate KIR has been difficult to determine because of a comparative lack of cellular reagents. In this study, several non-human primate-specific amino acid residues were introduced into either KIR2DL1 or KIR2DL3. The results of these assays were interpreted in the context of the evolution of hominoid KIR. Indeed, the KIR-Fc HLA bead-binding assay has been used in previous studies to explore the binding characteristics of KIR in several simian primates. In Old World Monkeys, the *lineage III KIR* are represented by a single gene [71] while *lineage II KIR* genes have expanded and diversified. To identify their MHC epitope-specificity and avidity, a panel of rhesus macaque lineage II KIR-Fc was assayed [45]. Although MHC-C is not present in macaques, their KIR recognize HLA-C epitopes more effectively than they recognize HLA-A and HLA-B, suggesting that *MHC-C* evolved to become a stronger ligand for KIR than HLA-A and –B. The emergence of *MHC-C* in the orangutan was accompanied by an expansion of *lineage III KIR* and their evolution as MHC-C receptors [45]. All orangutan MHC-C allotypes have asparagine 80 and display the C1 epitope. Correspondingly, the results from the KIR-Fc

HLA bead-binding assay showed that orangutan has C1-specific KIR but not C2-specific KIR [34]. In chimpanzees the MHC-C gene became fixed and the C2 epitope emerged. As a consequence, out of nine chimpanzee lineage III KIR genes [44], eight encode receptors with high avidity for HLA-C, comprising three C1-specific receptors and 5 C2-specific receptors [63]. Together, the results of the assays, from these studies, and those from my study, provide a compelling timeline for the evolution of hominoid KIR. However, one major confounding factor is that the results of these assays were interpreted without knowing how these human KIR mutants or naturally occurring non-human primate KIR-Fc react with their cognate MHC class I. The results of these assays correlate well with cytotoxicity assays using human NKL and 221 cells expressing HLA class I, but some simple experiments, for example transfecting a 221 cell with orangutan MHC-C would go some way to allay these concerns.

Chapter 2

Investigation of functional polymorphism in naturally occurring *lineage III KIR*

Chapter 1 details the results of my work that investigated the effect of mutation on six positively selected residues in human lineage III KIR. The results of that study not only shed light on the function of those six residues, but also provided insight into the broader characteristics of KIR2DL1 and KIR2DL3. KIR2DL1 was found to be a strong C2 receptor that was relatively resistant to changes in specificity whilst KIR2DL3 was found to be a weaker C1 specific receptor that was significantly more malleable in terms of both specificity and avidity for HLA class I. Varying only those residues that had been subject to positive diversifying selection, distilled the functional elements of those receptors. However, given that both *KIR2DL1* and *KIR2DL3* are highly polymorphic, with 26 and 38 allotypic variants having been described (at the outset of this second study) I wanted to investigate the functional consequences of this diversity and to try and identify some of the selective pressures that have driven this diversity in specific human populations. It is the results of these experiments, which focus on a genetically diverse southern African hunter-gatherer population, that are the subject of this chapter.

For reasons of practicality, the functional properties of KIR2DL1 and KIR2DL2/3 have been studied mainly in the context of allotypic variants that combine high avidity, high specificity and high frequency in Europeans [2]. In contrast, for sub-Saharan African populations, which have the highest genetic diversity [72, 73] and among the highest mortality from infectious disease and pregnancy complications [74], *KIR* investigation is in its infancy and has so far focused on West African and Bantu-speaking populations [75]. Within sub-Saharan Africa, some indigenous populations are as different from each other as they are from Europeans [72, 73]. Notably, the KhoeSan who reside across Southern Africa descend from the deepest human population divergence and have among the greatest genetic diversity

of any population [76, 77]. During the last 2,000 years there has been admixture between the KhoeSan and Bantu-speaking agriculturalists who expanded southwards. More recently, the arrival of European colonists over the past 500 years has introduced novel infectious diseases including smallpox and tuberculosis. In this study I undertook high-resolution genetic and functional studies on the HLA-C specific KIR of the KhoeSan and four other global populations that represent the range of human immunogenetic diversity.

Summary of results and key findings

Two novel KIR2DL1 alleles are unique to the KhoeSan

From analysis of 61 KhoeSan ten *KIR2DL1* alleles were identified. Of these, two alleles, subsequently given the designations *2DL1*022* and *2DL1*026,* were new discoveries that have frequencies in the KhoeSan of 17.2% and 4.2%, respectively. Being absent from all previously studied populations suggested that *2DL1*022* and *2DL1*026* are specific to the KhoeSan. To test this hypothesis we examined additional populations for the presence of these alleles. We first examined data from the 1000 Genomes project dataset by probing for sequence-specific reads that correspond to the *KIR2DL1*022* and *2DL1*026* alleles. *KIR3DL3*, a framework gene present on all *KIR* haplotypes, served as the positive control. All 2,496 individuals sampled had reads corresponding to *KIR3DL3* but none of the 2496 individuals in the current release of the 1000 Genome dataset, representing 26 different populations worldwide, was found to have either *2DL1*022* or *2DL1*026*. Because the 1000 Genome dataset represents a limited subset of sub-Saharan African population diversity, we expanded our search to include four further groups including three hunter-gatherer populations (the Tanzanian Hadza, Mbuti and Baka Pygmies) and the South African Zulu. Neither allele was found in the hunter-gatherer populations, but we did detect both *KIR2DL1*022* and *KIR2DL1*026* present at 1.5% and 1% respectively in the Zulu population. Haplotype analysis and admixture mapping were consistent with these alleles having been recently transferred from the KhoeSan into the Zulu. Together, these

data support an evolutionary model in which *2DL1*022* and *2DL1*026* increased in frequency in the KhoeSan people after their divergence from other populations.

*Neither KIR2DL1*022 nor KIR2DL1*026 can mediate NK cell responses via HLA-C2*

*KIR2DL1*022* differs from *2DL1*001*, also present in the KhoeSan, by a single non-synonymous substitution in codon 44. Thus *2DL1*022* likely evolved from *2DL1*001* by a point mutation that caused methionine to be replaced by lysine at position 44. Position 44 dimorphism determines whether a given KIR2DL has specificity for the C1 or C2 epitope of HLA-C [36]. Prior to investigation of the KhoeSan, all the known KIR2DL1 allotypes (n=23) had methionine 44 and were predicted to be C2-specific. Conversely, and in complementary fashion, the known KIR2DL2/3 allotypes (n=36) all had lysine 44 and were predicted to be C1 specific. Using the same assay described in chapter 1 and critically reviewed in chapter 4 of this thesis, we showed that KIR2DL1*022 binds to all nine C1-bearing HLA-C allotypes but to none of the seven C2-bearing HLA-C allotypes in the test panel. Indeed, 2DL1*022 has higher avidity for C1 than any of the KIR2DL2/3 allotypes we tested, but no significant C2 cross reactivity.

*KIR2DL1*026*, the other KhoeSan-specific *KIR2DL1* allele, differs from *2DL1*012*, also present in the KhoeSan, by one nucleotide substitution. Thus *KIR2DL1*026* likely arose from *2DL1*012* by point mutation. This substitution converted the tryptophan codon at position 246 to a termination codon. Position 246 is situated at the boundary between the transmembrane domain and the cytoplasmic tail. Consequently, 2DL1*026 lacks the immunoreceptor tyrosine-based inhibitory motifs (ITIMs) of the cytoplasmic tail that mediate inhibitory signaling function [78]. Less obvious is the effect that absence of a cytoplasmic tail could have on the association of 2DL1*026 with cellular membranes. Thus, the mutation that created *2DL1*026* clearly has a major effect in abrogating inhibitory

signaling function, but it also has potential to alter the amount of receptor that reaches the NK cell-surface.

Polymorphism produces KIR with a range of avidity and specificity for HLA-C

As predicted, 2DL1*022 functions as a C1-specific receptor and not a C2-specific receptor like eleven of the 13 other KIR2DL1-Fc. These eleven KIR2DL1-Fc varied in their avidity for C2 by half an order of magnitude. In contrast, 2DL1*013N-Fc and 2DL1*014-Fc bound to no HLA class I allotype. For 2DL1*013N this result was anticipated, because the protein is a fragment that terminates prematurely at residue 34 in the D1 domain. On the other hand, 2DL1*014 was expected to bind HLA class I, because it differs from 2DL1*003 only by substitution of glycine for serine at position 179 in the D2 domain. KIR2DL2/3 exhibit a range of avidity for C1, but with increasing avidity for C1 there is also rising cross-reactivity with C2. This is not the case for 2DL1*022, which has a higher avidity for C1 than any of the KIR2DL2/3 allotypes, but no significant C2 cross reactivity. Overall, these results vividly illustrate how the natural polymorphism of KIR2DL1 and KIR2DL2/3 modulates the avidity, specificity and functionality of these NK cell receptors in human populations.

The KhoeSan have a high frequency of weak C2 receptors

Unlike some populations, there is no single *KIR2DL1* allele that is present at high frequency in the KhoeSan. The ten KhoeSan *KIR2DL1* alleles vary in frequency from 1.1-21.3%. In addition, 18% of KhoeSan *KIR* haplotypes lack the *KIR2DL1* gene, constituting an eleventh allele: the '*blank*'. In addition to KIR2DL1*022 and 2DL1*026 that have lost the ability to mediate an inhibitory signal via engagement with C2 the KhoeSan have a high frequency of weak inhibitory C2 receptors. Amongst these are the 'blank' and 2DL1*004 and 2DL1*011 receptors that have low avidity for C2 as well as reduced signaling capacity [52]. In sum, the frequency of weak or inactive KIR2DL1 allotypes in the KhoeSan is 71.8% whereas the

28.2% frequency of strong KIR2DL1 allotypes in the KhoeSan and much lower than that of other populations (Figure 2).

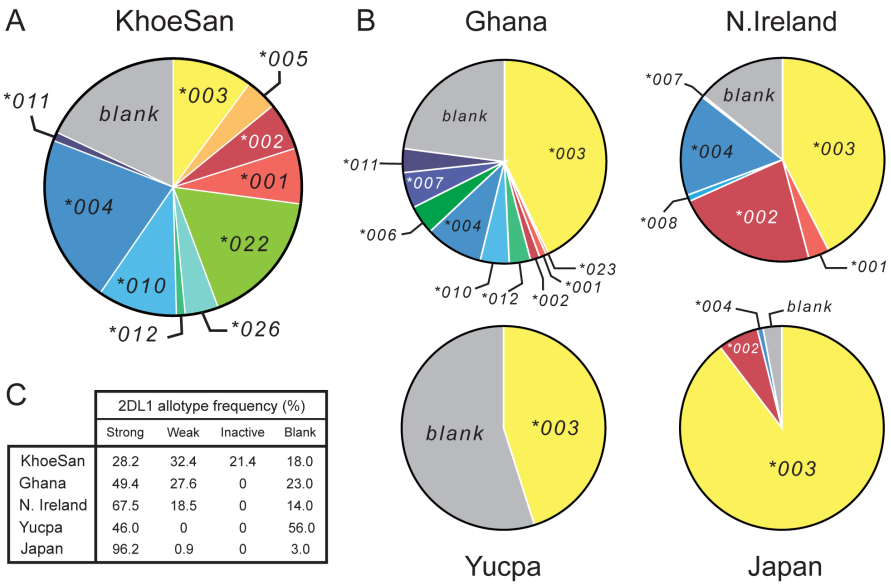

C

	2DL1 allotype frequency (%)			
	Strong	Weak	Inactive	Blank
KhoeSan	28.2	32.4	21.4	18.0
Ghana	49.4	27.6	0	23.0
N. Ireland	67.5	18.5	0	14.0
Yucpa	46.0	0	0	56.0
Japan	96.2	0.9	0	3.0

Figure 2: *The KhoeSan have high KIR2DL1 diversity compared to other human populations* (A and B) The pie charts show the number and relative frequencies of *KIR2DL1* alleles in the KhoeSan of Southern Africa (A), and four other populations representing four continents (B): the Ga-Adangbe from Ghana in Western Africa [14], Northern Ireland Caucasians from Europe [21], Japanese from East Asia [24] and Yucpa Amerindians from South America [20]. The 'blank' is the frequency of *KIR* haplotypes that lack the*KIR2DL1* gene. (C) Also compared in the five populations are the frequencies of strong KIR2DL1, weak KIR2DL1, KIR2DL1 that are not inhibitory C2 receptors (inactive) and the absence of KIR2DL1 (blank).

Polymorphism produces KIR with a range of cell-surface expression

KIR2DL1*026 and KIR2DL1*012 encode identical extracellular domains that bind C2 with high avidity and specificity. To determine if 2DL1*026, which lacks a cytoplasmic tail, reaches the cell-surface, we examined the expression of FLAG-tagged 2DL1*026 and 2DL1*012 in transiently transfected HeLa cells. For comparison, eight other KIR2DL1 allotypes were included in the analysis. KIR2DL1*026 is cell-surface expressed at a significantly lower level than 2DL1*012 (p=0.0087), but within the range observed for other KIR2DL1 allotypes. Although KIR2DL1*026 cannot mediate NK cell inhibition directly, because it lacks a cytoplasmic domain,

it could have indirect effects, either by preventing C2 from binding to other receptors or by contributing to the adhesive interactions of NK cells with target cells. That 2DL1*014 is not cell-surface expressed and cannot bind HLA class I suggests that its defining residue, serine 179, prevents proper protein folding. Other KIR allotypes with impaired folding that causes intracellular retention have been described [79-82].

Major conclusions

This study showed how KIR2DL1 polymorphism has given rise to NK cell receptors that vary substantially in their capacity to recognize HLA-C and propagate intracellular signals. Emphasizing the value of defining structural and functional KIR variation at high resolution is our discovery in the KhoeSan of two unusual allotypes of KIR2DL1 (2DL1*022 and 2DL1*026), both of which have lost the ability to recognize the C2 epitope of HLA-C. That KIR2DL1*022 and KIR2DL1*026 have lost the capacity to function as inhibitory C2 receptors, exemplifies the accumulation of KIR2DL1 allotypes in the KhoeSan with low avidity or weakened signaling function, as well as *KIR B* haplotypes lacking the *KIR2DL1* gene. We hypothesize that the emergence of 2DL1*022 and 2DL1*026, as well as the general increase of weaker inhibitory KIR2DL1 allotypes in the KhoeSan could have acted to reduce the incidence of preeclampsia, to which the KhoeSan are likely to be predisposed on account of their high frequency of the C2 epitope [23, 24].

For other allotypes of KIR2DL1 and KIR2DL2/3, the effects of their defining substitutions can act to alter different functional properties: receptor avidity [53, 69, 70], stability [81, 82], cell-surface abundance and signal transduction [52]. Throughout the KIR molecule are sites where natural substitutions affect receptor functions. Many of these are away from the HLA-C binding site and likely involve conformational changes, including ones that affect the relative orientation of the extracellular D1 and D2 domains that combine the form the binding site [69, 70].

Critical review of results

In this study we showed that allotypic variation of KIR2DL1 and KIR2DL2/3 results in receptors that display a range of avidity for HLA-C. This functional range was shown using the HLA class I bead-binding assay that is discussed in greater detail in chapter 4. Although the results of this assay correspond well with cell-based assays of cytotoxicity, this correlation has been studied only superficially and with receptor variants that bind with high avidity or no avidity to the HLA-C ligand under test. As a result, there is little information regarding how minor changes in avidity between KIR and HLA class I influence downstream NK cell function. Our interpretation has been that the changes in avidity represent a linear functional range i.e. that a receptor that binds with twice the avidity of its counterpart will educate an NK cell twice as well. However, NK cell reactivity may be determined by threshold rather than a true linear response. In this model, any receptor-ligand interaction above a certain threshold would educate the NK cell similarly, effectively nullifying any effect from higher avidity interactions. Similarly, a threshold effect may occur at the lower end of the binding spectrum such that any interactions below a given threshold are insufficient to induce receptor signaling via ligand engagement. To determine whether the linear or threshold models better fits with true NK cell biology would need extensive cellular assays. Other than the time constraints, one potential problem with this approach is that cellular assays of cytotoxicity have a notoriously high noise to signal readout. Indeed, it was this characteristic of these tests that first inspired our development of the bead-based assay. Flow cytometric analysis of cytoplasmic tail phosphorylation may be an appropriate experimental approach to investigate this open question.

In addition to the variation that we observed in receptor avidity and specificity, we also showed that KIR2DL1 receptors display a range of cell-surface expression. A similar criticism could be leveled at this work; the functional implications of this variation are not clear. Our assumption has been that an increase in cell-surface expression of a given receptor correlates

with an increase in the potential of that receptor to educate an NK cell via engagement with an HLA class I ligand. However, evidence for this assumption is lacking. Differences in the expression of HLA-C have been correlated with disease outcome [83], but it remains unknown as to whether this effect is mediated via engagement of NK cell receptors, TCR, or another immune system receptor. One pitfall of attempting to address this question is that an assay would have to be designed in which the cell-surface expression of a given KIR would have to be modified without influencing the avidity of binding to HLA-C. In this capacity, 2DL1*003 and 2DL1*005, which share an identical extracellular domain, but have different cell-surface expression, have potential. However, experimental design would need to ensure that the mutation in the cytoplasmic tail that distinguishes these allotypes does not play a role in regulating intracellular signaling.

This study concentrated on the functional aspects of single KIR allotypes, documenting the functional variation that is the result of genetic polymorphism. We did not consider the broader functional characteristics of the combinations of KIR allotypes inherited on specific KIR haplotypes. This is a deficiency that I sought to address in a follow-up study. The results of this in-depth characterization of the functional variation between the *KIR A* and *B* haplotypes that results from allotypic variation in HLA-C receptors is the subject of Chapter 3.

Chapter 3

Contribution of polymorphism to diversification of *KIR* haplotypes

The human *KIR* locus comprises two haplotype groups, termed *A* and *B*. *KIR A* haplotypes encode a fixed suite of largely inhibitory receptors whereas *KIR B* haplotypes have a variable number of inhibitory receptors and several activating receptors. That these haplotype groups are present in all human populations but with different relative frequencies, suggests that they have different functional properties that have been subject to balancing selection.

In addition to their accumulation of activating receptors, the *KIR B* haplotypes also have a subset of alleles for the inhibitory receptor genes that are common to *KIR A* and *B* haplotypes [37, 50, 84]. Furthermore, although a limited number of *KIR* haplotypes have been studied in detail there appears to be functional differences between the inhibitory receptors encoded by the *KIR A* and *B* haplotypes [52, 60, 68, 69]. In this chapter I present the findings from my study that determined the haplotypic association, phylogeny and function of every *KIR2DL1*, *KIR2DL2/3* and *KIR2DS1* allele yet defined. The results from this study shed light on the evolution and function of human HLA-C receptors and their contribution to the distinct functions of the *KIR A* and *B* haplotypes.

Summary of results and key findings

KIR2DL1/S1 and KIR2DL2/3 form four distinct phylogenetic clades that segregate on distinct haplotypes

KIRs that recognize HLA-C divide into two groups on the basis of their epitope recognition: the inhibitory KIR2DL2/3 recognize the C1 epitope of HLA-C, and the inhibitory KIR2DL1 and activating KIR2DS1 recognize the C2 epitope of HLA-C. Both *KIR2DL2/3* and *KIR2DL1* are highly polymorphic whereas *KIR2DS1* is relatively conserved [35].

Phylogenetic analysis of the coding sequence of 26 *KIR2DL1* and *KIR2DS1* alleles distinguishes four clades of *KIR* (Figure 3).

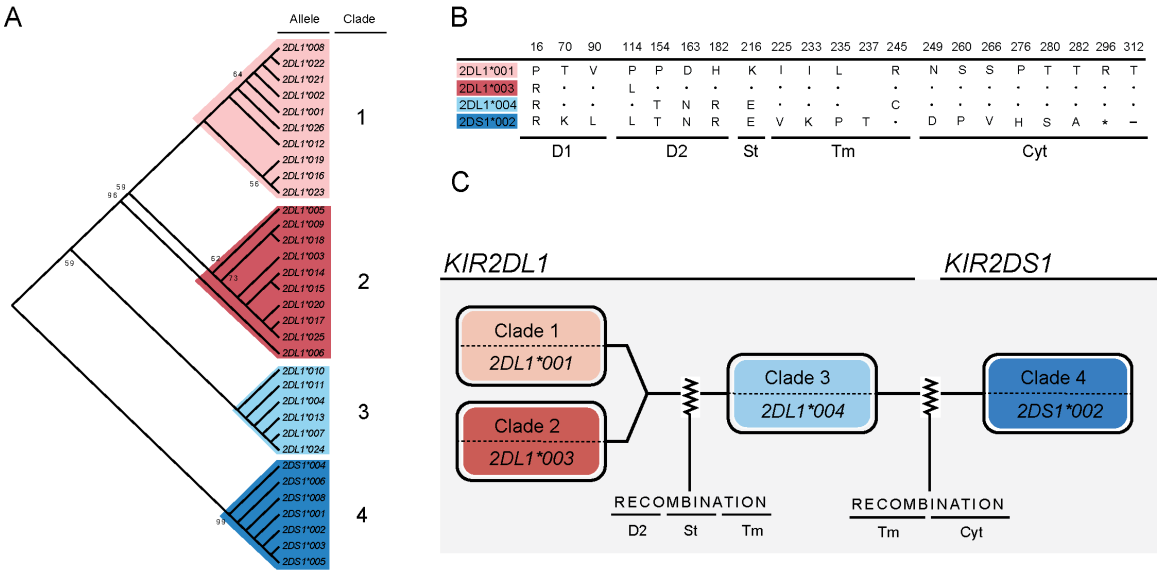

Figure 3: *KIR2DL1 and KIR2DS1 form four phylogenetic clades*

(A) Shown is a phylogenetic analysis of 33 KIR2DL1 and 2DS1 nucleotide sequences representing the domains encoding amino acids 1-328. The phylogenetic relationships were inferred using three tree-building algorithms that showed broad consensus. Shown is a representative tree created using the Neighbor-Joining Method [85]. The analysis identified four clades that have been color shaded for clarity. The optimal tree with sum of branch length = 0.071 is shown. The percentage of replicate trees in which the associated taxa clustered together in the bootstrap test (500 replicates) is shown next to the branches when greater than, or equal to, 50. The evolutionary distances were computed using the Tamura-Nei method and are in the units of the number of base substitutions per site. All positions containing gaps and missing data were eliminated. In the final dataset there was a total of 872 positions. Evolutionary analysis was conducted in MEGA6 [86]. (B) Shown is a sequence alignment of the most common allotypes in each of the four KIR2DL1 and 2DS1 clades identified by the phylogenetic analysis. Dots indicate identity with consensus (2DL1*001) and an asterisk indicates a termination codon. The lines beneath the alignment show the structural domains: Ig-like domains (D1+D2), stem (St), transmembrane domain (Tm) and cytoplasmic tail (Cyt). (C) Schematic diagram indicating the likely sites of recombination that define the four phylogenetic clades of KIR2DL1 and 2DS1 identified in (A).

The alleles grouped in clades 1 and 2 are associated with the centromeric part of the *KIR A* haplotype (*Cen-A*). Exceptions are the KhoeSan specific alleles *KIR2DL1*022* and *KIR2DL1*026* (discussed in detail in chapter 2) that phylogenetically form part of clade 1, but genetically associate with centromeric *KIR B* haplotypes (*Cen-B*) [54]. Clade 3 contains six *KIR2DL1*004*-like alleles, whose products are distinguished from those of clades 1 and 2 by a 4 amino acid sequence motif comprising threonine 154, asparagine 163, arginine 182 and glutamate 216. Clade 3 alleles map to the *Cen-B* haplotype with one exception (*KIR2DL1*011*) that maps to the *Cen-A haplotype*. That this motif is shared by KIR2DS1 suggests that *KIR2DL1* acquired this motif by recombination with *KIR2DS1*. Clade 4 comprises the *KIR2DS1* alleles that are found in the telomeric region of *KIR B* haplotypes. (*Tel-B*).

The *KIR2DL2/3* gene encodes receptors that recognize HLA-C allotypes carrying the C1 epitope. In an analogous fashion to that identified for *KIR2DL1*, phylogenetic analysis of *KIR2DL2/3* identified 4 clades of alleles that segregate with specific *KIR* haplotypes (Figure 4). Clades 1 and 2 comprise 24 *KIR2DL3* alleles that predominantly map to *Cen-A* (*KIR2DL3*014 and 2DL3*018* are exceptions found on *Cen-B*); clades 3 and 4 comprise 11 *KIR2DL2* alleles that map to *Cen-B*. In summary, for both *KIR2DL1* and *KIR2DS1* and *KIR2DL2/3* there are four phylogenetic clades of alleles that correlate with genomic location in the *Cen-A*, *Cen-B* or *Tel-B* region of *KIR* haplotypes.

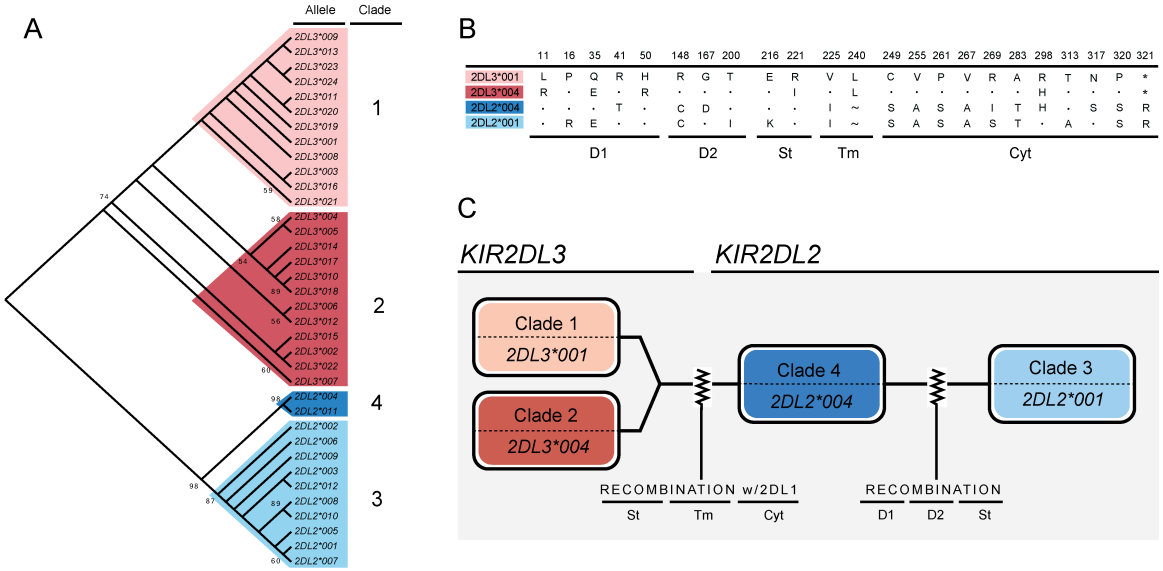

Figure 4: *KIR2DL2 and KIR2DL3 form four phylogenetic clades*

(A) Shown is a phylogenetic analysis of 36 *KIR2DL2/3* nucleotide sequences representing the domains encoding amino acids 1-328. The phylogenetic relationships were inferred using three tree-building algorithms. Shown is a representative tree created using the Neighbor-Joining Method [85]. The analysis identified four clades that have been color shaded for clarity. The optimal tree with sum of branch length = 0.079 is shown. The percentage of replicate trees in which the associated taxa clustered together in the bootstrap test (500 replicates) is shown next to the branches when greater than or equal to 50. The evolutionary distances were computed using the Tamura-Nei method and are in the units of the number of base substitutions per site. All positions containing gaps and missing data were eliminated. In the final dataset there was a total of 952 positions. Evolutionary analysis was conducted in MEGA6 [86].(B) Shown is an alignment of four KIR2DL2/3 allotypes representing the four clades identified using phylogenetic analysis. Dots indicate identity with the consensus (2DL3*001) and an asterisk indicates a termination codon. The lines beneath the alignment show the structural domains: Ig-like domains (D1+D2), stem (St), transmembrane domain (Tm) and cytoplasmic tail (Cyt). (C) Schematic diagram indicating the likely sites of recombination that define the four phylogenetic clades identified in part (A).

Cen A encodes stronger C2 receptors and weaker C1 receptors than Cen B

A synthesis of the binding data from each of the receptors encoded by alleles associated with the *Cen-A* or *Cen-B* haplotypes showed that KIR2DL1 encoded by *Cen-A* alleles bind C2 with significantly greater avidity than *Cen-B* encoded KIR2DL1. Receptor function of three *Cen-B*

associated KIR2DL1 allotypes is further weakened by substitutions in the transmembrane or cytoplasmic domain [52, 54]. A similar analysis for KIR2DL2/3 allotypes showed that *Cen-A* encoded KIR2DL2 and KIR2DL3 receptors have significantly lower avidity for C1 than do the *Cen-B* encoded KIR2DL2 and KIR2DL3 receptors.

*Four D2 domain substitutions give Cen A associated KIR2DL1*003 and Cen B associated KIR2DL1*004 different C2 avidity*

To determine the basis for the weaker C2 avidity of *Cen-B* associated KIR2DL1, we compared *KIR2DL1*003* and *KIR2DL1*004*, respectively the most common *Cen-A* and *Cen-B* associated alleles [51, 87-91]. In the D1 and D2 domains that form the ligand-binding site, KIR2DL1*003 and KIR2DL1*004 differ only in D2, at positions 114, 154, 163 and 182. We made KIR-Fc fusion proteins from KIR2DL1*003, KIR2DL1*004 and the set of 14 KIR2DL1 mutants that represents all possible combinations of the four dimorphic positions. These 16 KIR-Fc fusion proteins were tested for binding to the panel of 97 HLA class I allotypes. Substitution at all of the four positions affects receptor avidity for HLA-C2 with single mutations at three of the positions (154, 163 and 182) showing that the residue present in KIR2DL1*003 increases and the KIR2DL1*004 residue decreases avidity. For position 114 the opposite effect was seen. Thus, the four dimorphic sites have not co-evolved to produce the strongest and weakest C2 receptors possible. Instead, there exists a more moderate balance between a stronger and a weaker C2 receptor.

The N-terminal half of the KIR2DL1 transmembrane domain is essential for cell-surface expression

KIR2DL1*004 is one example of a *Cen-A* associated allotype that is functionally affected by polymorphism at the junction between the transmembrane and cytoplasmic domains. Another is KIR2DL1*026 that has a termination codon at position 246. This substitution has two effects. First, it eliminates the cytoplasmic tail with its ITIMs that mediate inhibitory signaling function [78]. Second, it reduces the cell surface expression of

KIR2DL1*026 [54]. This observation raised the question: how much of the transmembrane domain is necessary for KIR2DL1 to become surface associated? To address this question we introduced termination codons at five evenly spaced positions within the sequence encoding the transmembrane domain (residues 225-245) of KIR2DL1*003, as well as at position 224 in the stem domain and positions 246, 250 and 256 in the cytoplasmic tail. After incorporation of N-terminal FLAG tags, we determined the cell-surface expression of the 12 mutant constructs and wild-type KIR2DL1*003 using an anti-FLAG antibody.

Termination in the N-terminal half of the transmembrane region (residues 225-235) completely abrogated cell-surface expression of the mutant KIR2DL1*003. In contrast, termination in the carboxyl-terminal half of the transmembrane domain (residues 236-245) permitted cell surface expression of mutant KIR2DL1*003, with levels corresponding to 53-72% of the wild-type. Thus, the N-terminal half of the transmembrane domain is required for membrane association of KIR2DL1.

*A terminal mutation in KIR2DL1*014 prevents its cell-surface expression*

KIR2DL1*014 differs from KIR2DL1*003 by substitution of glycine for serine at position 179 in the D2 domain. Serine 179 prevents cell surface expression of KIR2DL1*014 and the binding of KIR2DL1*014-Fc to HLA class I [54]. These properties suggest that serine 179 prevents KIR2DL1*014 from folding properly, thereby leading to its intracellular retention.

We used confocal microscopy to examine the intracellular localization of the FLAG-tagged KIR2DL1*014 in HeLa cells, showing that although KIR2DL1*014 protein is produced, it is retained in the interior of the cell, consistent with an unfolded protein response. An analysis of the three-dimensional structure of KIR2DL1*001 (*PDB: 1NKR*) [47] showed that position 179 of the D2 domain is buried beneath the binding site for HLA-C. We modeled the effect of replacing glycine 179 of KIR2DL1*001 with the

serine 179 of KIR2DL1*014. In this model the side chain substitution of a hydrogen atom for a methyl group displaces the tyrosine at position 134 and this is the likely mechanism that disrupts the folding of the receptor.

Variation at positions 16 and 148 diversifies the recognition of HLA-C by KIR2DL2/3

Moesta et al. previously showed that the residues at positions 16 and 148 in the hinge region of the KIR molecule account for KIR2DL2*001 and KIR2DL3*001 having different avidities for HLA-C [69]. Having proline 16 and arginine 148 renders KIR2DL3*001 a C1-specific receptor of moderate avidity. In contrast, arginine 16 and cysteine 148 give KIR2DL2*001 higher avidity for C1 and cross-reactivity with C2 [36, 69]. Sequence comparison of 61 KIR2DL1, KIR2DL2 and KIR2DL3 variants showed that arginine and proline are the only residues present at position 16, whereas arginine, proline and cysteine can occur at position 148. Five of the six possible combinations are represented in the 36 KIR2DL2/3 allotypes, but only two combinations are represented in the 33 KIR2DL1 and KIR2DS1 allotypes. To see how the variability at positions 16 and 148 influence avidity and specificity for HLA-C, I made 18 KIR-Fc fusion proteins in which all six combinations of the natural residues at positions 16 and 148 were introduced into KIR2DL1*003, KIR2DL2*001 and KIR2DL3*001.

Consistent with the findings presented in chapter 1, KIR2DL1 appears comparatively insensitive to mutation, with 5 of the 6 KIR2DL1 mutants exhibiting <15% variability in the binding to HLA-C. In contrast, the mutant combining proline 16 with proline 148 retained high specificity for C2 but with avidity only 60% of wild-type. In comparison with the relative insensitivity of KIR2DL1 to mutation, all KIR2DL2 and KIR2DL3 mutants exhibited detectable differences. For KIR2DL2, the major effect of mutation was to change the avidity, whereas the specificity of stronger binding to C1 and weaker binding to C2 was largely preserved. By contrast, the five KIR2DL3 mutants showed greater cross-reactivity with C2 than wild-type

KIR2DL3*001. For both KIR2DL2 and KIR2DL3, mutants with arginine 16 and arginine 148 produce receptors with high avidity for HLA-C whereas mutants with proline 16 and proline 148 consistently produced receptors with low avidity for HLA-C.

In summary, these results indicate that polymorphism in all of the structural domains of the mature KIR protein can impact the function of KIR with respect to the initiation and propagation of inhibitory or activating signals. Substitutions that change the avidity of KIR2DL1 for HLA-C are usually in the D2 domain, whereas substitutions that change the avidity of KIR2DL2/3 for HLA-C are usually in the hinge region connecting the D1 and D2 domains. The only site where substitution has significant impact on the specificity of KIR2DL1 for C2 or KIR2DL2/3 for C1, is position 44 in the D1 domain. Substitutions that affect the cell surface expression of KIR2DL are more often in the transmembrane or the cytoplasmic domain, but there are also substitutions in the extracellular domains that alter receptor function in this way. An extreme example is KIR2DL1*014, which is completely retained inside the cell as a consequence of having serine, rather than glycine at position 179 in the D2 domain.

Major conclusions

This study showed that inhibitory *KIR2DL1*, activating *KIR2DS1*, and inhibitory *KIR2DL2*/3 alleles form distinctive clades that associate with specific *KIR* haplotypes. Typifying *KIR Cen-A* haplotypes are *KIR2DL1* alleles that encode strong inhibitory C2 receptors and *KIR2DL2/3* alleles encoding weak inhibitory C1 receptors. In striking contrast, *Cen-B* haplotypes combine *KIR2DL1* alleles that encode weak inhibitory C2 receptors with *KIR2DL2/3* alleles encoding strong inhibitory C1 receptors.

Although the relative frequency of KIR A and B haplotypes varies substantially across the world, as do C1 and C2 frequencies, there is a strong correlation between C2 and KIR B and a corresponding inverse correlation between C2 and KIR A. thus, it appears that in populations with high C2

frequency, such as those in Africa, there has been selection for weak C2 receptors and strong C1 receptors (found on KIR B haplotypes). Underlying these observations and implicating a strong inhibitory C2 receptor-ligand interaction in their pathogenesis, are correlations with pregnancy syndromes. Thus, women who are pregnant with a fetus expressing C2 are at increased risk of preeclampsia. Those same strong inhibitory KIR-ligand interactions are, however, vital for the development of well-educated NK cells that are both self-tolerant and responsive to virally infected and malignantly transformed cells. Thus, a pattern emerges in which KIR haplotypes with contrasting functional properties are subject to selection in response to the relative abundance of HLA-C ligand. In this way, we propose that the KIR system may be considered a buffering mechanism by which optimal NK cell function is preserved, despite fluctuations in the frequency of available ligand.

Critical review of results

A key finding of this study was that *KIR Cen-A* haplotypes encode stronger C2 receptors and weaker C1 receptors than *Cen-B* haplotypes. Supporting this conclusion was our analysis in which we compared the avidity and specificity of allotypes known to segregate with specific *KIR* haplotypes. However, there are three major weaknesses of this analysis:

1. *Incomplete haplotype and allele data:* because the high-resolution genotyping of *KIR* remains in its infancy, both the true allelic diversity of *KIR2DL1* and *KIR2DL2/3* and their haplotype associations are yet to be fully elucidated. Because our analysis used only known alleles with known haplotype associations, this dearth of information may skew the results of our analysis. Repeating our analysis using every known allele with putative haplotype associations confirmed our original findings. However, this secondary analysis may erroneously include alleles that display "haplotype infidelity" and skew the results for this reason.

2. *Signaling capacity and cell-surface expression not included in allotype weighting*: our analysis accounted for the avidity and specificity of the allotypes of KIR2DL1 and KIR2DL2/3 as measured by the KIR-Fc bead binding assay, but did not account for the differences in either cell-surface expression or the variable signaling capacity of the allotypes. Our rationale for excluding cell-surface expression information was twofold: (a) little is known regarding how cell-surface expression influences downstream NK cell education and function and (b) this study did not investigate the cell-surface expression of KIR2DL2/3. Our rationale for excluding signaling capacity was the lack of information available for KIR2DL2/3. Thus, as an example, the *Cen-B* associated allotype KIR2DL1*026, which binds strongly and specifically to HLA-C2, but does not generate an inhibitory signal because it lacks a cytoplasmic domain, artificially decreases the significance of the association that found. Conversely, the *Cen-A* associated KIR2DL1*006, which binds strongly and specifically to HLA-C2 but is weakened due to having cysteine at position 245, biases the finding in the opposite direction.

3. *Frequency of alleles not accounted for in analysis*: In this comparative analysis, each allele is weighted equally, regardless of their frequency in a given population. As an example, *KIR2DL1*022* is included in the *Cen-B* associated alleles. This allele encodes a receptor that does not recognize HLA-C2. However, our work (presented in chapter 2) showed that this allele is has a very restricted population distribution, being found almost exclusively in the southern African hunter-gatherer KhoeSan population. As a result, low frequency alleles or those that have a very restricted distribution may have too great an influence on the results of our analysis. A further analysis (which is currently being performed) that combines the frequency of specific *KIR* alleles with their functional capacity would go some way to address this weakness.

Chapter 4

Refining the production of KIR-Fc fusion proteins and their use in a multiplex binding assay

One of the central methodological advancements that allowed us to map the functional variation of KIR-HLA-C receptor ligand interactions (presented in chapters 1-3) was the development and refinement of the KIR-Fc - HLA class I multiplex binding assay. First described by *Moesta et al* [69] for the investigation of the reactivity of KIR2DL2 and KIR2DL3, this test has since been adopted widely in the field of NK cell biology [34, 45, 53-55, 62-64, 70]. The first studies that described this assay produced just a few KIR-Fc proteins whose reactivity was tested on the new multiplex platform [64, 69]. My research has expanded the use of these KIR-Fc proteins, mapping the reactivity of over 100 KIR-Fc that represent both naturally occurring KIR allotypes as well as mutant KIR, created to investigate the function of specific amino acid residues [53-55]. This exponential expansion in KIR-Fc production required devising new protein production systems, internal quality assurance controls and standard assay operating procedures [56]. These advances, which are the subject of this chapter, have increased the reproducibility and functionality of this assay.

NK cells encode a diverse repertoire of receptors that complicates understanding of how single receptors contribute to NK reactivity

Because the genes encoding KIR and HLA class I are on different chromosomes, their independent segregation during meiosis produces diversity in the number and type of *KIR-HLA* gene combinations inherited in individuals [67, 92]. The result is that NK cells from individuals of different genetic backgrounds are educated by different receptor ligand combinations resulting in a range of NK cell function. Further, NK cells can express more than one KIR at a time. This inherent diversity complicates the investigation of the specific KIR-HLA class I interactions that modulate immune response. Development of soluble KIR proteins, for which the reactivity for single HLA class I molecules was determined by direct binding assay, facilitated

understanding of how particular receptor-ligand combinations contributed to NK cell reactivity [93]. These recombinant proteins were made in a mammalian cell expression system by fusing the extracellular domains of a two-domain KIR with two Fc domains of a human IgG1 to form a soluble homodimer (Figure 5).

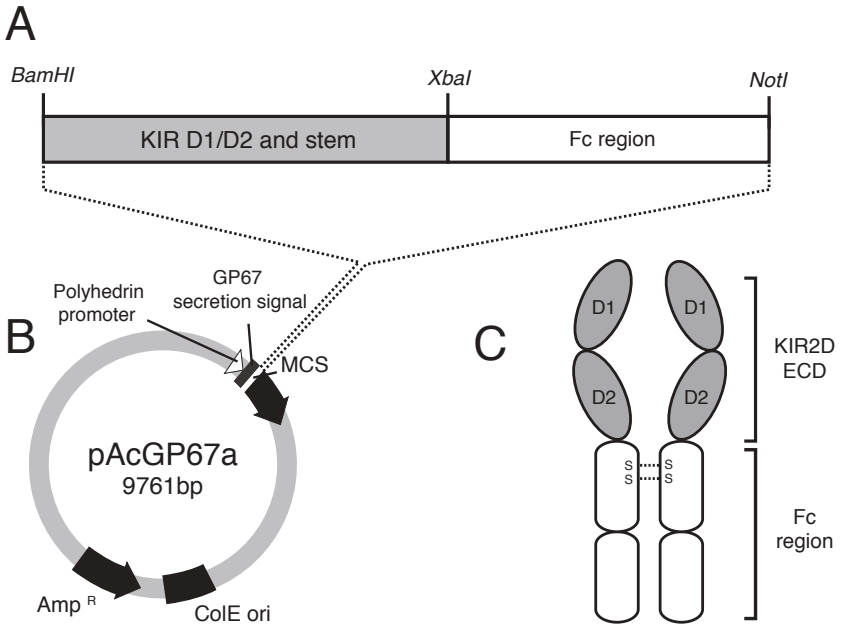

Figure 5: (A) Schematic diagram showing the configuration of a recombinant KIR-Fc fusion gene. The recombinant fusion gene consisting of the D1, D2 and stem domains of a KIR2D molecule (grey box) and the Fc region of a human IgG1 antibody (white box) is cloned using *BamH1* and *Not1* restriction sites into the multiple cloning site (MCS) of the pAcGP67a vector (B) downstream of the polyhedrin and GP67 promoters. Transfection into insect cells produces a soluble recombinant KIR-Fc dimer (C) consisting of the D1, D2 and stem regions (extracellular domain – ECD) of the KIR molecule (grey ovals) and the Fc region (white ovals) of the IgG1 antibody. (S-S) shows the location of the di-sulphide bonds that lead to formation of a dimer.

The reactivity of these KIR-Fc was then tested in a cellular binding assay [93]. Whilst this approach was critical to determining the basic "rules" that governed KIR and HLA class I interaction, the assay had two major drawbacks: (1) mammalian cells are comparatively difficult and expensive to culture and they produce relatively small quantities of protein and (2) the

assay only allowed examination of the reactivity between one specific KIR and one specific HLA class I molecule at any time. To address these issues, *Moesta et al*. [69] first developed a method for the production of KIR-Fc from insect cells and secondly, adapted an assay originally designed for the identification of human alloantibodies to test the reactivity of a single KIR for around 100 HLA class I molecules at one time.

KIR-Fc production from insect cells

The advantages of insect cells are that they are simple to culture. They also have a short doubling time that facilitates scaling and they are capable of higher protein yields than comparative mammalian cell expression systems. Because of these advantages, the baculovirus-insect cell system is now one of the most widely used methods for the production of recombinant proteins [94]. Although not equivalent to higher eukaryotic cells, most post-translational modifications are made correctly in insect cells, and proteins unable to be expressed in *E.coli* have been successfully expressed in the insect cell system [95]. The baculovirus family are species-specific double-stranded DNA viruses that infect insects as their natural host [96]. Once inserted into the host nucleus, the baculovirus is packaged into flexible nucelocapsids, into which foreign DNA may readily be inserted. The target gene, in our case the *KIR-Fc* fusion gene, is inserted into a transfer vector and positioned between sequences that are homologous to the ones in the baculoviral genome. When the viral genome and transfer vector are transfected into insect cells, recombination occurs and produces intact viral genomes harboring the target-gene sequence. The strong promoter of the *polyhedrin* gene is co-opted for production of recombinant target protein.

Development of a multiplex KIR-Fc binding assay

In seeking to improve upon previous iterations of the KIR-Fc binding assay (that investigated the reactivity of a single HLA class I allotype using a cell-based assay), *Moesta et al* [69] developed a multiplex assay that detects the binding of KIR-Fc to 97 HLA class I allotypes. This assay uses the Luminex platform, in which the antigenic targets are not cells but microbeads, each

coated with a defined HLA class I allotype. Such beads were developed originally for studying the specificity of human alloantibodies [97], but the platform was adapted for use with recombinant two-domain KIR-Fc fusion proteins [69] and monoclonal antibodies [57] (see chapter 5). By adjusting the relative concentration of two fluorescent dyes, a set of 97 individually identifiable beads is generated. Each bead is then coated with a different HLA class I allotype, allowing the results of the immune assay to be correlated with HLA class I specificity. The panel of HLA class I allotypes annealed to the beads represents a broad range of the HLA class I diversity found worldwide, allowing evaluation of interactions between KIR-Fc and rare, population specific and divergent HLA class I allotypes. Crucially, although HLA-C represents the minority of the HLA class I allotypes found in the panel (16/97 allotypes), both HLA-C1 and HLA-C2 encoding alleles are well represented.

The results of this assay can be used to predict the reactivity of KIR expressing NK and T cells when their KIR bind to cognate HLA class I ligands. It is designed to inform cellular assays of lymphocyte function in which receptor deficient effector NK cells transfected with a specific KIR are incubated with ligand-deficient target cells transfected with a specific HLA class I molecule. The correlation between the results from our multiplex assay and assays of lymphocyte function is very strong. As an example, our initial study with the bead-binding assay showed that KIR2DL2*001-Fc recognized HLA-C2 allotypes with higher avidity than its allotypic variant KIR2DL3*001-Fc. A cellular cytotoxicity assay subsequently showed that KIR2DL2*001, but not KIR2DL3*001 effectively inhibited lysis when incubated with HLA class deficient target cells transfected with the HLA-C2 bearing allotype HLA-C*04:01 [69]. Other groups have also demonstrated similar correlations between the bead-binding assay and assays of lymphocyte function, as well as assays such as surface plasmon resonance that directly measure the avidity of binding between two protein moieties [70].

Summary of results and key findings

In refining this assay I sought to address two major problems: (1) variable baculovirus amplification from *Sf9* insect cells and variable protein yield from *Hi5* insect cells and (2) inter-assay variability and high background binding. In previous iterations of the protocol, the failure of baculovirus amplification was only evidenced by a failure of protein production from *Hi5* cells. A positive control (using *Sf9* supernatant with known capacity to produce recombinant protein) could be used to determine whether the *Hi5* cells were functional, but this method still required several weeks of work without positive evidence of success. Additionally, first-time users were at a significant disadvantage if they did not have access to a suitable positive control. In combating these deficiencies I introduced steps aimed at (a) optimizing baculoviral recombination during initial transfection (b) ensuring optimal cell health during culture and detecting unhealthy cells or contamination early (c) using an independent marker of baculoviral amplification to determine successful viral infection and replication. To reduce inter-assay variability and background binding in the assay itself I introduced a series of standard operating procedures that addressed these deficiencies. These refinements to the protocol are summarized in the paragraphs below.

Creating optimal insect cell health and assessing baculoviral amplification

For the formation of intact baculovirus it is essential that transfer vector and linearized baculoviral DNA recombine during initial co-transfection of *Sf9* cells. We have obtained the best results with freshly isolated transfer vector and baculoviral DNA that has not been stored at 4°C for more than two weeks. Additionally, freeze/thaw cycles of the transfer vector should be avoided where possible. Because the linearized baculovirus is a large DNA fragment (~130kb), it is particularly susceptible to shear stress; over-zealous pipetting during transfection should therefore be avoided to minimize DNA damage and maximize transfection success.

Sf9 cells should have a doubling time of between 24 and 30h. *Hi5* cells should have a doubling time of between 18 and 24 hours. Slow doubling times usually indicate that *Sf9* of *Hi5* cell cultures are unhealthy. Unhealthy cells will not amplify baculovirus successfully or produce adequate recombinant protein. Cell viability for both *Sf9* and *Hi5* cells, as determined by trypan blue staining, should be greater than 95% at all times. Both bacterial and fungal infections in the insect cell culture will reduce viability and doubling times. These can be prevented with good cell culture technique and the addition of antibiotics (1% Penicillin-Streptomycin) and/or anti-fungals (0.25ug/ml Amphotericin B) to the culture medium. Cultures should be discarded immediately if there is evidence of microorganism contamination. A second reason for slow-doubling times is oxygen restriction. If the cell culture does not have sufficient surface area exposed to the air, cell growth will be retarded. This can be prevented by ensuring that the flasks are filled not more than one-third (by volume) with culture medium. Shaking the flasks between 120 and 150 rpm also ensures adequate oxygenation. Shaking at a higher rpm may lead to cell damaging shearing stress and should be avoided.

Identification of baculovirus-infected Hi5 cells by flow cytometry

GP64 is a baculovirus encoded glycoprotein that is expressed on insect cells upon infection with baculovirus [98]. As a result, identification of the expression of this surface protein by flow cytometry can be used as a proxy for the successful amplification of baculovirus in *Sf9* cells. We showed that GP64 expression is not detected on un-transfected Hi5 cells but is expressed following transfection with high viral titre Sf9 supernatant. P0 viral stock was not sufficient to induce GP64 expression whereas surface expression was typically detected after transfection with P1 viral stock and with each subsequent amplified viral stock. Surface expression of GP64 was sensitive to the baculoviral titre with P2 transfected *Hi5* cells showing a 40% increase in surface expression of G964 as compared to *Hi5* cells transfected with P1 viral stocks. That P3 stocks induced only marginally greater GP64 surface expression than P2 viral stocks suggests that GP64 is either maximally up-

regulated by a given viral titre or *Sf9* cells reach maximal viral amplification between the second and third amplification rounds. Because the titre of the transfecting supernatant corresponds to the degree of cell-surface expression of GP64, this method can be used to distinguish *Sf9* supernatants with a range of baculoviral titres.

Reducing inter-assay variability and background binding

We determined that the following steps reduce both inter-assay variability and high background binding. For the purposes of this assay we have defined high background readings as those in which the negative control bead binding is greater than 1% of the highest positive reading obtained.

Although not always the case, some KIR-Fc are not stable when stored at 4°C and consequently, their use in the assay can lead to high background readings. Our assumption has been that this occurs because of aggregation of protein, though we lack strong evidence to support this hypothesis. To control for this issue, we assessed the stability of the KIR-Fc fusion proteins when stored at -80°C. Freezing the KIR-Fc is assumed to prevent the protein degradation, aggregation and misfolding that may occur when stored at 4°C. We determined that flash freezing of the recombinant proteins in liquid nitrogen, followed by storage of up to 12 months at -80°C maintained the stability of the proteins well (as evidenced by minimal inter-assay variability). Similarly, HLA class I microbeads that have been thawed and stored at 4°C do not remain stable for more than 3 months and are a potential source of inter-assay variability and high background readings. The beads should be divided into 10µl aliquots and frozen at -80°C if they are unlikely to be used within this time frame. A final standard assay operation that we introduced was to make certain that during the wash and incubation phases of the protocol that all the reagents were chilled to 4°C and that wash steps be completed as quickly as possible if they are unable to be performed in a cold room. To monitor for inter-assay variability and high background, we also routinely include KIR-Fc with very well characterized HLA-C1 and HLA-C2 binding repertoires as positive controls.

Major conclusions

This chapter described the production of KIR-Fc fusion proteins in an insect cell expression system and their interaction in a multiplex binding assay with a panel of 97 HLA class I allotypes. KIR-Fc production in insect cells is relatively simple, allowing production of large amounts of recombinant protein in around 20 days. The assay is sensitive enough to discriminate between single amino acid substitutions in the extracellular domains of the KIR molecule and has, as a result, greatly facilitated investigation of even closely related KIR allotypes. Furthermore, the results of the direct binding assay correlate well with the results of cytotoxicity assays and the direct binding assays that were used to discover the KIR and first investigate their specificity for HLA class I.

Critical review of results

The microbeads we used in this assay are produced in a proprietary process by One Lambda (Canoga Park, CA, USA). As a result, we have limited information regarding their manufacture, specifically regarding the cellular origin of the HLA class I allotypes that are subsequently annealed to the microbeads. This dearth of knowledge influences the interpretation of our assay results in two significant ways. Firstly, we have no information regarding the peptide content of the HLA class I allotypes annealed to each bead. Given that the HLA class I protein is likely harvested from 221 cells transfected with a specific HLA class I variant, the peptide repertoire is considered to be heterogeneous, but we have no direct evidence to support that hypothesis. There are myriad ways in which the peptide content of the HLA class I presented on these microbeads might be skewed. As an example, the process by which the HLA class I proteins are annealed to the microbeads could select for just those complexes that are particularly stable. Given that the stability of a specific HLA class I is often directly related to the peptide that it is presenting, this process might easily skew the peptide content presented by HLA class I on the microbeads (and hence to KIR). Although the peptide specificity of KIR is unlikely to rival that of the TCR, with which it shares an overlapping (but different) binding footprint on HLA

class I [46, 47], recent work has shown that several two-domain KIR do display significant peptide specificity. Thus, any bias in peptide presentation might influence the results of our assay.

The second feature of the microbeads that might influence KIR reactivity is the number of open conformers of HLA class I that are present on the microbeads. As noted above, we have little information regarding the nature of the process by which HLA class I protein is annealed to the surface of the microbeads. It is possible (indeed unpublished data seems to suggest it might be common) that several open conformers (those that lack a peptide), might be presented on the surface of the microbeads. Although there are no reports of two-domain KIR recognizing open conformers of HLA class I, this feature has been observed for other members of the KIR family [99, 100]. It has also been hypothesized that many activating KIR (for which traditional HLA class I ligands have not been identified) might preferentially recognize open conformers of certain HLA class I. Thus, the presence of open conformers of HLA class I on the microbeads might influence the binding of certain KIR, especially activating variants, inducing a "false" positive result. Adding an additional antibody control (e.g. HC-10 which recognizes open HLA class I conformers) would determine the relative amount of unfolded HLA class I protein present on the beads. However, if positive, we would still be unable to distinguish KIR binding to open HLA class I conformers as compared to correctly folded conformers replete with peptide.

Although two-domain KIR are easily and reliably produced and purified from insect cell cultures, three-domain KIR (KIR3D) do not assemble efficiently. The insect cell system is capable of producing the protein, but we have not been able to detect reactivity of these KIR3D-Fc to any HLA class I. Because KIR3D are widely known to recognize the Bw4 epitope of HLA-A and HLA-B, this result suggests that the insect cells are incapable of producing an efficiently folded three-domain KIR-Fc. Recently however, three-domain KIR tetramers have been produced efficiently from insect cells [101] and KIR3D-Fc have been produced from HEK 293 cells [102].

Multiplex assays using these reagents have contributed a wealth of new information regarding the reactivity of KIR3DL1 allotypes.

This protocol uses a protein-A bead purification step to purify the recombinant KIR-Fc from other proteins produced by the insect cells. The KIR-Fc are subsequently eluted from the beads using an acid wash. This method produces a high concentration of pure KIR-Fc, as evidenced by visualization on a SDS-page gel. However, the acid-wash step may result in some denaturation of the protein, which would not be detected on a protein gel as it measures only the size of the protein, and not it's biological activity or structure. The result is that our determination of the concentration of the purified protein by Bradford assay may overestimate the true amount of biologically active protein. A second purification step, for example using a liquid chromatography column (FPLC), would allow visualization of the purity of the protein and allow efficient separation of any aggregated or unfolded recombinant protein. If present, any denatured protein might contribute to the small amount of variable background binding that we observe in this assay. The steps that we have taken in refining the protocol have reduced background binding over previous iterations of the assay, but there remains a consistent background level of approximately 1-2% background binding. Evidence that supports the claim that further purification might reduce background binding comes from KIR tetramer binding studies in which the proteins used have been purified by FPLC and have almost no detectable background binding.

Chapter 5

Adapting the multiplex platform to identify monoclonal antibody epitopes on HLA class I

In chapter 4 I described our adaptation of a commercially available HLA class I bead-binding assay to test the reactivity of KIR-Fc fusion proteins. We have also adapted this assay to map the polymorphic epitopes of a panel of monoclonal antibodies and it is the results of these experiments that are the subject of this chapter.

Monoclonal antibodies that recognize HLA class I have been an invaluable tool for basic and clinical research in human immunology. Such antibodies can be divided into two groups according to the types of epitope they recognize [103]. Monomorphic antibodies, such as W6/32, recognize monomorphic determinants that are common to all HLA class I variants, whereas polymorphic antibodies, the subject of the following two chapters, recognize determinants carried by a subset of such variants. In this study we examined the reactivity of four polymorphic monoclonal anti-HLA class I antibodies: PA2.1, BB7.1, BB7.2 and MA2.1.

Originally, PA2.1 and BB7.2 were seen to be specific for HLA-A2 [103-105], but with more extensive characterization were also shown to recognize and define HLA-A*69, a variant that is a recombinant of HLA-A*02 and HLA-A*68 [106]. In similar fashion, BB7.1 was originally seen to be specific for HLA-B*07 [103] but was subsequently shown to recognize HLA-B*42 [107], a recombinant of HLA-B*07 and HLA-B*08 [108] that is characteristic of African populations. MA2.1, which was originally described as recognizing HLA-A2 and HLA-B17 antigens [109] has been shown to react with both the B*57 and B*58 components of HLA-B17 [110], but no additional reactivity has been reported.

In large part, the HLA class I specificity of monoclonal antibodies has been determined using panels of cells each of which minimally expresses one

HLA-A, one HLA-B and one HLA-C allotype and more commonly express two allotypes for each. This complexity means that binding reactions cannot be directly attributed to particular HLA class I variants but must be inferred through various types of correlation. As a consequence, there are limitations in the extent to which data can be interpreted and thus in the resolution and accuracy of the data. An initial approach to address these limitations was the use of mutant cell lines that lacked endogenous HLA class I expression and could be transfected to express a single HLA class I allotype [111]. A more recent approach has been to replace cells as the target antigen with synthetic beads each of which is coated with a single HLA class I allotype [97]. Comparison of the reactivity patterns from the >90 HLA class I allotypes represented in the synthetic bead panel allows refinement of the epitopes recognized by each of these polymorphic monoclonal antibodies.

Summary of results and key findings

Specificity of the MA2.1 monoclonal antibody

MA2.1 bound strongly to the five HLA-A*02 subtypes tested and also to HLA-B*57:01, B*57:03 and B*58:01 (which correspond to the serological B17 antigen). These results are consistent with the previously defined specificity of MA2.1 for the HLA-A2 and B-17 antigens [109]. However, we also observed weak reactivity of MA2.1 with HLA-B*15:16 and an even weaker one with HLA-A*11.

The critical epitope for MA2.1 recognition is the GETR motif at positions 62-65 in the helix of the α-1 domain [112]. Within this motif, glycine 62 is the only residue that is not found in any of the other 89 HLA-A, -B or –C allotypes tested. HLA-B*15:16 and HLA-A*11 differ only at position 62, having RETR and QETR motifs respectively, which correlates with them having some avidity for MA2.1.

Specificity of the PA2.1 and BB7.2 monoclonal antibodies

When used at a concentration of 1μg/ml, the PA2.1 and BB7.2 antibodies gave similarly strong reactions with five subtypes of HLA-A*02 and with

HLA-A*69:01. However, when a much higher concentration was used (50μg/ml), cross-reactions of the PA2.1 and BB7.2 antibodies were observed with HLA-A*23:01, A*24:02, A*24:03, A*68:01, A*68:02 and A*69:01. These cross-reactions correspond well with the cross-reactivity first described in the 1960s [113] between the serological A2, A28 (A*68 and A*69) and A9 (A*23 and A*24) antigens and more recently described for cell-binding assays with the I-145 monoclonal antibody [114]. These cross-reactions were stronger for BB7.2 than PA2.1 and much stronger for A*24:03 than either A*24:02 or A*23:01. This must be due to the two substitutions that distinguish A*24:03 from the other allotypes and which are at positions 166 and 167 in the α-2 domain. The combination of sequence comparisons [103, 104, 106, 110] and site-directed mutagenesis [112, 115, 116] has shown that tryptophan 107 in the α-2 domain is a critical factor in forming the epitope recognized by PA2.1 and BB7.2. In addition, mutations at positions 161, 163, 166, 167 and 169 can lead to loss of binding by PA2.1 and BB7.2, showing that these residues also contribute to forming the epitope [115, 117].

Specificity of the BB7.1 monoclonal antibody

BB7.1 reacts with HLA-B*07:02 and HLA-B*42:01. In addition, we found that HLA-B*81:01, an African allotype [118, 119] also strongly reacts with BB7.1, which fits with both HLA-B*81:01, B*42:01 and B*07:01 having α-1 domains with identical sequence and residues 63-70 of the α-1 domain being critical for the BB7.1 epitope [103, 107, 120-124]. Both HLA-B*56:01 and B*82:01 have identical α-1 domains with identical sequence to that of HLA-B*07:02, B*42:01 and B*81:01 but these allotypes are not bound by BB7.1 suggesting that residues in the α-2 domain abrogate their recognition. *HLA-B*07:02*, *B*42:01* and *B*81:01* encode arginine at position 131 whereas *B*56:01* and *B*82:01* encode serine at this position. Similarly, both *B*56:01* and *B*82:01* encode leucine at position 163 whereas HLA-B*07:02 and B*81:01 both have glutamic acid. That BB7.1 interacts with residues in the α-2 domain is further supported by the observation that mutation at positions 166 and 169 of HLA-B*07 eliminates

the BB7.1 epitope [121]. Therefore, whilst the α-1 domain residues between positions 63-71 likely form the dominant epitope for recognition by BB7.1, binding is influenced by polymorphism in the α-2 domain, suggesting that this antibody binds both the α-1 and α-2 regions of HLA class I. Given that this footprint would span the peptide binding cleft, peptide variability is likely to influence BB7.1 recognition of HLA class I.

In summary, we find that the patterns of antibody reactivity observed here are entirely consistent with those obtained previously and extend those results by being able to detect and distinguish reactions and cross-reactions in a quantitative manner, All the observed reactions are with HLA-A and HLA-B variants, with no cross-reactivity for HLA-C, further emphasizing the distinct properties of HLA-C [125-127].

Using the multiplex platform to map the reactivity of the monoclonal antibody 10A5

Counterparts to the *HLA class I* genes are restricted to simian primates, and the chimpanzee (*Pan troglodytes*) has orthologs of all six expressed *HLA class I* genes [40]. For some 50% of chimpanzee *MHC* haplotypes, these genes (*Patr-A, B, C, E, F and G*) are the only expressed *MHC class I* genes, but the other 50% of haplotypes have a seventh expressed gene, *Patr-AL*, that is within an additional ~125kb block of genomic DNA that is next to the ~80kb block containing the *Patr-A* gene [128]. More closely related to *Patr-A* than the other expressed genes, *Patr-AL* is one of a group of *A*-related genes (hence the name *A-like*) that includes the non-functional *MHC-H* and *MHC-J* genes [129]. Although not yet proved, there is evidence for the existence of two forms of human *MHC* haplotype that correspond to the *Patr-AL+* and *Patr-AL-* haplotypes [128]. Called *HLA-Y*, the human equivalent of *Patr-AL* is non-functional and contains a 5' region of high sequence similarity with *Patr-AL* that is recombined with a 3' region from another *A*-related gene [128]. Neither *Patr-AL* nor *HLA-Y* exhibit significant polymorphism. *Patr-AL* originated long before the separation of human and chimpanzee ancestors [128, 129] and was specifically inactivated during

human evolution. Such inactivation could have been driven by selection or by the demographic factors of population bottleneck and genetic drift. Study of *Patr-AL* will therefore define an immune system component that humans have lost.

Patr-AL forms a heterotrimeric complex with β_2-microglobulin (β_2m) and nonamer peptides to give a three-dimensional structure in which the Cα traces of the H chain and β_2M superimpose with their counterparts in other HLA class I structures [128]. The peptide-binding specificity of Patr-AL is essentially the same as that of HLA-A*02, although the two molecules differ by >40 amino acid substitutions, of which 30 are in the α-1 and α-2 domains and 13 are predicted to contact peptide [128]. These properties suggest that Patr-AL, like HLA-A and Patr-A, presents peptide antigens to αβ TCRs. Supporting this hypothesis, Patr-AL is an alloantigen recognized by the highly specific cytotoxic CD8 αβ T cells that are present in chimpanzees lacking Patr-AL [128]. This implies that Patr-AL is expressed in the thymus and mediates negative selection.

The major structural difference between Patr-AL and other human and chimpanzee MHC class I molecules is the upper face of the α helix of the α-2 domain, which is unusually electropositive and makes Patr-AL exceptional in having a basic isoelectric point [128]. Previous preliminary analysis of mRNA levels indicated that the expression of Patr-AL was either very low or restricted to a minority of PBMCs [129]. In the investigation reported in this chapter, Abs against Patr-AL were made and used to study both endogenous Patr-AL protein expression and recombinant Patr-AL stably expressed in an MHC class I–deficient cell line and compared its expression with the well-characterized human HLA-A*02 protein. Central to this process was the characterization of the reactivity of the 10A5 (anti-Patr-AL) antibody using the multiplex antibody-binding assay described in this chapter.

The anti Patr-AL monoclonal antibody 10A5 does not recognize HLA class I on either cells or microbeads

Previously it was shown that the Patr-AL protein can be detected in chimpanzee PBMCs and B lymphoblastoid cell lines (BLCL), but at a much lower level than classical MHC class I molecules [129]. To facilitate further expression of Patr-AL expression, mAbs from the B cells of mice immunized with soluble, recombinant Patr-AL were made. This Ag comprised the extracellular domains of Patr-AL, β_2M and the nonamer Patr-AL binding peptide ALDKATVLL [128]. Of the many mAbs obtained, the 10A5 antibody was selected for further investigation because it bound strongly to Patr-AL but exhibited no detectable interaction with other MHC class I transfected into HLA class I deficient cell lines. Thus, 10A5 binds to HLA-A, B, -C deficient 221 cells transfected with Patr-AL, but not to untransfected 221 cells or to 221 cells transfected with either HLA-A or Patr-A.

The exquisite specificity of the 10A5 Ab for Patr-AL was demonstrated by analysis to measure the binding of 10A5 to the wider HLA class I panel represented in the Luminex panel described above and comparing the results to the binding achieved with W6/32. Whereas the binding of W6/32 to the 97 HLA class I coated beads varied between a fluorescence intensity of 17,715 and 28,136, the binding of 10A5 varied between 9 and 77. Thus, none of the 31 HLA-A, 50 HLA-B and 16 HLA-C allotypes was bound significantly by the anti-Patr-AL mouse mAb 10A5.

Critical review of results

Although we have speculated based on the predicted epitopes of the monoclonal antibodies that we investigated in this chapter that peptide may play an important role in the reactivity of certain monoclonal antibodies directed against HLA class I, we have little information regarding the peptide content of the beads used in this assay, although we have assumed them to be heterogeneous in nature. A simple cellular experiment documenting the binding effect of different pulsed peptides by flow

cytometry would go some way to confirm the true role of peptide in the antibody epitopes.

In similar fashion, if a particular antibody is highly sensitive to bound peptide, it is possible for an antibody to display no reactivity to HLA class I-peptide repertoire presented in the bead binding assay but to have specific reactivity to a particular peptide or group of peptides presented by an identical HLA class I allotype in a cellular system. This has particular relevance to our investigation of the 10A5 antibody that we demonstrated has no reactivity for HLA class I.

In designing this assay we used a wide range of antibody concentrations and interpreted the relatively low levels of binding seen with some antibodies as weak cross-reactivity for an epitope. However, as previously stated in chapter 4, there is a possibility that a portion of the HLA class I molecules annealed to the beads are present in the form of open conformers (unfolded HLA class I lacking peptide). As a result, these low levels of binding at high concentration may simply represent exposed epitopes to which the antibody would otherwise have no distinguishable reactivity. The result is that we over estimate the number and types of residues that form the binding epitopes for these antibodies.

Concluding remarks

This thesis summarizes the results from 6 published studies that investigated how genetic variation of KIR and HLA-C contributes to the functional diversity found in human immune systems. Also presented are several methodological advances that have facilitated our understanding of these complex immune interfaces.

Each of the six positions that have undergone positive selection in the extracellular ligand binding domains of KIR contribute to differences in binding to HLA-C. Position 44 governs the specificity of these interactions whereas position 70 plays the dominant role in the avidity of interactions.

The critical role of position 44 was further highlighted by our study of *KIR2DL1*022*. This allele, which evolved in the KhoeSan and is not found in other human populations, has switched specificity from HLA-C2 to HLA-C1. The increase in the frequency of this allele, and other weakened *KIR2DL1* alleles that predominate in the KhoeSan likely occurred to balance the unusually high frequency of the HLA-C2 epitope in this population.

The balance that characterizes the distribution and function of *KIR* and *HLA-C* in the KhoeSan is also evident for *KIR* haplotypes more generally. *KIR A* haplotypes are replete with alleles that encode strong HLA-C2 receptors but weak HLA-C1 receptors. Conversely, *KIR B* haplotypes have alleles that encode weaker HLA-C2 receptors but stronger HLA-C1 receptors.

Our results highlight the need for determining both the *KIR* and *HLA class I* genotype at the highest possible resolution and the need for functional studies that document the functional consequences of that variation. Such studies are likely to be critical for determining immune responses in individuals at the dawn of a new age of personalized medicine.

References

1. Cooper, M.A., M. Colonna, and W.M. Yokoyama, *Hidden talents of natural killers: NK cells in innate and adaptive immunity.* EMBO Rep, 2009. **10**(10): p. 1103-10.
2. Parham, P. and A. Moffett, *Variable NK cell receptors and their MHC class I ligands in immunity, reproduction and human evolution.* Nat Rev Immunol, 2013. **13**(2): p. 133-44.
3. Kiessling, R., et al., *"Natural" killer cells in the mouse. II. Cytotoxic cells with specificity for mouse Moloney leukemia cells. Characteristics of the killer cell.* Eur J Immunol, 1975. **5**(2): p. 117-21.
4. Kiessling, R., E. Klein, and H. Wigzell, *"Natural" killer cells in the mouse. I. Cytotoxic cells with specificity for mouse Moloney leukemia cells. Specificity and distribution according to genotype.* Eur J Immunol, 1975. **5**(2): p. 112-7.
5. Pross, H.F. and M. Jondal, *Cytotoxic lymphocytes from normal donors. A functional marker of human non-T lymphocytes.* Clin Exp Immunol, 1975. **21**(2): p. 226-35.
6. Pross, H.F. and M. Jondal, *Letter: Spontaneous cytotoxic activity as a test of human lymphocyte function.* Lancet, 1975. **1**(7902): p. 335-6.
7. Caligiuri, M.A., *Human natural killer cells.* Blood, 2008. **112**(3): p. 461-9.
8. Vivier, E., et al., *Functions of natural killer cells.* Nat Immunol, 2008. **9**(5): p. 503-10.
9. Clark, R. and G.M. Griffiths, *Lytic granules, secretory lysosomes and disease.* Curr Opin Immunol, 2003. **15**(5): p. 516-21.
10. Thiery, J., et al., *Perforin pores in the endosomal membrane trigger the release of endocytosed granzyme B into the cytosol of target cells.* Nat Immunol, 2011. **12**(8): p. 770-7.
11. Cooper, M.A., et al., *Human natural killer cells: a unique innate immunoregulatory role for the CD56(bright) subset.* Blood, 2001. **97**(10): p. 3146-51.
12. De Maria, A., et al., *Revisiting human natural killer cell subset function revealed cytolytic CD56(dim)CD16+ NK cells as rapid producers of abundant IFN-gamma on activation.* Proc Natl Acad Sci U S A, 2011. **108**(2): p. 728-32.
13. Moffett, A. and F. Colucci, *Uterine NK cells: active regulators at the maternal-fetal interface.* J Clin Invest, 2014. **124**(5): p. 1872-9.

14. Parham, P., *MHC class I molecules and KIRs in human history, health and survival.* Nat Rev Immunol, 2005. **5**(3): p. 201-14.
15. Braud, V.M., et al., *HLA-E binds to natural killer cell receptors CD94/NKG2A, B and C.* Nature, 1998. **391**(6669): p. 795-9.
16. Guethlein, L.A., et al., *Co-evolution of MHC class I and variable NK cell receptors in placental mammals.* Immunol Rev, 2015. **267**(1): p. 259-82.
17. Alter, G., et al., *HIV-1 adaptation to NK-cell-mediated immune pressure.* Nature, 2011. **476**(7358): p. 96-100.
18. Khakoo, S.I., et al., *HLA and NK cell inhibitory receptor genes in resolving hepatitis C virus infection.* Science, 2004. **305**(5685): p. 872-4.
19. Wauquier, N., et al., *Association of KIR2DS1 and KIR2DS3 with fatal outcome in Ebola virus infection.* Immunogenetics, 2010. **62**(11-12): p. 767-71.
20. Luszczek, W., et al., *Gene for the activating natural killer cell receptor, KIR2DS1, is associated with susceptibility to psoriasis vulgaris.* Hum Immunol, 2004. **65**(7): p. 758-66.
21. Suzuki, Y., et al., *Genetic polymorphisms of killer cell immunoglobulin-like receptors are associated with susceptibility to psoriasis vulgaris.* J Invest Dermatol, 2004. **122**(5): p. 1133-6.
22. van der Slik, A.R., et al., *KIR in type 1 diabetes: disparate distribution of activating and inhibitory natural killer cell receptors in patients versus HLA-matched control subjects.* Diabetes, 2003. **52**(10): p. 2639-42.
23. Hiby, S.E., et al., *Combinations of maternal KIR and fetal HLA-C genes influence the risk of preeclampsia and reproductive success.* J Exp Med, 2004. **200**(8): p. 957-65.
24. Nakimuli, A., et al., *A KIR B centromeric region present in Africans but not Europeans protects pregnant women from pre-eclampsia.* Proc Natl Acad Sci U S A, 2015. **112**(3): p. 845-50.
25. Cooley, S., et al., *Donor killer cell Ig-like receptor B haplotypes, recipient HLA-C1, and HLA-C mismatch enhance the clinical benefit of unrelated transplantation for acute myelogenous leukemia.* J Immunol, 2014. **192**(10): p. 4592-600.
26. Cooley, S., et al., *Donor selection for natural killer cell receptor genes leads to superior survival after unrelated transplantation for acute myelogenous leukemia.* Blood, 2010. **116**(14): p. 2411-9.

27. Karre, K., et al., *Selective rejection of H-2-deficient lymphoma variants suggests alternative immune defence strategy.* Nature, 1986. **319**(6055): p. 675-8.
28. Anfossi, N., et al., *Human NK cell education by inhibitory receptors for MHC class I.* Immunity, 2006. **25**(2): p. 331-42.
29. Kim, S., et al., *HLA alleles determine differences in human natural killer cell responsiveness and potency.* Proc Natl Acad Sci U S A, 2008. **105**(8): p. 3053-8.
30. Yu, J., et al., *Hierarchy of the human natural killer cell response is determined by class and quantity of inhibitory receptors for self-HLA-B and HLA-C ligands.* J Immunol, 2007. **179**(9): p. 5977-89.
31. Ogasawara, K., et al., *Function of NKG2D in natural killer cell-mediated rejection of mouse bone marrow grafts.* Nat Immunol, 2005. **6**(9): p. 938-45.
32. Oppenheim, D.E., et al., *Sustained localized expression of ligand for the activating NKG2D receptor impairs natural cytotoxicity in vivo and reduces tumor immunosurveillance.* Nat Immunol, 2005. **6**(9): p. 928-37.
33. Sun, J.C. and L.L. Lanier, *Tolerance of NK cells encountering their viral ligand during development.* J Exp Med, 2008. **205**(8): p. 1819-28.
34. Older Aguilar, A.M., et al., *Coevolution of killer cell Ig-like receptors with HLA-C to become the major variable regulators of human NK cells.* J Immunol. **185**(7): p. 4238-51.
35. Robinson, J., et al., *IPD--the Immuno Polymorphism Database.* Nucleic Acids Res, 2013. **41**(Database issue): p. D1234-40.
36. Winter, C.C. and E.O. Long, *A single amino acid in the p58 killer cell inhibitory receptor controls the ability of natural killer cells to discriminate between the two groups of HLA-C allotypes.* J Immunol, 1997. **158**(9): p. 4026-8.
37. Uhrberg, M., P. Parham, and P. Wernet, *Definition of gene content for nine common group B haplotypes of the Caucasoid population: KIR haplotypes contain between seven and eleven KIR genes.* Immunogenetics, 2002. **54**(4): p. 221-9.
38. Stewart, C.A., et al., *Recognition of peptide-MHC class I complexes by activating killer immunoglobulin-like receptors.* Proc Natl Acad Sci U S A, 2005. **102**(37): p. 13224-9.

39. Liu, J., et al., *Activating killer cell immunoglobulin-like receptor 2DS2 binds to HLA-A*11.* Proc Natl Acad Sci U S A, 2014. **111**(7): p. 2662-7.
40. Adams, E.J. and P. Parham, *Species-specific evolution of MHC class I genes in the higher primates.* Immunol Rev, 2001. **183**: p. 41-64.
41. Blokhuis, J.H., et al., *The mosaic of KIR haplotypes in rhesus macaques.* Immunogenetics, 2010. **62**(5): p. 295-306.
42. Kruse, P.H., C. Rosner, and L. Walter, *Characterization of rhesus macaque KIR genotypes and haplotypes.* Immunogenetics, 2010. **62**(5): p. 281-93.
43. LaBonte, M.L., et al., *The KIR and CD94/NKG2 families of molecules in the rhesus monkey.* Immunol Rev, 2001. **183**: p. 25-40.
44. Abi-Rached, L., et al., *Human-specific evolution and adaptation led to major qualitative differences in the variable receptors of human and chimpanzee natural killer cells.* PLoS Genet, 2010. **6**(11): p. e1001192.
45. Guethlein, L.A., et al., *Evolution of killer cell Ig-like receptor (KIR) genes: definition of an orangutan KIR haplotype reveals expansion of lineage III KIR associated with the emergence of MHC-C.* J Immunol, 2007. **179**(1): p. 491-504.
46. Boyington, J.C., et al., *Crystal structure of an NK cell immunoglobulin-like receptor in complex with its class I MHC ligand.* Nature, 2000. **405**(6786): p. 537-43.
47. Fan, Q.R., E.O. Long, and D.C. Wiley, *Crystal structure of the human natural killer cell inhibitory receptor KIR2DL1-HLA-Cw4 complex.* Nat Immunol, 2001. **2**(5): p. 452-60.
48. Trowsdale, J., *Genetic and functional relationships between MHC and NK receptor genes.* Immunity, 2001. **15**(3): p. 363-74.
49. Wilson, M.J., et al., *Plasticity in the organization and sequences of human KIR/ILT gene families.* Proc Natl Acad Sci U S A, 2000. **97**(9): p. 4778-83.
50. Uhrberg, M., et al., *Human diversity in killer cell inhibitory receptor genes.* Immunity, 1997. **7**(6): p. 753-63.
51. Pyo, C.W., et al., *Different patterns of evolution in the centromeric and telomeric regions of group A and B haplotypes of the human killer cell Ig-like receptor locus.* PLoS One, 2010. **5**(12): p. e15115.
52. Bari, R., et al., *Significant functional heterogeneity among KIR2DL1 alleles and a pivotal role of arginine 245.* Blood, 2009. **114**(25): p. 5182-90.

53. Hilton, H.G., et al., *Mutation at positively selected positions in the binding site for HLA-C shows that KIR2DL1 is a more refined but less adaptable NK cell receptor than KIR2DL3.* J Immunol, 2012. **189**(3): p. 1418-30.
54. Hilton, H.G., et al., *Loss and Gain of Natural Killer Cell Receptor Function in an African Hunter-Gatherer Population.* PLoS Genet, 2015. **11**(8): p. e1005439.
55. Hilton, H.G., et al., *Polymorphic HLA-C Receptors Balance the Functional Characteristics of KIR Haplotypes.* J Immunol, 2015. **195**(7): p. 3160-70.
56. Hilton, H.G., et al., *The production of KIR-Fc fusion proteins and their use in a multiplex HLA class I binding assay.* J Immunol Methods, 2015. **425**: p. 79-87.
57. Hilton, H.G. and P. Parham, *Direct binding to antigen-coated beads refines the specificity and cross-reactivity of four monoclonal antibodies that recognize polymorphic epitopes of HLA class I molecules.* Tissue Antigens, 2013. **81**(4): p. 212-20.
58. Goyos, A., et al., *A Distinctive Cytoplasmic Tail Contributes to Low Surface Expression and Intracellular Retention of the Patr-AL MHC Class I Molecule.* J Immunol, 2015. **195**(8): p. 3725-36.
59. Biassoni, R., et al., *Role of amino acid position 70 in the binding affinity of p50.1 and p58.1 receptors for HLA-Cw4 molecules.* Eur J Immunol, 1997. **27**(12): p. 3095-9.
60. Winter, C.C., et al., *Direct binding and functional transfer of NK cell inhibitory receptors reveal novel patterns of HLA-C allotype recognition.* J Immunol, 1998. **161**(2): p. 571-7.
61. Vilches, C. and P. Parham, *KIR: diverse, rapidly evolving receptors of innate and adaptive immunity.* Annu Rev Immunol, 2002. **20**: p. 217-51.
62. Moesta, A.K., et al., *Humans differ from other hominids in lacking an activating NK cell receptor that recognizes the C1 epitope of MHC class I.* J Immunol, 2010. **185**(7): p. 4233-7.
63. Moesta, A.K., et al., *Chimpanzees use more varied receptors and ligands than humans for inhibitory killer cell Ig-like receptor recognition of the MHC-C1 and MHC-C2 epitopes.* J Immunol, 2009. **182**(6): p. 3628-37.
64. Graef, T., et al., *KIR2DS4 is a product of gene conversion with KIR3DL2 that introduced specificity for HLA-A*11 while diminishing avidity for HLA-C.* J Exp Med, 2009. **206**(11): p. 2557-72.
65. Dohring, C., et al., *A human killer inhibitory receptor specific for HLA-A1,2.* J Immunol, 1996. **156**(9): p. 3098-101.

66. Pende, D., et al., *The natural killer cell receptor specific for HLA-A allotypes: a novel member of the p58/p70 family of inhibitory receptors that is characterized by three immunoglobulin-like domains and is expressed as a 140-kD disulphide-linked dimer.* J Exp Med, 1996. **184**(2): p. 505-18.
67. Valiante, N.M., et al., *Functionally and structurally distinct NK cell receptor repertoires in the peripheral blood of two human donors.* Immunity, 1997. **7**(6): p. 739-51.
68. Yawata, M., et al., *MHC class I-specific inhibitory receptors and their ligands structure diverse human NK-cell repertoires toward a balance of missing self-response.* Blood, 2008. **112**(6): p. 2369-80.
69. Moesta, A.K., et al., *Synergistic polymorphism at two positions distal to the ligand-binding site makes KIR2DL2 a stronger receptor for HLA-C than KIR2DL3.* J Immunol, 2008. **180**(6): p. 3969-79.
70. Frazier, W.R., et al., *Allelic Variation in KIR2DL3 Generates a KIR2DL2-like Receptor with Increased Binding to its HLA-C Ligand.* J Immunol, 2013.
71. Sambrook, J.G., et al., *Single haplotype analysis demonstrates rapid evolution of the killer immunoglobulin-like receptor (KIR) loci in primates.* Genome Res, 2005. **15**(1): p. 25-35.
72. Henn, B.M., et al., *Hunter-gatherer genomic diversity suggests a southern African origin for modern humans.* Proc Natl Acad Sci U S A, 2011. **108**(13): p. 5154-62.
73. Tishkoff, S.A., et al., *The genetic structure and history of Africans and African Americans.* Science, 2009. **324**(5930): p. 1035-44.
74. Nakimuli, A., et al., *Pregnancy, parturition and preeclampsia in women of African ancestry.* Am J Obstet Gynecol, 2014. **210**(6): p. 510-520 e1.
75. Norman, P.J., et al., *Co-evolution of human leukocyte antigen (HLA) class I ligands with killer-cell immunoglobulin-like receptors (KIR) in a genetically diverse population of sub-Saharan Africans.* PLoS Genet, 2013. **9**(10): p. e1003938.
76. Lachance, J., et al., *Evolutionary history and adaptation from high-coverage whole-genome sequences of diverse African hunter-gatherers.* Cell, 2012. **150**(3): p. 457-69.
77. Schuster, S.C., et al., *Complete Khoisan and Bantu genomes from southern Africa.* Nature, 2010. **463**(7283): p. 943-7.

78. Burshtyn, D.N., et al., *Recruitment of tyrosine phosphatase HCP by the killer cell inhibitor receptor.* Immunity, 1996. **4**(1): p. 77-85.
79. Pando, M.J., et al., *The protein made from a common allele of KIR3DL1 (3DL1*004) is poorly expressed at cell surfaces due to substitution at positions 86 in Ig domain 0 and 182 in Ig domain 1.* J Immunol, 2003. **171**(12): p. 6640-9.
80. Thomas, R., et al., *Novel KIR3DL1 alleles and their expression levels on NK cells: convergent evolution of KIR3DL1 phenotype variation?* J Immunol, 2008. **180**(10): p. 6743-50.
81. VandenBussche, C.J., et al., *A single polymorphism disrupts the killer Ig-like receptor 2DL2/2DL3 D1 domain.* J Immunol, 2006. **177**(8): p. 5347-57.
82. VandenBussche, C.J., et al., *Dramatically reduced surface expression of NK cell receptor KIR2DS3 is attributed to multiple residues throughout the molecule.* Genes Immun, 2009. **10**(2): p. 162-73.
83. Apps, R., et al., *Influence of HLA-C expression level on HIV control.* Science. **340**(6128): p. 87-91.
84. Shilling, H.G., et al., *Evidence for recombination as a mechanism for KIR diversification.* Immunogenetics, 1998. **48**(6): p. 413-6.
85. Saitou, N. and M. Nei, *The neighbor-joining method: a new method for reconstructing phylogenetic trees.* Mol Biol Evol, 1987. **4**(4): p. 406-25.
86. Tamura, K., et al., *MEGA6: Molecular Evolutionary Genetics Analysis version 6.0.* Mol Biol Evol, 2013. **30**(12): p. 2725-9.
87. Gendzekhadze, K., et al., *Co-evolution of KIR2DL3 with HLA-C in a human population retaining minimal essential diversity of KIR and HLA class I ligands.* Proc Natl Acad Sci U S A, 2009. **106**(44): p. 18692-7.
88. Hou, L., et al., *African Americans exhibit a predominant allele in the midst of extensive KIR2DL1 allelic diversity.* Tissue Antigens, 2010. **76**(1): p. 31-4.
89. Hou, L.H., et al., *KIR2DL1 allelic diversity: four new alleles characterized in a bone marrow transplant population and three families.* Tissue Antigens, 2007. **69**(3): p. 250-4.
90. Middleton, D., et al., *Killer immunoglobulin receptor gene and allele frequencies in Caucasoid, Oriental and Black populations from different continents.* Tissue Antigens, 2008. **71**(2): p. 105-13.
91. Vierra-Green, C., et al., *Allele-level haplotype frequencies and pairwise linkage disequilibrium for 14 KIR loci in 506*

European-American individuals. PLoS One, 2012. **7**(11): p. e47491.
92. Norman, P.J., et al., *Meiotic recombination generates rich diversity in NK cell receptor genes, alleles, and haplotypes.* Genome Res, 2009. **19**(5): p. 757-69.
93. Winter, C.C. and E.O. Long, *Binding of soluble KIR-Fc fusion proteins to HLA class I.* Methods Mol Biol, 2000. **121**: p. 239-50.
94. Hitchman, R.B., R.D. Possee, and L.A. King, *Baculovirus expression systems for recombinant protein production in insect cells.* Recent Pat Biotechnol, 2009. **3**(1): p. 46-54.
95. Victor, M.E., et al., *Insect cells are superior to Escherichia coli in producing malaria proteins inducing IgG targeting PfEMP1 on infected erythrocytes.* Malar J, 2010. **9**: p. 325.
96. Kost, T.A. and J.P. Condreay, *Recombinant baculoviruses as expression vectors for insect and mammalian cells.* Curr Opin Biotechnol, 1999. **10**(5): p. 428-33.
97. Pei, R., et al., *Simultaneous HLA Class I and Class II antibodies screening with flow cytometry.* Hum Immunol, 1998. **59**(5): p. 313-22.
98. Blissard, G.W. and G.F. Rohrmann, *Location, sequence, transcriptional mapping, and temporal expression of the gp64 envelope glycoprotein gene of the Orgyia pseudotsugata multicapsid nuclear polyhedrosis virus.* Virology, 1989. **170**(2): p. 537-55.
99. Goodridge, J.P., et al., *HLA-F and MHC class I open conformers are ligands for NK cell Ig-like receptors.* J Immunol, 2013. **191**(7): p. 3553-62.
100. Goodridge, J.P., et al., *HLA-F and MHC-I open conformers cooperate in a MHC-I antigen cross-presentation pathway.* J Immunol, 2013. **191**(4): p. 1567-77.
101. Saunders, P.M., et al., *The interaction of KIR3DL1*001 with HLA class I molecules is dependent upon molecular microarchitecture within the Bw4 epitope.* J Immunol, 2015. **194**(2): p. 781-9.
102. Boudreau, J.E., J.B. Le Luduec, and K.C. Hsu, *Development of a novel multiplex PCR assay to detect functional subtypes of KIR3DL1 alleles.* PLoS One, 2014. **9**(6): p. e99543.
103. Brodsky, F.M., et al., *Monoclonal antibodies for analysis of the HLA system.* Immunol Rev, 1979. **47**: p. 3-61.
104. Parham, P. and W.F. Bodmer, *Monoclonal antibody to a human histocompatibility alloantigen, HLA-A2.* Nature, 1978. **276**(5686): p. 397-9.

105. Parham, P. and F.M. Brodsky, *Partial purification and some properties of BB7.2. A cytotoxic monoclonal antibody with specificity for HLA-A2 and a variant of HLA-A28.* Hum Immunol, 1981. **3**(4): p. 277-99.
106. Holmes, N. and P. Parham, *Exon shuffling in vivo can generate novel HLA class I molecules.* EMBO J, 1985. **4**(11): p. 2849-54.
107. Parham, P., et al., *Further studies on the epitopes of HLA-B7 defined by murine monoclonal antibodies.* Hum Immunol, 1986. **15**(1): p. 44-67.
108. Cao, K., et al., *Analysis of the frequencies of HLA-A, B, and C alleles and haplotypes in the five major ethnic groups of the United States reveals high levels of diversity in these loci and contrasting distribution patterns in these populations.* Hum Immunol, 2001. **62**(9): p. 1009-30.
109. McMichael, A.J., et al., *A monoclonal antibody that recognizes an antigenic determinant shared by HLA A2 and B17.* Hum Immunol, 1980. **1**(2): p. 121-9.
110. Ways, J.P. and P. Parham, *The binding of monoclonal antibodies to cell-surface molecules. A quantitative analysis with immunoglobulin G against two alloantigenic determinants of the human transplantation antigen HLA-A2.* Biochem J, 1983. **216**(2): p. 423-32.
111. Shimizu, Y., et al., *Transfer of cloned human class I major histocompatibility complex genes into HLA mutant human lymphoblastoid cells.* Mol Cell Biol, 1986. **6**(4): p. 1074-87.
112. Santos-Aguado, J., et al., *Molecular characterization of serologic recognition sites in the human HLA-A2 molecule.* J Immunol, 1988. **141**(8): p. 2811-8.
113. Svejgaard, A. and F. Kissmeyer-Nielsen, *Complement-fixing platelet iso-antibodies. V. HL-A typing.* Vox Sang, 1970. **18**(1): p. 12-20.
114. Mizuno, S., et al., *A new murine lymphocytotoxic monoclonal antibody recognizing HLA-A2, -A28 and -A9.* Tissue Antigens, 1996. **48**(3): p. 224-7.
115. Hogan, K.T. and S.L. Brown, *Localization and characterization of serologic epitopes on HLA-A2.* Hum Immunol, 1992. **33**(3): p. 185-92.
116. Salter, R.D., et al., *In vitro mutagenesis at a single residue introduces B and T cell epitopes into a class I HLA molecule.* J Exp Med, 1987. **166**(1): p. 283-8.
117. Taketani, S., et al., *Structural analysis of HLA-A2 antigen from immunoselected mutant 8.6.1: further definition of an*

HLA-A2-specific serological determinant. J Immunol, 1983. **131**(6): p. 2935-8.
118. Ellexson, M.E., et al., *Nucleotide sequence analysis of HLA-B*1523 and B*8101. Dominant alpha-helical motifs produce complex serologic recognition patterns for the HLA-B"DT" and HLA-B"NM5" antigens.* Hum Immunol, 1995. **44**(2): p. 103-10.
119. Vilches, C., et al., *Molecular characterization of the new alleles HLA-B*8101 and B*4407.* Tissue Antigens, 1996. **47**(2): p. 139-42.
120. Domenech, N., J. Santos-Aguado, and J.A. Lopez de Castro, *Antigenicity of HLA-A2 and HLA-B7. Loss and gain of serologic determinants induced by site-specific mutagenesis at residues 62 to 80.* Hum Immunol, 1991. **30**(2): p. 140-6.
121. McCutcheon, J.A. and C.T. Lutz, *Mutagenesis around residue 176 on HLA-B*0702 characterizes multiple distinct epitopes for anti-HLA antibodies.* Hum Immunol, 1992. **35**(2): p. 125-31.
122. Parham, P., *Antigenic determinants of the HLA-B7 molecule; Bw6- and B7-specific determinants are spatially separate.* Immunogenetics, 1983. **18**(1): p. 1-16.
123. Toubert, A., et al., *Epitope mapping of HLA-B27 and HLA-B7 antigens by using intradomain recombinants.* J Immunol, 1988. **141**(7): p. 2503-9.
124. Wan, A.M., et al., *The primary structure of HLA-A32 suggests a region involved in formation of the Bw4/Bw6 epitopes.* J Immunol, 1986. **137**(11): p. 3671-4.
125. Zemmour, J. and P. Parham, *Distinctive polymorphism at the HLA-C locus: implications for the expression of HLA-C.* J Exp Med, 1992. **176**(4): p. 937-50.
126. Sibilio, L., et al., *A single bottleneck in HLA-C assembly.* J Biol Chem, 2008. **283**(3): p. 1267-74.
127. Sibilio, L., et al., *Impaired assembly results in the accumulation of multiple HLA-C heavy chain folding intermediates.* J Immunol, 2005. **175**(10): p. 6651-8.
128. Gleimer, M. and P. Parham, *Stress management: MHC class I and class I-like molecules as reporters of cellular stress.* Immunity, 2003. **19**(4): p. 469-77.
129. Adams, E.J., S. Cooper, and P. Parham, *A novel, nonclassical MHC class I molecule specific to the common chimpanzee.* J Immunol, 2001. **167**(7): p. 3858-69.

Mutation at Positively Selected Positions in the Binding Site for HLA-C Shows That KIR2DL1 Is a More Refined but Less Adaptable NK Cell Receptor Than KIR2DL3

Hugo G. Hilton,*,†,1 Luca Vago,*,†,‡,1 Anastazia M. Older Aguilar,*,† Achim K. Moesta,*,† Thorsten Graef,*,† Laurent Abi-Rached,*,† Paul J. Norman,*,† Lisbeth A. Guethlein,*,† Katharina Fleischhauer,§ and Peter Parham*,†

Through recognition of HLA class I, killer cell Ig-like receptors (KIR) modulate NK cell functions in human immunity and reproduction. Although a minority of HLA-A and -B allotypes are KIR ligands, HLA-C allotypes dominate this regulation, because they all carry either the C1 epitope recognized by KIR2DL2/3 or the C2 epitope recognized by KIR2DL1. The C1 epitope and C1-specific KIR evolved first, followed several million years later by the C2 epitope and C2-specific KIR. Strong, varying selection pressure on NK cell functions drove the diversification and divergence of hominid KIR, with six positions in the HLA class I binding site of KIR being targets for positive diversifying selection. Introducing each naturally occurring residue at these positions into KIR2DL1 and KIR2DL3 produced 38 point mutants that were tested for binding to 95 HLA- A, -B, and -C allotypes. Modulating specificity for HLA-C is position 44, whereas positions 71 and 131 control cross-reactivity with HLA-A*11:02. Dominating avidity modulation is position 70, with lesser contributions from positions 68 and 182. KIR2DL3 has lower avidity and broader specificity than KIR2DL1. Mutation could increase the avidity and change the specificity of KIR2DL3, whereas KIR2DL1 specificity was resistant to mutation, and its avidity could only be lowered. The contrasting inflexibility of KIR2DL1 and adaptability of KIR2DL3 fit with C2-specific KIR having evolved from C1-specific KIR, and not vice versa. Substitutions restricted to activating KIR all reduced the avidity of KIR2DL1 and KIR2DL3, further evidence that activating KIR function often becomes subject to selective attenuation. ***The Journal of Immunology*****, 2012, 189: 1418–1430.**

Major histocompatibility complex class I molecules function as ligands for a variety of activating and inhibitory receptors expressed by NK cells and CD8 T cells (1–4). In the human MHC, the HLA complex, six genes encode MHC class I molecules: HLA-A, -B, -C, -E, -F, and -G; all, with the exception of HLA-F, are known to interact with NK cell receptors. Of these, HLA-E is the oldest and most conserved; it binds a restricted set of peptides that is largely derived from the leader sequences of other HLA class I molecules and is the ligand for conserved CD94:NKG2 lectin-like receptors (5, 6).

In contrast, HLA-A, -B, -C, and -G bind diverse peptides and furnish ligands for diverse and polymorphic killer cell Ig-like receptors (KIR). This family of variable NK cell receptors is of very recent origin, being restricted to the simian primates: monkeys, apes, and humans (7, 8). HLA-G, the ligand for KIR2DL4, is expressed only by extravillous trophoblast (EVT) and is implicated in the interactions between EVT and uterine NK cells, which are critical for placentation and successful reproduction (9–11). HLA-A, -B, and -C are highly polymorphic and function as ligands for both KIR and the αβ TCR of CD8 T cells. Of these three, HLA-C is the most recently evolved and the only one for which all of the variant forms (allotypes) are ligands for KIR (12–14). Dimorphism at position 80 in HLA-C defines two epitopes, C1 (asparagine 80) and C2 (lysine 80), which are ligands for different forms of KIR (15). In contrast, only approximately one third of the HLA-A and HLA-B allotypes has the capacity to interact with KIR (8). Such comparisons indicate that HLA-C, which arose from an HLA-B–like ancestor (16), diverged under selection to become a specialized and dominant source of ligands for KIR. That HLA-C but not HLA-A or -B is expressed by EVT, and uterine NK cells selectively express KIR that recognize HLA-C, further argues that selection pressure from reproduction contributed to the evolution of HLA-C (17, 18).

The C2 epitope, carried by the subset of HLA-C allotypes having lysine 80, is recognized by the inhibitory receptor KIR2DL1 and the activating receptor KIR2DS1. The signaling domains of these two receptors are divergent, but their Ig-like domains, which form the ligand binding site, have high sequence similarity. The C1 epitope, carried by the subset of HLA-C allotypes having asparagine 80, and two unusual HLA-B allotypes (HLA-B*46:01 and HLA-B*73:01) are recognized by the inhibitory receptor KIR2DL2/3 (19–21). Corresponding to the dimorphism at position 80 in HLA-C is a dimorphism at position 44 in the D1 domain of the KIR that determines the receptors' specificities. Thus, C2-

*Department of Structural Biology, Stanford University School of Medicine, Stanford, CA 94305; †Department of Microbiology and Immunology, Stanford University School of Medicine, Stanford, CA 94305; ‡Hematology and Bone Marrow Transplantation Unit, San Raffaele Scientific Institute, 20132 Milan, Italy; and §Unit of Molecular and Functional Immunogenetics, San Raffaele Scientific Institute, 20132 Milan, Italy

[1]H.G.H. and L.V. contributed equally to this work.

Received for publication February 9, 2011. Accepted for publication May 24, 2012.

This work was supported by National Institutes of Health Grant AI22039 (to P.P.) and Telethon Foundation Grant GGP08201 (to K.F.). H.G.H. was also supported by the March of Dimes Prematurity Center at Stanford University School of Medicine, Clinical and Translational Science Awards Grant UL1 RR025744, and a Stanford University School of Medicine Dean's Fellowship.

Address correspondence and reprint requests to Prof. Peter Parham, Department of Structural Biology, Stanford University, Fairchild D-157, 299 Campus Drive West, Stanford, CA 94305. E-mail address: peropa@stanford.edu

Abbreviations used in this article: EVT, extravillous trophoblast; KIR, killer cell Ig-like receptor; siRNA, small interfering RNA; wt, wild-type.

specific KIR2DL1 and KIR2DS1 have methionine 44, whereas C1-specific KIR2DL2/3 has lysine 44. That mutation at this position was demonstrated to be sufficient to swap the receptors' specificities led to position 44 being described as the specificity-determining residue (22, 23). Functional studies and clinical correlations point to the C1 and C2 epitopes of HLA-C being the dominant ligands for KIR (24–26). And because C1 and C2 are alternatives, all human individuals have at least one of these epitopes and some have both of them; this is not the case for the A*03/11 epitope of HLA-A recognized by KIR3DL2 (27, 28) or the Bw4 epitope of HLA-A and -B recognized by KIR3DL1 (29, 30). The KIR that recognize epitopes of HLA-A and -B form a phylogenetic lineage (lineage II KIR) that is distinguished from the lineage III KIR to which the HLA-C receptors belong (31).

Comparison of primate species shows how KIR coevolve with their cognate MHC class I ligands. Old World monkeys have *MHC class I* genes resembling *HLA-A* and *-B* but no equivalent to *HLA-C*. Correspondingly, in these species there are multiple lineage II *KIR* genes but only one lineage III *KIR* (32–37). An equivalent to *HLA-C* is present only in the hominids (great apes and humans) and exists in a more primitive state in the orangutan *MHC* where the gene is not fixed, as it is in human and chimpanzee *MHCs*, and all of the allotypic variants carry the C1 epitope (12, 13). Nonetheless, there are multiple lineage III *KIR* in the orangutan but only one lineage II *KIR*, indicating the functional impact of the emergence of MHC-C and its cognate lineage III KIR.

By the time of the last common ancestor of humans and chimpanzees, the C2 epitope and its interaction with lineage III KIR had evolved from the C1 epitope and its cognate receptors. The chimpanzee maintains a diverse array of nine lineage III KIR that recognize the C1 and C2 epitopes with good avidity, which includes both inhibitory and activating KIR (7). In contrast, of the seven human lineage III KIR, only four bind to HLA-C, and the other three have no demonstrable binding to any HLA class I allotype (38, 39). These comparisons show how the selection pressures acting upon the interactions of lineage III KIR with human HLA-C, and its *MHC-C* counterparts in other species, have been remarkably variable throughout hominid evolution.

To investigate the effects of natural selection on hominid lineage III KIR, we identified sites of positive diversifying selection within the ligand binding site and assessed the functional effects of this variation by mutagenesis directed at these sites in human C2-specific KIR2DL1 and C1-specific KIR2DL2/3. For *KIR2DL1*, the *2DL1*003* allele was chosen as the target for mutagenesis, because it is the most common allele in many human populations. *KIR2DL2/3* has two distinctive allelic lineages: *KIR2DL2* and *KIR2DL3*. We chose *2DL3*001*, the most frequent *KIR2DL3* allele, as the target for mutagenesis because KIR2DL2 is a recombinant form (with greater sequence similarity to KIR2DL3 in the Ig-like domains and to KIR2DL1 in the stem, trans-membrane, and cytoplasmic regions) that, in functional assays, recognizes both C1 and C2, whereas KIR2DL3 appears functionally specific for C1, although it exhibits some cross-reactivity with C2-bearing allotypes in direct-binding assays (21). The disadvantage to choosing KIR2DL3 over KIR2DL2 is the availability of a crystallographic structure only for KIR2DL2 bound to HLA-C (40) but not for KIR2DL3 bound to HLA-C.

Materials and Methods

Cell lines

The human cell line NKL was maintained as described (41). The G4-NKL cell line was derived from NKL by specific small interfering RNA (siRNA) knockdown of LILRB1 expression using the pSIREN-RetroQ vector (Clontech, Mountain View, CA) (42). Transduction of NKL and G4-NKL with wild-type (wt) and mutant KIR was performed as described (13), with minor modifications. The full-length KIR-coding region was cloned into the pIB2 expression vector (kindly provided by Dr. Mark Davis, Stanford University) and transduced into Phi-NX cells (kindly provided by Dr. Garry Nolan, Stanford University) to generate recombinant amphotrophic retrovirus, which was then used to infect NKL cells. After 2 wk of infection, the NKL cells were FACS purified using KIR-specific mAbs. After such selection, >95% of the cells expressed KIR. Transduced cells were periodically checked for surface expression of KIR using specific mAbs.

Transduced NKL cells express GFP driven by an internal ribosome entry site from the same promoter as the *KIR*. This allowed cells transduced with different KIR to be sorted by FACS for equivalent GFP expression. Subsequently, the sorted transductants were analyzed for KIR expression using several KIR-specific mAbs that interact with lineage III KIR (EB-6, CH-L, anti-2DS4, and NKVFS1) (BD Biosciences, San Jose, CA). Among these, the reactivity of NKVFS1, which has a very broad reactivity for lineage III KIR from all hominid species, was particularly constant and allowed us to select cells with similar levels of KIR expression for use in functional assays (13, 21, 38, 39).

The HLA-A, HLA-B, and HLA-C–deficient cell-line 721.221 (subsequently referred to as 221 cells) was transfected with individual HLA class I alleles that had been mutated in the leader peptide so that, on binding to HLA-E, the derived peptides do not permit interaction with CD94:NKG2A (43). Lacking transporter-associated proteins, the T2 human cell line has a reduced amount of HLA-A*02 on the cell surface and no detectable amount of the other endogenous HLA class I allotypes (44). Permanent transduction of T2 with HLA-A*11:02 was achieved using the Amaxa Nucleofector Kit (Lonza, Cologne, Germany), according to the manufacturer's instructions. After transduction and 2 wk of growth in selective medium, T2 HLA-A*11:02 cells were pulsed with the A*11-specific peptide RLRAEAQVK, and cells with high expression of HLA-A*11 were FACS purified using mAb specific for HLA-A*11 (One Lambda, Canoga Park, CA). The new nomenclature for HLA class I is used throughout this article (45).

T2 cell incubation with synthetic peptides

The HLA-A*11–restricted RLRAEAQVK peptide from EBV and the HLA-A*02–restricted NLVPMVATV peptide from CMV were purchased from Synthetic Biomolecules (San Diego, CA). A total of 10^6 T2 cells was incubated overnight in 500 μl serum-free medium with peptide at a final concentration of 100 μM. To assess cell surface expression of HLA-A*11:02 by peptide-pulsed cells, the cells were first incubated with unconjugated monoclonal anti–HLA-A*11 Ab (reconstituted in 100 μl distilled water; 2 μl used per test) (One Lambda), followed by goat anti-mouse FITC-conjugated secondary Ab (10 μg/ml; Southern Biotech, Birmingham, AL), and then analyzed by flow cytometry.

Assay of NK cell cytotoxicity

NKL-mediated cell lysis was assessed in the standard 4-h chromium-release assay, as described (21). Effector cells were incubated with ^{51}Cr-labeled target cells at various E:T ratios. For Ab-inhibition experiments, ^{51}Cr-labeled 221-A*11:02 target cells (10^6) were incubated for 30 min at 37°C in 10 μl undiluted anti–HLA-A*11 mAb (One Lambda) and then washed two times before incubation with effector cells. Following 4 h of incubation at 37°C, cell supernatants were harvested, and [^{51}Cr] content was quantified using a Wallac gamma counter (Turku, Finland). Specific lysis was calculated using the formula (specific release − spontaneous release)/(total release − spontaneous release). Each set of conditions was performed in triplicate; each experiment was independently replicated three or more times.

Generation of KIR-Fc fusion proteins

Wt and mutant KIR-Fc fusion proteins were generated according to published protocols (21, 46). The insect cell lines Sf9 and Hi5 (kindly provided by Dr. K. Chris Garcia, Stanford University) were cultured as described (47). Regions encoding the Ig-like domains and the stem of KIR2DL1*003 and KIR2DL3*001 were fused with the region encoding the Fc portion of the human IgG1 H chain. Site-directed mutagenesis was performed with the QuikChange Kit (Stratagene, La Jolla, CA), according to the manufacturer's instructions. The chimeric constructs were transferred into the pACgp67 vector and cotransfected into Sf9 cells with linearized baculovirus (BD Biosciences), using Cellfectin (Invitrogen, Carlsbad, CA). After two rounds of amplification, high-titer virus was used to infect Hi5 cells for 72 h. Cell supernatant was then collected, filtered, and neutralized with HEPES-buffered saline. After overnight incubation with protein A conjugated to Sepharose beads (Invitrogen), the beads were washed with PBS,

and the KIR-Fc fusion proteins were then eluted from the beads with 0.1 M glycine (pH 2.7) and immediately neutralized using 0.2 M Tris-base (pH 9).

Binding assay of KIR-Fc fusion proteins to beads coated with HLA class I

KIR-Fc fusion proteins were tested for binding to a panel of microbeads, with each bead coated with one of 95 HLA class I allotypes: 29 HLA-A, 50 HLA-B, and 16 HLA-C (LABScreen Single-Antigen Bead Sets; One Lambda). These beads were originally developed for studying the specificity of human alloantibodies (48, 49) and were subsequently adapted by our group for the study of KIR specificity (21). The HLA class I proteins that coat the beads are purified from EBV-transformed B cell lines and, therefore, are highly heterogeneous with regard to bound peptide.

KIR-Fc fusion proteins, at a concentration of 100 μg/ml, were incubated with LABScreen microbeads for 60 min at 4˚C on a shaker. After three washes, secondary staining with anti-human Fc-PE (One Lambda) was performed for 60 min. Samples were then analyzed on a Luminex 100 reader (Luminex, Austin, TX). Independently, the beads were incubated with W6/32 (50 μg/ml) an anti-HLA class I Ab that recognizes an epitope shared by HLA-A, -B, and -C variants (50), which showed strong binding to all 95 microbeads, and with limited variability (<20%) in the amount bound. To take into account differences in the amount of HLA class I protein coating each bead, the binding obtained with KIR was normalized to the binding obtained with W6/32. Thus, the binding avidities for KIR-Fc were expressed as relative fluorescence ratios and calculated using the formula (specific binding − bead background fluorescence)/(W6/32 binding − bead background fluorescence) to normalize KIR-Fc binding to the amount of HLA class I on each bead type. Comparison of the specificity and avidity of W6/32 for HLA class I with other monoclonal anti-HLA class I Ab, particularly the anti–β_2-microglobulin Ab BBM1 (51) that recognizes an epitope away from the polymorphic HLA class I H chain and involving arginine 45 of β_2-microglobulin (52), is consistent with W6/32 recognizing an epitope shared by all HLA-A, -B, and -C allotypes (53, 54).

Results

Six positively selected residues in the HLA binding site of lineage III KIR

KIR of phylogenetic lineage III, which includes all of the KIR that recognize HLA-C, comprises three inhibitory receptors (KIR2DL1, 2, and 3) and five activating receptors (KIR2DS1, 2, 3, 4, and 5). In addition to sequence variation among the different receptors, all of them exhibit allelic polymorphism, but to a varying degree (http://www.ebi.ac.uk/ipd/kir/). To identify sites of sequence variation that have been subject to natural selection, we previously performed maximum-likelihood analysis on the aligned sequences of 110 lineage III KIR from humans and apes (7). Positive diversifying selection was evident at 16 sites in the extracellular, ligand-binding domains of the KIR molecule: positions 6, 13, 16, 44, 50, 68, 70, 71, 84, and 90 in the D1 domain and positions 119, 123, 131, 148, 182, and 190 in the D2 domain. Examination of the crystallographic structures of HLA-C bound to KIR2DL (40, 55) showed that six of the positively selected residues lay within regions that directly contact HLA class I (Fig. 1A, 1B): positions 44, 68, 70, and 71 in the D1 domain (Fig. 1C) and positions 131 and 182 in the D2 domain. Therefore, these positions were chosen for further study.

For these six positions, sequence variability is notably higher in the D1 domain than in the D2 domain, both in the number of positively selected positions and the number of alternative residues at each position (Fig. 2). Nonetheless, there is a variety of residues with distinctive chemistry and functional potential at all six positions. Lysine 44, proline 68, arginine 131, and arginine 182 are the only residues present in all five hominoid species examined, consistent with them having been present in the common hominoid ancestor. Greater variability and species specificity are observed for positions 70 and 71. Position 70 stands out for its diversification in humans but relative conservation in other species, whereas position 71 is more variable in chimpanzees and gorillas than in humans, particularly for the inhibitory KIR (Fig. 2). Given these properties, we hypothesized that variation at these six positions had been selected for its direct effect on the functional interactions of hominoid lineage III KIR with MHC class I. To test this hypothesis, we introduced all naturally occurring variations at the six positions (Fig. 2) into human C2-specific KIR2DL1 and C1-specific KIR2DL3 and then determined the effects of these mutations on KIR specificity and avidity for HLA class I.

Fc fusion proteins were made from the mutant and wt KIR and tested for binding to 95 HLA class I allotypes using a robust, sensitive assay in which the targets are microbeads, each coated with a single HLA class I allotype (13, 21, 39, 42, 56). Being purified from EBV-transformed B cell lines, each single HLA class I allotype is highly diverse with regard to the sequence of the bound peptide (48).

Variation at position 44 modulates specificity and strength of KIR recognition of MHC-C

Consistent with previous studies (22, 23), we find that swapping the position 44 residues of KIR2DL1 and KIR2DL3 is sufficient to swap their HLA class I specificities. Thus, the 2DL3-44M mutant has C2 specificity like KIR2DL1 (Fig. 3A), and the 2DL1-44K mutant has C1 specificity like KIR2DL3 (Fig. 3B). Two exceptional HLA-B allotypes, B*46:01 and HLA-B*73:01, also carry the C1 epitope (21, 57) and bind well to both KIR2DL3 and mutant 2DL1-44K (Fig. 3C). It is on the basis of data such as these that position 44 has been described as the specificity-determining position of the lineage III KIR (22, 23).

On average, the binding of KIR2DL1 to C2 (Fig. 3A) was approximately twice that of KIR2DL3 to C1 (Fig. 3B), indicating that KIR2DL1 is a stronger receptor than KIR2DL3. That mutant 2DL1-44K bound C1 at a much higher level (180%) than KIR2DL3 (Fig. 3B) confirms that 2DL1 is an inherently stronger receptor, as well as demonstrating that substitutions other than the lysine–methionine dimorphism at position 44 contribute to the avidity difference. However, the observation that mutant 2DL3-44M binds C2 almost as well (85%) as KIR2DL1 shows clearly that methionine 44 must also contribute to KIR2DL1 having higher avidity than KIR2DL3 (Fig. 3A). Consistent with this proposition, the mean binding of mutant 2DL1-K44 to C1 is 83% of that achieved by 2DL1 to C2, a comparison in which the only difference between the two KIR-Fc is at position 44 (Fig. 3). Likewise, the mean binding of 2DL3 to C1 (not including the poorly reactive HLA-C*12:03 and HLA-C*14:02) is 69% of that achieved by 2DL3-M44 binding to C2 (Fig. 3). These comparisons show that methionine 44 produces a stronger avidity than does lysine 44, consistent with the qualitatively different bonding patterns observed between KIR residue 44 and HLA-C residue 80 in the crystallographic structures of complexes of KIR2D and HLA-C (40, 55, 58).

Threonine 44 is naturally present in KIR2DS3 and KIR2DS5 (Fig. 1A), activating receptors exhibiting no detectable avidity for any HLA class I allotype when tested in the same binding assay as that used in this study (39). In contrast, KIR2DL1 and KIR2DL3 mutants with threonine 44 recognize some HLA-C allotypes. Replacement of lysine 44 by threonine in KIR2DL3 (mutant 2DL3-44T) abrogated binding to C1, with the exception of C*16:01, which retained ~50% of binding (Fig. 3B). Accompanying the loss of C1 reactivity was acquisition of C2 specificity by 2DL3-44T, but with much lower avidity than KIR2DL1 or 2DL3-44M (Fig. 3A). The 2DL1-44T mutant retained the C2 specificity of KIR2DL1 but with avidity reduced by ~50%. The avidity of

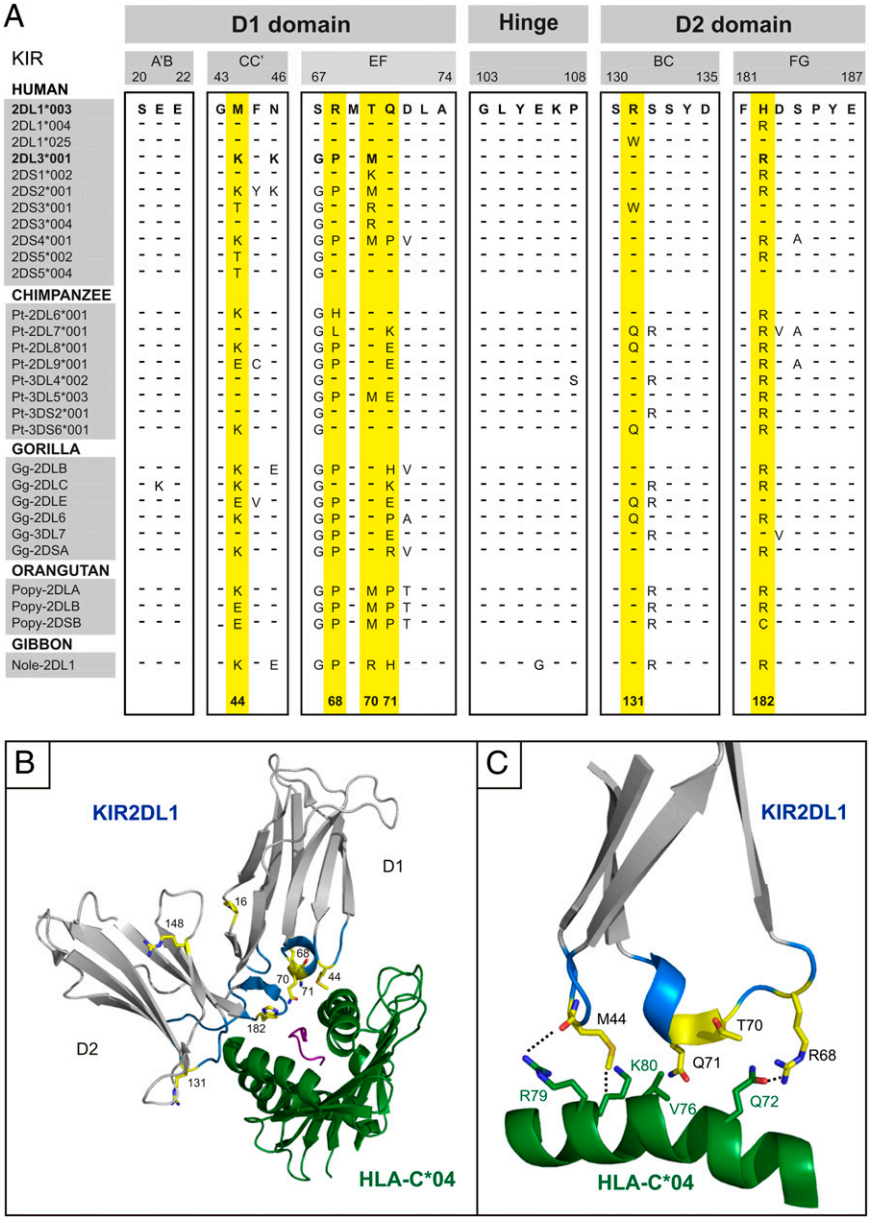

FIGURE 1. Six positively-selected residues in the binding site of hominoid lineage III KIR. (**A**) Alignment of partial amino acid sequences of hominoid lineage III KIR showing the loops of the D1 and D2 domains that contact HLA-C. Sequences were aligned to 2DL1*003, with identities indicated by dashes (-). The six positively selected residues in the binding site for HLA class I are highlighted in yellow. (**B**) Ribbon diagram of KIR2DL1 (gray) bound to HLA-C*04:01 (green) (PDB1IM9) (55). The loops of the KIR molecule that contact HLA ligands are blue, and positively selected residues are yellow, as in (A). (**C**) Details of the binding between the D1 domain contact loop of KIR2DL1*003 (in blue with positively selected residues in yellow) and the α_1 domain helix of HLA-C*04:01 (green).

2DL1-44T for C2 was greater than that of 2DL3-44T, the same hierarchy as observed for the 2DL1 and 2DL3 mutants with methionine and lysine at position 44. Moreover, the avidity of 2DL1-44T for C2 (Fig. 3A) is comparable to that of 2DL3 for C1 (Fig. 3B), well within the functional range of inhibitory NK cell receptors. Thus, human lineage III KIR with threonine 44 have the potential to be C2-specific receptors, suggesting that KIR2DS3 and KIR2DS5, for which ligands remain unknown (39, 59, 60),

	D1																D2					
	44				68				70				71							131			182		
SPECIES	E	M	K	T	H	L	R	P	K	M	R	T	E	H	K	P	Q	R	Q	R	W	C	H	R
Human		–	–				–	–		–	–	–				–			–	–			–	–
		+	+	+			+	+	+	+		+				+	+			+	+		+	+
Chimpanzee	–	–	–		–	–	–	–		–		–	–		–	–	–		–	–				–
		+	+				+					+					+		+	+				+
Gorilla	–	–	–				–	–				–	–	–	–	–			–	–			–	–
			+					+				+						+		+				+
Orangutan	–		–					–		–						–				–				–
	+		+					+		+						+				+		+		
Gibbon			–					–			–			–						–				–

FIGURE 2. Sequence variation in human and ape lineage III KIR at each of the six positively selected positions located within the binding site for MHC-C. For each of the six positions (44, 68, 70, 71, 131, and 182), the variety of residues is shown. For each species, the presence of a given residue in their KIR is indicated by a gray-shaded box; a box with a dash (–) denotes its presence in inhibitory KIR, and a box with a plus sign (+) denotes its presence in activating KIR.

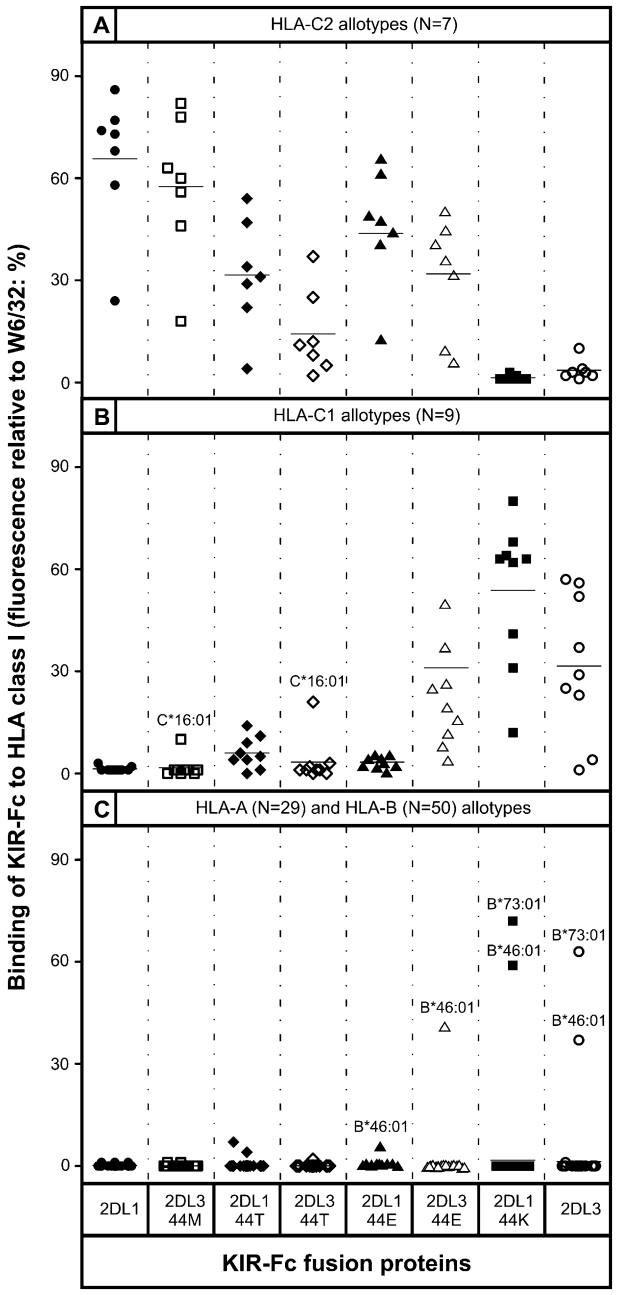

FIGURE 3. The residue at position 44 determines the HLA-C specificity of lineage III KIR. Shown are the results of assays to measure the binding of wt and mutant KIR2DL1-Fc and KIR2DL3-Fc fusion proteins to beads coated with a representative range of HLA-A, -B, and -C allotypes. Mutations were restricted to position 44 where KIR2DL1 has methionine and KIR2DL3 has lysine. Fusion proteins tested were 2DL1 (●), 2DL3-44M (□), 2DL1-44T (♦), 2DL3-44T (◇), 2DL1-44E (▲), 2DL3-44E (△), 2DL1-44K (■), and 2DL3-WT (○). Shown are representative results from 7 C2-bearing HLA-C allotypes (**A**), 9 C1-bearing HLA-C allotypes (**B**), and 29 HLA-A and 50 HLA-B allotypes (**C**). The mean value for each allotype group is denoted by a horizontal line. Allotypes showing unusual patterns of binding are indicated by their official names (45).

evolved from activating C2 receptors that lost the capacity to bind HLA class I through selected substitutions at positions other than 44. That threonine 44 is present only in human lineage III KIR suggests that these receptors both arose and became attenuated during the course of human evolution.

Although orangutan, gorilla, and chimpanzee have KIR with glutamate 44, such KIR were lost during human evolution (Fig. 2). Mutant 2DL1-44E retained the C2 specificity of KIR2DL1 but with 36% loss of avidity (Fig. 3A), properties similar to those of chimpanzee KIR2DL9 that has glutamate 44 (38). In contrast, mutant 2DL3-44E acquired reactivity with C2, while retaining 87% of the avidity for C1. Consequently, 2DL3-44E binds with comparable avidity to C1 and C2, thus having pan specificity for HLA-C (Fig. 3A, 3B). This C1+C2 specificity of 2DL3-44E is very similar to that of Popy-2DLB and Popy-2DSB, paired inhibitory and activating orangutan KIR that have glutamate 44 (13). The only difference between 2DL3-44E and the orangutan KIR is in the recognition of the two C1-bearing HLA-B allotypes; the orangutan KIR recognize both HLA-B*46:01 and HLA-B*73:01, whereas 2DL3-44E recognizes only HLA-B*46:01 (Fig. 3C).

Variation at positions 68, 70, and 182 modulates the avidity of KIR2DL for MHC-C

Substitution at position 68 did not perturb the specificities of KIR2DL1 and KIR2DL3 for HLA-C, but it did affect their avidities for HLA-C. Mutation of arginine 68 in KIR2DL1 to histidine or proline (the residue present in KIR2DL3) had little effect, but mutation to leucine reduced the avidity by 34% while preserving C2 specificity (Fig. 4A). For KIR2DL3, mutation of proline 68 to histidine, leucine, or arginine reduced the avidity for C1 by 19–40% (mean, 27%), while preserving C1 specificity (Fig. 4B). Thus, KIR2DL3 is seen to be more sensitive than KIR2DL1 to substitution at position 68.

Substitutions at position 70 had no effect on either the C2 specificity of KIR2DL1 or the C1 specificity of KIR2DL3, but they altered their avidities to a greater extent than seen for the position 68 mutations. Substitution of threonine 70 in KIR2DL1 to lysine, methionine, or arginine reduced the avidity by 43–66%, with the greatest effect seen with methionine, the residue present at position 70 in KIR2DL3 (Fig. 4C). In contrast, substitution of methionine 70 in KIR2DL3 with arginine or threonine (the residue present in KIR2DL1) gave a modest increase (16–38%) in the avidity for C1, whereas the lysine substitution reduced the avidity by 48% (Fig. 4D). The results obtained for the position 70 swap mutants indicate that the threonine–methionine difference at position 70 is a major factor contributing to the higher avidity of KIR2DL1 and lower avidity of KIR2DL3.

Substitution of histidine 182 in KIR2DL1 for arginine (the residue in KIR2DL3) had no effect, whereas substitution for cysteine reduced the avidity for C2 by 50% (Fig. 4E). The effect of the cysteine substitution in KIR2DL3 was even greater. When arginine 182 of KIR2DL3 was replaced by cysteine, the avidity for C1 was reduced by 87%, whereas the introduction of histidine had only a modest effect (10% reduction) (Fig. 4F). A common property of the mutations at positions 68, 70, and 182 is that they affect the avidity, but not the specificity, of the receptors. For KIR2DL1, these mutations led only to retention or reduction of avidity for C2, whereas for KIR2DL3, they could also lead to increased avidity for C1. Comparison of the properties of the swap mutations between 2DL1 and 2DL3 at positions 68, 70, and 182 indicates that the difference at position 70 contributes significantly to the differential avidity of the two receptors, whereas the effects of the reciprocal substitutions at positions 68 and 182 are weaker and less clear cut.

*Position 71 and 131 variation can alter avidity for HLA-C and introduce recognition of HLA-A*11:02*

Both KIR2DL1 and KIR2DL3 have glutamine 71. In KIR2DL1, its substitution with glutamate, histidine, and proline had little effect on the specificity or avidity for C2. In contrast, the 2DL1-71R

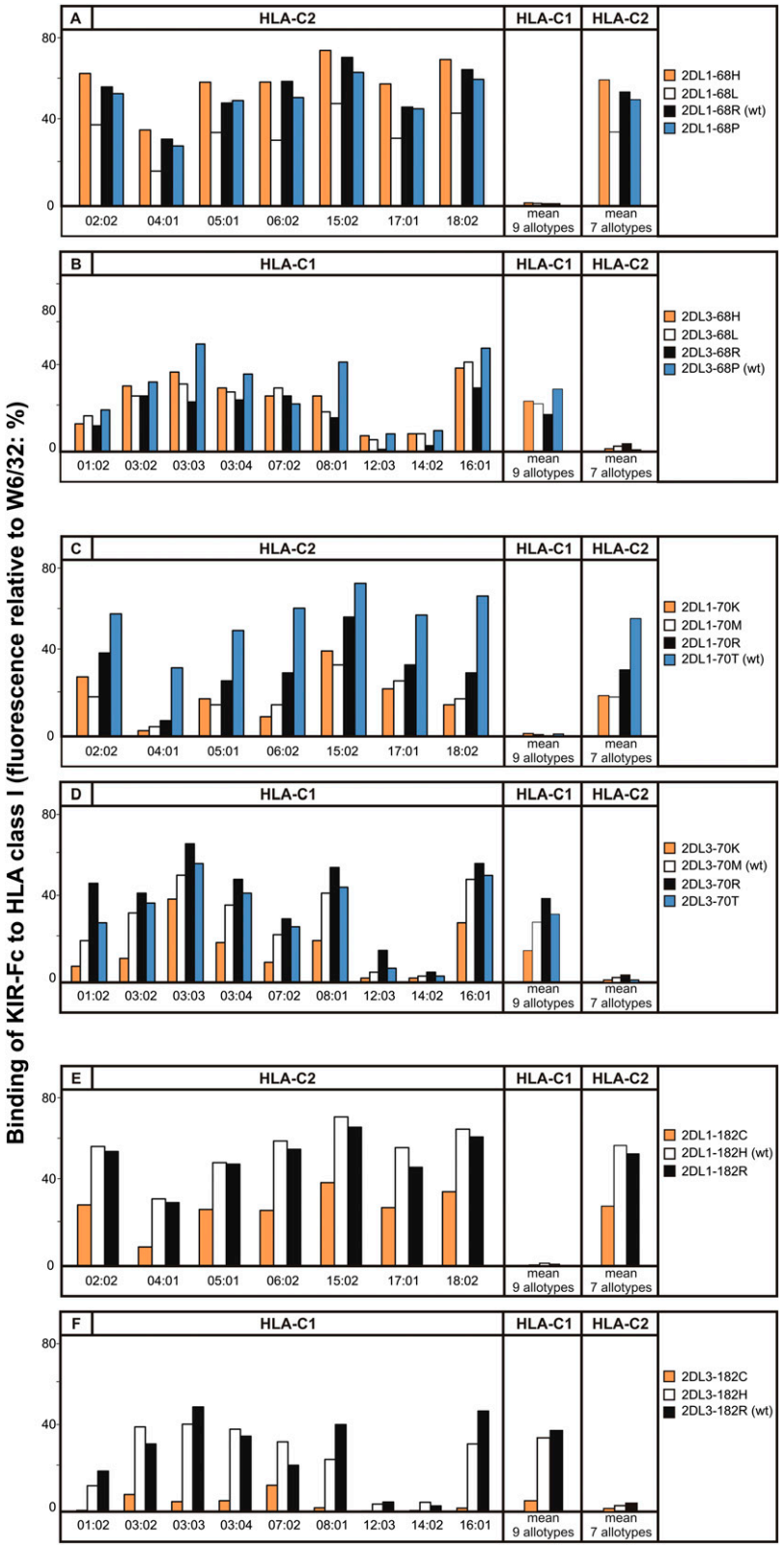

FIGURE 4. The avidity of KIR2D for MHC-C has been modulated by positive selection at positions 68, 70, and 182. Shown is the binding of wt and mutant KIR2DL-Fc fusion proteins to beads coated with 16 HLA-C allotypes: 9 having the C1 epitope (HLA-C1) and 7 having the C2 epitope (HLA-C2). Binding to each HLA-C allotype is given (*left panels*), as well as mean values for the HLA-C1 and HLA-C2 allotype groups (*middle* and *right panels*). (**A**) Mutation at position 68 of KIR2DL1: 2DL1-68H, 2DL1-68L, 2DL1-68R (wt), and 2DL1-68P. (**B**) Mutation at position 68 of KIR2DL3: 2DL3-68H, 2DL3-68L, 2DL3-68R, and 2DL3-68P (wt). (**C**) Mutation at position 70 of KIR2DL1: 2DL1-70K, 2DL1-70M, 2DL1-70R, and 2DL1-70T (wt). (**D**) Mutation at position 182 of KIR2DL3: 2DL3-70K, 2DL3-70M (wt), 2DL3-70R, and 2DL3-70T. (**E**) Mutation at position 182 of KIR2DL1: 2DL1-182C, 2DL1-182H (wt), and 2DL1-182R. (**F**) Mutation at position 182 of KIR2DL3: 2DL3-182C, 2DL3-182H, and 2DL3-182R (wt). HLA-C*12:03 and C*14:02 routinely bind weakly compared to other C1-bearing allotypes.

mutant exhibited a general reduction of avidity, while preserving C2 specificity (Fig. 5A). For HLA-C*04:01, the avidity was diminished by 88%; for other C2-bearing allotypes, the reduction was 38% (Fig. 5A). For the 2DL1-71K mutant, this selective trend was more extreme: binding to HLA-C*04:01 was reduced by 82%, whereas the binding to other C2-bearing allotypes was unperturbed.

Replacing glutamine 71 in KIR2DL3 with either glutamate or histidine had little effect on C1 specificity or avidity. In contrast, lysine 71 abrogated the interaction of KIR2DL3 with C1, and arginine 71 reduced the mean avidity for C1 by 64% while increasing the avidity for C1-bearing HLA-C*12:03 (Fig. 5B). Proline 71 caused a modest decrease in the avidity for C1 (25%), but it broadened the specificity of mutant 2DL3-71P to include

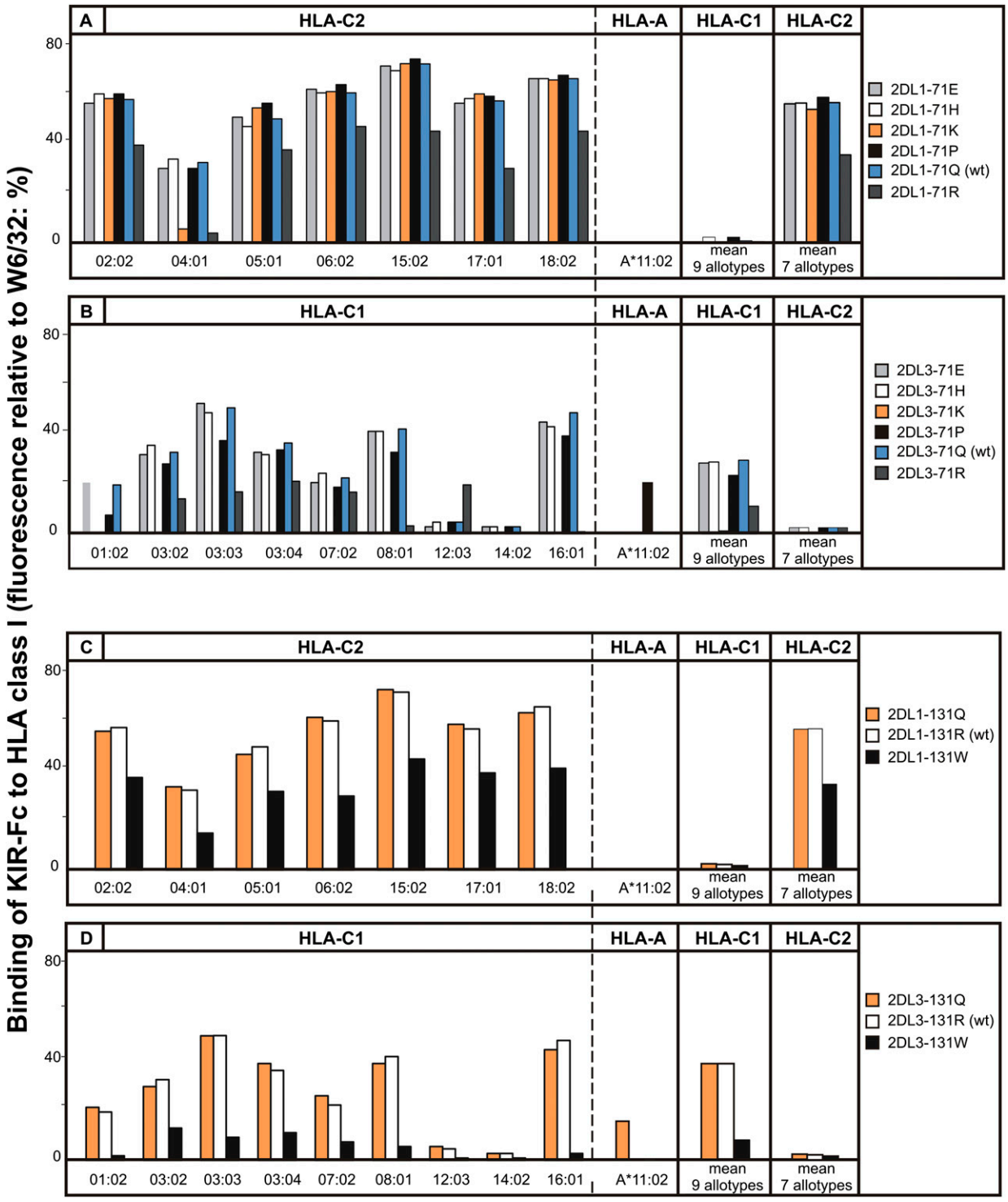

FIGURE 5. Positive selection at positions 71 and 131 of KIR2D can introduce reactivity with HLA-A*11:02 and alter avidity for HLA-C. Shown is the binding of wt and mutant KIR2D-Fc fusion proteins to beads coated with HLA-C (nine HLA-C1 and seven HLA-C2) and A*11:02 allotypes. (**A**) Mutation at position 71 of KIR2DL1: 2DL1-71E, 2DL1-71H, 2DL1-71K, 2DL1-71P, 2DL1-71Q (wt), and 2DL1-71R. (**B**) Mutation at position 71 of KIR2DL3: 2DL3-71E, 2DL3-71H, 2DL3-71K, 2DL3-71P, 2DL3-71Q (wt), and 2DL3-71R. (**C**) Mutation at position 131 of KIR2DL1: 2DL1-131Q, 2DL1-131R (wt), and 2DL1-131W. (**D**) Mutation at position 131 of KIR2DL3: 2DL3-131Q, 2DL1-131R (wt), and 2DL1-131W. HLA-C*12:03 and C*14:02 routinely bind weakly compared with other C1-bearing allotypes.

HLA-A*11:02 (Fig. 5B). KIR2DS4 is an activating lineage III KIR that naturally has proline 71 and exhibits similar reactivity with HLA-A*11:02 (42). However, proline 71 is not necessary for recognition of HLA-A*11:02, as became apparent from analysis of the position 131 mutants (Fig. 5C, 5D). Substitution of arginine 131 in KIR2DL3 with glutamine introduced reactivity with HLA-A*11:02 while preserving avidity for C1-bearing HLA-C (Fig. 5D). In contrast, substitution of arginine 131 for tryptophan caused 86% loss of avidity for C1 but no binding to HLA-A*11:02. For KIR2DL1, replacement of arginine 131 by glutamine preserved the avidity and specificity for C2, with no acquisition of reactivity toward HLA-A*11:02, whereas replacement

with tryptophan preserved a pure C2 specificity but reduced avidity by 40% (Fig. 5C).

In structural and functional studies of KIR interaction with HLA-C, it has been common practice to use HLA-C*04:01 as the prototypical C2-bearing allotype (23, 55, 61). Because the selective loss of HLA-C*04:01 reactivity by the 2DL1-71K and 2DL1-71R (Fig. 5A) implies that HLA-C*04:01 has unusual properties, we investigated the capacity of 2DL1-71K to recognize HLA-C*04:01 in a functional assay of NK cell killing (Fig. 6). NKL cells transduced with 2DL1, 2DL1-71K, 2DL3, and 2DL3-71K lysed untransfected 221 cells effectively and to a similar degree (Fig. 6B). KIR-Fc fusion constructs made from 2DL1, 2DL1-71K, 2DL3, and 2DL3-71K bound to transfected 221 cells expressing HLA-C*03:04 (C1) and HLA-C*04:01 (C2) with similar specificities and avidities to those obtained in the bead-binding assay. Thus, KIR2DL3 bound to 221-C*03:04 (Fig. 6C) but not to 221-C*04:01 (Fig. 6D), whereas KIR2DL1 bound to 221-C*04:01 (Fig. 6D) but not 221-C*03:04 (Fig. 6C). No binding of 2DL3-71K was detected on either target cell, whereas 2DL1-71K bound weakly, but specifically, to 221-C*04:01 (Fig. 6D). In cytolytic assays, 221-C*03:04 cells were resistant to lysis by NKL cells expressing KIR2DL3, but they were killed by NKL cells expressing KIR2DL1, 2DL1-71K, or 2DL3-71K (Fig. 6E). Conversely, 221-C*04:01 cells were resistant to lysis by NKL cells expressing KIR2DL1, but they were killed by NKL cells expressing either KIR2DL3 or 2DL3-71K (Fig. 6F). NKL cells expressing 2DL1-71K lysed 221-C*04:01 cells to a much lesser extent than did KIR2DL1, consistent with the weak, but detectable signal observed with 2DL1-71K in the binding assay (Fig. 6D). In conclusion, a positive correlation was observed between the results obtained in the direct binding assay and functional assays of cellular cytotoxicity. Consequently, our analysis points to HLA-C*04:01 having unusual properties that could challenge its prototypical stature.

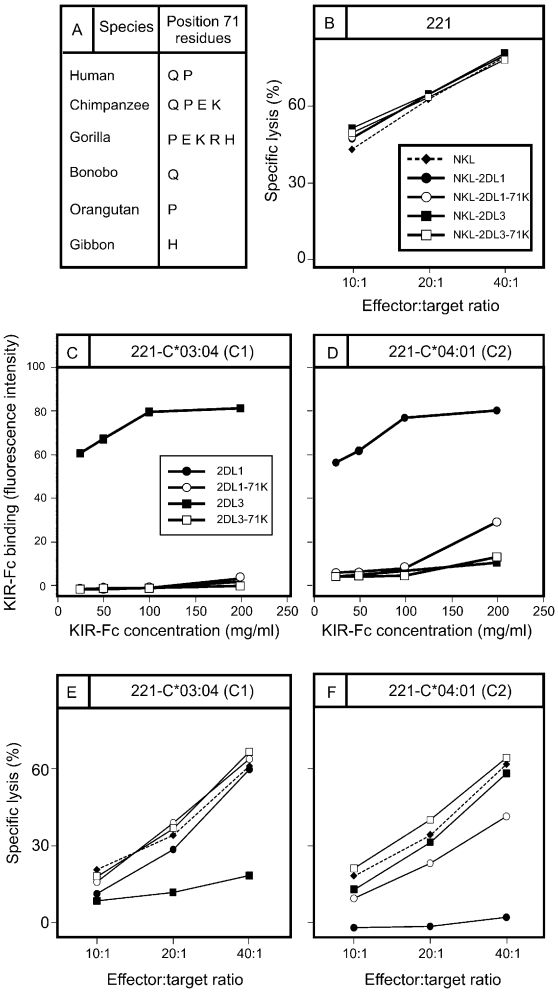

FIGURE 6. Lysine 71 abrogates interaction of KIR2DL3 with HLA-C and selectively impairs interaction of KIR2DL1 with HLA-C*04:01. (**A**) Shown are the residues present at position 71 in hominoid lineage III KIR. Notably, lysine 71 is absent from humans but present in chimpanzees and gorillas. (**B**) Killing of class I-deficient 221 cells by NKL cells (♦) and by NKL cells transduced with KIR2DL1 (●), 2DL1-71K (○), KIR2DL3 (■), and 2DL3-71K (□). Binding to 221 cells expressing C1-bearing HLA-C*03:04 (**C**) and C2-bearing HLA-C*04:01 (**D**) of KIR2DL-Fc fusion proteins: KIR2DL1, 2DL1-71K, 2DL3, and 2DL3-71K. Killing of 221 target cells expressing HLA-C*03:04 (**E**) and HLA-C*04:01 (**F**) by NKL cells expressing KIR2DL1 (●), 2DL1-71K (○), 2DL3 (■), and 2DL3-71K (□).

*Functional recognition of HLA-A*11:02 by mutant KIR2DL3-71P*

Of the four HLA class I epitopes (A3/11, Bw4, C1, and C2) recognized by KIR, the functional significance of A3/11 remains uncertain. Carried by HLA-A*03 and HLA-A*11 allotypes, the A3/A11 epitope was first shown to engage the lineage III KIR, KIR3DL2 (28, 62). Although Bw4, C1, and C2 mediate robust inhibition and education of NK cells on binding their cognate KIR, the interaction of the A3/11 epitope with 3DL2 provides weak inhibition (25) and no detectable education (63, 64). In previous studies of lineage III KIR2DS4 (42) and orangutan lineage III (13), we detected binding HLA-A allotypes carrying the A3/11 epitope, for which the strength of binding is A*11:02 > A*11:01 > A*03:01. This hierarchy is again seen for mutant 2DL3-71P, which binds significantly to A*11:02 but not to A*11:01 or A*03:01 (Fig. 6A). With this background and context, we tested whether the recognition of HLA-A*11:02 by 2DL2-71P could influence NK cell function.

In cytotoxic assays, NKL cells killed 221 cells (Fig. 7A) but not 221 cells transfected with HLA-A*11:02 (Fig. 7B), an inhibitory effect not seen with 221 cells expressing either C*03:04 or C*04:01 (20) (Fig. 6E, 6F). Because the leader peptides of the transfected HLA class I are all nonpermissive for HLA-E interaction with CD94:NKG2A, the enhanced inhibition of cytolysis achieved by A*11:02 was unlikely to be mediated through this receptor. Alternatively, the inhibition could arise from interaction of HLA-A*11:02 with the LILRB1 receptor on NKL cells. Consistent with this mechanism, G4-NKL, a derivative of NKL having siRNA that reduces LILRB1 expression by >90%, killed 221-A*11:02 cells much more effectively than NKL cells (Fig. 7B). Our observations that HLA-C*03:04 and HLA-C*04:01 are not good functional ligands for LILRB1 agree with the results of previous studies. Using a similar assay system, LILRB1 was seen to bind HLA-G, HLA-A*03:01, B*27:02, and B*27:05 but not HLA-C*03:01 (65). Likewise, a LILRB1-Fc fusion protein bound well to a variety of HLA-A and -B allotypes at cell surfaces but not to HLA-C*04:01 or C*07:02 and only weakly to C*03:04 (66). In contrast, in noncellular-binding assays, LILRB1 has detectable avidity for the spectrum of HLA-C allotypes (67, 68). The mechanisms underlying the differing results obtained in cellular- and molecular-binding assays, as well as between HLA-A and -B compared with HLA-C, have yet to be determined. To identify and avoid the inhibitory effects of LILRB1, our experiments to investigate the capacity for HLA-A*11:02 to be a KIR ligand were performed using both NKL (Fig. 7A–C, *left panels*) and G4-NKL cells (Fig. 7A–C, *right panels*).

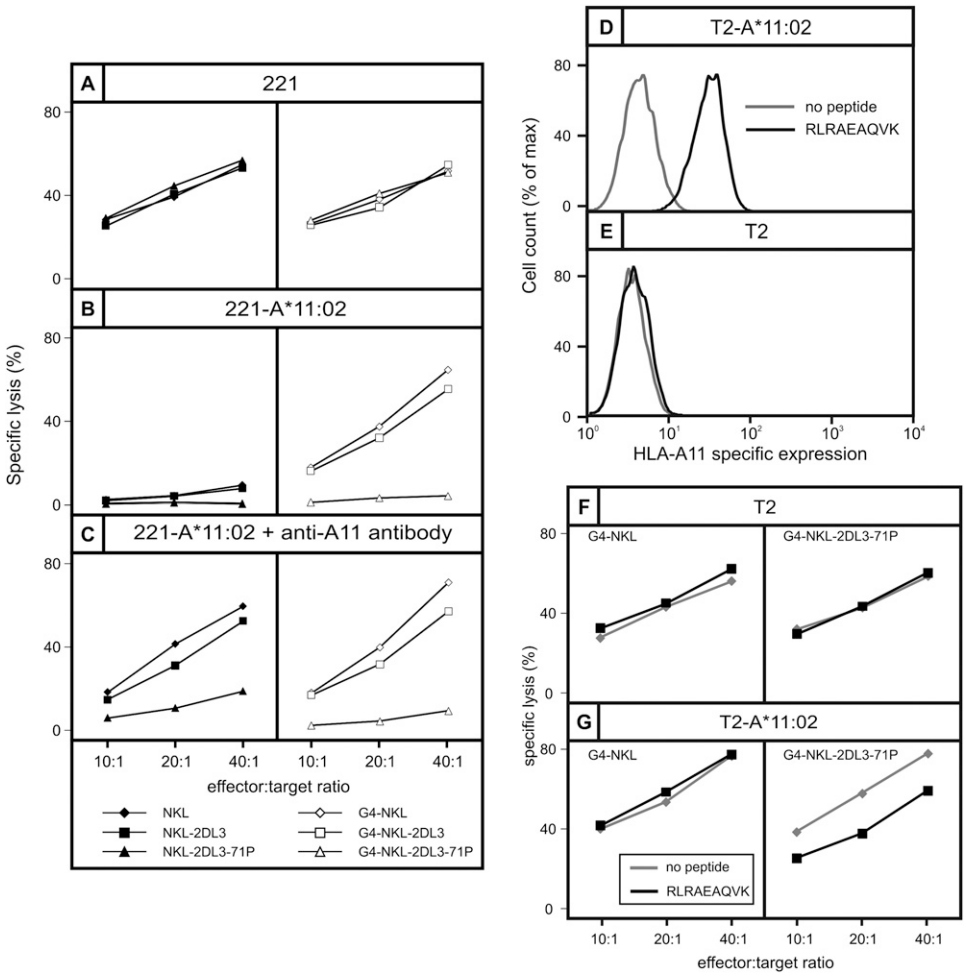

FIGURE 7. Proline 71 present in KIR2DS4 and KIR3DL2 confers specificity for HLA-A*11:02 on KIR2DL3 but not on KIR2DL1. Results of cytotoxicity assays in which the target cells are class I-deficient 221 cells (**A**), 221 cells expressing HLA-A*11:02 (**B**), or 221 cells expressing HLA-A*11:02 cells preincubated with Ab specific for HLA-A*11 (**C**). *Left panels*: the effector cells included NKL cells, NKL cells expressing 2DL3, and NKL cells expressing 2DL3-71P. *Right panels*: the effector cells included G4-NKL cells, G4-NKL cells expressing 2DL3, and G4-NKL cells expressing 2DL3-71P. NKL cells express the HLA class I receptor LILRB1, whereas G4-NKL is an NKL cell in which LILRB1 expression is suppressed. Flow cytometric analysis of the binding of anti-A*11 Ab to T2 cells transfected with HLA-A*11:02 (T2-A*11:02) (**D**) and untransfected T2 cells (**E**), following overnight incubation in the presence (black line) or absence (gray line) of the RLRAEAQVK peptide that binds HLA-A*11. Results of cytotoxicity assays in which the targets were T2-A*11:02 cells (**F**) and T2 cells (**G**), following overnight incubation in the presence (black line) or absence (gray line) of peptide RLRAEAQVK. Effector cells were G4-NKL cells (*left panels*) and G4-NKL cells expressing 2DL3-71P (*right panels*).

That G4-NKL cells expressing KIR2DL3 killed 221-A*11:02 cells shows that A*11:02 is not a ligand for wt KIR2DL3 (Fig. 7B, *right panel*). In contrast, killing of 221-A*11:02 was strongly inhibited when G4-NKL cells expressed the 2DL3-71P mutant, showing that binding of A*11:02 to 2DL3-71P is a functional ligand–receptor interaction that leads to the transduction of an inhibitory signal (Fig. 7B, *right panel*). Preincubation of 221-A*11:02 with an anti-A11 mAb had little effect on the interaction between 2DL3-71P and HLA-A*11:02 (Fig. 7C, *right panel*), but it rendered the cells susceptible to lysis by NKL cells, with an efficiency similar to that achieved by siRNA-mediated downregulation of LILRB1 (Fig. 7C, *left panel*). This result, suggesting that the Ab recognizes an epitope of HLA-A*11:02 in or near the binding site for LILRB1, but away from the binding site for 2DL3-71P, is consistent with crystallographic studies showing that LILRB1 interacts with the conserved Ig-like domains (α_3 and β_2-microglobulin) of HLA class I (69), whereas lineage III KIR interact with the highly polymorphic α_1 and α_2 domains (58).

*Mutant KIR2DL3-71P can recognize the complex of HLA-A*11:02 and a peptide derived from EBV*

Comparison of five peptides that bind to HLA-A*03:01 and five peptides that bind to HLA-A*11:01 showed that peptide RLRAEAQVK from the EBNA3A protein of EBV, which binds both A*03:01 and A*11:01, was the only peptide that permitted interaction with KIR3DL2 (27, 28, 62). With this precedent, we investigated whether this peptide could bind to HLA-A*11:02 and form a functional ligand for the KIR2DL3-71P mutant. To do this, we transfected the TAP-deficient T2 cell line with A*11:02. T2 cells present very few endogenous peptides, giving a minimal surface expression of HLA class I unless binding peptide is supplied exogenously. In the absence of peptide, basal expression of A*11:02 on transfected T2 cells was undetectable (Fig. 7E). T2 and T2-A*11:02 cells were incubated overnight either in the absence or presence of peptide RLRAEAQVK (27). Incubation of T2-A*11:02 cells with peptide increased the amount of A*11:02 on the cell surface 10-fold over T2-A*11:02 cells incubated in the absence of peptide (Fig. 7D) or T2 cells incubated either in the

presence or absence of peptide (Fig. 7E). This result shows that A*11:02 does bind the RLRAEAQVK peptide (Fig. 7F). Consequently, the substitution of lysine for glutamate at position 19 that distinguishes HLA-A*11:02 from A*11:01 does not affect the binding of this peptide.

In cytotoxicity assays, T2 cells that were incubated in the presence or absence of peptide were killed to a similar extent by G4-NKL cells and G4-NKL cells expressing the 2DL3-71P mutant (Fig. 7F). G4-NKL and G4-NKL–2DL3-71P resulted in a similarly effective killing of T2-A*11:02 cells that had been incubated in the absence peptide. In contrast, T2-A*11:02 cells that had been incubated with peptide exhibited a resistance to killing by G4–2DL3-71P (Fig. 7G). This result indicates that 2DL3-71P recognizes the complex of RLRAEAQVK bound to A*11:02 to generate a functional signal that inhibits NK cells.

Discussion

MHC-C–mediated regulation of NK cells is of recent and rapid evolution and is specific to hominids: humans and great apes. In humans it comprises a bipartite system of two mutually exclusive epitopes that are defined by dimorphism at position 80 of HLA-C and that serve as ligands for different lineage III KIR (15, 19, 31). In this study, we compared KIR2DL3 that recognizes the C1 epitope (asparagine 80) with KIR2DL1 that recognizes the C2 epitope (lysine 80). Comparison of >100 hominid lineage III KIR identified six positions of sequence variation that have been subject to positive diversifying selection and are situated in the part of the KIR molecule that forms the binding site for HLA-C, as visualized at high resolution in three-dimensional crystallographic structures (55, 58, 70). To assess the effects of natural selection upon the interactions of KIR with MHC-C, we studied the strength and specificity of mutant KIR2DL3 and KIR2DL1 receptors, each one substituted with one of the natural variations identified at the six positively selected sites. Thus, each wt receptor was compared to 18 mutants. The results of this analysis are summarized for each mutant in Fig. 8.

Overall, mutation had a wider range of effects on KIR2DL3 than on KIR2DL1. The C1 specificity of KIR2DL3 was changed in two ways: a major broadening to give a pan HLA-C receptor with C1 plus C2 specificity and a minor broadening to give reactivity with HLA-A*11:02, as well as C1. The avidity of KIR2DL3 was also changed in two ways: 2 of the mutations increased avidity for C1 by >10%, 13 decreased the avidity by >10%, and 3 had little effect (Fig. 8). In comparison with KIR2DL3, the ligand-binding properties of KIR2DL1 were more resistant to mutation: none of the 18 mutations altered the C2 specificity, and none of them increased the avidity for C2. Ten mutations in KIR2DL1 reduced C2 avidity by >10%, and eight had little effect. Consideration of all of the mutants, with the exception of those at specificity-determining position 44, shows that all KIR2DL1 mutants retained a minimum of 32% of the wt binding, with an average of 75%, whereas the binding of KIR2DL3 mutants ranged from 0–138% of wt binding, with an average of 68%. Exemplifying the variety of effects that mutation had on KIR2DL3 and their limited effect on KIR2DL1 are the avidities and specificities of the mutants containing glutamate 44, proline 71, and glutamine 13 (Fig. 9).

In functional and epidemiological studies, the interactions of KIR2DL1 with C2 and KIR2DL2/3 with C1 are often considered complementary but equivalent. From the molecular analysis a different picture emerges, one in which KIR2DL1 is seen as the stronger and more selective receptor, which appears to have been optimized for high-avidity recognition of C2 and, as a consequence, became relatively resistant to further functional change by point mutation. In contrast, KIR2DL3 is seen as the weaker and less selective receptor, which, by being less refined, retains greater potential for improvement and change. Having acquired a strong and exquisite specificity for C2, KIR2DL1 is now specialized and inflexible; by retaining a weaker C1 specificity that cross-reacts with C2 (21, 22, 30), KIR2DL3 is less specialized but more flexible and adaptable.

These contrasting and complementary properties fit well with an evolutionary model in which the C1 epitope and their cognate C1-specific KIR evolved first and subsequently underwent mutation and selection to give rise to the C2 epitope and C2-specific KIR (13). The crucial feature of this model is the flexibility of the C1 receptor and its cross-reactivity with C2, which, while maintaining function as a C1 receptor, provides a potential C2 receptor prior to formation of the C2 epitope. Thus, the inherent flexibility of the C1 receptor allows C2 and C2-specific KIR to evolve by stepwise point mutation through a series of intermediate forms that all have biological function and could be maintained by natural selection. The model's first intermediate is a receptor with broad MHC-C reactivity like the 2DL3-44E mutant (Fig. 8). The presence of this C1+C2 specific receptor sets the stage for mutation at position 80 of MHC-C to produce C2 from C1 and for it to be a functional KIR ligand. With both C1 and C2 in place, further mutation of the KIR, including the key introduction of methionine 44, then gave rise to highly specific C2 receptors, such as KIR2DL1.

Hominid variation at three of the six positively selected positions is associated with changes in receptor specificity: position 44 controls HLA-C specificity, and positions 71 and 131 affect the recognition of HLA-A*11:02. Variation at all six positions influences receptor avidity, but the major players are positions 70 and

		D1																		D2					
		44				68				70				71						131			182		
KIR	HLA	E	M	K	T	H	L	R	P	K	M	R	T	E	H	K	P	Q	R	Q	R	W	C	H	R
2DL1	C1	1	2	52	6	1	1	2	2	1	1	1	2	1	1	1	2	2	1	2	2	0	0	2	1
	C2	40	62	1	33	64	39	62	59	21	20	34	62	60	60	59	62	62	37	62	62	37	30	62	59
	A*11:02	0	0	0	0	0	0	0	0	0	0	0	0	0	0	0	0	0	0	0	0	0	0	0	0
2DL3	C1	28	3	32	4	25	25	19	32	16	32	44	37	30	30	0	24	32	11	33	32	6	4	27	32
	C2	34	54	2	17	2	1	1	2	1	2	2	2	1	1	0	2	2	0	3	2	0	0	2	2
	A*11:02	0	0	0	0	0	0	0	0	0	0	0	0	0	0	0	19	0	0	11	0	0	0	0	0

FIGURE 8. Summary of the binding avidity of KIR2DL1 and KIR2DL3 mutants for the C1 and C2 epitopes of HLA-C and for HLA-A*11:02. Each value is the binding of the KIR-Fc protein to the target HLA class I expressed as a percentage of the binding of the W6/32 mAb to the same HLA class I allotype. Values for C1 and C2 are the means from nine C1-bearing and seven C2-bearing HLA-C allotypes, respectively. Gray shading indicates the residues in KIR2DL1*003 and KIR2DL3*001.

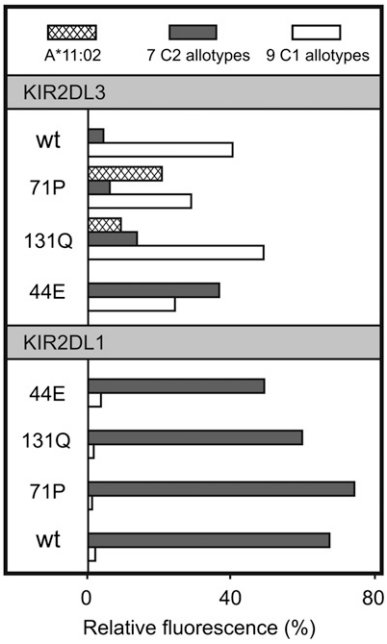

FIGURE 9. KIR2DL1 has stronger avidity and narrower HLA class I specificity than KIR2DL3. Shown is the binding of wt and mutant KIR2DL3-Fc (*upper panel*) and KIR2DL1-Fc (*lower panel*) fusion proteins to beads coated with HLA-A*11:02 (cross-hatched bars), HLA-C2 allotypes (dark gray bars; mean value for seven allotypes), and HLA-C1 allotypes (white bars; mean value for nine allotypes). The specificity and avidity of KIR2DL1 are markedly more resistant to mutation at positions 44, 71, and 131 compared with the specificity and avidity of KIR2DL3.

44. In determining both specificity and avidity, residues of the D1 domain are the dominant influence, with D2 domain residues taking the minor role. Because KIR2DL1*003 and KIR2DL3*001 are identical at positions 71 and 131, only positions 44, 68, 70, and 182 can contribute to their functional differences. That dimorphism at position 44 determines receptor specificity is well known (22, 23), but this difference of methionine in KIR2DL1 and lysine in KIR2DL3 also contributes to their relative strength.

The major modulator of avidity is residue 70: threonine in KIR2DL1 and methionine in KIR2DL3. By rough estimate, 67% of the avidity difference comes from position 70, and 19% comes from position 44. The remaining 14% could involve synergism between positions 44 and 70, which would go undetected in this study of single mutations, or contributions from other positions, including 68, 182, and the 10 positively selected positions away from the binding site (7). A precedent for such possibilities is the synergistic contribution that distal residues 16 and 148 make to KIR2DL2*001 being a stronger C1 receptor than KIR2DL3*001 (21). Although residue 70 is the major influence on receptor avidity, it has no role in receptor specificity. In their respective crystallographic structures, glutamine 70 of KIR2DL1 makes no direct contact with HLA-C*04, whereas glutamine 70 of KIR2DL2 forms a hydrophobic bond with arginine 69 of HLA-C*03 (55, 58, 70). It is not known whether glutamine 70 of KIR2DL3 makes a similar contact with HLA-C, because a pertinent crystallographic structure has yet to be determined

Interaction of KIR2DL3 with HLA-A*11:02 was achieved by mutation at either position 71 or 131. The A3/11 epitope, carried by HLA-A*03 and HLA-A*11, was first described as the ligand for KIR3DL2, a lineage II KIR (28, 62). Subsequently, lineage III KIR2DS4 was shown to bind HLA-A*11 but not HLA-A*03, a property associated with the proline 71 valine 72 motif acquired from a KIR3DL2-like lineage II gene and not present in other lineage III KIR (42). We now show that introduction of proline 71 into KIR2DL3 is sufficient to confer reactivity with HLA-A*11:02, but it is not necessary to achieve this effect. Mutating arginine 131 to glutamine in KIR2DL3 also conferred recognition of HLA-A*11:02. Popy-2DLA, an orangutan receptor that has lysine 44, proline 71, and arginine 131, also recognizes HLA-A*11:02. Unlike C1, C2 (23), and Bw4 (71), the A3/11 epitope cannot be described in terms of a single specificity-determining residue.

Of the four HLA class I epitopes recognized by KIR, the A3/11 epitope is the least studied, and its functional significance remains uncertain. Although all human populations have the Bw4, C1, and C2 epitopes, the A3/11 epitope appears dispensable [e.g., it is absent from Native American populations: http://www.allelefrequencies.net (72)]. Functionally, interactions of Bw4, C1, and C2 with cognate KIR mediate robust inhibition and education of NK cells, whereas KIR3DL2 engagement of A3/11 provides weak inhibition (25) and no detectable education (63, 64). Of 10 viral or self-peptides that bind to HLA-A*03 and/or HLA-A*11, only peptide RLRAEAQVK from EBV was shown to permit interaction with KIR3DL2 (27), raising the possibility that only a small fraction of the HLA-A*11 and HLA-A*03 molecules on cell surfaces functions as a ligand for KIR3DL2. The biological relevance of these interactions remains an open question, and another function for KIR3DL2 as a receptor and transporter of CpG oligodeoxynucleotides has been proposed (73).

A possible consequence of rapidly coevolving NK cell receptors and MHC ligands is the circumstance of NK cell receptors losing function, by failure to keep up with changes in MHC class I imposed by selected pressures from other functions, such as Ag presentation to CD8 T cells. Surviving such a crisis, with subsequent evolution of a new set of variable NK cell receptors, could explain how humans and mice came to use completely unrelated proteins as variable NK cell receptors. The human KIR and mouse Ly49 became MHC class I receptors through convergent evolution; being subject to similar selection pressure caused them to acquire several similar functional characteristics, including activating and inhibitor receptors with the same MHC class I specificity. The activating receptors have a greater tendency than do their inhibitory counterparts to accumulate substitutions causing loss of receptor avidity (40, 74), a trend well illustrated by human activating lineage III KIR: 2DS1 has half the C2 avidity of 2DL1; 2DS4 binds weakly to just a few HLA class I allotypes; and 2DS2, 2DS3, and 2DS5 exhibit almost no binding to HLA class I.

Five of the substitutions that we studied are principally found in activating KIR (threonine 44, lysine 70, arginine 71, tryptophan 131, and cysteine 182) and, therefore, were likely acquired through mutation of the activating KIR and not from the inhibitory KIR from which they were formed by recombinations (74). When introduced into KIR2DL1 and KIR2DL3, these residues had no effect upon receptor specificity, but they all reduced avidity for HLA-C: KIR2DL1 avidity for C2 was reduced by 38–66% (mean, 51%), and KIR2DL3 avidity for C1 was reduced by 65–90% (mean, 74%). That positions 44, 70, 71, 131, and 182 were subject to positive selection implies there was a functional advantage to reducing the potency of activating receptors with the introduction of threonine 44, lysine 70, arginine 71, tryptophan 131, and cysteine 182. Exemplifying this phenomenon is KIR2DS1*002 (the common 2DS1 allele), in which lysine substituted for threonine 70 was responsible for reducing C2 avidity to half of that of KIR2DL1*003 (39, 75).

At an early stage of pregnancy, interplay and balance between KIR2DL1 and KIR2DS1 appear to modulate interactions between fetal trophoblast and maternal uterine NK cells that facilitate

placentation. In pregnancies in which the fetus expresses C2, the risk for preeclampsia and other disorders is less if the mother has both KIR2DL1 and KIR2DS1 than if she has only KIR2DL1 (76). If this balance were improved by having an activating receptor less avid than its inhibitory partner, it could explain the positive selection of lysine 70 in KIR2DS1.

Within the groups of C1-bearing and C2-bearing HLA-C, there is a considerable and reproducible range of avidity for the cognate KIR. Because the observed binding is stable to washing, and residues 7 and 8 of HLA-C bound peptide contact KIR (55, 70), we suspect that the observed avidity differences are the consequence of substitutions in the peptide binding site that cause different populations of peptides to be bound by the various HLA-C allotypes. In this context, the selective and almost complete loss of binding to HLA-C*04:01 by mutant 2DL1-71P is a striking example of the increasing number of allotype-specific effects that are being uncovered in the study of HLA-C binding to lineage III KIR. This result is not an artifact of the direct-binding assay, because 2DL1-71P on NK cell surfaces similarly fails to engage HLA-C*04:01 on target cells. In many studies of KIR specificity, HLA-C*04:01 and HLA-C*03:04 provided the representative C2 and C1 epitopes, respectively (22, 23, 61, 77). Notably, these allotypes formed the complexes with KIR that were used to determine the canonical three-dimensional structures (55, 70). Although a good ligand for KIR2DL1 in cellular assays of NK cell function, we noticed that the binding of KIR2DL1 to HLA-C*04:01 is generally lower than for other C2-bearing allotypes. Such observations suggested that HLA-C*04:01 could have some properties that are not representative of other C2-bearing HLA-C, a possibility that is strengthened by our results.

Disclosures

The authors have no financial conflicts of interest.

References

1. Caligiuri, M. A. 2008. Human natural killer cells. *Blood* 112: 461–469.
2. Campbell, K. S., and A. K. Purdy. 2011. Structure/function of human killer cell immunoglobulin-like receptors: lessons from polymorphisms, evolution, crystal structures and mutations. *Immunology* 132: 315–325.
3. Lanier, L. L. 1998. NK cell receptors. *Annu. Rev. Immunol.* 16: 359–393.
4. Moretta, A., C. Bottino, M. Vitale, D. Pende, R. Biassoni, M. C. Mingari, and L. Moretta. 1996. Receptors for HLA class-I molecules in human natural killer cells. *Annu. Rev. Immunol.* 14: 619–648.
5. Braud, V. M., D. S. Allan, C. A. O'Callaghan, K. Söderström, A. D'Andrea, G. S. Ogg, S. Lazetic, N. T. Young, J. I. Bell, J. H. Phillips, et al. 1998. HLA-E binds to natural killer cell receptors CD94/NKG2A, B and C. *Nature* 391: 795–799.
6. Pérez-Villar, J. J., I. Melero, F. Navarro, M. Carretero, T. Bellón, M. Llano, M. Colonna, D. E. Geraghty, and M. López-Botet. 1997. The CD94/NKG2-A inhibitory receptor complex is involved in natural killer cell-mediated recognition of cells expressing HLA-G1. *J. Immunol.* 158: 5736–5743.
7. Abi-Rached, L., A. K. Moesta, R. Rajalingam, L. A. Guethlein, and P. Parham. 2010. Human-specific evolution and adaptation led to major qualitative differences in the variable receptors of human and chimpanzee natural killer cells. *PLoS Genet.* 6: e1001192.
8. Parham, P., P. J. Norman, L. Abi-Rached, and L. A. Guethlein. 2012. Human-specific evolution of killer cell immunoglobulin-like receptor recognition of major histocompatibility complex class I molecules. *Philos. Trans. R. Soc. Lond. B Biol. Sci.* 367: 800–811.
9. Rajagopalan, S., and E. O. Long. 1999. A human histocompatibility leukocyte antigen (HLA)-G-specific receptor expressed on all natural killer cells. *J. Exp. Med.* 189: 1093–1100.
10. Ponte, M., C. Cantoni, R. Biassoni, A. Tradori-Cappai, G. Bentivoglio, C. Vitale, S. Bertone, A. Moretta, L. Moretta, and M. C. Mingari. 1999. Inhibitory receptors sensing HLA-G1 molecules in pregnancy: decidua-associated natural killer cells express LIR-1 and CD94/NKG2A and acquire p49, an HLA-G1-specific receptor. *Proc. Natl. Acad. Sci. USA* 96: 5674–5679.
11. Kovats, S., E. K. Main, C. Librach, M. Stubblebine, S. J. Fisher, and R. DeMars. 1990. A class I antigen, HLA-G, expressed in human trophoblasts. *Science* 248: 220–223.
12. Guethlein, L. A., A. M. Older Aguilar, L. Abi-Rached, and P. Parham. 2007. Evolution of killer cell Ig-like receptor (KIR) genes: definition of an orangutan KIR haplotype reveals expansion of lineage III KIR associated with the emergence of MHC-C. *J. Immunol.* 179: 491–504.
13. Older Aguilar, A. M., L. A. Guethlein, E. J. Adams, L. Abi-Rached, A. K. Moesta, and P. Parham. 2010. Coevolution of killer cell Ig-like receptors with HLA-C to become the major variable regulators of human NK cells. *J. Immunol.* 185: 4238–4251.
14. Older Aguilar, A. M., L. A. Guethlein, M. Hermes, L. Walter, and P. Parham. 2011. Rhesus macaque KIR bind human MHC class I with broad specificity and recognize HLA-C more effectively than HLA-A and HLA-B. *Immunogenetics* 63: 577–585.
15. Mandelboim, O., H. T. Reyburn, M. Valés-Gómez, L. Pazmany, M. Colonna, G. Borsellino, and J. L. Strominger. 1996. Protection from lysis by natural killer cells of group 1 and 2 specificity is mediated by residue 80 in human histocompatibility leukocyte antigen C alleles and also occurs with empty major histocompatibility complex molecules. *J. Exp. Med.* 184: 913–922.
16. Mizuki, N., H. Ando, M. Kimura, S. Ohno, S. Miyata, M. Yamazaki, H. Tashiro, K. Watanabe, A. Ono, S. Taguchi, et al. 1997. Nucleotide sequence analysis of the HLA class I region spanning the 237-kb segment around the HLA-B and -C genes. *Genomics* 42: 55–66.
17. King, A., T. D. Burrows, S. E. Hiby, J. M. Bowen, S. Joseph, S. Verma, P. B. Lim, L. Gardner, P. Le Bouteiller, A. Ziegler, et al. 2000. Surface expression of HLA-C antigen by human extravillous trophoblast. *Placenta* 21: 376–387.
18. King, A., C. Boocock, A. M. Sharkey, L. Gardner, A. Beretta, A. G. Siccardi, and Y. W. Loke. 1996. Evidence for the expression of HLAA-C class I mRNA and protein by human first trimester trophoblast. *J. Immunol.* 156: 2068–2076.
19. Colonna, M., G. Borsellino, M. Falco, G. B. Ferrara, and J. L. Strominger. 1993. HLA-C is the inhibitory ligand that determines dominant resistance to lysis by NK1- and NK2-specific natural killer cells. *Proc. Natl. Acad. Sci. USA* 90: 12000–12004.
20. Colonna, M., T. Spies, J. L. Strominger, E. Ciccone, A. Moretta, L. Moretta, D. Pende, and O. Viale. 1992. Alloantigen recognition by two human natural killer cell clones is associated with HLA-C or a closely linked gene. *Proc. Natl. Acad. Sci. USA* 89: 7983–7985.
21. Moesta, A. K., P. J. Norman, M. Yawata, N. Yawata, M. Gleimer, and P. Parham. 2008. Synergistic polymorphism at two positions distal to the ligand-binding site makes KIR2DL2 a stronger receptor for HLA-C than KIR2DL3. *J. Immunol.* 180: 3969–3979.
22. Winter, C. C., J. E. Gumperz, P. Parham, E. O. Long, and N. Wagtmann. 1998. Direct binding and functional transfer of NK cell inhibitory receptors reveal novel patterns of HLA-C allotype recognition. *J. Immunol.* 161: 571–577.
23. Winter, C. C., and E. O. Long. 1997. A single amino acid in the p58 killer cell inhibitory receptor controls the ability of natural killer cells to discriminate between the two groups of HLA-C allotypes. *J. Immunol.* 158: 4026–4028.
24. Moffett, A., and C. Loke. 2006. Immunology of placentation in eutherian mammals. *Nat. Rev. Immunol.* 6: 584–594.
25. Valiante, N. M., M. Uhrberg, H. G. Shilling, K. Lienert-Weidenbach, K. L. Arnett, A. D'Andrea, J. H. Phillips, L. L. Lanier, and P. Parham. 1997. Functionally and structurally distinct NK cell receptor repertoires in the peripheral blood of two human donors. *Immunity* 7: 739–751.
26. Velardi, A., L. Ruggeri, A. Mancusi, F. Aversa, and F. T. Christiansen. 2009. Natural killer cell allorecognition of missing self in allogeneic hematopoietic transplantation: a tool for immunotherapy of leukemia. *Curr. Opin. Immunol.* 21: 525–530.
27. Hansasuta, P., T. Dong, H. Thananchai, M. Weekes, C. Willberg, H. Aldemir, S. Rowland-Jones, and V. M. Braud. 2004. Recognition of HLA-A3 and HLA-A11 by KIR3DL2 is peptide-specific. *Eur. J. Immunol.* 34: 1673–1679.
28. Döhring, C., D. Scheidegger, J. Samaridis, M. Cella, and M. Colonna. 1996. A human killer inhibitory receptor specific for HLA-A1,2. *J. Immunol.* 156: 3098–3101.
29. Cella, M., A. Longo, G. B. Ferrara, J. L. Strominger, and M. Colonna. 1994. NK3-specific natural killer cells are selectively inhibited by Bw4-positive HLA alleles with isoleucine 80. *J. Exp. Med.* 180: 1235–1242.
30. Gumperz, J. E., V. Litwin, J. H. Phillips, L. L. Lanier, and P. Parham. 1995. The Bw4 public epitope of HLA-B molecules confers reactivity with natural killer cell clones that express NKB1, a putative HLA receptor. *J. Exp. Med.* 181: 1133–1144.
31. Rajalingam, R., P. Parham, and L. Abi-Rached. 2004. Domain shuffling has been the main mechanism forming new hominoid killer cell Ig-like receptors. *J. Immunol.* 172: 356–369.
32. Palacios, C., L. C. Cuervo, and L. F. Cadavid. 2011. Evolutionary patterns of killer cell Ig-like receptor genes in Old World monkeys. *Gene* 474: 39–51.
33. Sambrook, J. G., A. Bashirova, S. Palmer, S. Sims, J. Trowsdale, L. Abi-Rached, P. Parham, M. Carrington, and S. Beck. 2005. Single haplotype analysis demonstrates rapid evolution of the killer immunoglobulin-like receptor (KIR) loci in primates. *Genome Res.* 15: 25–35.
34. Blokhuis, J. H., M. K. van der Wiel, G. G. Doxiadis, and R. E. Bontrop. 2010. The mosaic of KIR haplotypes in rhesus macaques. *Immunogenetics* 62: 295–306.
35. LaBonte, M. L., K. L. Hershberger, B. Korber, and N. L. Letvin. 2001. The KIR and CD94/NKG2 families of molecules in the rhesus monkey. *Immunol. Rev.* 183: 25–40.
36. Kruse, P. H., C. Rosner, and L. Walter. 2010. Characterization of rhesus macaque KIR genotypes and haplotypes. *Immunogenetics* 62: 281–293.
37. Hershberger, K. L., J. Kurian, B. T. Korber, and N. L. Letvin. 2005. Killer cell immunoglobulin-like receptors (KIR) of the African-origin sabaeus monkey: evidence for recombination events in the evolution of KIR. *Eur. J. Immunol.* 35: 922–935.
38. Moesta, A. K., L. Abi-Rached, P. J. Norman, and P. Parham. 2009. Chimpanzees use more varied receptors and ligands than humans for inhibitory killer cell Ig-

like receptor recognition of the MHC-C1 and MHC-C2 epitopes. *J. Immunol.* 182: 3628–3637.
39. Moesta, A. K., T. Graef, L. Abi-Rached, A. M. Older Aguilar, L. A. Guethlein, and P. Parham. 2010. Humans differ from other hominids in lacking an activating NK cell receptor that recognizes the C1 epitope of MHC class I. *J. Immunol.* 185: 4233–4237.
40. Boyington, J. C., S. A. Motyka, P. Schuck, A. G. Brooks, and P. D. Sun. 2000. Crystal structure of an NK cell immunoglobulin-like receptor in complex with its class I MHC ligand. *Nature* 405: 537–543.
41. Robertson, M. J., K. J. Cochran, C. Cameron, J. M. Le, R. Tantravahi, and J. Ritz. 1996. Characterization of a cell line, NKL, derived from an aggressive human natural killer cell leukemia. *Exp. Hematol.* 24: 406–415.
42. Graef, T., A. K. Moesta, P. J. Norman, L. Abi-Rached, L. Vago, A. M. Older Aguilar, M. Gleimer, J. A. Hammond, L. A. Guethlein, D. A. Bushnell, et al. 2009. KIR2DS4 is a product of gene conversion with KIR3DL2 that introduced specificity for HLA-A*11 while diminishing avidity for HLA-C. *J. Exp. Med.* 206: 2557–2572.
43. Michaëlsson, J., C. Teixeira de Matos, A. Achour, L. L. Lanier, K. Kärre, and K. Söderström. 2002. A signal peptide derived from hsp60 binds HLA-E and interferes with CD94/NKG2A recognition. *J. Exp. Med.* 196: 1403–1414.
44. Cerundolo, V., J. Alexander, K. Anderson, C. Lamb, P. Cresswell, A. McMichael, F. Gotch, and A. Townsend. 1990. Presentation of viral antigen controlled by a gene in the major histocompatibility complex. *Nature* 345: 449–452.
45. Marsh, S. G., E. D. Albert, W. F. Bodmer, R. E. Bontrop, B. Dupont, H. A. Erlich, M. Fernández-Viña, D. E. Geraghty, R. Holdsworth, C. K. Hurley, et al. 2010. Nomenclature for factors of the HLA system, 2010. *Tissue Antigens* 75: 291–455.
46. Winter, C. C., and E. O. Long. 2000. Binding of soluble KIR-Fc fusion proteins to HLA class I. *Methods Mol. Biol.* 121: 239–250.
47. Dukkipati, A., J. Vaclavikova, D. Waghray, and K. C. Garcia. 2006. In vitro reconstitution and preparative purification of complexes between the chemokine receptor CXCR4 and its ligands SDF-1alpha, gp120-CD4 and AMD3100. *Protein Expr. Purif.* 50: 203–214.
48. Pei, R., J. H. Lee, N. J. Shih, M. Chen, and P. I. Terasaki. 2003. Single human leukocyte antigen flow cytometry beads for accurate identification of human leukocyte antigen antibody specificities. *Transplantation* 75: 43–49.
49. El-Awar, N., J. Lee, and P. I. Terasaki. 2005. HLA antibody identification with single antigen beads compared to conventional methods. *Hum. Immunol.* 66: 989–997.
50. Barnstable, C. J., W. F. Bodmer, G. Brown, G. Galfre, C. Milstein, A. F. Williams, and A. Ziegler. 1978. Production of monoclonal antibodies to group A erythrocytes, HLA and other human cell surface antigens-new tools for genetic analysis. *Cell* 14: 9–20.
51. Brodsky, F. M., W. F. Bodmer, and P. Parham. 1979. Characterization of a monoclonal anti-beta 2-microglobulin antibody and its use in the genetic and biochemical analysis of major histocompatibility antigens. *Eur. J. Immunol.* 9: 536–545.
52. Parham, P., M. J. Androlewicz, N. J. Holmes, and B. E. Rothenberg. 1983. Arginine 45 is a major part of the antigenic determinant of human beta 2-microglobulin recognized by mouse monoclonal antibody BBM.1. *J. Biol. Chem.* 258: 6179–6186.
53. Brodsky, F. M., and P. Parham. 1982. Evolution of HLA antigenic determinants: species cross-reactions of monoclonal antibodies. *Immunogenetics* 15: 151–166.
54. Brodsky, F. M., and P. Parham. 1982. Monomorphic anti-HLA-A,B,C monoclonal antibodies detecting molecular subunits and combinatorial determinants. *J. Immunol.* 128: 129–135.
55. Fan, Q. R., E. O. Long, and D. C. Wiley. 2001. Crystal structure of the human natural killer cell inhibitory receptor KIR2DL1-HLA-Cw4 complex. *Nat. Immunol.* 2: 452–460.
56. Older Aguilar, A. M., L. A. Guethlein, L. Abi-Rached, and P. Parham. 2011. Natural variation at position 45 in the D1 domain of lineage III killer cell immunoglobulin-like receptors (KIR) has major effects on the avidity and specificity for MHC class I. *Immunogenetics* 63: 543–547.
57. Barber, L. D., L. Percival, N. M. Valiante, L. Chen, C. Lee, J. E. Gumperz, J. H. Phillips, L. L. Lanier, J. C. Bigge, R. B. Parekh, and P. Parham. 1996. The inter-locus recombinant HLA-B*4601 has high selectivity in peptide binding and functions characteristic of HLA-C. *J. Exp. Med.* 184: 735–740.
58. Boyington, J. C., and P. D. Sun. 2002. A structural perspective on MHC class I recognition by killer cell immunoglobulin-like receptors. *Mol. Immunol.* 38: 1007–1021.
59. Della Chiesa, M., E. Romeo, M. Falco, M. Balsamo, R. Augugliaro, L. Moretta, C. Bottino, A. Moretta, and M. Vitale. 2008. Evidence that the KIR2DS5 gene codes for a surface receptor triggering natural killer cell function. *Eur. J. Immunol.* 38: 2284–2289.
60. VandenBussche, C. J., T. J. Mulrooney, W. R. Frazier, S. Dakshanamurthy, and C. K. Hurley. 2009. Dramatically reduced surface expression of NK cell receptor KIR2DS3 is attributed to multiple residues throughout the molecule. *Genes Immun.* 10: 162–173.
61. Wagtmann, N., S. Rajagopalan, C. C. Winter, M. Peruzzi, and E. O. Long. 1995. Killer cell inhibitory receptors specific for HLA-C and HLA-B identified by direct binding and by functional transfer. *Immunity* 3: 801–809.
62. Pende, D., R. Biassoni, C. Cantoni, S. Verdiani, M. Falco, C. di Donato, L. Accame, C. Bottino, A. Moretta, and L. Moretta. 1996. The natural killer cell receptor specific for HLA-A allotypes: a novel member of the p58/p70 family of inhibitory receptors that is characterized by three immunoglobulin-like domains and is expressed as a 140-kD disulphide-linked dimer. *J. Exp. Med.* 184: 505–518.
63. Andersson, S., C. Fauriat, J. A. Malmberg, H. G. Ljunggren, and K. J. Malmberg. 2009. KIR acquisition probabilities are independent of self-HLA class I ligands and increase with cellular KIR expression. *Blood* 114: 95–104.
64. Yawata, M., N. Yawata, M. Draghi, F. Partheniou, A. M. Little, and P. Parham. 2008. MHC class I-specific inhibitory receptors and their ligands structure diverse human NK-cell repertoires toward a balance of missing self-response. *Blood* 112: 2369–2380.
65. Colonna, M., F. Navarro, T. Bellón, M. Llano, P. García, J. Samaridis, L. Angman, M. Cella, and M. López-Botet. 1997. A common inhibitory receptor for major histocompatibility complex class I molecules on human lymphoid and myelomonocytic cells. *J. Exp. Med.* 186: 1809–1818.
66. Fanger, N. A., D. Cosman, L. Peterson, S. C. Braddy, C. R. Maliszewski, and L. Borges. 1998. The MHC class I binding proteins LIR-1 and LIR-2 inhibit Fc receptor-mediated signaling in monocytes. *Eur. J. Immunol.* 28: 3423–3434.
67. Jones, D. C., V. Kosmoliaptsis, R. Apps, N. Lapaque, I. Smith, A. Kono, C. Chang, L. H. Boyle, C. J. Taylor, J. Trowsdale, and R. L. Allen. 2011. HLA class I allelic sequence and conformation regulate leukocyte Ig-like receptor binding. *J. Immunol.* 186: 2990–2997.
68. Shiroishi, M., K. Tsumoto, K. Amano, Y. Shirakihara, M. Colonna, V. M. Braud, D. S. Allan, A. Makadzange, S. Rowland-Jones, B. Willcox, et al. 2003. Human inhibitory receptors Ig-like transcript 2 (ILT2) and ILT4 compete with CD8 for MHC class I binding and bind preferentially to HLA-G. *Proc. Natl. Acad. Sci. USA* 100: 8856–8861.
69. Willcox, B. E., L. M. Thomas, and P. J. Bjorkman. 2003. Crystal structure of HLA-A2 bound to LIR-1, a host and viral major histocompatibility complex receptor. *Nat. Immunol.* 4: 913–919.
70. Boyington, J. C., A. G. Brooks, and P. D. Sun. 2001. Structure of killer cell immunoglobulin-like receptors and their recognition of the class I MHC molecules. *Immunol. Rev.* 181: 66–78.
71. Sanjanwala, B., M. Draghi, P. J. Norman, L. A. Guethlein, and P. Parham. 2008. Polymorphic sites away from the Bw4 epitope that affect interaction of $Bw4^+$ HLA-B with KIR3DL1. *J. Immunol.* 181: 6293–6300.
72. Gonzalez-Galarza, F. F., S. Christmas, D. Middleton, and A. R. Jones. 2011. Allele frequency net: a database and online repository for immune gene frequencies in worldwide populations. *Nucleic Acids Res.* 39(Database issue): D913–D919.
73. Sivori, S., M. Falco, S. Carlomagno, E. Romeo, C. Soldani, A. Bensussan, A. Viola, L. Moretta, and A. Moretta. 2010. A novel KIR-associated function: evidence that CpG DNA uptake and shuttling to early endosomes is mediated by KIR3DL2. *Blood* 116: 1637–1647.
74. Abi-Rached, L., and P. Parham. 2005. Natural selection drives recurrent formation of activating killer cell immunoglobulin-like receptor and Ly49 from inhibitory homologues. *J. Exp. Med.* 201: 1319–1332.
75. Biassoni, R., A. Pessino, A. Malaspina, C. Cantoni, C. Bottino, S. Sivori, L. Moretta, and A. Moretta. 1997. Role of amino acid position 70 in the binding affinity of p50.1 and p58.1 receptors for HLA-Cw4 molecules. *Eur. J. Immunol.* 27: 3095–3099.
76. Hiby, S. E., R. Apps, A. M. Sharkey, L. E. Farrell, L. Gardner, A. Mulder, F. H. Claas, J. J. Walker, C. W. Redman, L. Morgan, et al. 2010. Maternal activating KIRs protect against human reproductive failure mediated by fetal HLA-C2. *J. Clin. Invest.* 120: 4102–4110.
77. Litwin, V., J. Gumperz, P. Parham, J. H. Phillips, and L. L. Lanier. 1994. NKB1: a natural killer cell receptor involved in the recognition of polymorphic HLA-B molecules. *J. Exp. Med.* 180: 537–543.

PLOS | GENETICS

RESEARCH ARTICLE

Loss and Gain of Natural Killer Cell Receptor Function in an African Hunter-Gatherer Population

Hugo G. Hilton[1], Paul J. Norman[1]*, Neda Nemat-Gorgani[1], Ana Goyos[1], Jill A. Hollenbach[2], Brenna M. Henn[3], Christopher R. Gignoux[4], Lisbeth A. Guethlein[1], Peter Parham[1]

1 Departments of Structural Biology and Microbiology & Immunology, Stanford University School of Medicine, Stanford, California, United States of America, **2** Department of Neurology, University of California, San Francisco, California, United States of America, **3** Department of Ecology and Evolution, Stony Brook University, Stony Brook, New York, United States of America, **4** Department of Genetics, Stanford University School of Medicine, Stanford, California, United States of America

* paul.norman@stanford.edu

Citation: Hilton HG, Norman PJ, Nemat-Gorgani N, Goyos A, Hollenbach JA, Henn BM, et al. (2015) Loss and Gain of Natural Killer Cell Receptor Function in an African Hunter-Gatherer Population. PLoS Genet 11(8): e1005439. doi:10.1371/journal.pgen.1005439

Editor: Sarah A Tishkoff, University of Pennsylvania, UNITED STATES

Received: December 17, 2014

Accepted: July 13, 2015

Published: August 20, 2015

Data Availability Statement: A curated database of KIR alleles including novel alleles identified in the current paper (GU323355 and JX523630) are available at http://www.ebi.ac.uk/ipd/kir/. All other relevant data are within the paper and its Supporting Information files.

Funding: This study was supported by National Institutes of Health grant AI17892 and AI090905 to PP and GM109030 to PP and JAH. HGH was also supported by the March of Dimes Prematurity Center at Stanford University School of Medicine, Clinical and Translational Science Awards Grant ULI

Abstract

Modulating natural killer cell functions in human immunity and reproduction are diverse interactions between the killer cell immunoglobulin-like receptors (KIR) of Natural Killer (NK) cells and HLA class I ligands on the surface of tissue cells. Dominant interactions are between KIR2DL1 and the C2 epitope of HLA-C and between KIR2DL2/3 and the C1 epitope of HLA-C. KhoeSan hunter-gatherers of Southern Africa represent the earliest population divergence known and are the most genetically diverse indigenous people, qualities reflected in their *KIR* and *HLA* genes. Of the ten KhoeSan *KIR2DL1* alleles, *KIR2DL1*022* and *KIR2DL1*026* likely originated in the KhoeSan, and later were transmitted at low frequency to the neighboring Zulus through gene flow. These alleles arose by point mutation from other KhoeSan *KIR2DL1* alleles that are more widespread globally. Mutation of *KIR2DL1*001* gave rise to *KIR2DL1*022*, causing loss of C2 recognition and gain of C1 recognition. This makes KIR2DL1*022 a more avid and specific C1 receptor than any KIR2DL2/3 allotype. Mutation of *KIR2DL1*012* gave rise to *KIR2DL1*026*, causing premature termination of translation at the end of the transmembrane domain. This makes KIR2DL1*026 a membrane-associated receptor that lacks both a cytoplasmic tail and signaling function. At higher frequencies than their parental allotypes, the combined effect of the KhoeSan-specific KIR2DL1*022 and KIR2DL1*026 is to reduce the frequency of strong inhibitory C2 receptors and increase the frequency of strong inhibitory C1 receptors. Because interaction of KIR2DL1 with C2 is associated with risk of pregnancy disorder, these functional changes are potentially advantageous. Whereas all other KhoeSan *KIR2DL1* alleles are present on a wide diversity of centromeric *KIR* haplotypes, *KIR2DL1*026* is present on a single *KIR* haplotype and *KIR2DL1*022* is present on two very similar haplotypes. The high linkage disequilibrium across their haplotypes is consistent with a recent emergence for these *KIR2DL1* alleles that have distinctive functions.

RR025744 and a Stanford University School of Medicine Dean's Postdoctoral Fellowship.The funders had no role in study design, data collection and analysis, decision to publish, or preparation of the manuscript.

Competing Interests: The authors have declared that no competing interests exist.

Author Summary

The genes that control the response of the human immune system vary enormously between individuals. Understanding the evolution of these genetic differences and how they individualize immune responses is central to understanding how the immune system works in health and disease. In this regard, the KhoeSan of southern Africa are particularly informative because they are genetically diverse, divergent from other modern human populations and have been subject to unique demographic history. In the KhoeSan population, we studied variable genes that control natural killer cell function. We identified two recently evolved, novel gene variants that have unusual function; one completely changed its ligand specificity and the other lost its capacity for signal transduction.

Introduction

Natural killer (NK) cells are versatile lymphocytes that contribute to reproduction and immune defense [1,2]. Modulating the activities of human NK-cells are the killer-cell immunoglobulin-like receptors (KIR). These receptors engage the HLA class I ligands (HLA-A, -B and -C) expressed on the surface of most human cells. Such interactions direct NK cells to kill virus-infected cells and tumor cells; they also induce the secretion of cytokines that activate other leukocytes or guide fetal trophoblast cells to invade the uterus during pregnancy. In human populations, both receptors and ligands are highly polymorphic. Their combinatorial diversity contributes to the resistance of individuals to infection, and their susceptibility to autoimmunity and pregnancy syndromes [1,3]. A minority of HLA-A and -B allotypes are ligands for KIR, whereas all HLA-C allotypes fulfill this role. HLA-C arose more recently than HLA-A and -B and has evolved to become the predominant polymorphic KIR ligand [4]. In reproduction it is the only polymorphic ligand, because HLA-C is expressed by fetal trophoblast cells whereas HLA-A and -B are not [1].

KIR engage the upward face of the HLA class I molecule formed by the α_1 domain, the α_2 domain and the bound peptide antigen [5]. αβ T cell receptors engage the same face, in an overlapping but different way [6]. Dimorphism at position 80 in the α_1 domain of HLA-C defines two mutually exclusive epitopes, C1 (asparagine 80) and C2 (lysine 80), recognized by different KIR [7]. All the numerous (>1,700) HLA-C allotypes have either the C1 or C2 epitope. Human KIR are comprised of four phylogenetic lineages, of which the KIR that recognize HLA-C are all lineage III [4]. They have two extracellular immunoglobulin-like domains (D1 and D2), which together form the site that binds HLA-C [5]. Within the binding site, dimorphism at position 44 in the D1 domain determines if a KIR is specific for C1 (lysine 44) or C2 (methionine 44). *KIR2DL1* and *KIR2DS1* encode inhibitory and activating C2 receptors, respectively. *KIR2DL2/3* encodes inhibitory C1 receptors. (There is no activating C1 receptor). The inhibitory receptors are highly polymorphic, with 25 KIR2DL1 and 36 KIR2DL2/3 variants being defined, whereas KIR2DS1 with seven variants is relatively conserved.

Among individuals and populations, *KIR* are further diversified by gene content variation [8]. Whereas *KIR2DL2/3* is present on almost every human *KIR* haplotype described, neither *KIR2DL1* nor *KIR2DS1* are present on every haplotype. Represented in every human population are two distinctive *KIR* haplotype groups: *A* and *B* [1]. KIR *A* haplotypes encode high avidity inhibitory receptors for HLA class I and have one activating receptor gene; *B* haplotypes encode low avidity inhibitory receptors for HLA class I and have several activating receptor genes. This bipartite system of functionally distinctive *KIR* haplotypes appears unique to humans because it is not present in chimpanzees or any other species investigated [9].

For reasons of practicality, the functional properties of KIR2DL1 and KIR2DL2/3 have been studied mainly in the context of allotypic variants that combine high avidity, high specificity and high frequency in Europeans [1]. In contrast, for sub-Saharan African populations, which have the highest genetic diversity [10–12] and among the highest mortality from infectious disease and pregnancy complications [13], KIR investigation is in its infancy and has so far focused on West African and Bantu-speaking populations [14]. Within sub-Saharan Africa, some indigenous populations are as different from each other as they are from Europeans [10,12,15]. Notably, the KhoeSan who reside across southern Africa descend from the deepest human population divergence and have among the greatest genetic diversity of any population [10,16,17]. During the last 2,000 years there has been admixture between the KhoeSan and Bantu-speaking agriculturalists who expanded southwards [11,18]. More recently, the arrival of European colonists over the past 500 years has introduced novel infectious diseases including smallpox and tuberculosis [19]. Here we describe high-resolution genetic and functional studies on the HLA-C specific KIR of the KhoeSan and their comparison to other populations.

Results

Two unusual *KIR2DL1* alleles evolved in the KhoeSan after their divergence from other modern humans

From analysis of 61 KhoeSan we identified ten *KIR2DL1* alleles (Fig 1A and S1A Fig). Of these, *2DL1*022* and *2DL1*026* are new discoveries that have frequencies in the KhoeSan of 17.2% and 4.2%, respectively. Being absent from all previously studied populations [14,20–24], suggested that *2DL1*022* and *2DL1*026* are specific to the KhoeSan. To test this hypothesis we examined additional populations for the presence of these alleles. We first examined data from the 1000 Genomes project dataset [25] by probing for sequence-specific reads that correspond to the *2DL1*022* and *2DL1*026* alleles. *KIR3DL3*, a framework gene present on all *KIR* haplotypes, served as the positive control. All 2,496 individuals sampled had reads corresponding to *KIR3DL3*, as did the eight KhoeSan who were analyzed similarly by whole-exome sequencing [26]. The eight KhoeSan individuals also gave allele-specific *KIR2DL1* reads consistent with their high-resolution *KIR2DL1* genotype (S2A Fig). In this context it is striking that none of the 2,496 individuals, representing 26 different populations worldwide (S2B Fig), was found to have either *2DL1*022* or *2DL1*026* (S2C Fig). Because the 1000 Genome dataset represents a limited subset of sub-Saharan African population diversity [12,27], we expanded our search to include four further groups.

To determine if *2DL1*022* or *2DL1*026* are present in African hunter-gatherer populations other than the KhoeSan we examined three groups: the Hadza who are an isolated click-speaking population that live in northern Tanzania [10] and the central African Mbuti and Baka Pygmies. Together with the KhoeSan, these hunter-gatherer groups may have formed a larger proto-KhoeSan-Pygmy population prior to their divergence 50,000–100,000 years ago [12,28,29]. Neither *2DL1*022* nor *2DL1*026* was detected in any Hadza or Pygmy individual (S2C Fig). Despite the relatively low number of individuals sampled (52 Hadza and 40 Pygmies) this result indicates that *2DL1*022* and *2DL1*026* are not present at any appreciable frequency in these groups.

To determine whether *2DL1*022* and *2DL1*026* are present in other southern African populations, we examined 100 Zulu individuals whose genomes were sequenced as part of the African Genome Variation Project [27]. With the same approach used to probe the 1000 Genomes dataset, we identified three Zulus having *2DL1*022* and two having *2DL1*026* (S2C Fig). As these five individuals were all *2DL1* heterozygous, we estimate that the frequencies of *2DL1*022* and *2DL1*026* in the Zulu population are approximately 1.5% and 1%, respectively.

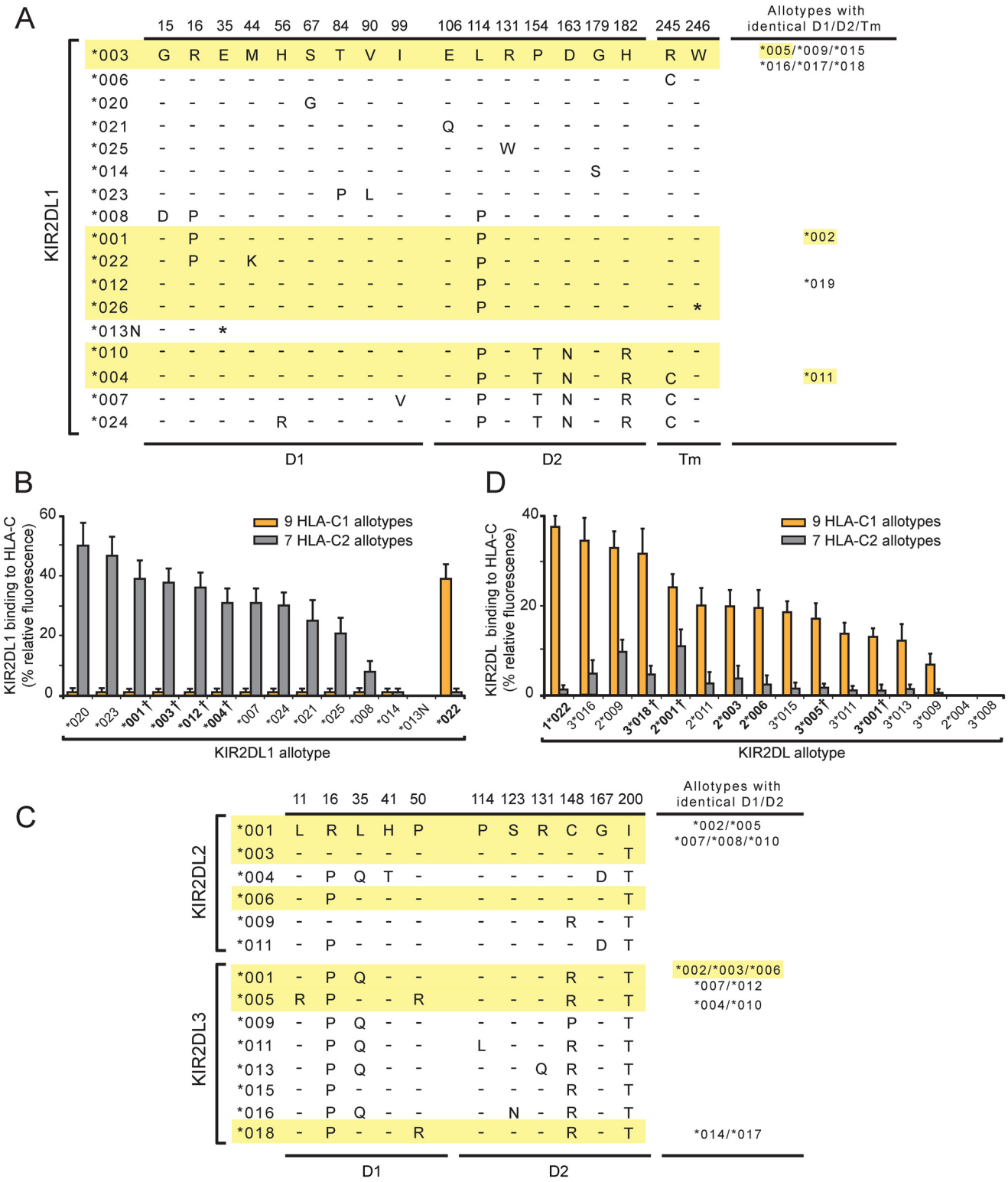

Fig 1. A variant of KIR2DL1 originating in the KhoeSan is a C1-specific receptor and not a C2-specific receptor like other KIR2DL1. (A) This alignment of KIR2DL1 sequence differences shows the sites of polymorphism in the D1 domain (D1), the D2 domain (D2) and the transmembrane region (Tm). Dashes denote identity with the KIR2DL1*003 sequence, an asterisk denotes a termination codon. Sequences of the KhoeSan KIR2DL1 allotypes are highlighted in yellow. The names of allotypes with D1, D2 and Tm identical to an aligned sequence are listed in the column at the right. (B) Binding of KIR2DL1-Fc fusion proteins to microbeads coated with C1-bearing and seven C2-bearing HLA-C allotypes. Each binding value was normalized to that of the

W6/32 antibody and these normalized values were averaged for the C1 (N = 9) and C2 (N = 7) allotype groups. The names of allotypes present in the KhoeSan are boldened. A dagger following the listed allotype indicates that the allotype represents a group of two or more alleles that encode identical ligand binding domains (see Panel A). (C) This alignment of KIR2DL2/3 sequence differences shows the sites of polymorphism in the D1 and D2 domains. Dashes denote identity with the KIR2DL2*001 sequence Sequences of the KhoeSan KIR2DL2/3 allotypes are highlighted in yellow. The names of allotypes with D1 and D2 identical to an aligned sequence are listed in the column at the right. (D) Binding of KIR2DL2/3-Fc fusion proteins to microbeads coated with C1-bearing and C2-bearing HLA-C allotypes. Each binding value was normalized to that of the W6/32 antibody and these normalized values were averaged for the C1 (N = 9) and C2 (N = 7) groups. The names of allotypes present in the KhoeSan are boldened. Groups of allotypes with identical D1 and D2 domains, and which are represented by a single KIR2DL2/3-Fc, are as shown in the column on the right of Panel A. A dagger following the listed allotype indicates that the allotype represents a group of two or more alleles that encode identical ligand binding domains (see Panel A).

doi:10.1371/journal.pgen.1005439.g001

Examination of the centromeric half of the *KIR* haplotypes, the location of the *KIR2DL1* gene, showed that each Zulu allele is likely present on the identical haplotype background to that found in the KhoeSan (S3 Fig). Together with their low frequencies, this suggests that these alleles were introduced into the Zulu population as a result of admixture with KhoeSan hunter-gatherers. This interpretation is supported by studies that have demonstrated recent KhoeSan admixture with the Zulus [10,11,18,27] and by the absence of both *2DL1*022* and *2DL1*026* from a Bantu-speaking population in east Africa (Kenyan Luhya from the 1000 Genomes dataset). These data support an evolutionary model in which *2DL1*022* and *2DL1*026* rose in frequency in the KhoeSan populations sometime after their divergence from the other groups and thus within the past 100,000 years [12,28,29].

*KIR2DL1*022* differs from *2DL1*001*, also present in the KhoeSan, by a single non-synonymous substitution in codon 44 (Fig 1A). Thus *2DL1*022* likely evolved from *2DL1*001* by a point mutation that caused methionine to be replaced by lysine at position 44 (Fig 1A). Position 44 dimorphism determines whether a given KIR2DL has specificity for the C1 or C2 epitope of HLA-C [7]. Prior to investigation of the KhoeSan, all the known KIR2DL1 allotypes (n = 23) had methionine 44 and were predicted to be C2-specific. Conversely, and in complementary fashion, the known KIR2DL2/3 allotypes (n = 36) all had lysine 44 and were predicted to be C1 specific. In this context, 2DL1*022 appears an extraordinary KIR2DL1 allotype, being predicted to be a C1 receptor and not a C2 receptor like other KIR2DL1 allotypes. Thus, the mutation that created *2DL1*022* had two important functional effects: loss of C2 recognition and gain of C1 recognition.

*KIR2DL1*026*, the other KhoeSan-specific *KIR2DL1* allele, differs from *2DL1*012*, also present in the KhoeSan, by one nucleotide substitution. Thus *KIR2DL1*026* likely arose from *2DL1*012* by point mutation. This substitution converted the tryptophan codon at position 246 to a termination codon (Fig 1A). Position 246 is situated at the boundary between the transmembrane domain and the cytoplasmic tail. Consequently, 2DL1*026 lacks the immunoreceptor tyrosine-based inhibitory motifs of the cytoplasmic tail that mediate inhibitory signaling function [30]. Less obvious is the effect that absence of a cytoplasmic tail could have on the association of 2DL1*026 with cellular membranes. Thus, the mutation that created *2DL1*026* clearly has a major effect in abrogating inhibitory signaling function, but it also has potential to alter the amount of receptor that reaches the NK cell-surface.

KhoeSan specific 2DL1*022 is an unusually strong and specific C1 receptor

To determine the avidity and specificity of 2DL1*022 for HLA class I, and also to compare its binding reactivity with other KIR2DL1 allotypes, we made a panel of 14 KIR2DL1-Fc fusion proteins that covers the allotypic range of KIR2DL1 binding sites (Fig 1A). Each KIR-Fc was tested for binding to a panel of 97 microbeads in which each bead is coated with one of 31 HLA-A, 50 HLA-B and 16 HLA-C allotypes. Our previous work has shown that the results

obtained with this cell-free bead-binding assay correlate well with those derived from in vitro functional assays of NK cell cytotoxicity [31,32].

Assessment of the pairwise interactions between 14 KIR2DL1-Fc and 16 HLA-C allotypes shows that 2DL1*022 binds to all nine C1-bearing HLA-C allotypes but to none of the seven C2-bearing HLA-C allotypes in the test panel (Fig 1B). KIR2DL1*022 also binds HLA-B*46:01 and HLA-B*73:01, two exceptional C1-bearing HLA-B allotypes but to no other HLA-B allotype, or any HLA-A allotype. Eleven HLA-C1 bearing allotypes are present in the KhoeSan (S1C Fig). Neither HLA-B*46:01 or HLA-B*73:01 are present in the KhoeSan, their distributions being focused on Southeast Asia (B*46:01) or West Asia (B*73:01) [9,33,34]. As we predicted, 2DL1*022 functions as a C1-specific receptor and not a C2-specific receptor like eleven of the 13 other KIR2DL1-Fc. These eleven KIR2DL1-Fc molecules varied in their avidity for C2 by half an order of magnitude. In contrast, 2DL1*013N-Fc and 2DL1*014-Fc bound to no HLA class I allotype (Fig 1B). For 2DL1*013N this result was anticipated, because the protein is a fragment that terminates prematurely at residue 34 in the D1 domain. On the other hand, 2DL1*014 was expected to bind HLA class I, because it differs from 2DL1*003 only by substitution of glycine for serine at position 179 in the D2 domain (Fig 1A). Neither the 2DL1*013N nor the 2DL1*014 allotype is present in the KhoeSan. Overall, these results vividly illustrate how the natural polymorphism of KIR2DL1 modulates the avidity, specificity and functionality of this NK cell receptor in human populations.

In the KhoeSan, mutation of 2DL1*001, a strong C2 receptor, produced the C1 receptor, 2DL1*022. We therefore examined how the properties of 2DL1*022 compare to the prototypical C1 receptors encoded by the *KIR2DL2/3* gene. (This gene has two distinctive allelic lineages, *2DL2* and *2DL3*, hence the *KIR2DL2/3* name). KIR-Fc proteins were made from six 2DL2 and nine 2DL3 allotypes (Fig 1C) and their binding to HLA class I coated beads was compared to 2DL1*022 (Fig 1D). As a group, the KIR2DL2/3 allotypes are not as specific for C1 as the KIR2DL1 allotypes are for C2. KIR2DL2/3 exhibit a range of avidity for C1, but increasing avidity for C1 is accompanied by increased cross-reactivity with C2 (Fig 1D). This is, however, not the case for 2DL1*022, which has a higher avidity for C1 than any of the KIR2DL2/3 allotypes, but no significant C2 cross-reactivity. KIR2DL1*022 has completely lost recognition of C2 while gaining a stronger, more specific, recognition of C1 than any KIR2DL2/3 allotype. Thus KIR2DL1*022 is seen to have unique functional properties, ones that will clearly have a profound functional impact on the KhoeSan and Zulu individuals who carry this allele.

The interactions of KIR2DL with HLA-C are not only diversified by KIR2DL1 and KIR2DL2/3 polymorphism, but also by polymorphism within the subsets of C1-bearing and C2-bearing HLA-C allotypes. Binding to C2 by the 11 KIR2DL1 allotypes varied over half an order of magnitude and with a similar hierarchy for each of the KIR allotypes (Fig 2A). Thus HLA-C*15:02 is always the strongest ligand for KIR2DL1 and HLA-C*04:01 the weakest. Analogous patterns were observed for the binding of 2DL1*022 and the 15 KIR2DL2/3 allotypes to C1-bearing HLA-B and -C allotypes (Fig 2B). Here, HLA-B*73:01 is the strongest ligand for 2DL1*022 and KIR2DL2/3 and HLA-C*16:01 the weakest. The basis for these hierarchies within the C1- and C2-bearing allotypes arise from either the differing peptide repertoires presented by specific HLA-C or by polymorphism at sites other than position 80 that defines the C1 and C2 epitopes.

KhoeSan specific 2DL1*026 lacks a cytoplasmic tail but is cell-surface expressed

*KIR2DL1*026* and *2DL1*012* encode identical extracellular domains that bind C2 with high avidity and specificity (Fig 1B). To determine if 2DL1*026, which lacks a cytoplasmic tail,

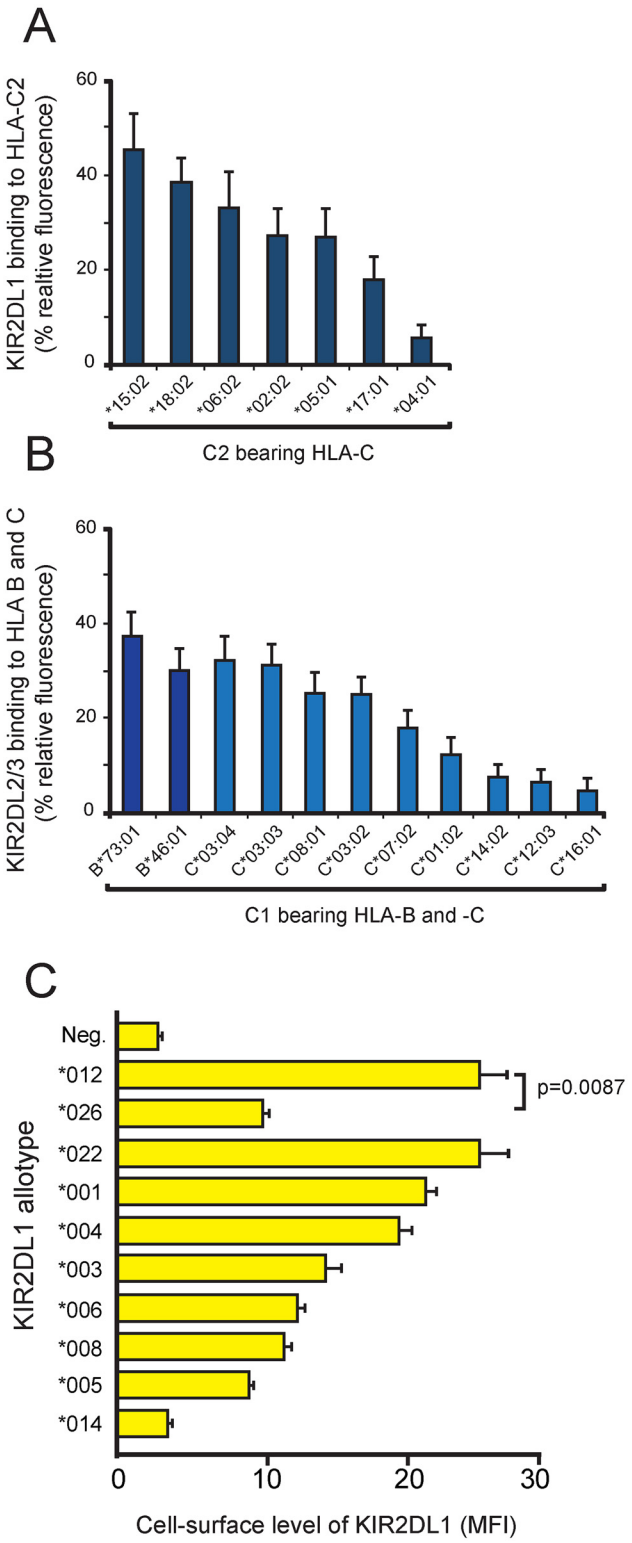

Fig 2. KIR polymorphism modulates the avidity and specificity for HLA-C, as well as KIR abundance at the cell surface. (A) Binding of KIR2DL1-Fc fusion proteins to C2-bearing HLA-C allotypes. For each C2-bearing HLA-C allotype, the KIR2DL1 binding is the mean of the values obtained with 11 different KIR2DL1-Fc (2DL1*001, *003, *004, *007, *008, *012, *020, *021, *023 *024, *025). Each individual binding value was normalized to the binding of the W6/32 antibody before calculating the average. (B)

Binding of KIR2DL1*022-Fc and KIR2DL2/3-Fc fusion proteins to C1-bearing HLA-B and -C allotypes. For each C1-bearing HLA-B and HLA-C allotype, the KIR2DL2/3 binding is the mean of the values obtained with 16 KIR2DL-Fc fusion proteins (2DL1*022; 2DL2*001,*003, *004, *006, 009 *011; and 2DL3*001, *005, *008, *009, *011, *013, *015, *016, *018). The proteins were tested against microbeads coated with one of nine C1 HLA-C or two C1 HLA-B allotypes. Each individual binding value was normalized to the binding to that of the W6/32 antibody before calculating the average. (C) Variable cell-surface expression of KIR2DL1. FLAG-tagged KIR2DL1 allotypes were transfected into HeLa cells. Cell-surface expression was detected using FLAG-specific antibody and analysis by flow cytometry. MFI = median fluorescence intensity. The experiment was performed in triplicate, error bars give the standard deviation. The difference between 2DL1*012 and 2DL1*026 is statistically significant as assessed by a two-tailed t-test.

doi:10.1371/journal.pgen.1005439.g002

reaches the cell-surface, we examined the expression of FLAG-tagged 2DL1*026 and 2DL1*012 in transiently transfected HeLa cells. For comparison, eight other KIR2DL1 allotypes were included in the analysis (Fig 2C). KIR2DL1*026 is cell-surface expressed at a significantly lower level than 2DL1*012 ($p = 0.0087$), but within the range observed for other KIR2DL1 allotypes. Although KIR2DL1*026 cannot mediate NK cell inhibition directly, because it lacks a cytoplasmic domain, it could have indirect effects, either by preventing C2 from binding to other receptors or by contributing to the adhesive interactions of NK cells with target cells. That 2DL1*014 is not cell-surface expressed and cannot bind HLA class I suggests that its defining residue, serine 179, prevents proper protein folding. Other KIR allotypes with impaired folding that causes intracellular retention have been described [35–37].

Characterizing the KhoeSan population is a high frequency of weak C2 receptors

Unlike some other populations, there is no single *2DL1* allele that is present at high frequency in the KhoeSan (Fig 3 and S1A Fig). The ten KhoeSan *2DL1* alleles vary in frequency from 1.1–21.3%. In addition, 18% of KhoeSan *KIR* haplotypes lack the *KIR2DL1* gene, constituting an eleventh allele: the 'blank'. The frequency of *2DL1*022*, (17.2%) is more than double that of *2DL1*001* (7.0%), the parental allele from which it evolved. Likewise, *2DL1*026* (4.2%) has a higher frequency than *2DL1*012* (1.1%), the parental allele from which it evolved. The impact of both *2DL1*022* and *2DL1*026* has been to reduce the capacity of KIR2DL1 to function as an inhibitory C2 receptor in the KhoeSan.

This effect of the KhoeSan-specific *KIR2DL1* alleles is reinforced by the relatively low frequency in the KhoeSan of other alleles encoding strong inhibitory C2 receptors (2DL1*001, *002, *003 and *005) and relatively high frequency of alleles encoding weaker inhibitory C2 receptors. Included in the latter are the 'blank', the 2DL1*004, 2DL1*010 and 2DL1*011 receptors that have reduced avidity for C2 (Fig 1B and S4 Fig) and the 2DL1*004 and 2DL1*011 allotypes that have reduced signaling capacity caused by the cysteine residue at position 245 [38] (Fig 1A). In sum, the frequency of weak or inactive 2DL1 allotypes in the KhoeSan is 71.8%, whereas the 28.2% frequency of strong 2DL1 allotypes in the KhoeSan is much lower than that of other populations (Fig 3C).

*KIR2DL1*022* and *2DL1*026* are present on conserved haplotypes that are recently evolved

To examine the genetic background of *KIR2DL1*022* and *KIR2DL1*026*, we determined structures for the *KIR2DL1*-containing centromeric region of KhoeSan *KIR* haplotypes. Extensive diversity was observed, there being 70 different haplotypes among a total of 110 haplotypes characterized from 55 unrelated individuals. For each *KIR2DL1* allele we determined how

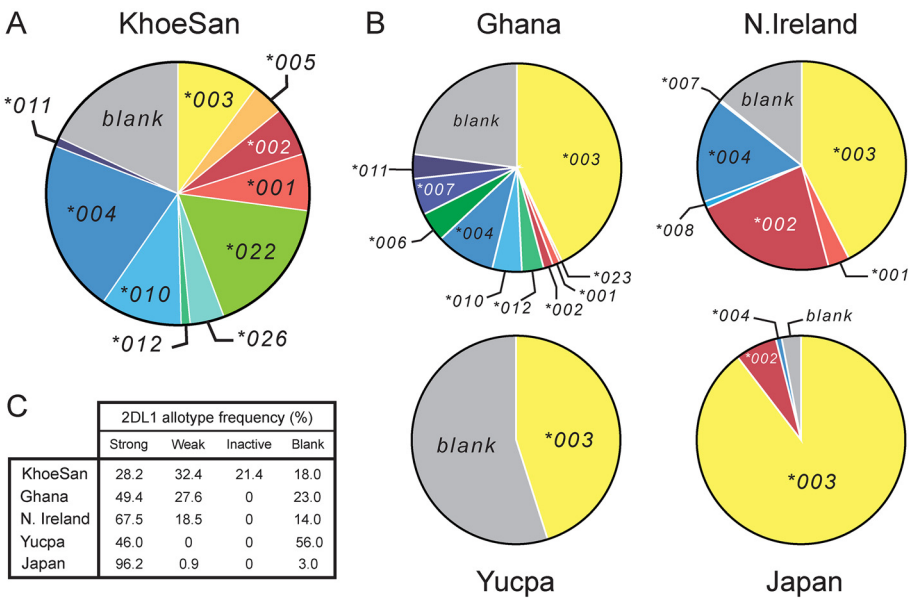

C

	2DL1 allotype frequency (%)			
	Strong	Weak	Inactive	Blank
KhoeSan	28.2	32.4	21.4	18.0
Ghana	49.4	27.6	0	23.0
N. Ireland	67.5	18.5	0	14.0
Yucpa	46.0	0	0	56.0
Japan	96.2	0.9	0	3.0

Fig 3. The KhoeSan have high *KIR2DL1* diversity compared to other human populations. (A and B) The pie charts show the number and relative frequencies of *KIR2DL1* alleles in the KhoeSan of Southern Africa (A), and four other populations representing four continents (B): the Ga-Adangbe from Ghana in Western Africa [14], Northern Ireland Caucasians from Europe [21], Japanese from East Asia [24] and Yucpa Amerindians from South America [20]. The 'blank' is the frequency of *KIR* haplotypes that lack the *KIR2DL1* gene. (C) Also compared in the five populations are the frequencies of strong KIR2DL1, weak KIR2DL1, KIR2DL1 that are not inhibitory C2 receptors (inactive) and the absence of KIR2DL1 (blank). The definition and designation of these KIR2DL1 categories are given in S4 Fig.

doi:10.1371/journal.pgen.1005439.g003

many different haplotypes have the allele and what their frequencies are in the KhoeSan. Because the linkage disequilibrium (LD) between nine of the eleven KhoeSan *2DL1* alleles and other genes of the centromeric region is low, there is a strong positive correlation ($r^2 = 0.96$) between an allele's frequency and the number of different haplotypes on which it occurs (Fig 4A). For example, a total of seven haplotypes have *2DL1*001* and they are all different in their linked *KIR* alleles and genes (Fig 4A). That we find numerous different haplotypes reflects the high diversity of KhoeSan genomes [10,16]. Dramatic exceptions to this pattern are the haplotypes containing the KhoeSan specific *KIR2DL1* alleles, which are in complete LD with the other centromeric *KIR* genes and alleles. Among the 23 haplotypes containing *2DL1*022* only two are unique, and they differ only in *KIR3DL3* at the centromeric end of the *KIR* locus (Fig 4B). The six haplotypes containing *2DL1*026* are all identical (Fig 4B). The high LD across these haplotypes shows that they have not been broken and mixed by meiotic recombination, which is consistent with their recent evolution [39] (Fig 4C).

Discussion

Our study shows how *KIR2DL1* polymorphism has given rise to NK cell receptors that vary substantially in their capacity to recognize HLA-C and propagate intracellular signals. Emphasizing the value of defining structural and functional KIR variation at high resolution is our discovery in the KhoeSan of two unusual allotypes of KIR2DL1, the inhibitory NK cell receptor for the C2 epitope of HLA-C. The alleles encoding these allotypes were derived by point mutation from older, more widespread *KIR2DL1* alleles that encode strong, inhibitory C2 receptors.

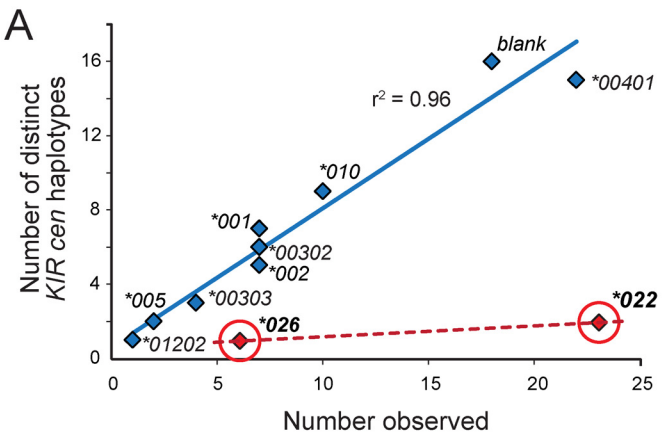

B

	N	3DL3	2DS2	2DL2/3	2DL5	2DS5	2DL1
*022	17	*038	*001	2*003	B*018	*00502	***022**
*022	6	*020	*001	2*003	B*018	*00502	***022**
Par?	1	*038	*001	2*003	B*018	*00502	*001
*026	6	*038	*001	2*003	B*00803	*006	***026**
Par?	1	*056		3*018	B*00803	*006	*01201

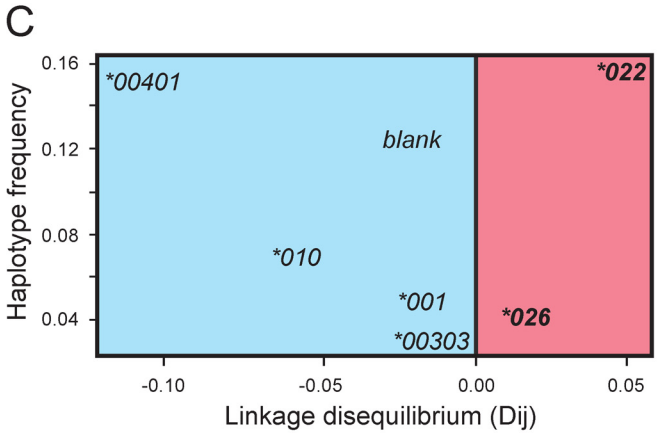

Fig 4. *KIR2DL1*022* and *2DL1*026* are of recent origin compared to other KhoeSan *KIR2DL1* alleles. (A) For each KhoeSan *KIR2DL1* allele, the number of centromeric *KIR* haplotypes on which the allele is present in the KhoeSan (number observed) is plotted against the number of different (distinct) haplotypes on which the allele is present. In total, 110 haplotypes were analyzed. Haplotypes that lack *KIR2DL1* are denoted 'blank'. The r^2 was calculated from Pearson correlation of the alleles shown in blue. This analysis excluded *2DL1*022* and **026* (shown in red). (B) Shows the allele content of centromeric *KIR* haplotypes containing either *2DL1*022* (purple) or *2DL1*026* (yellow). The observed number of each haplotype is given on the left. Also shown (in white) are the KhoeSan haplotypes that are the putative parents (Par?) of the derived *2DL*022*-containing and *2DL1*026*-containing haplotypes. The putative parents are the haplotypes that differ from the derived haplotypes by the least number of nucleotide substitutions. (C) Plot of haplotype frequency against linkage disequilibrium (LD). The analysis was conditioned so that *2DL2*003*-bearing haplotypes were analyzed. The figure illustrates the high level of linkage disequilibrium observed for haplotypes containing *2DL1*022* and *2DL1*026* suggesting they appeared more recently in the KhoeSan population than other *KIR2DL1* alleles.

doi:10.1371/journal.pgen.1005439.g004

In stark contrast to the parental allotypes, neither progeny is a strong, inhibitory C2 receptor. KIR2DL1*026 has no capacity for signal transduction and 2DL1*022 recognizes C1 with specificity and avidity that exceeds that of any KIR2DL2/3 allotype, the archetypal C1 receptor. The methionine to lysine substitution at position 44 that defines KIR2DL1*022 occurs within the HLA-C binding site of the KIR [5]. Here, residue 44 in the D1 domain of the KIR interacts with residue 80 of the α_1 domain of HLA-C. For KIR2DL1*001, the parent allele of KIR2DL1*022, methionine 44 binds to lysine 80 of the C2 epitope of HLA-C [5,7]. In contrast, lysine 44 in KIR2DL1*022 binds to asparagine 80 of the C1 epitope of HLA-C.

KIR2DL1*022 is the most vivid example of how genetic polymorphism can change KIR specificity for HLA class I. For other allotypes of KIR2DL1 and KIR2DL2/3, the effects of their defining substitutions can act to alter different functional properties: receptor avidity [31,32,40], stability, cell-surface abundance and signal transduction [38]. Throughout the KIR molecule are sites where natural substitutions affect receptor functions. Many of these are away from the HLA-C binding site and likely involve conformational changes, including ones that affect the relative orientation of the extracellular D1 and D2 domains that combine to form the binding site [31,40]. That KIR2DL1*022 and 2DL1*026 have lost their parents' capacity to function as inhibitory C2 receptors, exemplifies a more widespread trend in the KhoeSan. That is an accumulation of KIR2DL1 allotypes with low avidity for HLA-C2 or weakened signaling function, as well as *KIR B* haplotypes lacking the *KIR2DL1* gene (Fig 3C).

In human populations worldwide there is an inverse correlation between the frequency of HLA-C allotypes carrying the C2 epitope and the frequency of the *KIR A* haplotypes encoding strong KIR2DL1 allotypes. This correlation reflects the increased risk of spontaneous abortion, preeclampsia, and low birth-weight that is associated with pregnancies in which a *KIR A* homozygous mother who lacks the C2 epitope is carrying a fetus that expresses a C2 epitope of paternal origin [41,42]. In these pregnancies, the interaction of paternal C2 on extravillous trophoblast cells with maternal uterine NK cells expressing the strong KIR2DL1 encoded by *KIR A* haplotypes can lead to incomplete placentation. In general, Africans have a higher frequency of the C2 epitope than other populations and the C2 frequency of the KhoeSan is particularly high (63.4%; Fig 5). The reasons for the high C2 frequency are unknown, but may include

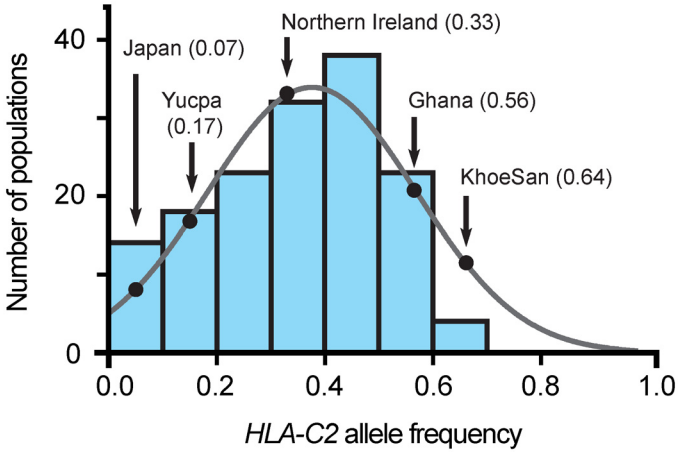

Fig 5. The C2 frequency in the KhoeSan is unusually high. Each of the seven blue-shaded vertical bars gives the number of populations, of 140 considered [34], that have a C2 frequency within the range covered by the bar, given on the horizontal axis. The frequency data are not significantly different from a normal distribution (grey line). The black-shaded dots on the curve give the frequencies for the KhoeSan and the four other populations for which *KIR2DL1* allele frequencies are given in Fig 3.

doi:10.1371/journal.pgen.1005439.g005

protection against specific diseases though interaction of C2-expressing HLA-C with NK cells or CD8 T cells. Thus the emergence of 2DL1*022 and 2DL1*026, as well as the general increase of weaker inhibitory KIR2DL1 allotypes, in the KhoeSan could have acted to reduce the incidence of preeclampsia. In this manner, the KhoeSan retained the ability to both fight infection and reproduce efficiently.

In assessing the effect of a high C2 frequency on the KhoeSan, it is informative to consider the Yucpa, an indigenous South American population that has a low frequency of C2 and a high frequency of C1 (82.7%) [20]. Accompanying the abundance of C1 are two Yucpa-specific *KIR2DL3* alleles, both arising by point mutation of the older, widespread *2DL3*001*. KIR2DL3*009 has lower C1 avidity than 2DL3*001 and 2DL3*008N is non-functional. These Yucpa specific 2DL3 have a frequency of 41.8% compared to 8.2% for their 2DL3*001 parent. In the Yucpa, the high C1 frequency combines with a much-reduced frequency of strong inhibitory C1 receptors, whereas in KhoeSan, the high C2 frequency combines with a much-reduced frequency of strong inhibitory C2 receptors. These analogous behaviors at the two extremes of the frequency spectrum appear to reflect a buffering mechanism that maintains a balance between C1, C2 and their inhibitory receptors in human populations.

One possibility is that *2DL1*022* and *2DL1*026* increased in frequency as a consequence of genetic drift. Thus, they would represent two of the many private alleles that are present in the KhoeSan because of their unique demographic history [12]. Unlike other African hunter-gatherer groups, the KhoeSan have maintained a large effective population size and high levels of genetic diversity [10,43]. These characteristics argue against the KhoeSan having been subject to a classic bottleneck of the type experienced by other African hunter-gatherer populations, such as the Tanzanian Hadza [10], or migrant modern humans who left Africa and populated other continents [44]. An alternative interpretation is that *2DL1*022* and *2DL1*026* rose in frequency in the KhoeSan under positive selection. Supporting this model are the distinctive functional properties of the 2DL1*022 and 2DL1*026 proteins, the evidence for balancing selection at the *KIR* locus [20,24,45,46] and the evidence for diversifying selection at position 44, where lysine determines the unique functionality of KIR2DL1*022 [9]. To establish if drift or selection is responsible for emergence of the new, variant KIR, will require extensive demographic simulations and the development of appropriate programs that simulate co-evolution between unlinked, highly polymorphic loci.

Materials and Methods

Ethics statement

Sampling of the ≠Khomani San in Upington, South Africa and neighboring villages occurred in 2006. Institution Review Board (IRB) approval was obtained from Stanford University [Protocol 13829] for assessment of genetic diversity and ancestry inference. Individuals who were still living in 2011 were re-consented (IRB approved from Stanford University and Stellenbosch University, South Africa). ≠Khomani N|u-speaking individuals, local community leaders, traditional leaders, non-profit organizations and a legal counselor were all consulted regarding the aims of this research, prior to collection of DNA. All individuals consented orally to participation, with a second, local native speaker witnessing and were re-consented with written consent. DNA was collected via saliva and all individuals were as described in previous studies [10,26].

Study populations

Genomic DNA samples were isolated from saliva samples donated by 61 KhoeSan individuals of the ≠Khomani San population as described by Henn et al. [10]. *KIR2DL1*, *KIR2DL2/3* and

HLA-C allele frequencies were determined for 55 unrelated individuals. The additional six individuals comprised five additional family members of two of the 55 unrelated individuals, and a sibling of another. The sequences and frequencies of KhoeSan *KIR* and *HLA-C* alleles were compared to those of Ghanaians [14], Northern Irish [21] Japanese [24] and South Amerindians [20], and also to three non-KhoeSan hunter-gatherer populations. These comprised 20 Mbuti and 20 Baka Pygmies from The Democratic Republic of Congo and Cameroon, and 52 Hadza from northern Tanzania [10]. We also analyzed the *KIR* sequence data of 100 Zulus from South Africa [27]. Allele frequencies for the C1 and C2 epitopes of HLA-C were determined using data deposited at www.allelefrequencies.net [34]. The 140 populations analyzed were chosen for being anthropologically well characterized, for having minimal admixture with other populations, and for having a size of 40 individuals or more. This panel of populations is described in Abi Rached et al. [33].

High-resolution *KIR2DL1* and *KIR2DL2/3* genotyping

Nucleotide sequences were determined for all exons of *KIR2DL1 and KIR2DL2/3* genes from sixteen randomly selected unrelated KhoeSan individuals as well as the seven-member family. Sequences for two previously unknown alleles, *KIR2DL1*022* (GU323355) and *KIR2DL1*026* (JX523630) were confirmed by re-amplification, cloning and sequencing, as described [26]. A pyrosequencing-based method for allele-level *KIR2DL1* and *KIR2DL2/3* genotyping [14], was expanded to include detection of the new KhoeSan variants (S5 Fig). This method provides a semi-quantitative measure of SNP genotypes (the peak-height ratio) that determines both allele identity and copy-number genotype [14]. Centromeric *KIR* haplotypes were characterized as described [14], with modification to accommodate the newly-discovered *3DL3*038* and *2DL5B*018* alleles [26]. Pyrosequencing and standard Sanger sequencing were used to determine the *2DL1* alleles present in the Pygmy and Hadza populations.

High-resolution *HLA* genotyping

The 61 KhoeSan individuals were *HLA-C* genotyped at allele-level resolution using bead-based SSOP hybridization (One Lambda) and detection by a Luminex-100 instrument (Luminex corp. Austin, TX).

KIR nomenclature

KIR genes and alleles were named by the KIR nomenclature committee [47] formed from members of the WHO Nomenclature Committee for factors of the HLA system, and the HUGO Genome Nomenclature Committee. A curated database is available at http://www.ebi.ac.uk/ipd/kir/ [47].

Searching for *KIR2DL1*022* and *KIR2DL1*026* alleles in the 1000 Genomes and African Genome Variation Project datasets

The high-coverage exome data from the May 2013 release of the 1000 Genomes project [25] were used to determine the frequency of *KIR2DL1*022* and *KIR2DL1*026* in populations worldwide. All read-pairs that map to the *KIR* regions (Build Hg19: chr19:55,228,188–55,383,188 and GL000209.1) were extracted using SAMtools 0.1.18 [48]. For 39 individuals the data have insufficient coverage and were excluded from the analysis, which was performed on data from 2,496 individuals representing 26 populations (S2B Fig). Individual fastq files were probed using locus-specific and allele-specific sequence-string searches. Where required, individual fastq files were filtered for locus-specificity using Bowtie (version 0.12.7) [49], aligned to references and

the SNP genotypes inspected manually. As controls we included data from eight KhoeSan individuals who had previously been sequenced using Illumina whole-exome paired end technology [26] and, independently, KIR genotyped to allele-level resolution by pyrosequencing [14]. Three of the eight individuals have *KIR2DL1*022*, and one other has *KIR2DL1*026*.

We used the same method to determine the frequencies of *2DL1*022* and *2DL1*026* in 100 Zulus whose genomes were sequenced as part of the African Genome Variation project [27]. Zulus are a Bantu-speaking population from southern Africa, who show evidence for recent admixture with the KhoeSan [11,18]. For each Zulu individual having either *2DL1*022* or *2DL1*026* we used manual inspection of sequence reads mapped to each *KIR* gene to infer the likely centromeric *KIR* haplotype structure.

Binding assay of KIR-Fc fusion proteins to beads coated with HLA class I

KIR-Fc fusion proteins were generated from insect cells (cabbage looper moth *Hi5* cells, kindly provided by Prof. K.C. Garcia, Stanford University) infected with baculovirus as described [50]. The KIR-Fc fusion protein corresponding to each 2DL1, 2DL2 and 2DL3 allotype was tested for binding to a panel of microbeads, each of which is coated with one of 31 HLA-A, 50 HLA-B and 16 HLA-C allotypes (LabScreen Single-Antigen Beads, One Lambda, lot #8). To account for differences in the amount of HLA class I protein coating each bead, the binding of each KIR-Fc fusion protein was normalized to the binding of W6/32, a monoclonal antibody detecting a common epitope of HLA class I. Binding values were calculated using the formula (specific binding—bead background fluorescence)/(W6/32 binding—bead background fluorescence).

Cell-surface expression of KIR2DL1 in transiently transfected HeLa

Recombinant cDNA encoding the extracellular, stem, transmembrane and cytoplasmic domain (amino acids 1–336) of *KIR2DL1*003* with an N-terminal 3X FLAG-tag was manufactured by Genscript (Piscataway, NJ) and cloned into the pcDNA3.1+ expression vector. Site-directed mutagenesis was performed with the QuikChange Kit (Stratagene), according to the manufacturer's instructions, to generate nine further *KIR2DL1* variants. HeLa cells (ATCC Cell Lines, VA) were plated in 15.6mm wells at 5 x 10^4 cells/well in 500μl DMEMc for 24hrs and then transfected with a pcDNA3.1+ vector encoding FLAG-tagged KIR2DL1 allotypes using the Fugene transfection reagent (Promega). After 36h, adherent cells were dissociated from the wells using 200μl 0.05% trypsin EDTA solution and stained with 25μl mouse polyclonal FITC-conjugated FLAG-specific antibody (Sigma-Aldrich) at a final concentration of 3μg/ml. Cells expressing FLAG-tagged KIR2DL1 allotypes were detected by flow cytometry (Accuri C6 cytometer, BD Biosciences). Dead cells were identified by staining with propidium iodide and excluded from the analysis. The median fluorescence intensity (MFI) of FITC-conjugated anti-FLAG antibody bound to each positively staining cell was used as a measure of the cell-surface expression of KIR2DL1. At least 50,000 such cells were analyzed in each experiment. Three independent transfections were performed for each allotype.

Population and molecular genetic analysis

The *KIR* locus has extensive structural and allelic polymorphism [8,51], as well as recombination hotspots that flank the centromeric *KIR* region [52,53]. These characteristics preclude the use of methods that use SNP analysis and the identification of regions of extended haplotype homozygosity as evidence for selection [54–56]. We examined the patterns of LD associated with specific alleles, using a method designed for analysis of a polymorphic multigene family

[39,57]. This approach was applied to the analysis of the haplotypes in centromeric region of the KhoeSan *KIR* locus, the regions containing the *KIR2DL1* gene.

Supporting Information

S1 Fig. Comparison of the *KIR2DL1*, *KIR2DL2/3* and *HLA-C* allele frequencies in five human populations. The *KIR2DL1* (A) and *KIR2DL2/3* (B) alleles of the KhoeSan are compared to those of the Ga-Adangbe, a Ghanaian population, the Caucasian population of Northern Ireland, the Yucpa South Amerindians from Venezuela and Japanese [14,20,21,24]. (C) Shown are the frequencies of *HLA-C* alleles from each of the five populations described above. The alleles are grouped into those encoding HLA-C allotypes with the C1 epitope and those encoding HLA-C allotypes with the C2 epitope.
(PDF)

S2 Fig. *KIR2DL1*022* and *2DL1*026* evolved in the KhoeSan after their divergence from other modern human populations. (A) Shown are the results from a search, of whole-exome genome data from eight KhoeSan individuals [26], for sequence reads corresponding to *KIR2DL1* and to the *2DL1*022* and *2DL1*026* alleles. Shown on the left are the *KIR2DL1* genotypes of each individual as assessed by pyrosequencing. Shown on the right are the numbers of *KIR2DL1*, *2DL1*022* and *2DL1*026* reads obtained from the exome data and the percentage of total *2DL1*-specific reads that they constitute. (B) Shown is the number of individuals from each of 26 populations covered by the 1000 Genomes dataset [25]. (C) Shown is the number of individuals from the 1000 Genomes project [25] and African Genome Variation project (AGVP) [27] datasets that tested positive for *2DL1*022* and *2DL1*026*, using the same probes as for panel (A). For no individual in the 1000 Genomes dataset did >1% of the reads that covered the SNP location match the tested allele (*2DL1*022* or *2DL1*026*), whereas for the control individuals the read ratio matched the expected genotype. Five Bantu-speaking Zulu individuals from the AGVP dataset had reads consistent with heterozygosity for either *2DL1*022* or *2DL1*026*. Also shown are the frequencies of *3DL3*, *2DL1*, *2DL1*022* and *2DL1*026* in two non-KhoeSan hunter-gatherer populations: the Mbuti and Baka Pygmies (central Africa) and the Hadza (Tanzania). Genotype data for these populations were obtained by whole-exome sequencing.
(PDF)

S3 Fig. In the Bantu-speaking Zulu population of southern Africa, *2DL1*022* and *2DL1*026* are present on that same *KIR* haplotypes as in the KhoeSan. (A) Allele content of centromeric *KIR* haplotypes containing either *2DL1*022* (purple) or *2DL1*026* (yellow) that were defined from analysis of 61 KhoeSan individuals. The number of haplotypes observed is given on the left under 'N'. Also shown are KhoeSan *KIR* haplotypes that are putative parents (Par?) of the haplotypes containing *2DL1*022* or *2DL1*026* haplotypes (white boxes). (B) Inferred allele content of centromeric *KIR* haplotypes containing either *2DL1*022* (purple) or *2DL1*026* (yellow) that were defined from analysis of 100 Bantu-speaking Zulu individuals. The number of haplotypes observed is given on the left under 'N'.
(PDF)

S4 Fig. KIR2DL1 allotypes can be classified into functional groups based on HLA-C2 binding and signaling capacity. (A) KIR2DL1 allotypes were classified into three functional groups on the basis of their binding to C2 targets and their predicted signaling capacity. KIR2DL1 allotypes were classified as strong if they had a mean binding to C2 that is greater than 50% of the strongest known 2DL1 allotype (2DL1*020). Allotypes were considered weak if they had either a mean binding to C2 that is less than 50% of the strongest 2DL1 allotype or if they have a

cysteine residue at position 245, which is known to reduce inhibitory signaling capacity [38]. KIR2DL1 allotypes with no detectable binding to HLA-C2 or no capacity to transduce an inhibitory signal were classified as inactive. (B) Table showing the classification of KIR2DL1 allotypes into groups of strong, weak and inactive receptors.
(PDF)

S5 Fig. Oligonucleotide primers used to amplify single *KIR2DL1* exons. An initial PCR was performed using the amplification primers shown in the upper panel. Pyrosequencing was performed following a second (nested) amplification; (o-) indicates biotin and (nnnn-) indicates random oligonucleotides (to prevent fragment looping). The pyrosequencing reactions were performed using the primers shown in the lower panel. When required, standard Sanger sequencing was performed using the amplification primers.
(PDF)

Acknowledgments

The authors thank Lluis Quintana-Murci, Carlos Bustamante and Martin Sikora for providing genomic DNA samples from the Mbuti and Baka people and Joanna Mountain for providing genomic DNA samples from the Hadza people. We thank the ≠Khomani San community for their generous donation of DNA to facilitate genetic research.

Author Contributions

Conceived and designed the experiments: HGH PJN. Performed the experiments: HGH NNG AG. Analyzed the data: HGH PJN NNG AG JAH LAG. Contributed reagents/materials/analysis tools: BMH CRG. Wrote the paper: HGH PJN LAG PP.

References

1. Parham P, Moffett A (2013) Variable NK cell receptors and their MHC class I ligands in immunity, reproduction and human evolution. Nat Rev Immunol 13: 133–144. doi: 10.1038/nri3370 PMID: 23334245
2. Cooper MA, Colonna M, Yokoyama WM (2009) Hidden talents of natural killers: NK cells in innate and adaptive immunity. EMBO Rep 10: 1103–1110. doi: 10.1038/embor.2009.203 PMID: 19730434
3. Bashirova AA, Martin MP, McVicar DW, Carrington M (2006) The killer immunoglobulin-like receptor gene cluster: tuning the genome for defense. Annu Rev Genomics Hum Genet 7: 277–300. PMID: 16824023
4. Parham P, Norman PJ, Abi-Rached L, Guethlein LA (2012) Human-specific evolution of killer cell immunoglobulin-like receptor recognition of major histocompatibility complex class I molecules. Philos Trans R Soc Lond B Biol Sci 367: 800–811. doi: 10.1098/rstb.2011.0266 PMID: 22312047
5. Boyington JC, Motyka SA, Schuck P, Brooks AG, Sun PD (2000) Crystal structure of an NK cell immunoglobulin-like receptor in complex with its class I MHC ligand. Nature 405: 537–543. PMID: 10850706
6. Bjorkman PJ, Saper MA, Samraoui B, Bennett WS, Strominger JL, et al. (1987) The foreign antigen binding site and T cell recognition regions of class I histocompatibility antigens. Nature 329: 512–518. PMID: 2443855
7. Winter CC, Long EO (1997) A single amino acid in the p58 killer cell inhibitory receptor controls the ability of natural killer cells to discriminate between the two groups of HLA-C allotypes. J Immunol 158: 4026–4028. PMID: 9126959
8. Uhrberg M, Valiante NM, Shum BP, Shilling HG, Lienert-Weidenbach K, et al. (1997) Human diversity in killer cell inhibitory receptor genes. Immunity 7: 753–763. PMID: 9430221
9. Abi-Rached L, Moesta AK, Rajalingam R, Guethlein LA, Parham P (2010) Human-specific evolution and adaptation led to major qualitative differences in the variable receptors of human and chimpanzee natural killer cells. PLoS Genet 6: e1001192. doi: 10.1371/journal.pgen.1001192 PMID: 21079681
10. Henn BM, Gignoux CR, Jobin M, Granka JM, Macpherson JM, et al. (2011) Hunter-gatherer genomic diversity suggests a southern African origin for modern humans. Proc Natl Acad Sci U S A 108: 5154–5162. doi: 10.1073/pnas.1017511108 PMID: 21383195

11. Petersen DC, Libiger O, Tindall EA, Hardie RA, Hannick LI, et al. (2013) Complex patterns of genomic admixture within southern Africa. PLoS Genet 9: e1003309. doi: 10.1371/journal.pgen.1003309 PMID: 23516368
12. Tishkoff SA, Reed FA, Friedlaender FR, Ehret C, Ranciaro A, et al. (2009) The genetic structure and history of Africans and African Americans. Science 324: 1035–1044. doi: 10.1126/science.1172257 PMID: 19407144
13. Nakimuli A, Chazara O, Byamugisha J, Elliott AM, Kaleebu P, et al. (2014) Pregnancy, parturition and preeclampsia in women of African ancestry. Am J Obstet Gynecol 210: 510–520 e511. doi: 10.1016/j.ajog.2013.10.879 PMID: 24184340
14. Norman PJ, Hollenbach JA, Nemat-Gorgani N, Guethlein LA, Hilton HG, et al. (2013) Co-evolution of human leukocyte antigen (HLA) class I ligands with killer-cell immunoglobulin-like receptors (KIR) in a genetically diverse population of sub-Saharan Africans. PLoS Genet 9: e1003938. doi: 10.1371/journal.pgen.1003938 PMID: 24204327
15. Bryc K, Auton A, Nelson MR, Oksenberg JR, Hauser SL, et al. (2010) Genome-wide patterns of population structure and admixture in West Africans and African Americans. Proc Natl Acad Sci U S A 107: 786–791. doi: 10.1073/pnas.0909559107 PMID: 20080753
16. Schuster SC, Miller W, Ratan A, Tomsho LP, Giardine B, et al. (2010) Complete Khoisan and Bantu genomes from southern Africa. Nature 463: 943–947. doi: 10.1038/nature08795 PMID: 20164927
17. Lachance J, Vernot B, Elbers CC, Ferwerda B, Froment A, et al. (2012) Evolutionary history and adaptation from high-coverage whole-genome sequences of diverse African hunter-gatherers. Cell 150: 457–469. doi: 10.1016/j.cell.2012.07.009 PMID: 22840920
18. Chimusa ER, Meintjies A, Tchanga M, Mulder N, Seioghe C, et al. (2015) A genomic portrait of haplotype diversity and signatures of selection in indigenous southern African populations. PLoS Genet 11: e1005052. doi: 10.1371/journal.pgen.1005052 PMID: 25811879
19. Howell N (2007) Demography of the Dobe! Kung. New Brunswick, N.J.: AldineTransaction.
20. Gendzekhadze K, Norman PJ, Abi-Rached L, Graef T, Moesta AK, et al. (2009) Co-evolution of KIR2DL3 with HLA-C in a human population retaining minimal essential diversity of KIR and HLA class I ligands. Proc Natl Acad Sci U S A 106: 18692–18697. doi: 10.1073/pnas.0906051106 PMID: 19837691
21. Middleton D, Meenagh A, Gourraud PA (2007) KIR haplotype content at the allele level in 77 Northern Irish families. Immunogenetics 59: 145–158. PMID: 17200871
22. Nemat-Gorgani N, Edinur HA, Hollenbach JA, Traherne JA, Dunn PP, et al. (2014) KIR diversity in Maori and Polynesians: populations in which HLA-B is not a significant KIR ligand. Immunogenetics 66: 597–611. doi: 10.1007/s00251-014-0794-1 PMID: 25139336
23. Vierra-Green C, Roe D, Hou L, Hurley CK, Rajalingam R, et al. (2012) Allele-level haplotype frequencies and pairwise linkage disequilibrium for 14 KIR loci in 506 European-American individuals. PLoS One 7: e47491. doi: 10.1371/journal.pone.0047491 PMID: 23139747
24. Yawata M, Yawata N, Draghi M, Little AM, Partheniou F, et al. (2006) Roles for HLA and KIR polymorphisms in natural killer cell repertoire selection and modulation of effector function. J Exp Med 203: 633–645. PMID: 16533882
25. Abecasis GR, Auton A, Brooks LD, DePristo MA, Durbin RM, et al. (2012) An integrated map of genetic variation from 1,092 human genomes. Nature 491: 56–65. doi: 10.1038/nature11632 PMID: 23128226
26. Kidd JM, Sharpton TJ, Bobo D, Norman PJ, Martin AR, et al. (2014) Exome capture from saliva produces high quality genomic and metagenomic data. BMC Genomics 15: 262. doi: 10.1186/1471-2164-15-262 PMID: 24708091
27. Gurdasani D, Carstensen T, Tekola-Ayele F, Pagani L, Tachmazidou I, et al. (2015) The African Genome Variation Project shapes medical genetics in Africa. Nature 517: 327–332. doi: 10.1038/nature13997 PMID: 25470054
28. Gronau I, Hubisz MJ, Gulko B, Danko CG, Siepel A (2011) Bayesian inference of ancient human demography from individual genome sequences. Nat Genet 43: 1031–1034. doi: 10.1038/ng.937 PMID: 21926973
29. Schlebusch CM, Skoglund P, Sjodin P, Gattepaille LM, Hernandez D, et al. (2012) Genomic variation in seven Khoe-San groups reveals adaptation and complex African history. Science 338: 374–379. doi: 10.1126/science.1227721 PMID: 22997136
30. Burshtyn DN, Scharenberg AM, Wagtmann N, Rajagopalan S, Berrada K, et al. (1996) Recruitment of tyrosine phosphatase HCP by the killer cell inhibitor receptor. Immunity 4: 77–85. PMID: 8574854
31. Moesta AK, Norman PJ, Yawata M, Yawata N, Gleimer M, et al. (2008) Synergistic polymorphism at two positions distal to the ligand-binding site makes KIR2DL2 a stronger receptor for HLA-C than KIR2DL3. J Immunol 180: 3969–3979. PMID: 18322206

32. Hilton HG, Vago L, Older Aguilar AM, Moesta AK, Graef T, et al. (2012) Mutation at positively selected positions in the binding site for HLA-C shows that KIR2DL1 is a more refined but less adaptable NK cell receptor than KIR2DL3. J Immunol 189: 1418–1430. doi: 10.4049/jimmunol.1100431 PMID: 22772445

33. Abi-Rached L, Jobin MJ, Kulkarni S, McWhinnie A, Dalva K, et al. (2011) The shaping of modern human immune systems by multiregional admixture with archaic humans. Science 334: 89–94. doi: 10.1126/science.1209202 PMID: 21868630

34. Gonzalez-Galarza FF, Christmas S, Middleton D, Jones AR (2011) Allele frequency net: a database and online repository for immune gene frequencies in worldwide populations. Nucleic Acids Res 39: D913–919. doi: 10.1093/nar/gkq1128 PMID: 21062830

35. VandenBussche CJ, Mulrooney TJ, Frazier WR, Dakshanamurthy S, Hurley CK (2009) Dramatically reduced surface expression of NK cell receptor KIR2DS3 is attributed to multiple residues throughout the molecule. Genes Immun 10: 162–173. doi: 10.1038/gene.2008.91 PMID: 19005473

36. Pando MJ, Gardiner CM, Gleimer M, McQueen KL, Parham P (2003) The protein made from a common allele of KIR3DL1 (3DL1*004) is poorly expressed at cell surfaces due to substitution at positions 86 in Ig domain 0 and 182 in Ig domain 1. J Immunol 171: 6640–6649. PMID: 14662867

37. Thomas R, Yamada E, Alter G, Martin MP, Bashirova AA, et al. (2008) Novel KIR3DL1 alleles and their expression levels on NK cells: convergent evolution of KIR3DL1 phenotype variation? J Immunol 180: 6743–6750. PMID: 18453594

38. Bari R, Bell T, Leung WH, Vong QP, Chan WK, et al. (2009) Significant functional heterogeneity among KIR2DL1 alleles and a pivotal role of arginine 245. Blood 114: 5182–5190. doi: 10.1182/blood-2009-07-231977 PMID: 19828694

39. Klitz W, Thomson G (1987) Disequilibrium pattern analysis. II. Application to Danish HLA A and B locus data. Genetics 116: 633–643. PMID: 3476350

40. Frazier WR, Steiner N, Hou L, Dakshanamurthy S, Hurley CK (2013) Allelic Variation in KIR2DL3 Generates a KIR2DL2-like Receptor with Increased Binding to its HLA-C Ligand. J Immunol.

41. Hiby SE, Walker JJ, O'Shaughnessy K M, Redman CW, Carrington M, et al. (2004) Combinations of maternal KIR and fetal HLA-C genes influence the risk of preeclampsia and reproductive success. J Exp Med 200: 957–965. PMID: 15477349

42. Nakimuli A, Chazara O, Hiby SE, Farrell L, Tukwasibwe S, et al. (2015) A KIR B centromeric region present in Africans but not Europeans protects pregnant women from pre-eclampsia. Proc Natl Acad Sci U S A 112: 845–850. doi: 10.1073/pnas.1413453112 PMID: 25561558

43. Kim HL, Ratan A, Perry GH, Montenegro A, Miller W, et al. (2014) Khoisan hunter-gatherers have been the largest population throughout most of modern-human demographic history. Nat Commun 5: 5692. doi: 10.1038/ncomms6692 PMID: 25471224

44. Oppenheimer S (2012) Out-of-Africa, the peopling of continents and islands: tracing uniparental gene trees across the map. Philos Trans R Soc Lond B Biol Sci 367: 770–784. doi: 10.1098/rstb.2011.0306 PMID: 22312044

45. Hollenbach JA, Nocedal I, Ladner MB, Single RM, Trachtenberg EA (2012) Killer cell immunoglobulin-like receptor (KIR) gene content variation in the HGDP-CEPH populations. Immunogenetics 64: 719–737. doi: 10.1007/s00251-012-0629-x PMID: 22752190

46. Norman PJ, Abi-Rached L, Gendzekhadze K, Korbel D, Gleimer M, et al. (2007) Unusual selection on the KIR3DL1/S1 natural killer cell receptor in Africans. Nat Genet 39: 1092–1099. PMID: 17694054

47. Robinson J, Halliwell JA, McWilliam H, Lopez R, Marsh SG (2013) IPD—the Immuno Polymorphism Database. Nucleic Acids Res 41: D1234–1240. doi: 10.1093/nar/gks1140 PMID: 23180793

48. Li H, Handsaker B, Wysoker A, Fennell T, Ruan J, et al. (2009) The Sequence Alignment/Map format and SAMtools. Bioinformatics 25: 2078–2079. doi: 10.1093/bioinformatics/btp352 PMID: 19505943

49. Langmead B, Trapnell C, Pop M, Salzberg SL (2009) Ultrafast and memory-efficient alignment of short DNA sequences to the human genome. Genome Biol 10: R25. doi: 10.1186/gb-2009-10-3-r25 PMID: 19261174

50. Hilton HG, Moesta AK, Guethlein LA, Blokhuis J, Parham P, et al. (2015) The production of KIR-Fc fusion proteins and their use in a multiplex HLA class I binding assay. Journal of Immunological Methods doi: 10.1016/j.jim.2015.06.012

51. Shilling HG, Guethlein LA, Cheng NW, Gardiner CM, Rodriguez R, et al. (2002) Allelic polymorphism synergizes with variable gene content to individualize human KIR genotype. J Immunol 168: 2307–2315. PMID: 11859120

52. Wilson MJ, Torkar M, Haude A, Milne S, Jones T, et al. (2000) Plasticity in the organization and sequences of human KIR/ILT gene families. Proc Natl Acad Sci U S A 97: 4778–4783. PMID: 10781084

53. Norman PJ, Cook MA, Carey BS, Carrington CV, Verity DH, et al. (2004) SNP haplotypes and allele frequencies show evidence for disruptive and balancing selection in the human leukocyte receptor complex. Immunogenetics 56: 225–237. PMID: 15185041

54. Hancock AM, Rienzo AD (2008) Detecting the Genetic Signature of Natural Selection in Human Populations: Models, Methods, and Data. Annu Rev Anthropol 37: 197–217. PMID: 20622977

55. Nielsen R (2005) Molecular signatures of natural selection. Annu Rev Genet 39: 197–218. PMID: 16285858

56. Oleksyk TK, Smith MW, O'Brien SJ (2010) Genome-wide scans for footprints of natural selection. Philos Trans R Soc Lond B Biol Sci 365: 185–205. doi: 10.1098/rstb.2009.0219 PMID: 20008396

57. Thomson G, Klitz W (1987) Disequilibrium pattern analysis. I. Theory. Genetics 116: 623–632. PMID: 3623083

Published August 26, 2015, doi:10.4049/jimmunol.1501358

Polymorphic HLA-C Receptors Balance the Functional Characteristics of *KIR* Haplotypes

Hugo G. Hilton,*,† Lisbeth A. Guethlein,*,† Ana Goyos,*,† Neda Nemat-Gorgani,*,† David A. Bushnell,* Paul J. Norman,*,† and Peter Parham*,†

The human killer cell Ig-like receptor (*KIR*) locus comprises two groups of *KIR* haplotypes, termed *A* and *B*. These are present in all human populations but with different relative frequencies, suggesting they have different functional properties that underlie their balancing selection. We studied the genomic organization and functional properties of the alleles of the inhibitory and activating HLA-C receptors encoded by *KIR* haplotypes. Because every HLA-C allotype functions as a ligand for KIR, the interactions between KIR and HLA-C dominate the HLA class I–mediated regulation of human NK cells. The C2 epitope is recognized by inhibitory KIR2DL1 and activating KIR2DS1, whereas the C1 epitope is recognized by inhibitory KIR2DL2 and KIR2DL3. This study shows that the *KIR2DL1, KIR2DS1*, and *KIR2DL2/3* alleles form distinctive phylogenetic clades that associate with specific *KIR* haplotypes. *KIR A* haplotypes are characterized by *KIR2DL1* alleles that encode strong inhibitory C2 receptors and *KIR2DL3* alleles encoding weak inhibitory C1 receptors. In striking contrast, *KIR B* haplotypes are characterized by *KIR2DL1* alleles that encode weak inhibitory C2 receptors and *KIR2DL2* alleles encoding strong inhibitory C1 receptors. The wide-ranging properties of KIR allotypes arise from substitutions throughout the KIR molecule. Such substitutions can influence cell surface expression, as well as the avidity and specificity for HLA-C ligands. Consistent with the crucial role of inhibitory HLA-C receptors in self-recognition, as well as NK cell education and response, most KIR haplotypes have both a functional C1 and C2 receptor, despite the considerable variation that occurs in ligand recognition and surface expression.
***The Journal of Immunology*, 2015, 195: 000–000.**

Natural killer cells are cytotoxic lymphocytes that kill virus infected (1) and malignantly transformed cells without prior sensitization (2). They also play an important role in early pregnancy where they control the trophoblast-mediated remodeling of maternal blood vessels during formation of the placenta (3). Controlling the development and function of NK cells are a wide array of activating and inhibitory cell surface receptors (4). A common feature of these germline-encoded receptors is their specificity for MHC class I ligands (in humans the HLA class I molecules). In catarrhine primates (humans, apes, and Old World monkeys) the ubiquitously expressed classical MHC class I molecules are recognized by the killer cell Ig-like receptor (KIR) family (5). Because both KIR and MHC class I are highly polymorphic, these interactions diversify and individualize NK cell responses. The functional importance of such interactions is illustrated by the association of various combinations of KIR and HLA class I with the outcome of viral infection (6–8), susceptibility to autoimmune disease (9–11), survival following bone marrow transplantation (12, 13), and reproductive success (14, 15).

The catarrhine primates share four phylogenetic lineages of KIR that have different structure and specificity for MHC class I molecules (3, 5). Lineage I KIRs recognize HLA-G, which has restricted expression on trophoblast cells and monocytes and is considered to be dedicated to reproductive function (16–18). Lineage II KIRs recognize the A3/A11 and Bw4 epitopes that are each carried by a different subset of HLA-A and HLA-B alleles. Lineage III KIRs, the subject of this study, recognize HLA-C ligands. A ligand for the lineage V KIRs, represented by KIR3DL3 in humans, has yet to be identified. In contrast to HLA-A and HLA-B, every HLA-C allotype forms a ligand for KIRs, and it is these interactions that dominate NK cell responses. Two mutually exclusive HLA-C epitopes are defined by the residue at position 80 in the α_1 domain and are recognized by different KIRs (19). Inhibitory KIR2DL1 and activating KIR2DS1 recognize the C2 epitope (lysine 80) whereas inhibitory KIR2DL3 recognizes the C1 epitope (asparagine 80) and inhibitory KIR2DL2 principally recognizes C1 but also has some cross-reactivity with C2 (20, 21).

The *KIR* gene family is diversified by both gene content variability and allelic polymorphism and is part of the leukocyte receptor complex on human chromosome 19 (22, 23). The basic organization of the *KIR* locus is conserved among the catarrhine primates, consisting of four framework genes (common to most haplotypes) and a suite of homologous genes that are variably present between species and individuals (24). A site of recombination at the center of the locus defines two distinct regions: one closer to the chromosomal centromere (termed centromeric), the other closer to the chromosomal telomere (termed telomeric) (25).

*Department of Structural Biology, Stanford University School of Medicine, Stanford, CA 94305; and †Department of Microbiology and Immunology, Stanford University School of Medicine, Stanford, CA 94305

ORCID: 0000-0002-6962-727X (A.G.).

Received for publication June 17, 2015. Accepted for publication July 22, 2015.

This work was supported by National Institutes of Health Grants AI22039 and AI17892. H.G.H. was also supported by the March of Dimes Prematurity Research Center at the Stanford University School of Medicine, Clinical and Translational Science Awards Grant ULI RR025744, and a Stanford University School of Medicine Dean's postdoctoral fellowship.

Address correspondence and reprint requests to Prof. Peter Parham, Stanford University School of Medicine, Sherman Fairchild Building, D157, 299 Campus Drive West, Stanford, CA 94305. E-mail address: peropa@stanford.edu

The online version of this article contains supplemental material.

Abbreviations used in this article: BB, blocking buffer; DMEMc, DMEM supplemented with FBS, streptomycin, penicillin, and L-glutamine; DPBS, Dulbecco's PBS; KIR, killer cell Ig-like receptor.

Since the time of their common ancestor, there has been species-specific reorganization of the centromeric and telomeric regions of the catarrhine primate *KIR* locus (5). Chimpanzees, orangutans, and gorillas expanded variable *KIR* genes in the centromeric region of the *KIR* locus but not in the telomeric region (26). In contrast, macaques and other Old World monkeys expanded variable *KIR* genes in the telomeric region but not in the centromeric region (27). The human species is unique in having expanded variable *KIR* genes in both the centromeric and telomeric regions (26). Each of these regions contains different genes and different alleles of shared genes, and it is these differences that are the basis for the division of human *KIR* haplotypes into two functional groups, *A* and *B* (28). *KIR A* haplotypes encode a fixed suite of largely inhibitory receptors whereas *KIR B* haplotypes have a variable number of inhibitory receptors and several activating receptors. That these haplotypes are found in all human populations but with different relative frequencies suggests they have different functional properties that are subject to balancing selection (29).

In addition to their accumulation of activating receptors, the *KIR B* haplotypes have accumulated a particular subset of alleles for the inhibitory receptor genes that are common to *KIR A* and *B* haplotypes (28, 30). Furthermore, although a limited number of *KIR* haplotypes have been studied in detail, there appears to be functional differences between the inhibitory receptors encoded by the *KIR A* and *B* haplotypes (21, 31–33). In this study we determined the haplotypic association, phylogeny, and function of every *KIR2DL1*, *KIR2DL2/3*, and *KIR2DS1* allele defined. In so doing we have shed light on the evolution and function of human HLA-C receptors and their contribution to the distinct functions of the *KIR A* and *B* haplotypes.

Materials and Methods

Genomic analyses

Sequences encoding the D1, D2, stem, transmembrane, and cytoplasmic tail domains (amino acids 1–328) of 26 *KIR2DL1*, 7 *KIR2DS1*, and 36 *KIR2DL2/3* alleles were aligned and analyzed by three methods: neighbor joining (using the Tamura–Nei pairwise substitution) (34), maximum likelihood, and parsimony, each with 500 replicates. The bootstrap support for each node is indicated when >50. Representative trees are shown in Figs. 1 and 3 and Supplemental Fig. 1. Evolutionary analyses were conducted in MEGA6 (35).

Binding assay of KIR-Fc fusion proteins to beads coated with HLA class I

KIR-Fc fusion proteins were generated from insect cells (provided by Prof. K.C. Garcia, Stanford University) and infected with baculovirus as described (36). The KIR-Fc fusion protein corresponding to each KIR2DL1, KIR2DL2, and KIR2DL3 allotype was tested for binding to a panel of microbeads, in which each bead is coated with 1 of 97 HLA class I allotypes (31 HLA-A, 50 HLA-B, and 16 HLA-C allotypes) (LABScreen single-antigen beads, One Lambda, lot no. 8). To account for differences in the amount of HLA class I protein coating each bead, the binding of each KIR-Fc fusion protein is normalized to the binding of W6/32, a mAb detecting a common epitope of HLA class I. Binding values were calculated using the formula: (specific binding − background bead fluorescence)/(W6/32 binding − background bead fluorescence).

Cell surface expression of KIR2DL1 allotypes

We examined the cell surface expression of four natural KIR2DL1 allotypes and nine KIR2DL1*003 mutants when transfected transiently into HeLa cells. N-terminal 3× FLAG-tags were attached to each *KIR2DL1* construct, so that the expression of each KIR2DL1 variant could be measured using the same anti-FLAG Ab binding to the identical FLAG epitope. Recombinant cDNA encoding the extracellular, stem, transmembrane, and cytoplasmic domains (amino acids 1–328) of KIR2DL1*003 with an N-terminal 3× FLAG-tag (amino acid sequence, DYKDHDGDYKDHDI-DYKDDDDK) was manufactured by GenScript (Piscataway, NJ) and subcloned into the pcDNA3.1$^+$ expression vector. Site-directed mutagenesis was performed with the QuikChange kit (Stratagene), according to the manufacturer's instructions, to generate three other natural *KIR2DL1* alleles and nine mutants containing termination codons at different positions in the sequence encoding the stem, transmembrane, and cytoplasmic tail domains. HeLa cells were cultured in DMEM (Life Technologies) supplemented with 10% FBS, 100 μg/ml streptomycin, 100 U/ml penicillin, and 2 mM L-glutamine (DMEMc). Cells were plated in 15.6-mm wells at 5×10^4 cells/well in 500 μl DMEMc for 24 h and then transfected with a pcDNA3.1$^+$ vector encoding FLAG-tagged KIR2DL1 allotypes using the FuGENE transfection reagent (Promega). Thirty-six hours after transfection, adherent cells were dissociated from the wells using 200 μl 0.05% trypsin-EDTA solution and washed with flow cytometry buffer (Dulbecco's PBS [DPBS] containing 2% EDTA and 1% BSA at 4°C). Cells were then stained with 25 μl FITC-conjugated mouse polyclonal anti-FLAG Ab (Sigma-Aldrich) at a final concentration of 3 μg/ml. Following a further wash, cells were suspended in 50 μl 50× propidium iodide (BD Biosciences) and fixed in 50 μl 2% paraformaldehyde. Cells expressing FLAG-tagged KIR2DL1 were detected by flow cytometry (Accuri C6 cytometer, BD Biosciences). Expression levels of each allotype or mutant were determined from the median fluorescence intensity of FITC-conjugated anti-FLAG Ab bound to each positive staining cell. Three independent transfections with at least 50,000 cells each were performed for each allotype tested.

Slide preparation and microscopy

HeLa cells were plated at 5×10^5 cells/well in 500 μl DMEMc on a 12-mm round no. 1 German glass poly-D-lysine–coated glass coverslip (BD Biosciences) and transfected with FLAG-tagged KIR2DL1 allotypes. Forty-eight hours after transfection the cells were fixed in 4% paraformaldehyde (Electron Microscopy Sciences) diluted in DPBS with magnesium and calcium (Life Technologies). DPBS (275 μl) containing glycine (25 mM) was added to quench reactive aldehydes. Cells were permeabilized with DPBS containing 0.04% saponin and blocked in blocking buffer (BB; DPBS containing 2% heat-inactivated goat serum, 1% BSA, 0.1% cold fish skin gelatin, 0.02% SDS, 0.1% Nonidet P-40, and 0.05% sodium azide [pH 7.2]). Rabbit polyclonal IgG anti-FLAG primary Ab (Sigma-Aldrich) was applied at 5 μg/ml in BB and incubated overnight at 4°C. After washing with BB, cells were incubated for 20 min at room temperature with 1 U Alexa Fluor 555 phalloidin solution diluted in BB. Cells were then washed with BB and incubated for 1 h at room temperature with Alexa Fluor 488 goat anti-rabbit IgG (Life Technologies) secondary Ab suspended in BB. Cells were washed in BB and DPBS and coverslips were mounted for microscopy in ProLong Gold antifade reagent (Life Technologies). Cells were analyzed by confocal laser-scanning microscopy using an upright system (DM6000, SP5; Leica) with an oil immersion objective (×63, 1.3 numerical aperture; HCX Plan-Apochromat; Leica) and argon (488-nm) and HeNe (543- and 633-nm) lasers. Images were acquired using LAS AF SP5 software (Leica) in sequential scan mode with a 400-Hz scan rate, line averages of two, and a 512 × 512-pixel resolution. Z-stacks were collected at 0.3-μm intervals. Raw images were processed using Volocity (PerkinElmer). To improve image quality, raw images were processed using a fine filter before any analysis was performed. The same settings were maintained for all samples within an experiment.

Quantification of colocalization of phalloidin and anti-FLAG channels

Quantitative colocalization analysis in three dimensions was performed between the phalloidin and anti-FLAG channels. Colocalized voxels were identified by performing colocalization analysis in Volocity (PerkinElmer) and generating channels that display the product of the differences of the mean, which were generated by calculating the product of the difference from the mean for each voxel intensity from the two channels analyzed. This gave a clear visual display of areas of positive (and negative) correlation. The total volume of colocalized voxels per cell was calculated in Volocity using eight cells for each of the six transfections performed.

Results

KIR2DL1 and KIR2DS1 alleles form four phylogenetic clades that segregate on different KIR haplotypes

KIRs that recognize HLA-C divide into two groups: the inhibitory KIR2DL2/3 that recognize the C1 epitope of HLA-C, and the inhibitory KIR2DL1 and activating KIR2DS1 that recognize the C2 epitope of HLA-C. *KIR2DL1* and *KIR2DL2/3* are highly

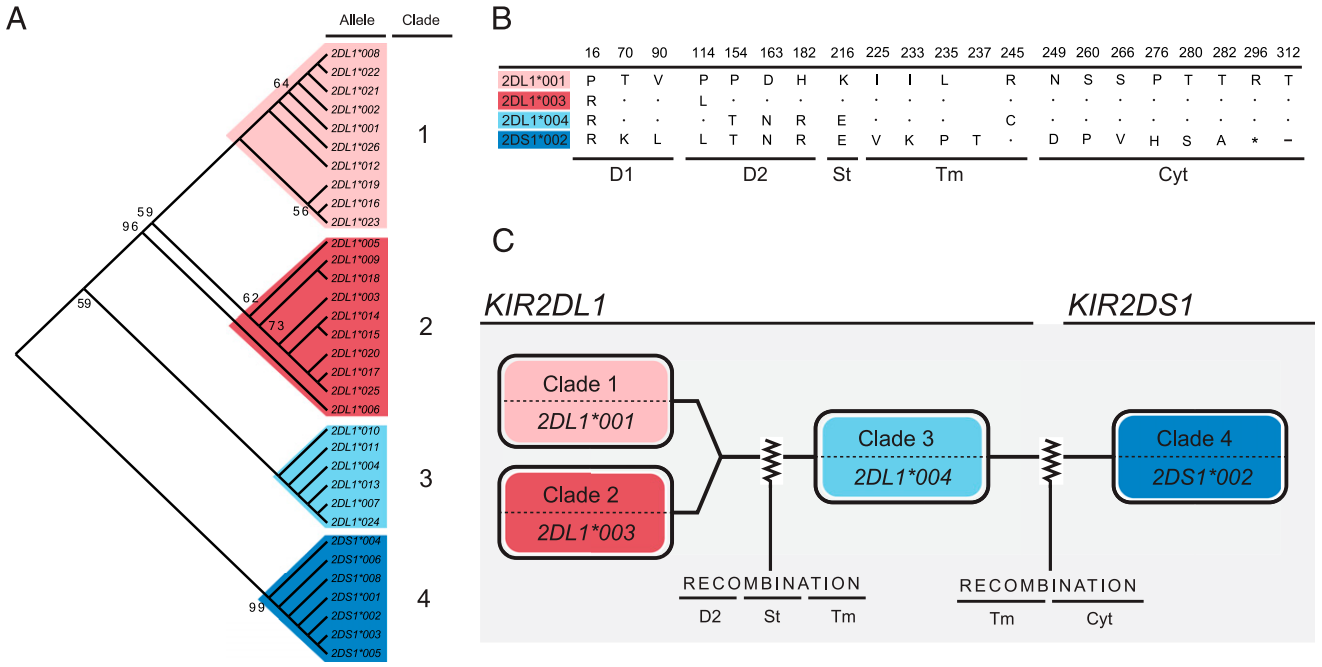

FIGURE 1. *KIR2DL1* and *KIR2DS1* form four phylogenetic clades. (**A**) Shown is a phylogenetic analysis of 33 *KIR2DL1* and *KIR2DS1* nucleotide sequences encoding amino acids 1–328. The phylogenetic relationships were inferred using three tree-building algorithms that showed broad consensus. Shown is a representative tree created using the neighbor-joining method (34). The analysis identified four clades, which are color shaded for clarity. The optimal tree, with sum of branch length of 0.071, is shown. The percentage of replicate trees in which the associated taxa clustered together in the bootstrap test (500 replicates) is shown next to the branches when ≥50. The evolutionary distances were computed using the Tamura–Nei method and are in the units of the number of base substitutions per site. All positions containing gaps and missing data were eliminated. In the final dataset there was a total of 872 positions. Evolutionary analysis was conducted in MEGA6 (35). (**B**) Shown is a sequence alignment of the most common allotypes in each of the four *KIR2DL1* and *KIR2DS1* clades identified by the phylogenetic analysis. Dots indicate identity with consensus (2DL1*001) and an asterisk indicates a termination codon. The lines beneath the alignment show the structural domains: Ig-like domains (D1 and D2), stem (St), transmembrane domain (Tm), and cytoplasmic tail (Cyt). (**C**) Schematic diagram indicating the likely sites of recombination that define the four phylogenetic clades of *KIR2DL1* and *KIR2DS1* identified in (A).

polymorphic, whereas *KIR2DS1* is relatively conserved (37) (http://www.ebi.ac.uk/ipd/kir/).

Phylogenetic analysis of the coding sequence of 26 *KIR2DL1* and 7 *KIR2DS1* alleles distinguishes four clades of *KIR* (Fig. 1A, Supplemental Fig. 1). The amino acid substitutions that distinguish representative members of the four clades are shown in Fig. 1B. Clade 1 comprises 10 *KIR2DL1*001*-like alleles (Fig. 1A), 7 of which have been mapped to *KIR* haplotypes (29, 38–44). Five of the seven are present in *Cen A*, the centromeric region of *KIR A* haplotypes (Fig. 2). In contrast, *KIR2DL1*022* and *KIR2DL1*026* are present in *Cen B*, the centromeric region of *KIR B* haplotypes (44). Clade 2 comprises 10 *KIR2DL1*003*-like alleles, of which 5 have been mapped to *KIR* haplotypes (Fig. 1A). These alleles segregate with *Cen A* (Fig. 2). Clade 3 comprises six *KIR2DL1*004*-like alleles, whose products are distinguished from those of clades 1 and 2 by a 4-aa sequence motif comprising threonine 154, asparagine 163, and arginine 182 of the D2 domain and glutamate 216 of the stem domain (Fig. 1B, Supplemental Fig. 2). This motif is shared with KIR2DS1, suggesting that *KIR2DL1* acquired this motif from *KIR2DS1* by recombination (Fig. 1C) (26). Clade 3 comprises six *KIR2DL1* alleles, of which three have been mapped to *Cen B* and one (*KIR2DL1*011*) to *Cen A* (Fig. 2). Clade 4 comprises the seven *KIR2DS1* alleles. KIR2DS1 is distinguished by having an additional residue in the transmembrane region, threonine 237, as well as lysine 233 that forms a noncovalent association with DAP12, a disulfide-bonded homodimer that contains an ITAM (45) (Fig. 1B). *KIR2DS1* alleles are all found in the telomeric region of *KIR B* haplotypes (*Tel B*). Four of these alleles have been identified in the course of high-resolution *KIR* haplotype studies (Fig. 2).

KIR2DL2/3 alleles form four phylogenetic clades that segregate on different KIR haplotypes

The *KIR2DL2/3* gene encodes receptors that recognize HLA-C allotypes carrying the C1 epitope. The alleles of *KIR2DL2/3* form two distinctive groups named *KIR2DL2* and *KIR2DL3*. Phylogenetic analysis of 36 *KIR2DL2/3* sequences identified four clades of alleles (Fig. 3A, Supplemental Figs. 1, 2B). The amino acid substitutions that distinguish representative members of the four clades are shown in Fig. 3B. Clades 1 and 2 comprise the 24 *KIR2DL3* alleles; clades 3 and 4 comprise the 11 *KIR2DL2* alleles (Fig. 3C). Clade 1 consists of 12 *KIR2DL3*001*-like alleles, and clade 2 consists of 12 *KIR2DL3*004*-like alleles. Of the 11 *KIR2DL3* alleles mapped to *KIR* haplotypes, 8 are in *Cen A* and 2 (*2DL3*014* and *2DL3*018*) in *Cen B* (Fig. 2). Although usually present in *Cen A*, *KIR2DL3*001* has been found in *Cen B*, but rarely (41).

The KIR2DL2 proteins encoded by clades 3 and 4 are distinguished from KIR2DL3 mainly by differences in the transmembrane region and the cytoplasmic tail (Fig. 3B). In this carboxyl-terminal part of the molecule, KIR2DL2 is more similar to KIR2DL1 than to KIR2DL3, indicating that *KIR2DL2* acquired this sequence from *KIR2DL1* by recombination (Fig. 3C) (21). Clade 3 comprises 10 of the 12 *KIR2DL2* alleles. Five clade 3 *KIR2DL2* alleles have been mapped to *KIR* haplotypes and shown to be present on *Cen B* (Fig. 2). Additionally, rare examples of *2DL2*003* and *2DL2*006* on *Cen A* have been reported (Fig. 2) (40, 41). Clade 4 comprises the *KIR2DL2*004* and *KIR2DL2*011* alleles. Their protein products are distinguished from other KIR2DL2/3 at positions 41, 167, 269, and 317 (Fig. 3B, Supplemental Fig. 2B). The clade 4 alleles are both present on *Cen B* (Fig. 2).

	KIR2DL1	KIR2DS1	KIR2DL2	KIR2DL3
Cen A	*001 (1) *003 (2) *002 (1) *006 (2) *008 (1) ***009*** (2) ***012*** (1) *020 (2) *023 (1) *011 (3)		*003 (3) *006 (3)	***001*** (1) *002 (2) *003 (1) *005 (2) *008 (1) *006 (2) *009 (1) *012 (2)
Cen B	*004 (3) *012 (1) *007 (3) *022 (1) *010 (3) *026 (1) *009 (2)		*001 (3) *007 (3) ***003*** (3) *004 (4) *005 (3) *011 (4) ***006*** (3)	*014 (2) *018 (2) *001 (1)
Tel B		*002 (4) *005 (4) *004 (4) *006 (4)		

FIGURE 2. *KIR2DL1*, *KIR2DS1*, and *KIR2DL2/3* segregate on distinct *KIR* haplotypes. Shown is a listing of the published associations of *KIR2DL1* and *KIR2DS1* and *KIR2DL2/3* alleles with the centromeric *KIR A* (*Cen A*, red), centromeric *KIR B* (*Cen B*, light blue), and telomeric *KIR B* (*Tel B*) haplotypes (29, 38–44). Alleles with a dual association are listed under both haplotypes with bold type indicating the more frequent association. Alleles that associate differently from the other alleles in their phylogenetic clade are highlighted with either light blue (phylogenetically *Cen B* but segregate with *Cen A*) or light red (phylogenetically *Cen A* but segregate with *Cen B*) shading. Alleles are grouped according to their clade that is shown in parentheses to the right of each allele.

In summary, these analyses (Figs. 1–3) show that for both *KIR2DL1* and *KIR2DS1* and *KIR2DL2/3* there are four phylogenetic clades of alleles that correlate with genomic location in the *Cen A*, *Cen B*, or *Tel B* regions of *KIR* haplotypes.

Cen A *encodes stronger C2 receptors and weaker C1 receptors than* Cen B

We investigated whether the receptors encoded by *Cen A* and *Cen B* alleles differ in their capacity to bind to a panel of nine C1 and seven C2 allotypes. All 10 KIR2DL1 allotypes encoded by *Cen A* (Fig. 2) have strong C2 specificity (Supplemental Fig. 3A). Of the seven KIR2DL1 encoded by *Cen B* (Fig. 2), six are specific for C2 (Supplemental Fig. 3A). The exception, KIR2DL1*022, has a methionine to lysine substitution at position 44 that gives it C1 specificity. From a synthesis of these binding data, we demonstrate that KIR2DL1 encoded by *Cen A* alleles binds C2 with greater avidity than does *Cen B*–encoded KIR2DL1, and the difference is statistically significant (two-tailed *t* test, $p < 0.01$) (Fig. 4,

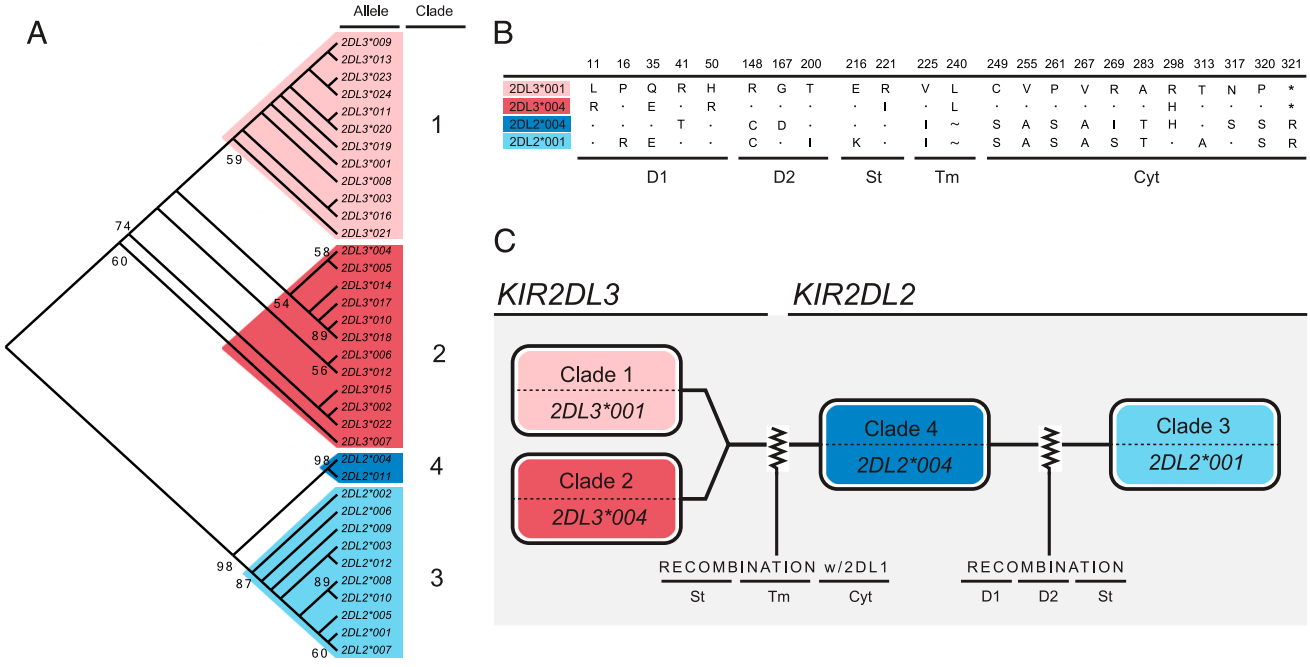

FIGURE 3. *KIR2DL2* and *KIR2DL3* form four phylogenetic clades. (**A**) Shown is a phylogenetic analysis of 36 *KIR2DL2/3* nucleotide sequences representing the domains encoding amino acids 1–328. The phylogenetic relationships were inferred using three tree-building algorithms that showed broad consensus. Shown is a representative tree created using the neighbor-joining method (34). The analysis identified four clades that have been color shaded for clarity. The optimal tree with sum of branch length of 0.079 is shown. The percentage of replicate trees in which the associated taxa clustered together in the bootstrap test (500 replicates) is shown next to the branches when ≥50. The evolutionary distances were computed using the Tamura–Nei method and are in the units of the number of base substitutions per site. All positions containing gaps and missing data were eliminated. In the final dataset there was a total of 952 positions. Evolutionary analysis was conducted in MEGA6 (35). (**B**) Shown is an alignment of four KIR2DL2/3 allotypes representing the four clades identified using phylogenetic analysis. Dots indicate identity with the consensus (2DL3*001) and an asterisk indicates a termination codon. The lines beneath the alignment show the structural domains: Ig-like domains (D1 and D2), stem (St), transmembrane domain (Tm), and cytoplasmic tail (Cyt). (**C**) Schematic diagram indicating the likely sites of recombination that define the four phylogenetic clades identified in (A).

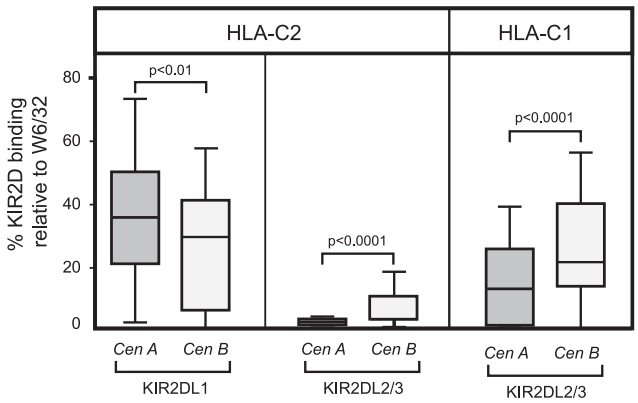

FIGURE 4. *KIR Cen A* encodes stronger C2 and weaker C1 receptors than does *Cen B*. *KIR2DL1* alleles that segregate on the *Cen A* haplotype encode receptors that bind to HLA-C2 targets with significantly greater avidity than those that segregate on the *Cen B* haplotype (two-tailed *t* test, $p < 0.01$) (*left panel*). In contrast, *KIR2DL2/3* alleles that segregate on the *Cen A* haplotype encode receptors that bind to HLA-C2 targets with significantly lower avidity than those on the *Cen B* haplotype (two-tailed *t* test, $p < 0.001$) (*center panel*). *KIR2DL2/3* alleles that segregate on the *Cen A* haplotype encode receptors that bind to HLA-C1 targets with significantly lower avidity than those on the *Cen B* haplotype (two-tailed *t* test, $p < 0.001$) (*right panel*). The binding avidity of each allotype was assessed using the binding of KIR-Fc fusion proteins to microbeads, each coated with one of nine HLA-C1 and seven HLA-C2 allotypes (Supplemental Fig. 3). Binding values are normalized to that of the W6/32 Ab that binds to all HLA class I allotypes with equal avidity.

left panel). Receptor function of three *Cen B*–associated KIR2DL1 allotypes is further weakened by substitutions in the transmembrane or cytoplasmic domain. The presence of cysteine 245 in KIR2DL1*004 and *007 (Supplemental Fig. 2A) reduces their signaling capacity (31), and that of KIR2DL1*026 is abrogated as a result of premature termination at codon 246 that eliminates the cytoplasmic tail (44, 46). Consistent with a persistent selection pressure to reduce the functionality of *Cen B*–encoded KIR2DL1, some allotypes are weakened by substitutions in both the ligand binding and signaling domains (Table I).

We performed similar analyses of the KIR2DL2/3 allotypes encoded by *Cen A* and *Cen B*. The seven *KIR2DL2* alleles generally associate with *Cen B*, although rare examples of *2DL2*003* and *2DL2*006* on *Cen A* have been reported (Fig. 2) (40, 41). Of these, *KIR2DL2*004* is inactivated (47) and does not encode a functional C1 receptor (44). The eight *KIR2DL3* alleles with defined haplotype association are all on *Cen A*. Among these is *KIR2DL3*008N* that does not encode a functional receptor (29). KIR2DL3*014 and 2DL3*018 are associated with *Cen B* and display strong binding to C1 and cross-reactivity with C2 (Supplemental Fig. 3B). These binding properties are more like KIR2DL2 allotypes than the *Cen A*–encoded KIR2DL3 allotypes. The *Cen A*–encoded KIR2DL2 and KIR2DL3 receptors have lower avidity for C1 than do the *Cen B*–encoded KIR2DL2 and KIR2DL3 receptors, and this is statistically significant (two-tailed *t* test, $p < 0.0001$) (Fig. 4, *right panel*). Thus, *Cen B*–associated KIR2DL2/3 have higher avidity for C2 than do *Cen A*–associated KIR2DL2/3 (two-tailed *t* test, $p < 0.0001$) (Fig. 4, *center panel*). This pattern is the opposite of that seen for KIR2DL1, where the *Cen A*–encoded allotypes have higher avidity for C2 than do those encoded by *Cen B*.

*Four D2 domain substitutions give Cen A–associated KIR2DL1*003 and Cen B–associated KIR2DL1*004 different C2 avidity*

To determine the basis for the weaker C2 avidity of *Cen B*–encoded KIR2DL1, we compared *KIR2DL1*003* and *KIR2DL1*004*, respectively, the most common *Cen A*– and *Cen B*–associated alleles (29, 38–44). In the D1 and D2 domains that form the ligand-binding site, KIR2DL1*003 and KIR2DL1*004 differ only in D2, at positions 114, 154, 163, and 182 (Fig. 5A). We made KIR-Fc fusion proteins from KIR2DL1*003, KIR2DL1*004, and the set of 14 KIR2DL1 mutants that represents all possible combinations of the four dimorphic positions. These 16 KIR-Fc fusion proteins were tested for binding to the panel of 97 HLA class I allotypes.

The 16 KIR2DL1-Fc bound only to the seven C2 allotypes, with the mean values being shown in Fig. 5B. Substitution at all four positions affects receptor avidity for C2. Single mutation at three of the positions (154, 163, and 182) showed that the KIR2DL1*003 residue increases and the KIR2DL1*004 residue decreases avidity. For position 114 the opposite effect was seen; that is, the KIR2DL1*003 leucine decreases avidity and the KIR2DL1*004 proline increases avidity. Receptors with higher C2 avidity than any natural KIR2DL1 allotype were made by introducing proline 114 into KIR2DL1*003 and histidine 182 into KIR2DL1*004, whereas the weakest of all the mutants tested is the KIR2DL1*004 mutant with leucine 114. In contrast to the striking differences seen among the single mutations, the mutants that differ by two substitutions from KIR2DL1*003 and KIR2DL1*004 are less varied and are all weaker C2 receptors than KIR2DL1*003. Notably, the combination of histidine 182 and proline 114, which individually give the strongest receptors, is a weaker receptor than KIR2DL1*003.

Each of the residues that contributes to the difference between KIR2DL1*003 and KIR2DL1*004 is present in 8 of the 16 KIR-Fc tested. By averaging the binding of the eight receptors

Table I. Single nucleotide polymorphisms inactivate six inhibitory lineage III KIR allotypes

Allele	Haplotype	Linked HLA-C Receptor	Mutation	Inactivation Mechanism	References
*2DL1*013N*	—	—	E35Ter	Truncated protein	(38)
*2DL1*014*	—	—	G179S	Misfolded protein and intracellular retention	(44)
*2DL1*022*	*Cen B*	*2DL2*003*	M44K	Specificity change to HLA-C1	(44)
*2DL1*026*	*Cen B*	*2DL2*003*	W246Ter	Truncated protein	(44)
2DL1 blank	*Cen B*	*2DL2*003* *2DL2*001* *2DL2*005*	NA	Gene absent	(38–44)
*2DL2*004*	*Cen B*	—	H41T	Misfolded protein and intracellular retention	(47)
*2DL3*008N*	*Cen A*	*2DL1*003*	Ins86/Ter124	Truncated protein	(29)

Haplotype association and identity of known linked HLA-C receptors for five HLA-C receptors that are unable to effect an inhibitory signal via engagement with HLA class I are shown. Also included is *KIR2DL1*022*, an allele that encodes a receptor that recognizes C1 but not C2 (44), and *2DL1 blank* (the absence of the *2DL1* gene). The amino acid mutation, termination (Ter) or insertion (Ins), and mechanism by which each allele encodes an inactivated protein is listed to the right with the reference that identified it. —, the allele listed has no known published association; NA; not applicable, indicates that the listed allele is not defined by an amino acid mutation.

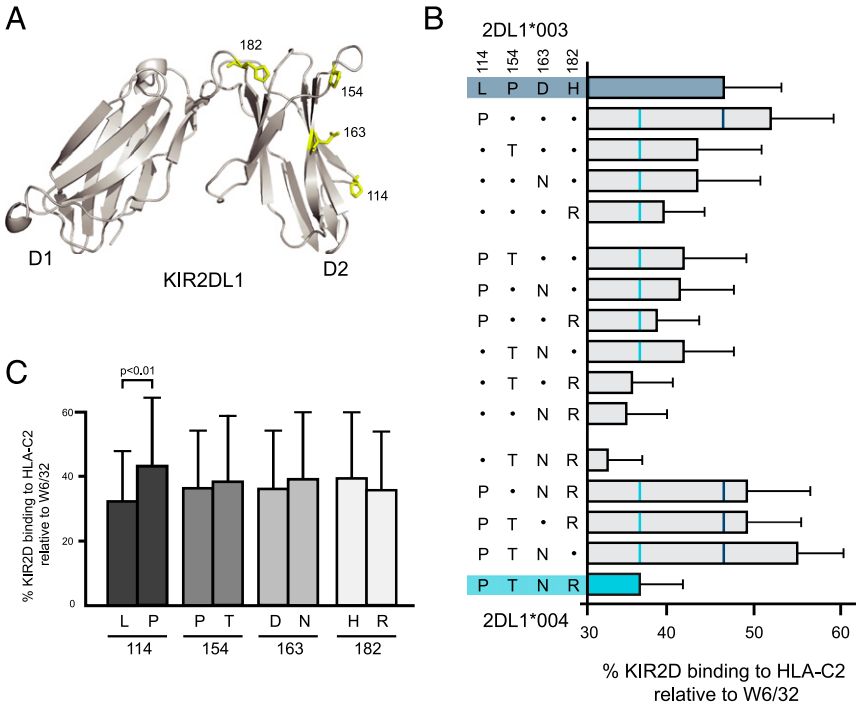

FIGURE 5. Variation at positions 154, 163, and 182 in the D2 domain reduces the avidity of KIR2DL1*004 for HLA-C2. (**A**) Structural representation of KIR2DL1 (PDB: 1NKR) (48) mapping the location of the four residues at which 2DL1*003 and 2DL1*004 differ. The protein backbone is shown in gray with the four positions of substitution highlighted in yellow. (**B**) Mean binding of 16 KIR2DL1-Fc fusion proteins to microbeads, each coated with one of seven C2 HLA-C allotypes. Shown is a sequential mutation analysis in which every possible residue or combination of residues at which 2DL1*003 and 2DL1*004 differ is tested for binding to HLA-C2. The alignment to the left shows the identity of the residues in each KIR-Fc mutant. Binding values are normalized to that of the W6/32 Ab that binds to all HLA class I allotypes with equal avidity. Broken vertical lines indicate the binding of 2DL1*003 (dark blue) and 2DL1*004 (light blue) for comparison. (**C**) Shown is the mean binding to HLA-C2 of every mutant KIR-Fc containing the listed amino acid residue at positions 114, 154, 163, and 182. KIR-Fc with leucine 114 bound to HLA-C2 with a significantly lower avidity than those with proline 114 (two-tailed *t* test, $p < 0.01$).

containing a particular residue we see that the mean values are very similar, except for that between the groups of receptors having leucine or proline at position 114 (Fig. 5C). These results are consistent with all four positions contributing to the binding and being affected by the particular residues present at the other positions. Thus, the four dimorphic sites have not coevolved to produce the strongest and weakest C2 receptors possible. Instead, there exists a more moderate balance between a stronger and a weaker C2 receptor. The dimorphism of arginine (KIR2DL1*003) and cysteine (KIR2DL1*004) at position 245 at the end of the transmembrane domain (Fig. 1B) also adds to the functional difference between KIR2DL1*003 and KIR2DL1*004. The cysteine 245 reduces the capacity of KIR2DL1*004 to develop inhibitory signals (31) and educate NK cells (33).

The N-terminal half of the KIR2DL1 transmembrane domain is essential for cell surface expression

KIR2DL1*004 is one example of a *Cen B*–associated allotype that is functionally affected by polymorphism at the junction between the transmembrane and cytoplasmic domains. Another is KIR2DL1*026 that has a termination codon at position 246 (Supplemental Fig. 2A). This substitution has two effects. First, it eliminates the cytoplasmic tail with its ITIMs that mediate inhibitory signaling function (46). Second, it reduces the cell surface expression of KIR2DL1*026, which is 32% that of KIR2DL1*012, the progenitor of KIR2DL1*026 (44). This observation raised the question: How much of the transmembrane domain is necessary for KIR2DL1 to become cell surface associated?

To address this question we introduced termination codons at five evenly spaced positions within the sequence encoding the transmembrane domain (residues 225–245) of KIR2DL1*003, as well as at position 224 in the stem domain and positions 246, 250, and 256 in the cytoplasmic tail (Fig. 6A). After incorporation of N-terminal 3× FLAG-tags, the 12 mutant constructs and wild-type *KIR2DL1*003* were transiently transfected into HeLa cells. After 48 h of culture the amounts of KIR2DL1 on the surface of the transfected HeLa cells were measured using anti-FLAG Ab and flow cytometry.

Termination in the N-terminal half of the transmembrane region (residues 225–235) completely abrogated cell surface expression of the mutant KIR2DL1*003. In contrast, termination in the carboxyl-terminal half of the transmembrane (residues 236–245) permitted cell surface expression of mutant KIR2DL1*003, with levels corresponding to 53–72% of the wild-type (Fig. 6A). These results show that the N-terminal half of the transmembrane domain is required for membrane association and cell surface expression of KIR2DL1. Mutants that terminate at positions 238, 242, and 246, and that lack a cytoplasmic tail, were expressed at slightly higher levels than mutants 250 and 256 that have a short, truncated cytoplasmic tail ($p = 0.0317$). Terminating at position 246, KIR2DL1*026 is in the former category.

*KIR2DL1*014 folds inefficiently and is retained inside the cell*

KIR2DL1*014 differs from KIR2DL1*003 by substitution of glycine for serine at position 179 in the D2 domain (Supplemental Fig. 2A). Serine 179 prevents cell surface expression of KIR2DL1*014 and the binding of KIR2DL1*014-Fc to HLA class I (44). These properties suggest that serine 179 prevents KIR2DL1*014 from folding properly, thereby leading to a denatured protein and its intracellular retention.

To test this hypothesis, confocal microscopy was used to examine the cellular localization of FLAG-tagged KIR2DL1*014 in

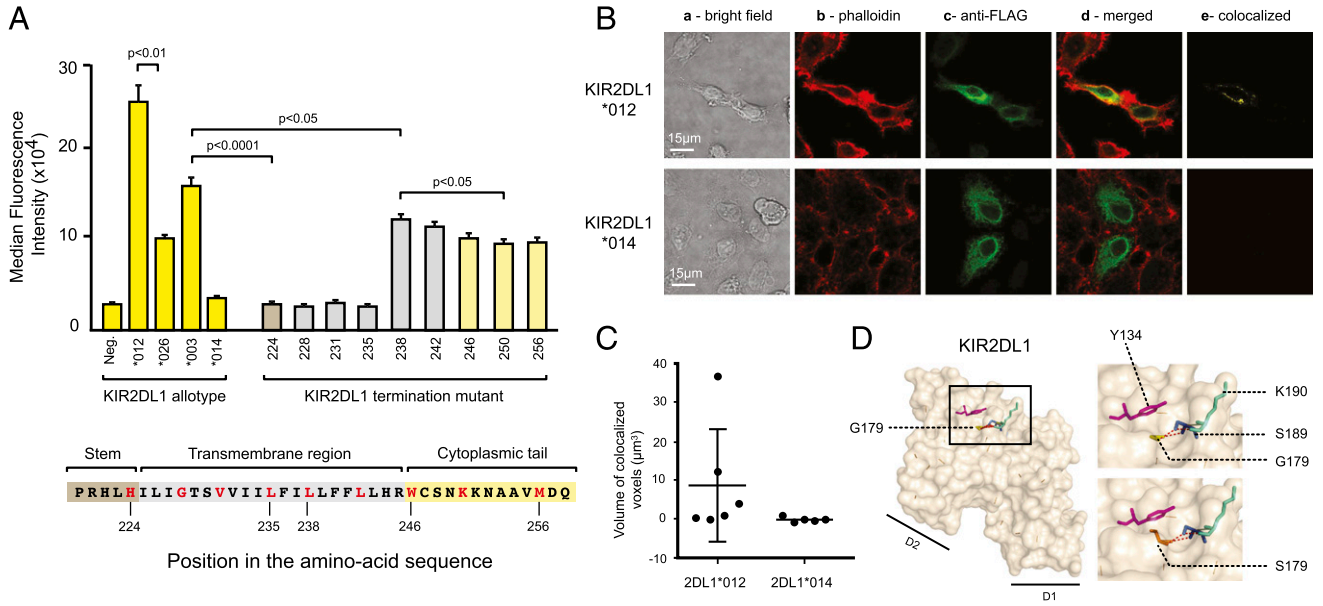

FIGURE 6. The N-terminal half of the KIR2DL1 transmembrane domain is essential for cell surface expression. (**A**) Cell surface expression of natural and mutant KIR2DL1. Constructs encoding FLAG-tagged KIR2DL1 were transiently transfected into HeLa cells. The binding of anti-FLAG Ab to the transfected cells was measured. Shown are median fluorescence intensity (MFI) values for the KIR2DL1*012, KIR2DL1*026, KIR2DL1*003, and KIR2DL1*014 natural allotypes and for nine KIR2DL1 mutants, each containing a termination codon at the listed residue. Termination codons were placed at position 224 in the stem region (brown), positions 228, 231, 235, 238, and 242 in the transmembrane region (gray) and positions 246, 250, and 256 in the cytoplasmic tail (pale yellow). Error bars give the SD for three separate experiments. Statistically significant differences are denoted by brackets. Shown below is the amino acid sequence at positions 220–258 in KIR2DL1*003. This sequence encompasses the stem region (brown), the transmembrane region (gray), and the cytoplasmic tail (yellow). Residues at which termination codons were introduced are shown in red. (**B**) Shown are confocal microscopy images of HeLa cells 48 h after transfection with FLAG-tagged KIR2DL1*012 (*upper panels*) and KIR2DL1*014 (*lower panels*). Columns a–e show the bright field image, staining with phalloidin–Alexa Fluor 555 to identify the area near the cell surface, staining with FITC-conjugated anti-FLAG Ab, a merged image of columns b and c, and the colocalization of anti-FLAG and phalloidin. (**C**) Shown is the quantitative colocalization analysis in three dimensions performed between the phalloidin and anti-FLAG channels. The total volume of colocalized voxels per cell was calculated in Volocity (PerkinElmer) using eight cells for each of the six transfections performed. (**D**) Structural representation of KIR2DL1 (PDB: 1NKR) (48) showing the location of glycine 179 (yellow) buried in the interior of the receptor architecture (*left panel*). As seen in the enlargement in the *right panels*, structural analysis showed that substitution of glycine for serine at position 179 is predicted to disrupt protein folding as a result of a side chain interaction between serine 179 and tyrosine 134.

transiently transfected HeLa cells (Fig. 6B). KIR2DL1*012, an allotype expressed highly at the cell surface, served as the control. Phalloidin, which binds to intracellular actin, was used as an independent marker of the underside of the cell surface (Fig. 6Bb). In cells expressing FLAG-tagged KIR2DL1*012, the distribution of the anti-FLAG Ab (Fig. 6Bc, *upper*) overlapped with that of phalloidin. This is further seen in a merge of the two images (Fig. 6Bd, *upper*) and determination of the extent of colocalization (Fig. 6Be, *upper*). In the cells expressing KIR2DL1*014 the anti-FLAG Ab was detected inside the transfected cells (Fig. 6Bc, *lower*) but not at the cell surface similar to phalloidin (Fig. 6Bb, *lower*). On merging the two images (Fig. 6Bd, *lower*) there was no detectable colocalization (Fig. 6Be, *lower*). Quantification of the extent of the colocalization of phalloidin and anti-FLAG Ab in transfected HeLa cells expressing KIR2DL1*012 and KIR2DL1*014 is shown in Fig. 6C. This analysis demonstrates that transfected cells expressing KIR2DL1*014 make the protein but do not transport it to the cell surface. These data are consistent with KIR2DL1*014 not folding properly.

Analysis of the three-dimensional structure of KIR2DL1*001 (*PDB:1NKR*) (48) showed that position 179 of the D2 domain is buried beneath the binding site for HLA-C (Fig. 6D, *left panel*). We modeled the effect of replacing glycine 179 of KIR2DL1*001 with the serine 179 of KIR2DL1*014. In this model, the side chain substitution of a hydrogen atom for a methyl group displaces the tyrosine at position 134 (Fig. 6D, *right panels*). We hypothesize that this displacement is incompatible with proper folding of the KIR2D molecule. Supporting this interpretation, tyrosine 134 and glycine 179 are conserved in hominoid lineage III KIR (Supplemental Fig. 4).

Variation at positions 16 and 148 diversifies the recognition of HLA-C by KIR2DL2/3

Analysis of hominoid KIR sequences demonstrated that positions 16 (D1 domain) and 148 (D2 domain) have been subject to positive selection during hominoid evolution (26). These residues juxtapose within the hinge region that connects the D1 and D2 domains (Fig. 7A) (49). Polymorphism at residues 16 and 148 of KIR2DL2/3 has been proposed to vary the angle between the D1 and D2 domains and account for KIR2DL2*001 and KIR2DL3*001 having different avidity and specificity for HLA-C (21, 50). Having proline 16 and arginine 148, KIR2DL3*001 is a C1-specific receptor of moderate avidity. In contrast, arginine 16 and cysteine 148 give KIR2DL2*001 high avidity for C1 and cross-reactivity with C2 (21, 32).

Sequence comparison of 61 KIR2DL1, KIR2DL2, and KIR2DL3 variants showed that arginine and proline are the only residues present at position 16, whereas arginine, proline, and cysteine can occur at position 148 (Fig. 7B). Five of the six possible combinations of these residues are present in human lineage III KIR. Absent is the combination of arginine 16 with proline 148 (Supplemental Fig. 4). The other five combinations are represented in the 36 KIR2DL2/3 allotypes, but only two combinations are represented in the 33 KIR2DL1 and 2DS1 allotypes (Fig. 7C). To see how the variability at positions 16 and 148 influence avidity

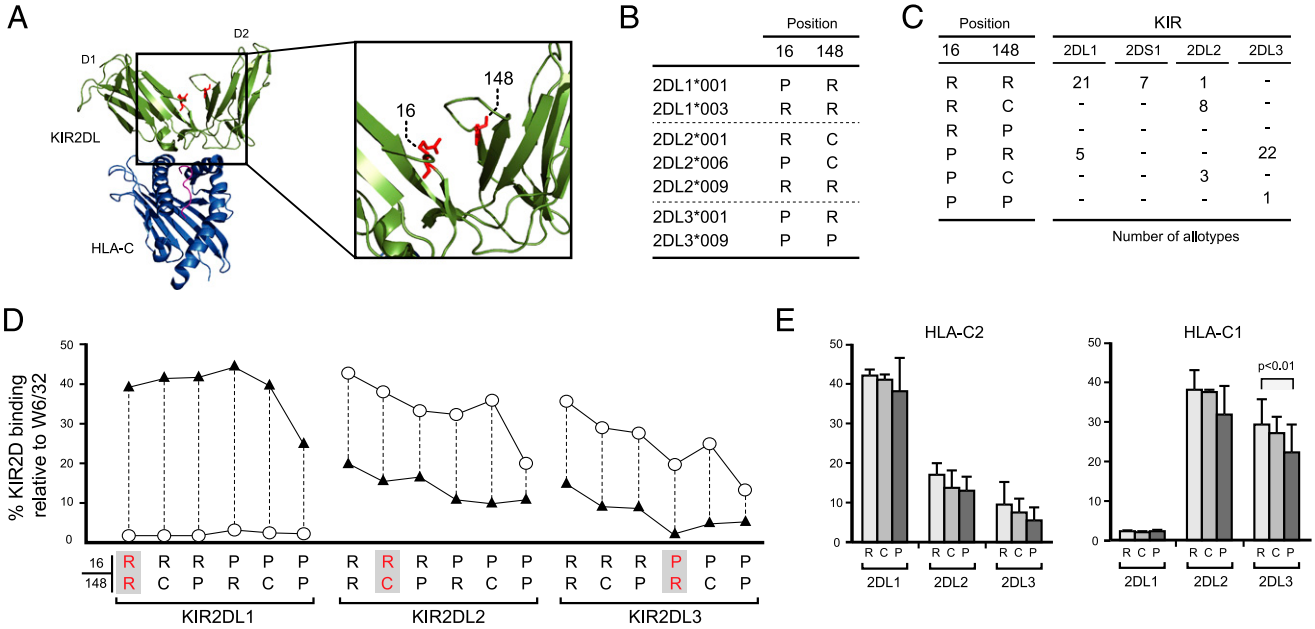

FIGURE 7. Residues at positions 16 and 148 diversify the binding of two-domain KIR to HLA-C. (**A**) Structural representation of a two-domain KIR (green) bound to HLA-C (blue) (PDB: 1EFX) (49). Shown in red and enlarged in the *right panel* is the position of residues 16 and 148 that occupy the hinge region of the receptor. (**B**) Alignment showing the amino acid variation at positions 16 and 148 in 61 KIR2DL1 and KIR2DL2/3 allotypes. One representative allele with a unique combination of residues is shown for KIR2DL1 and KIR2DL2/3. The allotypes listed differ at residues other than 16 and 148 (Supplemental Fig. 2). (**C**) For each unique combination of residues at positions 16 and 148, the number of KIR2DL1, KIR2DS1, KIR2DL2, and KIR2DL3 allotypes that encode that combination are listed. A dash (-) indicates the combination is not present in the listed gene. (**D**) Shown is the binding of six 2DL1-Fc, six 2DL2-Fc, and six 2DL3-Fc fusion proteins to nine HLA-C1 allotypes (○) and 7 HLA-C2 allotypes (▲). The residues at positions 16 and 148 were mutated to those listed below each KIR-Fc. The prototypical allotypes of each KIR (KIR2DL1*003, KIR2DL2*001, and KIR2DL3*001, respectively) are indicated with red lettering and gray shading. Binding values are normalized to that of the W6/32 Ab that binds to all HLA class I allotypes with equal avidity. (**E**) Shown is the mean binding to HLA-C2 and HLA-C1 of every KIR containing arginine at either position 16 or 148 (R), cysteine at either position (C), or proline at either position (P). KIR2DL3-Fc containing either R16 or R148 bound to C1-bearing allotypes with significantly greater avidity than those containing either P16 or P148 (two-tailed *t* test, $p < 0.01$).

for HLA-C, we made 18 KIR-Fc fusion proteins in which all six combinations of the natural residues at positions 16 and 148 were introduced into KIR2DL1*003, KIR2DL2*001, and KIR2DL3*001. These KIR-Fc fusion proteins were tested for binding to HLA class I.

KIR2DL1*003 and four of the five KIR2DL1 mutants have similarly high avidity and specificity for HLA-C, exhibiting <15% variability in the binding to any HLA-C allotype (Fig. 7D). In contrast, the mutant combining proline 16 with proline 148 retained high specificity for C2 but its avidity was reduced to 60% that of KIR2DL1*003.

In comparison with the relative insensitivity of KIR2DL1*003 to mutation, all the KIR2DL2 and KIR2DL3 mutants exhibit detectable differences (Fig. 7D). For KIR2DL2 the major effect of mutation was to change the avidity, whereas the specificity, of stronger binding to C1 and weaker binding to C2, was less affected. Arginine residues correlate with the highest binding. Thus, the mutant with arginine 16 and arginine 148 binds more strongly to HLA-C than does the wild-type KIR2DL2*001 that combines arginine 16 with cysteine 148. Alternatively, lower binding correlates with the presence of proline at positions 16 and 148, with the weakest receptor having proline 16 and proline 148. The effect of cysteine at position 148 is intermediate between that of arginine and proline. These general effects of arginine and proline are seen for KIR2DL1, KIR2DL2, and KIR2DL3 (Fig. 7E).

Three of the KIR2DL3 mutants have higher avidity for HLA-C than does wild-type KIR2DL3*001. What distinguishes KIR2DL3*001 from the five mutants is its minimal cross-reactivity with C2. It therefore appears that KIR2DL3*001 evolved under selection for C1 specificity, with avidity being of secondary importance. In contrast, the evolution of KIR2DL1*003 resulted in a receptor having both high avidity and high specificity for C2. The properties of KIR2DL2 are different again. KIR2DL2 recognizes both C1 and C2, making it a stronger C1 receptor than KIR2DL3 and a weaker C2 receptor than KIR2DL1. Thus, KIR2DL2 appears as an evolutionary compromise, or intermediate, between KIR2DL1 and KIR2DL3.

KIR2DS1 allotypes bind HLA-C2 with different avidity

KIR2DS1 has specificity for C2 (20), similar to KIR2DL1, but is less polymorphic. *KIR2DS1* alleles encoding seven KIR2DS1 allotypes have been described (37). *KIR2DS1*002* is by far the most frequent allele, being present in every population that has been *KIR* typed at allele-level resolution (29, 38–44). To study the avidity and specificity of KIR2DS1, we constructed KIR-Fc fusion proteins for the four KIR2DS1 allotypes that differ in the amino acid sequences of the D1 and D2 domains that bind HLA class I (Fig. 8A).

The four KIR2DS1 allotypes all bound to the seven C2-bearing HLA-C allotypes (Fig. 8B) but did not bind to the nine C1-bearing HLA-C allotypes (data not shown). KIR2DS1*001 has the highest avidity for C2, which correlates with arginine at position 70, where the other KIR2DS1 allotypes have lysine. KIR2DS1*008 has the lowest avidity for C2, which correlates with serine 123, where the other KIR2DS1 allotypes have tryptophan. Having a similar intermediate avidity for C2 are KIR2DS1*002 and KIR2DS1*004. They differ at position 90, where the valine–leucine dimorphism has little effect on the receptors' avidity. Thus, the

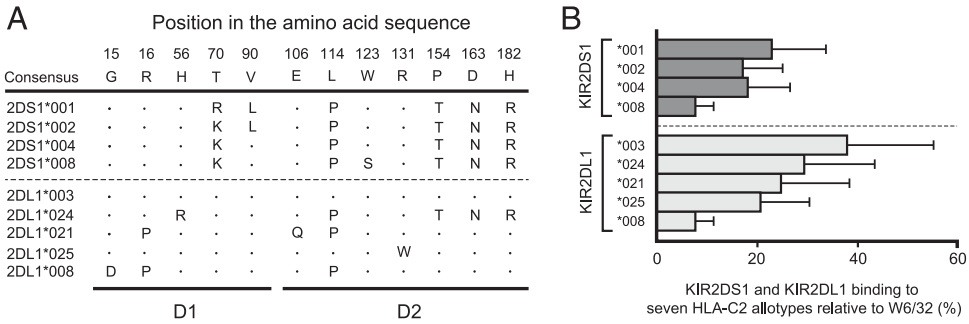

FIGURE 8. Substitutions in the extracellular binding domains regulate the avidity of KIR2DS1 allotypes for HLA-C2. (**A**) Shown is an alignment of the Ig-like domains (D1 and D2) of four allotypes of KIR2DS1 and four allotypes of KIR2DL1. Dots indicate identity with consensus. The position of the structural domain (D1 or D2) is indicated by a line below the alignment. (**B**) Binding of four naturally occurring KIR2DS1-Fc and KIR2DL1-Fc fusion proteins to microbeads coated with seven C2 HLA-C allotypes. Binding values are normalized to that of the W6/32 Ab that binds to all HLA class I allotypes with equal avidity.

observed differences in avidity can be attributed to the dimorphisms at position 70 in the D1 domain and 123 in the D2 domain. Position 70 has been subject to positive selection in hominoid KIR and has a dominant effect in modifying the avidity of KIR2DL1 and KIR2DL3 (51). Arginine at position 70 improves recognition of HLA-C as shown in this study for KIR2DS1 and previously for KIR2DL3 (51). Although, overall, KIR2DS1 allotypes are not as avid HLA-C2 receptors as KIR2DL1, there are KIR2DL1 allotypes that have similar HLA-C2 avidity to each of the KIR2DS1 allotypes (Fig. 8B).

Discussion

This study investigated the genetic and functional diversity of human HLA-C receptors. We showed that the inhibitory *KIR2DL1*, activating *KIR2DS1*, and inhibitory *KIR2DL2/3* alleles form distinctive phylogenetic clades that associate with specific *KIR* haplotypes. Typifying *KIR Cen A* haplotypes are *KIR2DL1* alleles that encode strong inhibitory C2 receptors and *KIR2DL2/3* alleles encoding weak inhibitory C1 receptors. In striking contrast, *Cen B* haplotypes combine *KIR2DL1* alleles that encode weak inhibitory C2 receptors with *KIR2DL2/3* alleles encoding strong inhibitory C1 receptors.

Our results are in accordance with the first descriptions of the genomic organization of *KIR* haplotypes (28, 52, 53). These studies identified the segregation of *KIR2DL3* with *KIR A* haplotypes and *KIR2DL2* with *KIR B* haplotypes. Subsequent work highlighted the functional differences between the receptors encoded by these allelic variants (21, 32). High-resolution *KIR* analysis of white populations consistently associated *KIR2DL1*004* with the *KIR B* haplotype, and in positive linkage disequilibrium with *KIR2DL2* (30). Functional differences between the *KIR2DL1* alleles of *KIR A* and *B* haplotypes were likewise discovered when NK cells expressing KIR2DL1*004 were found to be hyporesponsive in comparison with NK cells expressing KIR2DL1*003 (33). Dimorphism at position 245 in the transmembrane region of KIR2DL1 was demonstrated to be one mechanism that causes such functional differences (31).

We show that such attenuated function is not limited to KIR2DL1*004, or even to the group of KIR2DL1 allotypes having cysteine 245, but it is a defining characteristic of the KIR2DL1 encoded by *Cen B*–associated alleles. A variety of mechanisms cause functional attenuation, with mutations in the ligand-binding domains regulating the avidity and specificity of KIR2DL1 for HLA-C. Such changes can synergize with those in the transmembrane domain (which predominantly regulate cell surface expression and signaling function) to produce a broad range of functionally distinct receptors that share the common feature of being weakened in comparison with the KIR2DL1 allotypes associated with the *KIR A* haplotype.

Examination of KIR2DL2/3 allotypes revealed a range of functional properties, similar to those seen for KIR2DL1. In contrast to KIR2DL1, the weaker C1 receptors are associated with *KIR A* haplotypes and the stronger receptors are associated with *KIR B* haplotypes. Additionally, the weaker *KIR A*–associated receptors are more specific C1 receptors than the *KIR B*–associated receptors, which to varying degree exhibit cross-reactivity for C2. Unlike KIR2DL1, most functional differences between KIR2DL2/3 allotypes arise from amino acid substitutions in the ligand-binding domains.

Of interest in this regard are *KIR2DL2*008* and *KIR2DL2*010*, two alleles for which haplotype associations have yet to be determined. The ligand-binding domains are identical to those of the KIR2DL2*001 prototype. Where they differ from KIR2DL2*001, and all other KIR2DL2/3 allotypes, is in the transmembrane domain. They have cysteine instead of arginine at position 245. Given the functional attenuation caused by cysteine 245 in KIR2DL1 (31), it is likely that cysteine 245 in KIR2DL2*008 and KIR2DL1*010 weakens their function by reducing cell surface expression and inhibitory signaling. Supporting this hypothesis, KIR2DL2 and KIR2DL1 have almost identical transmembrane and cytoplasmic domains (21). We further predict that *KIR2DL2*008* and *KIR2DL2*010* associate with *Cen A* haplotypes, not *Cen B* haplotypes, similar to other *KIR2DL2* alleles. A precedent for such "haplotype infidelity" is that *KIR2DL3*014* and *KIR2DL3*018* are strong C1 receptors that cross-react with C2 and associate with *Cen B*.

Our results indicate that polymorphisms in all of the structural domains of the mature protein can impact the function of KIR with respect to the initiation and propagation of inhibitory or activating signals. Substitutions that change the avidity of KIR2DL1 for HLA-C are usually in the D2 domain, whereas substitutions that change the avidity of KIR2DL2/3 for HLA-C are usually in the hinge region connecting the D1 and D2 domains. The only site where substitution has significant impact on the specificity of KIR2DL1 for C2, or KIR2DL2/3 for C1, is position 44 in the D1 domain. Substitutions that affect the cell surface expression of KIR2DL are more often in the transmembrane or the cytoplasmic domain, but there are also substitutions in the extracellular domains that affect receptor function in this way. An extreme example is KIR2DL1*014, which is completely retained inside the cell as a consequence of having serine, rather than glycine, at position 179 in the D2 domain. We suspect that this substitution prevents proper folding of KIR2DL1*014.

Similar to KIR2DL1*014, KIR2DL1*013N, KIR2DL1*026, KIR2DL2*004, and KIR2DL3*008N are inhibitory lineage III *KIR* that are unlikely to be functional receptors (Table I). We examined the extent to which inactivation of these receptors affected the capacity of their haplotypes to provide inhibitory receptors that recognize C1 and C2. From the initial description of *KIR A* and *B* haplotypes it was appreciated that they both encode inhibitory receptors that recognize C1 and C2 (28, 52). Subsequent studies established the combination of *KIR2DL1* and *KIR2DL3* on *Cen A* and of *KIR2DL1* and *KIR2DL2* on *Cen B* (25, 30, 40–42). Overlaying our functional binding data onto the high-resolution *KIR* haplotypes of seven populations, we find that every KIR2DL1 allotype encoded by *Cen A* recognizes C2 and that every KIR2DL3 allotype encoded by *Cen A* recognizes C1. The exception is a *KIR A* haplotype of Yucpa Amerindians, which has a frequency of 7.4% and combines a strong, C2-specific receptor with the nonfunctional *KIR2DL3*008N* allele (29). Consequently, the receptors encoded by this haplotype cannot recognize C1, although the frequency of the haplotypes is such that <1% of individuals in the population would be deficient in C1 recognition.

Cen B haplotypes that encode KIR2DL1*022 and KIR2DL1*026 (neither of which can mediate inhibition via engagement with C2) are in strong linkage disequilibrium with *KIR2DL2*003* and are specific to the KhoeSan and immediately neighboring populations in southern Africa (44). *Cen B* haplotypes that lack the *KIR2DL1* gene (*KIR2DL1* blank) are widespread and associated with *KIR2DL2*003, KIR2DL2*001* and *KIR2DL2*005* (Table I) (38–44). These *Cen B* haplotypes retain some capacity to recognize C2 because their associated KIR2DL2 allotypes cross-react with C2 (Supplemental Fig. 3B). The functional importance of these cross-reactions needs to be assessed in cellular assays of NK cell education and effector response.

Although the relative frequency of *KIR A* and *B* haplotypes varies substantially across the world, as do C1 and C2 frequencies, there is a strong correlation between C2 and *KIR B* and a corresponding inverse correlation between C2 and *KIR A* (14). Thus, it appears that in populations with high C2 frequency, such as those in Africa, there has been selection for weak C2 receptors and strong C1 receptors (found on KIR B haplotypes) whereas in populations with high C1 frequency, such as those in Asia and the Americas, there has been selection for weak C1 receptors but strong C2 receptors (found on KIR A haplotypes). Underlying these observations, and implicating a strong inhibitory C2 receptor–ligand interaction in their pathogenesis, are correlations with pregnancy syndromes. Thus, women who are pregnant with a fetus expressing C2 are at increased risk of pre-eclampsia (14, 15). Those same strong inhibitory KIR–ligand interactions are, however, vital for the development of well-educated NK cells that are both self-tolerant and responsive to virally infected and malignantly transformed cells. Thus, a pattern emerges in which *KIR* haplotypes with contrasting functional properties are subject to selection in response to the relative abundance of HLA-C ligand. In this way, the KIR system may be considered a buffering mechanism by which optimal NK cell function is preserved, despite fluctuations in the frequency of available ligand.

Disclosures

The authors have no financial conflicts of interest.

References

1. Lanier, L. L. 2008. Evolutionary struggles between NK cells and viruses. *Nat. Rev. Immunol.* 8: 259–268.
2. Diefenbach, A., and D. H. Raulet. 2002. The innate immune response to tumors and its role in the induction of T-cell immunity. *Immunol. Rev.* 188: 9–21.
3. Parham, P., and A. Moffett. 2013. Variable NK cell receptors and their MHC class I ligands in immunity, reproduction and human evolution. *Nat. Rev. Immunol.* 13: 133–144.
4. Lanier, L. L. 2008. Up on the tightrope: natural killer cell activation and inhibition. *Nat. Immunol.* 9: 495–502.
5. Parham, P., L. Abi-Rached, L. Matevosyan, A. K. Moesta, P. J. Norman, A. M. Older Aguilar, and L. A. Guethlein. 2010. Primate-specific regulation of natural killer cells. *J. Med. Primatol.* 39: 194–212.
6. Alter, G., D. Heckerman, A. Schneidewind, L. Fadda, C. M. Kadie, J. M. Carlson, C. Oniangue-Ndza, M. Martin, B. Li, S. I. Khakoo, et al. 2011. HIV-1 adaptation to NK-cell-mediated immune pressure. *Nature* 476: 96–100.
7. Khakoo, S. I., C. L. Thio, M. P. Martin, C. R. Brooks, X. Gao, J. Astemborski, J. Cheng, J. J. Goedert, D. Vlahov, M. Hilgartner, et al. 2004. HLA and NK cell inhibitory receptor genes in resolving hepatitis C virus infection. *Science* 305: 872–874.
8. Wauquier, N., C. Padilla, P. Becquart, E. Leroy, and V. Vieillard. 2010. Association of KIR2DS1 and KIR2DS3 with fatal outcome in Ebola virus infection. *Immunogenetics* 62: 767–771.
9. Łuszczek, W., M. Mańczak, M. Cisło, P. Nockowski, A. Wiśniewski, M. Jasek, and P. Kuśnierczyk. 2004. Gene for the activating natural killer cell receptor, KIR2DS1, is associated with susceptibility to psoriasis vulgaris. *Hum. Immunol.* 65: 758–766.
10. Suzuki, Y., Y. Hamamoto, Y. Ogasawara, K. Ishikawa, Y. Yoshikawa, T. Sasazuki, and M. Muto. 2004. Genetic polymorphisms of killer cell immunoglobulin-like receptors are associated with susceptibility to psoriasis vulgaris. *J. Invest. Dermatol.* 122: 1133–1136.
11. van der Slik, A. R., B. P. Koeleman, W. Verduijn, G. J. Bruining, B. O. Roep, and M. J. Giphart. 2003. KIR in type 1 diabetes: disparate distribution of activating and inhibitory natural killer cell receptors in patients versus HLA-matched control subjects. *Diabetes* 52: 2639–2642.
12. Cooley, S., D. J. Weisdorf, L. A. Guethlein, J. P. Klein, T. Wang, C. T. Le, S. G. Marsh, D. Geraghty, S. Spellman, M. D. Haagenson, et al. 2010. Donor selection for natural killer cell receptor genes leads to superior survival after unrelated transplantation for acute myelogenous leukemia. *Blood* 116: 2411–2419.
13. Cooley, S., D. J. Weisdorf, L. A. Guethlein, J. P. Klein, T. Wang, S. G. Marsh, S. Spellman, M. D. Haagenson, K. Saeturn, M. Ladner, et al. 2014. Donor killer cell Ig-like receptor B haplotypes, recipient HLA-C1, and HLA-C mismatch enhance the clinical benefit of unrelated transplantation for acute myelogenous leukemia. *J. Immunol.* 192: 4592–4600.
14. Hiby, S. E., J. J. Walker, K. M. O'shaughnessy, C. W. Redman, M. Carrington, J. Trowsdale, and A. Moffett. 2004. Combinations of maternal KIR and fetal HLA-C genes influence the risk of preeclampsia and reproductive success. *J. Exp. Med.* 200: 957–965.
15. Nakimuli, A., O. Chazara, S. E. Hiby, L. Farrell, S. Tukwasibwe, J. Jayaraman, J. A. Traherne, J. Trowsdale, F. Colucci, E. Lougee, et al. 2015. A KIR B centromeric region present in Africans but not Europeans protects pregnant women from pre-eclampsia. *Proc. Natl. Acad. Sci. USA* 112: 845–850.
16. Kovats, S., E. K. Main, C. Librach, M. Stubblebine, S. J. Fisher, and R. DeMars. 1990. A class I antigen, HLA-G, expressed in human trophoblasts. *Science* 248: 220–223.
17. Rajagopalan, S., and E. O. Long. 1999. A human histocompatibility leukocyte antigen (HLA)-G-specific receptor expressed on all natural killer cells. *J. Exp. Med.* 189: 1093–1100.
18. Yang, Y., W. Chu, D. E. Geraghty, and J. S. Hunt. 1996. Expression of HLA-G in human mononuclear phagocytes and selective induction by IFN-γ. *J. Immunol.* 156: 4224–4231.
19. Winter, C. C., and E. O. Long. 1997. A single amino acid in the p58 killer cell inhibitory receptor controls the ability of natural killer cells to discriminate between the two groups of HLA-C allotypes. *J. Immunol.* 158: 4026–4028.
20. Moesta, A. K., T. Graef, L. Abi-Rached, A. M. Older Aguilar, L. A. Guethlein, and P. Parham. 2010. Humans differ from other hominids in lacking an activating NK cell receptor that recognizes the C1 epitope of MHC class I. *J. Immunol.* 185: 4233–4237.
21. Moesta, A. K., P. J. Norman, M. Yawata, N. Yawata, M. Gleimer, and P. Parham. 2008. Synergistic polymorphism at two positions distal to the ligand-binding site makes KIR2DL2 a stronger receptor for HLA-C than KIR2DL3. *J. Immunol.* 180: 3969–3979.
22. Barrow, A. D., and J. Trowsdale. 2008. The extended human leukocyte receptor complex: diverse ways of modulating immune responses. *Immunol. Rev.* 224: 98–123.
23. Trowsdale, J., R. Barten, A. Haude, C. A. Stewart, S. Beck, and M. J. Wilson. 2001. The genomic context of natural killer receptor extended gene families. *Immunol. Rev.* 181: 20–38.
24. Wilson, M. J., M. Torkar, A. Haude, S. Milne, T. Jones, D. Sheer, S. Beck, and J. Trowsdale. 2000. Plasticity in the organization and sequences of human KIR/ILT gene families. *Proc. Natl. Acad. Sci. USA* 97: 4778–4783.
25. Pyo, C. W., L. A. Guethlein, Q. Vu, R. Wang, L. Abi-Rached, P. J. Norman, S. G. Marsh, J. S. Miller, P. Parham, and D. E. Geraghty. 2010. Different patterns of evolution in the centromeric and telomeric regions of group A and B haplotypes of the human killer cell Ig-like receptor locus. *PLoS One* 5: e15115.
26. Abi-Rached, L., A. K. Moesta, R. Rajalingam, L. A. Guethlein, and P. Parham. 2010. Human-specific evolution and adaptation led to major qualitative differences in the variable receptors of human and chimpanzee natural killer cells. *PLoS Genet.* 6: e1001192.
27. Bimber, B. N., A. J. Moreland, R. W. Wiseman, A. L. Hughes, and D. H. O'Connor. 2008. Complete characterization of killer Ig-like receptor (KIR)

haplotypes in Mauritian cynomolgus macaques: novel insights into nonhuman primate KIR gene content and organization. *J. Immunol.* 181: 6301–6308.
28. Uhrberg, M., N. M. Valiante, B. P. Shum, H. G. Shilling, K. Lienert-Weidenbach, B. Corliss, D. Tyan, L. L. Lanier, and P. Parham. 1997. Human diversity in killer cell inhibitory receptor genes. *Immunity* 7: 753–763.
29. Gendzekhadze, K., P. J. Norman, L. Abi-Rached, T. Graef, A. K. Moesta, Z. Layrisse, and P. Parham. 2009. Co-evolution of KIR2DL3 with HLA-C in a human population retaining minimal essential diversity of KIR and HLA class I ligands. *Proc. Natl. Acad. Sci. USA* 106: 18692–18697.
30. Shilling, H. G., L. A. Guethlein, N. W. Cheng, C. M. Gardiner, R. Rodriguez, D. Tyan, and P. Parham. 2002. Allelic polymorphism synergizes with variable gene content to individualize human KIR genotype. *J. Immunol.* 168: 2307–2315.
31. Bari, R., T. Bell, W. H. Leung, Q. P. Vong, W. K. Chan, N. Das Gupta, M. Holladay, B. Rooney, and W. Leung. 2009. Significant functional heterogeneity among KIR2DL1 alleles and a pivotal role of arginine 245. *Blood* 114: 5182–5190.
32. Winter, C. C., J. E. Gumperz, P. Parham, E. O. Long, and N. Wagtmann. 1998. Direct binding and functional transfer of NK cell inhibitory receptors reveal novel patterns of HLA-C allotype recognition. *J. Immunol.* 161: 571–577.
33. Yawata, M., N. Yawata, M. Draghi, F. Partheniou, A. M. Little, and P. Parham. 2008. MHC class I-specific inhibitory receptors and their ligands structure diverse human NK-cell repertoires toward a balance of missing self-response. *Blood* 112: 2369–2380.
34. Saitou, N., and M. Nei. 1987. The neighbor-joining method: a new method for reconstructing phylogenetic trees. *Mol. Biol. Evol.* 4: 406–425.
35. Tamura, K., G. Stecher, D. Peterson, A. Filipski, and S. Kumar. 2013. MEGA6: molecular Evolutionary Genetics Analysis version 6.0. *Mol. Biol. Evol.* 30: 2725–2729.
36. Hilton, H. G., A. K. Moesta, L. A. Guethlein, J. Blokhuis, P. Parham, and P. J. Norman. 2015. The production of KIR-Fc fusion proteins and their use in a multiplex HLA class I binding assay. *J. Immunol. Methods* S0022-1759(15) 30014-4 10.1016/j.jim.2015.06.012.
37. Robinson, J., J. A. Halliwell, H. McWilliam, R. Lopez, and S. G. Marsh. 2013. IPD—the Immuno Polymorphism Database. *Nucleic Acids Res.* 41: D1234–D1240.
38. Hou, L., M. Chen, B. Jiang, D. Wu, J. Ng, and C. K. Hurley. 2010. Thirty allele-level haplotypes centered around KIR2DL5 define the diversity in an African American population. *Immunogenetics* 62: 491–498.
39. Hou, L., M. Chen, J. Ng, and C. K. Hurley. 2012. Conserved KIR allele-level haplotypes are altered by microvariation in individuals with European ancestry. *Genes Immun.* 13: 47–58.
40. Norman, P. J., J. A. Hollenbach, N. Nemat-Gorgani, L. A. Guethlein, H. G. Hilton, M. J. Pando, K. A. Koram, E. M. Riley, L. Abi-Rached, and P. Parham. 2013. Co-evolution of human leukocyte antigen (HLA) class I ligands with killer-cell immunoglobulin-like receptors (KIR) in a genetically diverse population of sub-Saharan Africans. *PLoS Genet.* 9: e1003938.
41. Vierra-Green, C., D. Roe, L. Hou, C. K. Hurley, R. Rajalingam, E. Reed, T. Lebedeva, N. Yu, M. Stewart, H. Noreen, et al. 2012. Allele-level haplotype frequencies and pairwise linkage disequilibrium for 14 KIR loci in 506 European-American individuals. *PLoS One* 7: e47491.
42. Middleton, D., A. Meenagh, and P. A. Gourraud. 2007. KIR haplotype content at the allele level in 77 Northern Irish families. *Immunogenetics* 59: 145–158.
43. Nemat-Gorgani, N., H. A. Edinur, J. A. Hollenbach, J. A. Traherne, P. P. Dunn, G. K. Chambers, P. Parham, and P. J. Norman. 2014. KIR diversity in Māori and Polynesians: populations in which HLA-B is not a significant KIR ligand. *Immunogenetics* 66: 597–611.
44. Hilton, H. G., P. J. Norman, N. Nemat-Gorgani, A. Goyos, J. A. Hollenbach, B. M. Henn, C. R. Gignoux, L. A. Guethlein, and P. Parham. 2015. Loss and gain of natural killer cell receptor function in an African hunter-gatherer population. *PLoS Genet.* 11: e1005439.
45. Lanier, L. L., B. C. Corliss, J. Wu, C. Leong, and J. H. Phillips. 1998. Immunoreceptor DAP12 bearing a tyrosine based activation motif is involved in activating NK cells. *Nature* 391: 703–707.
46. Burshtyn, D. N., A. M. Scharenberg, N. Wagtmann, S. Rajagopalan, K. Berrada, T. Yi, J. P. Kinet, and E. O. Long. 1996. Recruitment of tyrosine phosphatase HCP by the killer cell inhibitor receptor. *Immunity* 4: 77–85.
47. VandenBussche, C. J., S. Dakshanamurthy, P. E. Posch, and C. K. Hurley. 2006. A single polymorphism disrupts the killer Ig-like receptor 2DL2/2DL3 D1 domain. *J. Immunol.* 177: 5347–5357.
48. Fan, Q. R., L. Mosyak, C. C. Winter, N. Wagtmann, E. O. Long, and D. C. Wiley. 1997. Structure of the inhibitory receptor for human natural killer cells resembles haematopoietic receptors. *Nature* 389: 96–100.
49. Boyington, J. C., S. A. Motyka, P. Schuck, A. G. Brooks, and P. D. Sun. 2000. Crystal structure of an NK cell immunoglobulin-like receptor in complex with its class I MHC ligand. *Nature* 405: 537–543.
50. Frazier, W. R., N. Steiner, L. Hou, S. Dakshanamurthy, and C. K. Hurley. 2013. Allelic variation in KIR2DL3 generates a KIR2DL2-like receptor with increased binding to its HLA-C ligand. *J. Immunol.* 190: 6198–6208.
51. Hilton, H. G., L. Vago, A. M. Older Aguilar, A. K. Moesta, T. Graef, L. Abi-Rached, P. J. Norman, L. A. Guethlein, K. Fleischhauer, and P. Parham. 2012. Mutation at positively selected positions in the binding site for HLA-C shows that KIR2DL1 is a more refined but less adaptable NK cell receptor than KIR2DL3. *J. Immunol.* 189: 1418–1430.
52. Wilson, M. J., M. Torkar, and J. Trowsdale. 1997. Genomic organization of a human killer cell inhibitory receptor gene. *Tissue Antigens* 49: 574–579.
53. Uhrberg, M., P. Parham, and P. Wernet. 2002. Definition of gene content for nine common group B haplotypes of the Caucasoid population: KIR haplotypes contain between seven and eleven KIR genes. *Immunogenetics* 54: 221–229.

Journal of Immunological Methods 425 (2015) 79–87

Contents lists available at ScienceDirect

Journal of Immunological Methods

journal homepage: www.elsevier.com/locate/jim

The production of KIR–Fc fusion proteins and their use in a multiplex HLA class I binding assay

Hugo G. Hilton [a,b], Achim K. Moesta [c], Lisbeth A. Guethlein [a,b], Jeroen Blokhuis [a,b], Peter Parham [a,b], Paul J. Norman [a,b,*]

[a] Department of Structural Biology, Stanford University School of Medicine, Stanford, USA
[b] Department of Microbiology & Immunology, Stanford University School of Medicine, Stanford, USA
[c] Discovery Research, Amgen Inc., South San Francisco, CA, USA

ARTICLE INFO

Article history:
Received 28 May 2015
Received in revised form 16 June 2015
Accepted 17 June 2015
Available online 19 June 2015

Keywords:
Natural killer cells
MHC
Comparative immunology/evolution
Antigens/peptides/epitopes

ABSTRACT

Soluble recombinant proteins that comprise the extracellular part of a surface expressed receptor attached to the Fc region of an IgG antibody have facilitated the determination of ligand specificity for an array of immune system receptors. Among such receptors is the family of killer cell immunoglobulin-like receptors (KIR) that recognize HLA class I ligands. These receptors, expressed on natural killer (NK) cells and T cells, play important roles in both immune defense and placental development in early pregnancy. Here we describe a method for the production of two domain KIR–Fc fusion proteins using baculovirus infected insect cells. This method is more scalable than traditional mammalian cell expression systems and produces efficiently folded proteins that carry post-translational modifications found in native KIR. We also describe a multiplex binding assay using the Luminex platform that determines the avidity and specificity of two domain KIR–Fc for a panel of microbeads, each coated with one of 97 HLA class I allotypes. This assay is simple to perform, and represents a major improvement over the assays used previously, which were limited in the number of KIR and HLA class I combinations that could be assayed at any one time. The results obtained from this assay can be used to predict the response of NK cell and T cells when their KIR recognize HLA class I.

1. Introduction

Killer-cell immunoglobulin like receptors (KIR) are a family of germline encoded cell surface receptors that regulate the activity of natural killer (NK) cells and T cells in immunity and reproduction through interaction with HLA class I molecules (Parham and Moffett, 2013). Both KIR and HLA are encoded by polymorphic genes, which have numerous alleles encoding unique KIR and HLA class I proteins, which are known as allotypes. HLA class I proteins are expressed on the surface of most cell types and present a diverse repertoire of peptides that furnish ligands for KIR and other immune system receptors (Bjorkman et al., 1987; Colonna et al., 1992; Colonna and Samaridis, 1995; Moretta et al., 1993). The *HLA class I* locus contains three highly polymorphic genes, called *HLA-A*, *B* and *C*. *HLA-C* is the most recently evolved and the only one for which all the variant forms are KIR ligands (Guethlein et al., 2007; Older Aguilar et al., 2010, 2011). Dimorphism at position 80 in HLA-C defines two epitopes, C1 (asparagine 80) and C2 (lysine 80), which are ligands for two different forms of two-domain KIR (Mandelboim et al., 1996; Winter and Long, 1997). *KIR2DL1* encodes methionine at position 44 and binds to C2 bearing HLA-C, *KIR2DL2/3* encodes lysine at position 44 and binds to C1 bearing HLA-C allotypes.

Because the genes encoding KIR and HLA class I are on different chromosomes, their independent segregation during meiosis produces diversity in the number and type of *KIR–HLA* gene combinations inherited by individuals (Norman et al., 2013; Wilson et al., 2000). Further, NK cells can express more than one KIR at a time (Lanier, 1997; Valiante et al., 1997). This inherent diversity has complicated the investigation of the specific KIR–HLA class I interactions that modulate immune response. Development of soluble KIR proteins for which the reactivity for single HLA class I molecules was determined by direct binding assay, facilitated understanding of how particular receptor–ligand combinations contributed to NK cell reactivity (Winter et al., 1998). These recombinant proteins were made in a mammalian cell expression system by fusing the extracellular domains of a two-domain KIR with two Fc domains of a human IgG1 to form a soluble homodimer (Winter and Long, 2000).

We have adapted this method for the production of soluble KIR–Fc fusion proteins by using baculovirus-infected insect cells. The advantage of this approach is that insect cells are simple to culture. They have short doubling times that facilitate scaling and they are capable of higher protein yields than mammalian cell systems of expression. Because of these advantages, the baculovirus–insect cell system is now one of the most

* Corresponding author at: Department of Structural Biology, Stanford University, Fairchild D-159, 299 Campus Drive West, Stanford, CA 94305, USA.
E-mail address: paul.norman@stanford.edu (P.J. Norman).

http://dx.doi.org/10.1016/j.jim.2015.06.012
0022-1759/

widely used methods for the production of recombinant proteins (Hitchman et al., 2009). Although not equivalent to higher eukaryotic cells, most post-translational modifications are made correctly in insect cells, and proteins unable to be expressed in *E. coli* have been successfully expressed in the insect cell system (Victor et al., 2010). The baculovirus family are species-specific double-stranded DNA viruses that infect insects as their natural host (Kost and Condreay, 1999). Once inserted into the host nucleus, the baculovirus is packaged into flexible nucleocapsids, into which foreign DNA may readily be inserted. The target gene, in this case the KIR–Fc fusion construct, is inserted into a transfer vector and positioned between sequences that are homologous to the ones in the baculoviral genome. When the viral genome and transfer vector are transfected into insect cells, recombination occurs, and produces intact viral genomes harboring the target gene sequence. The target gene replaces the non-essential baculoviral polyhedrin gene. The strong promoter of the polyhedrin gene is co-opted for production of recombinant target protein.

We have also developed a multiplex assay that tests the binding of soluble KIR–Fc to 97 HLA class I allotypes. This assay uses the Luminex platform, in which the antigenic targets are microbeads, each coated with a defined HLA class I allotype. Such beads were developed originally for studying the specificity of human alloantibodies (Pei et al., 1998, 2003), but our group has successfully adapted this platform for use with recombinant two-domain KIR–Fc fusion proteins and monoclonal antibodies (Hilton and Parham, 2013; Moesta et al., 2008). By adjusting the relative concentration of two fluorescent dyes, a set of 100 individually identifiable beads is generated. Each bead is then coated with a different HLA class I allotype, allowing the results of the immunoassay to be correlated with HLA class I specificity.

The goal of the KIR–Fc HLA-bead binding assay is to determine the strength and specificity of the interactions between HLA class I and KIR using defined purified proteins. The results can be used to predict the reactivity of KIR expressing NK cells and T cells when their KIR recognize cognate HLA class I ligands. This assay represents a major advance from the cell-based direct binding assay in which the reactivity of only a few KIR and HLA class I combinations could be determined at any one time (Winter and Long, 2000). Moreover, the KIR–Fc HLA bead-binding assay is designed to inform cellular assays of lymphocyte function in which receptor deficient effector NK cells transfected with a specific KIR are incubated with ligand-deficient target cells transfected with a specific HLA class I molecule (Moesta et al., 2008).

The HLA class I specificity of several KIR allotypes has been investigated using various assays. Our initial study with the multiplex bead-binding assay showed that KIR2DL2*001–Fc recognized HLA-C2 allotypes with higher avidity than its allotypic variant KIR2DL3*001–Fc (Moesta et al., 2008). A cellular cytotoxicity assay subsequently showed that KIR2DL2*001, but not KIR2DL3*001 effectively inhibited lysis when incubated with HLA class I deficient 221 cells transfected with the HLA-C2 allotype, HLA-C*04:01 (Moesta et al., 2008). Another group investigated a second allotypic variant, KIR2DL3*005 (Frazier et al., 2013) using a similar multiplex assay. They showed that KIR2DL3*005–Fc bound HLA-C1 allotypes with higher avidity than KIR2DL3*001–Fc. This result was concordant with a cellular assay in which NK cells expressing either 2DL3*005 or 2DL3*001 respectively were incubated with 221 cells expressing the C1 bearing allotype HLA-C*03:04. Natural killer cells expressing 2DL3*005 exhibited a more potent inhibitory signal than those transfected with 2DL3*001 (Frazier et al., 2013). A third type of assay, surface plasmon resonance, confirmed that the 2DL3*005 variant bound with greater avidity than the 2DL3*001 variant to the HLA-C1 allotype HLA-C*03:04 (Frazier et al., 2013).

In summary, we have developed a simplified method for the production of KIR–Fc and designed an assay that tests their binding to 97 HLA class I allotypes simultaneously. The assay is easy to perform and correlates well with more complicated experimental techniques such as cellular cytotoxicity and surface plasmon resonance that have traditionally been used to determine the avidity and specificity of KIR for HLA class I ligands.

2. Materials and methods

KIR–Fc fusion protein generation.

This section describes the generation of a DNA insert, flanked by restriction sites, that encodes the first 224 amino acids of the KIR2D of interest and the Fc region of human IgG1 (Fig. 1A). This insert is first cloned into the pAcGP67a transfer vector (Fig. 1B). Subsequently it is co-transfected with linearized baculovirus into insect cells.

2.1. KIR–Fc fusion construct generation

Amplify the sequences encoding the D1, D2 and stem region of the selected KIR2D molecule by PCR (primers from Fig. 1D, upper panel). The forward primer annealing site is immediately downstream of the *KIR* signal sequence cleavage site and should contain a *BamHI* (New England BioLabs, Cat. #R0136) site. The reverse primer annealing site is immediately upstream of the transmembrane region and contains an *XbaI* (New England Biolabs, Cat. #R0145s) site.

Add a mix consisting of 20.2 μl PCR grade sterile water, 2.5 μl 10× cloned *Pfu* buffer, 0.5 μl forward primer (10 mM), 0.5 μl reverse primer (10 mM), 0.2 μl dNTP mix (40 mM) and 0.25 μl HotStart TAQ polymerase (Kit from Qiagen, Cat. #203203) to 1 μl of template DNA (10 ng/μl) and perform PCR using the following conditions: (5 min at 95 °C) × 1, (30 s at 94 °C, 1 min 25 s at 62 °C, 40 s at 72 °C) × 35, (10 min at 72 °C) × 1, and hold at 4 °C. Digest the amplification products with *BamHI* and *XbaI* and ligate into the *BamH1* and *XbaI* digested pAcGP67a vector (BD Pharmigen, Cat. #554758). Amplify the sequences encoding the hinge, CH2 and CH3 regions of human IgG1 using a forward primer containing an *XbaI* site and a reverse primer containing a *NotI* (New England Biolabs, Cat. #R0189) site (primers from Fig. 1D, upper panel). Digest the amplification products with *XbaI* and *NotI* and ligate into the *XbaI* and *NotI* digested pAcGP67a vector. Transform the ligation products into *E. coli* competent cells (Kit from Invitrogen, Cat. #K4510-20). Following overnight incubation select individual *E. coli* colonies, clonally amplify and prepare transfection quality DNA using Qiagen columns (Kit from Qiagen, Cat. #27104). Sequence each clone to confirm that the desired KIR–Fc fusion gene is inserted in frame behind the GP67 secretion signal sequence (primers from Fig. 1D, lower panel).

2.2. Site-directed mutagenesis of KIR–Fc constructs

Site-directed mutagenesis can be used to introduce non-synonymous mutations into the newly generated *KIR–Fc* fusion gene. This technique is useful for making comparisons of closely related KIR2D–Fc allotypes or to investigate the effect of alternative amino acids at a particular position on HLA class I recognition. Mutagenesis primers should have a melting temperature of at least 78 °C and the desired mutation should be situated in the center of the primer sequence. The website www.bioinformatics.org/primerx was used to design mutagenesis primers. Add a mix consisting of 40 μl PCR grade sterile water, 5 μl 10× cloned *Pfu* buffer (Agilent Technologies, Cat. #600153-82), 1 μl forward primer (10 mM), 1 μl reverse primer (10 mM), 1 μl dNTP mix (40 mM) and 1 μl Turbo polymerase (Agilent Technologies, Cat. #600252-52) to 1 μl of template DNA (50 ng/μl) and perform PCR using the following conditions: (30 s at 95 °C) × 1, (30 s at 95 °C, 60 s at 55 °C, 15 min at 68 °C) × 20, (7 min at 72 °C) × 1, and hold at 4 °C. A 15 min extension time is recommended, because of the large size of the pAcGP67a vector (9761 bp). Following the PCR, add 1 μl *DpnI* (New England BioLabs, Cat. #R0167S) to the reaction mixture and incubate for 30 min at 37 °C. *DpnI* digests the methylated template DNA and effectively increases the efficiency of mutated DNA transformation into competent *E. coli* cells. Following overnight incubation select individual

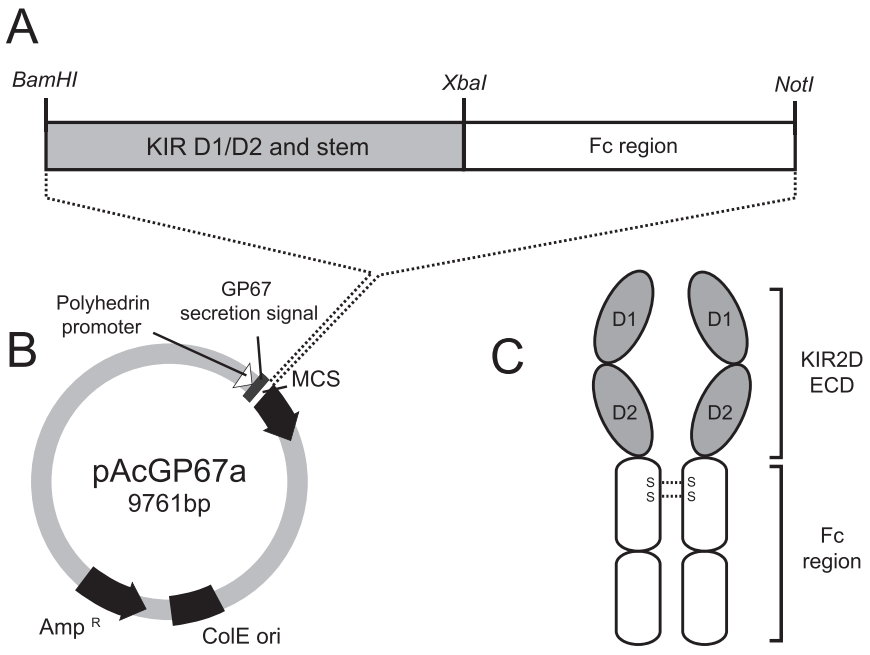

D

	Direction	Target	Rest. Site	Sequence (5' - 3')	GC content (%)	Tm (°C)	Length (bp)
Amplification	F	*KIR2DL1/2/3/S1/2*	*BamHI*	TA**GGATCC**CCATGAGGGAGTCCACAG	57.7	62.8	26
	F	*KIR2DS3/5*	*BamHI*	TA**GGATCC**CCATGAGGGATTCCGCAG	53.8	61.7	26
	F	*KIR2DS4*	*BamHI*	TA**GGATCC**CCAGGAGGAGTCCACAG	57.7	62.7	26
	R	*KIR2DL1/2*	*XbaI*	GTGCAGGTG**TCTAGA**GTTACCGGT	54.2	60.2	24
	R	*KIR2DL3/S2*	*XbaI*	ATGCAGGTG**TCTAGA**GTTACCGGT	50.0	59.5	24
	R	*KIR2DS1/4*	*XbaI*	ATGTAGGTG**TCTAGA**GTTACCGGT	45.8	56.7	24
	R	*KIR2DS3*	*XbaI*	GTGTAGGTG**TCTAGA**GTTACCGGT	50.0	57.4	24
	F	*Fc*	*XbaI*	**TCTAGA**CACCTGCACGAGCCCAAATCTTCTGACAAAACTCACACATGCCC	50.0	69.6	50
	R	*Fc*	*NotI*	AT**GCGGCCGC**TCATTTACCGGAGACAGGGAG	61.3	68.9	31
Sequencing	F	pAcGP67a	-	TTTACTGTTTTCGTAACAGTTTTG	29.2	50.3	24
	R	pAcGP67a	-	GGAAGCTGTCTTCCATGAAGCG	54.5	58.3	22

Fig. 1. (A) Schematic diagram showing the configuration of a recombinant *KIR–Fc* fusion gene. The recombinant fusion gene consisting of the D1, D2 and stem domains of a KIR2D molecule (gray box) and the Fc region of a human IgG1 antibody (white box) is cloned using *BamH1* and *Not1* restriction sites into the multiple cloning site (MCS) of the pAcGP67a vector (B) in frame behind the GP67 secretion signal sequence. Transfection into insect cells produces a soluble recombinant KIR–Fc dimer (C) consisting of the D1, D2 and stem regions (extracellular domain — ECD) of the KIR molecule (gray ovals) and the Fc region (white ovals) of the IgG1 antibody. (S–S) shows the location of the di-sulfide bonds that lead to formation of a dimer. (D) Table listing the primers for amplification and sequencing of KIR–Fc fusion genes representing inhibitory *KIR2DL1*, *2DL2/3* and activating *KIR2DS1*, *2DS2*, *2DS3*, *2DS4* and *2DS5*. The properties of each primer, including the GC content, melting temperature (Tm) and length are listed to the right. Restriction sites are shown in bold when present in a primer sequence.

E. coli colonies and then clonally amplify and prepare transfection quality DNA using Qiagen columns (Kit from Qiagen, Cat. #27104). Sequence each clone to confirm that the desired KIR–Fc fusion gene is inserted in frame with the GP67 secretion signal (primers from Fig. 1D, lower panel).

2.3. Co-transfection of KIR–Fc containing transfer vector and baculovirus into insect cells

Having constructed the *KIR-Fc* gene, cloned it into the pAcGP67a transfer vector and mutated it when required, the construct must now be combined with linearized baculovirus and transfected into insect cells. For the initial transfection, the insect cells derived from *Spodoptera frugiperda* (*Sf9*) (Invitrogen, Cat. #11496-015) are used. Both the *Sf9* insect cells and baculovirus should be handled in a sterile laminar flow hood. The *Sf9* cells should be cultured in Sf-900 II media (Invitrogen, Cat. #10902-096) supplemented with 10% heat inactivated fetal bovine serum (FBS), 1% Penicillin–Streptomycin and 1% L-Glutamine, shaking at 120 rpm at 27 °C. The *Sf9* cells should be maintained at between 4×10^5 and 2×10^6 cells/ml. When maintained at this density, *Sf9* cells have an approximate doubling time of 24 h; a slower doubling time may signify unhealthy cells (see Section 2.11). For each *KIR–Fc* transfection, seed one well of a sterile six-well plate (BD Falcon, Cat. #353046) with 2 ml *Sf9* cells at a density of 1×10^6 cells/ml and incubate for 60 min at 27 °C to allow adherence of *Sf9* cells. Concurrently, mix (gently using a pipette) 2 μg of purified transfer vector DNA with KIR–Fc insert from step 2.1 with 0.5 μg of linearized baculovirus DNA (Expression Systems, Cat. #91-002) in a sterile 2 ml microcentrifuge tube and incubate for 5 min at room temperature. This specific baculovirus has the chitinase and cathepsin loci deleted to remove a detrimental protease and reduce competition for resources for protein synthesis during late gene expression. Meanwhile, for each transfectant, mix 10 μl Cellfectin II (Invitrogen, Cat. #10362-100) with 100 μl unsupplemented Sf-900 II media (Invitrogen, Cat. #10902-096) and pipette to mix them together. Add this to the baculovirus/KIR–Fc construct mixture (immediately following the 5 min incubation), mix

gently using a pipette and incubate for a further 30 min at room temperature. Following the 30 min incubation, add 1.8 ml un-supplemented Sf-900 II media to complete each KIR–Fc transfection mixture. In summary, each KIR–Fc transfection mixture should contain *Sf9* cells, *KIR–Fc* fusion gene DNA in pAcGP67a transfer vector, linearized baculovirus DNA, Cellfectin and un-supplemented Sf-900 II media.

Remove the 6-well plate from incubation and replace the medium covering the adherent cells with the *KIR–Fc* transfection mixture. Incubate, covered but not shaking, for 3–5 h at 27 °C. Remove the supernatant from each well and replace with 3 ml Sf-900 II media (warmed to 27 °C and supplemented with 10% heat inactivated FBS, 1% Penicillin–Streptomycin and 1% L-Glutamine). Incubate, cover and seal, with laboratory film (Pechiney, Cat. #PM996), for 7 days at 27 °C. Remove the supernatant from each well and transfer to a sterile 15 ml tube. Separate the cells by centrifugation (1000 *g* for 10 min), discard the pellet and transfer the supernatant to a sterile 15 ml tube and store in the dark at 4 °C. This first transfectant, termed *P0*, and each subsequent *Sf9* amplification supernatant (*P1–P3*) may be placed without further modification at −80 °C for long-term storage.

2.4. Amplification of baculovirus in Sf9 cells — P1–3 production

Successive rounds of *Sf9* cell amplification are now used to amplify the baculovirus (now containing the *KIR–Fc* gene added in step 2.3). Add 30 ml *Sf9* cells at a density of 1×10^6 cells/ml to a 125 ml vented sterile Erlenmeyer flask (Thermo-Scientific, Cat. #4116-0125) and leave shaking at 115 rpm overnight at 27 °C. The following day, add 500 μl of *P0* virus stock to the flask and incubate for 4–5 days shaking at 120 rpm at 27 °C. Collect 14 ml suspension from each flask and transfer to a sterile 15 ml tube. Separate the cells by centrifugation (1000 *g* for 5 min) and transfer each supernatant to a new sterile 15 ml tube. Discard the pellet and store in the dark at 4 °C. This forms the *P1* viral stock. A second (*P2*) or third (*P3*) round of amplification in which each round is seeded with 50 μl of the preceding amplified supernatant, may be required to produce *Sf9* supernatant with a sufficiently high baculoviral titre for adequate protein production.

Quantification of baculovirus amplification in *Sf9* supernatant.

Before proceeding it is necessary to quantify the amount of baculovirus generated from the amplification of the *Sf9* cells in Sections 2.3 and 2.4. The amount of baculovirus generated is critical, as insufficient baculoviral amplification will result in low or absent protein yield. An estimation of viral titre can be made in two ways: directly, using small-scale protein production (protein mini-prep) (see Section 2.5) or indirectly, by flow cytometry, assessing baculoviral-induced up-regulation of surface glycoprotein 64 (GP64) (see Section 2.6).

2.5. KIR–Fc fusion protein — mini-prep

This small-scale protein production tests the capacity of the baculoviral infected *Sf9* supernatant from steps 2.3 and 2.4 to produce protein from *Trichopulsia ni* (*Hi5*) (Invitrogen, Cat. #B855-02) insect cells. *Hi5* cells are similar to *Sf9* cells but are optimized for recombinant protein production rather than baculoviral amplification. *Hi5* cells should be cultured, shaking at 27 °C in Express Five serum free media (Invitrogen, Cat. #10486-025) supplemented with 1% L-Glutamine. The cell density should be kept at between 4×10^5 and 3×10^6 cells/ml. Aggregation of cells, which is more likely to occur at densities higher than 3×10^6 cells/ml, is a sign of unhealthy cells and will reduce the possible protein yield from any preparation in which they are used (see Section 2.11). Seed each well of a sterile 6-well tissue culture plate with 2 ml *Hi5* cells at a density of 1×10^6 cells/ml. Add 100 μl of the viral stock under test (*P1*, *P2* or *P3*) to each well, seal the plate with laboratory film and incubate for 48 h (covered, shaking at 120 rpm, at 27 °C). To serve as a negative control, one well should contain *Hi5* cells but no *Sf9* supernatant. To serve as a positive control, one well should be transfected with an *Sf9* supernatant previously used to produce KIR–Fc protein. Transfer the contents of each well to a 2 ml microcentrifuge tube and separate the cells by centrifugation (1000 *g* for 5 min). Discard the pellet and transfer 1.5 ml of the supernatant to a clean 2 ml microcentrifuge tube, add 150 μl 10× Hepes Buffered Saline (HBS), pH 7.2 and 10 μl protein A Sepharose bead slurry (Invitrogen, Cat. #101142). Rotate the mixture overnight at 4 °C.

Separate the beads by centrifugation (2500 *g*, 15 min, 4 °C) and discard the supernatant. Add 20 μl Laemmli sample buffer (Bio-Rad, Cat. #161-0737) with 5% β-mercaptoethanol (Bio-Rad, Cat. #161-0710) and incubate the sample at 95 °C for 10 min. Load the sample onto a 12% SDS-PAGE gel (Bio-Rad, Cat. #456-1043) and run at 150 V for 1 h. Stain with Coomassie reagent (Bio-Rad, Cat. #161-0786) to identify an appropriately sized band. Although each KIR–Fc exists as a 102 kDa homodimer in native format (Fig. 1C), they run as a band of 51 kDa monomers (Fig. 3A) on an SDS gel. The reducing conditions in the sample application buffer disrupt the disulfide bonds that link the two monomers. The bands produced from successive *Sf9* amplifications of the same *KIR–Fc* construct should show increasing intensity. Amplification is considered sufficient when successive rounds of amplification produce bands of similar intensity. This indicates that the amplification of baculovirus from *Sf9* cells has reached capacity on SDS-PAGE.

2.6. Identification of baculovirus-infected Hi5 cells by flow cytometry

GP64 is a baculovirus encoded glycoprotein that is expressed on insect cells upon infection with baculovirus (Blissard and Rohrmann, 1989). Because the titre of the transfecting supernatant corresponds to the degree of cell-surface expression of GP64, this can be used as a proxy to assess viral amplification in *Sf9* supernatant. Seed an appropriate number of wells of a sterile six-well tissue culture plate with 2 ml *Hi5* cells at a density of 1×10^6 cells/ml. Add 100 μl of *P1*, *P2* or *P3* viral stock to each well, seal the plate with laboratory film and incubate for 24 h (covered, shaking at 120 rpm, at 27 °C). To serve as a negative control, one well should contain *Hi5* cells but no *Sf9* supernatant. To serve as a positive control for the ability of the *Hi5* cells to express GP64, one well should be transfected with a high baculoviral titre *Sf9* supernatant. Mix the cells and add 250 μl of the contents of the well to a 2 ml microcentrifuge tube and separate the cells via centrifugation (50 *g* for 2 min). In the following steps, all wash solutions should be at 4 °C. Resuspend the cells in flow cytometry buffer (FCB) (1× phosphate buffered saline [PBS — Cellgro, Cat. #21-031-CV] supplemented with 0.5% EDTA and 1% BSA) and wash twice. Following the second wash, resuspend the cells in 25 μl FCB and stain the cells with 1 μl anti-baculovirus GP64 antibody (eBioscience, Cat. #14-6995-81). Incubate for 30 min at 4 °C. Wash the cells a further three times in FCB, resuspending in 1 ml FCB after the final wash. Flow cytometry is then used to detect the presence of the PE-conjugated antibody bound to cell surface GP64. *Hi5* cells transfected with low viral titre *P0* or *P1* viral stocks show low or absent levels of surface GP64. Successive *Sf9* amplifications of the same *KIR–Fc* construct should show increasing levels of cell-surface GP64 (Fig. 2). Amplification is considered complete when successive rounds of amplification result in similar levels of cell-surface GP64. This indicates that the amplification of baculovirus from *Sf9* cells has reached capacity and typically occurs at the *P2* stage.

2.7. Harvest and purification of soluble KIR–Fc fusion proteins from baculovirus infected Hi5 cells

Once a suitable baculoviral *Sf9* stock has been produced and assessed for viral titre, a full-scale experiment to produce recombinant KIR–Fc protein can be performed. Grow a 1 l *Hi5* cell culture to a density of 2×10^6 cells/ml. Add 1 ml of high-titre *P2* or *P3* viral stock and incubate for 60 h (covered, shaking at 120 rpm, 27 °C). Separate cells by centrifugation (2500 *g* for 15 min, 4 °C). Discard the pellet and pass the

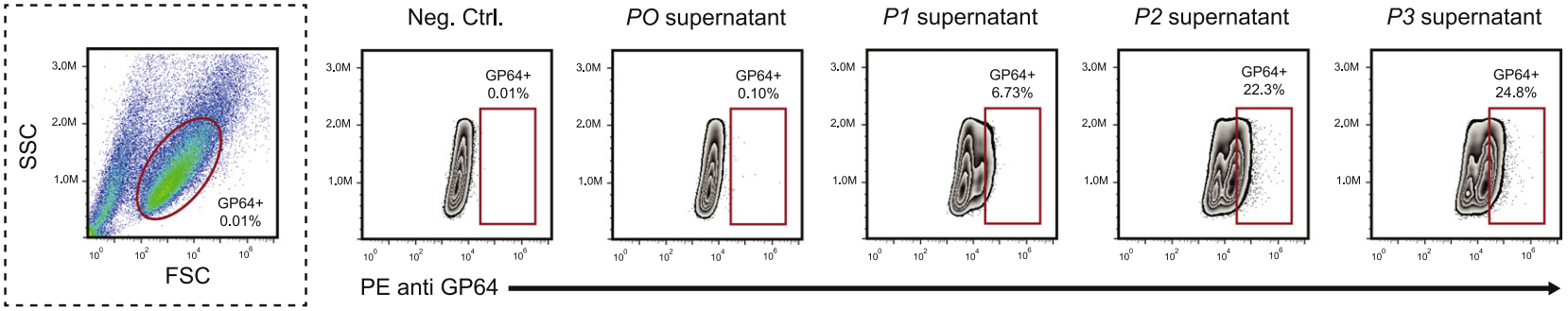

Fig. 2. (A) GP64 is up-regulated on the surface of *Hi5* cells following transfection with baculovirus infected *Sf9* supernatant. Shown is the gating strategy and representative flow cytometry plots from *Hi5* cells transfected with Sf9 supernatant from *P0*, *P1*, *P2* and *P3* viral stocks and stained with PE conjugated anti-GP64 antibody. *P0* viral stocks do not induce up-regulation of GP64 on the surface of *Hi5* cells. Transfection of *Hi5* cells with *P1* viral stocks induces partial up-regulation of GP64 whereas transfection of *Hi5* cells with *P2* or *P3* viral stocks maximally up-regulates GP64.

supernatant through a 0.2 μm filter (Nalgene, Cat. #450-0020) into a sterile container. Add 100 ml 10× HBS, pH 7.2 per 900 ml filtered Hi5 supernatant. Add 1 ml protein A Sepharose bead slurry and rotate bottles slowly overnight at 4 °C.

In the following steps, all wash solutions should be at 4 °C. Separate the protein A Sepharose beads from the *Hi5* supernatant by filtration using gravity flow through a Buchner funnel with fritted glass disk (Pyrex, Cat. #36060). Care should be taken to avoid the Sepharose beads running dry. Wash the beads with approximately 500 ml of 1× PBS and transfer to an empty 13 ml PD-10 column with a 20–85 μm frit filter (GE Healthcare, Cat. #17-0435-01) using a serological pipette. The beads should collect on the frit filter as the wash solution passes through by gravity flow.

Elute the KIR–Fc fusion protein from the collected beads in the PD-10 column using 100 mM glycine, pH 2.7 in 8 fractions of 800 μl each, neutralizing by elution into 8 separate microcentrifuge tubes, each containing 200 μl 1 M Tris, pH 9.0. The protein content of each elution fraction should be determined by Bradford assay (Kit from Bio-Rad, Cat. #500-0001).

Wash a Sephadex G-25 desalting column (GE Healthcare, Cat. #17-0851-01) with 25 ml 1× PBS. Load 2.5 ml of the fractions having the highest protein concentration onto the desalting column. Add 3.5 ml 1× PBS to the desalting column in 0.5 ml aliquots and collect seven 0.5 ml fractions in separate microcentrifuge tubes. Determine the protein content of each fraction by Bradford assay.

At this stage, it is best to estimate the purity of each eluted protein fraction by gel electrophoresis. Add 10 μl of each KIR–Fc eluent to an equal volume of Laemmli sample buffer with 5% β-mercaptoethanol and incubate the sample at 95 °C for 10 min. Transfer the sample onto a 15% SDS-PAGE gel and electrophorese at 150 V for 1 h. Stain with Coomassie reagent to identify the appropriately sized band (Fig. 3A).

2.8. Assessment of KIR–Fc integrity by flow cytometry

Having produced recombinant KIR–Fc protein from the full-scale prep as described in Section 2.7, it is now necessary to determine the integrity (i.e. correct protein folding) of the protein. This is achieved by flow-cytometry, using monoclonal antibodies specific for KIR. In the following steps, all wash solutions should be kept at 4 °C. Add 20 μl of anti-human IgG-coated beads (Bangs Laboratories, Cat. #BM562) to 500 μl KIR–Fc fusion protein (diluted in 1× PBS to 100 μg/ml). Ensure that the beads are vortexed gently to resuspend them prior to their use. Incubate, shaking gently for 30 min at 4 °C. Collect the beads by centrifugation (50 *g* for 2 min) and wash twice with FCB. Following the second wash, resuspend the beads in 25 μl FCB and add 2 μl PE-conjugated mouse anti-human KIR antibody (KIR2DL1: Beckman Coulter, Cat # EB6-PE; KIR2DL2/3, Beckman Coulter, Cat # DX27-PE; Lineage III KIR: AbD Serotec, Cat # NKVFS1). Incubate, shaking gently for 30 min at 4 °C. Collect the beads by centrifugation (50 *g* for 2 min) and wash a further two times with FCB. Resuspend the beads in 150 μl FCB. Flow cytometry is then used to detect the presence of the PE conjugated anti-KIR antibody bound to individual IgG coated beads (Fig. 3B).

2.9. Multiplex assay to detect binding of soluble KIR proteins to HLA class I single antigen beads

The purified, functional KIR–Fc fusion proteins are now ready to be tested for their capacity to recognize HLA class I allotypes. Each KIR–Fc protein is first incubated with approximately 10,000 individual beads, each coated with one of 97 HLA class I allotypes; the goal being to test the binding of the KIR–Fc to each HLA class I allotype approximately 100 times. In the second step of the assay, a secondary antibody is added that binds to the Fc portion of the KIR–Fc. The Luminex reader is able to simultaneously detect the identity of the bead (which correlates with a specific HLA class I) and the fluorescence of the antibody, which indicates the amount of KIR–Fc bound to the bead.

For each KIR–Fc protein to be tested, pre-wet one well of a 96-well 0.65 μm filter plate (Millipore, Cat. #MSDVN6510) with 200 μl 1× PBS. Remove the PBS from the wells by vacuum aspiration (manifold from Qiagen, Cat. #19504). Add 50 μl of soluble KIR protein (100 μg/ml) and 3 μl LABscreen microbeads (One Lambda, Cat. #LS1A04) to each pre-wetted well. Ensure that the beads are vortexed gently to resuspend them prior to aliquoting into each well. For each assay, 50 μl W6/32 antibody (Biolegend, Cat. #311402) (50 μg/ml) should be added to one well to control for antigen density on individual beads (see Section 2.10). Incubate the KIR–Fc proteins and W6/32 with the beads for 60 min, shaking gently and covered at 4 °C.

In the following steps, all wash and resuspension solutions should be at 4 °C. Wash the beads in each well four times with 1× Luminex wash buffer (One Lambda, Cat. #LS1A04). For each wash, add 200 μL of wash buffer to each well and gently pipette up and down several times. If more than one protein is being tested use a multi-channel pipette to ensure even washing of each KIR–Fc protein being tested. Care should be taken to avoid introducing air bubbles into the wells. Following each wash, aspirate the wash solution using a vacuum manifold, ensuring that the well does not become dry. The vacuum pressure should not exceed 100 mm Hg.

Following the first complete wash cycle (4 individual washes), resuspend the KIR–Fc fusion proteins in 100 μl PBS with 1% PE-conjugated goat anti-human IgG-Fc antibody (One Lambda, Cat. #LS-AB2). Suspend the beads incubated with W6/32 in 100 μl PBS with 1% PE-conjugated goat anti-mouse IgG-Fc antibody (BD Pharmigen, Cat. #550589). Incubate both KIR–Fc and W6/32 for a further 60 min, shaking gently and covered at 4 °C. Following the second incubation, wash the beads a further four times with 1× Luminex wash buffer, resuspend in 100 μl 1× PBS and transfer into a 96-well, 250 μl 'V' bottom microplate (Whatman, Cat. #7701-3250). The test plate should be transferred immediately into the Luminex reader (with pre-warmed lasers and beadset template entered to avoid delay in starting the assay).

2.10. Calculating fluorescence relative to HLA class I antigen density

To correct for differences in the absolute amount of HLA class I annealed to each microbead, the binding of KIR–Fc fusion proteins to a specific HLA class I should be calculated relative to the amount of HLA class I as determined by binding of W6/32, an antibody that recognizes an epitope common to all HLA class I allotypes. The relative fluorescence ratio of a given KIR–Fc is calculated using the formula (KIR–Fc binding − negative control bead binding) / (W6/32 binding − negative control bead binding).

2.11. Common problems and their solutions

The most common problem encountered in the protocol is failure of amplification of baculovirus in *Sf9* cell preps and failure of protein production from *Hi5* cell preps. We have introduced several steps to test baculoviral amplification, the goal being to identify insufficient baculoviral amplification early and take steps to correct it to minimize lost time. A common cause of amplification failure is unhealthy *Sf9* or *Hi5* cells. The following steps can be used to ensure healthy cells and detect unhealthy cells should they occur.

Sf9 cells should have a doubling time of between 24 and 30 h. *Hi5* cells should have a doubling time of between 18 and 24 h. Slow doubling times usually indicate that *Sf9* or *Hi5* cell cultures are unhealthy. Unhealthy cells will not amplify baculovirus successfully or produce adequate recombinant protein. Cell viability for both *Sf9* and *Hi5* cells, as determined by trypan blue staining, should be greater than 95% at all times. Both bacterial and fungal infections in the insect cell culture will reduce cell viability and doubling times. These can be prevented with good cell culture technique and the addition of antibiotics (1%

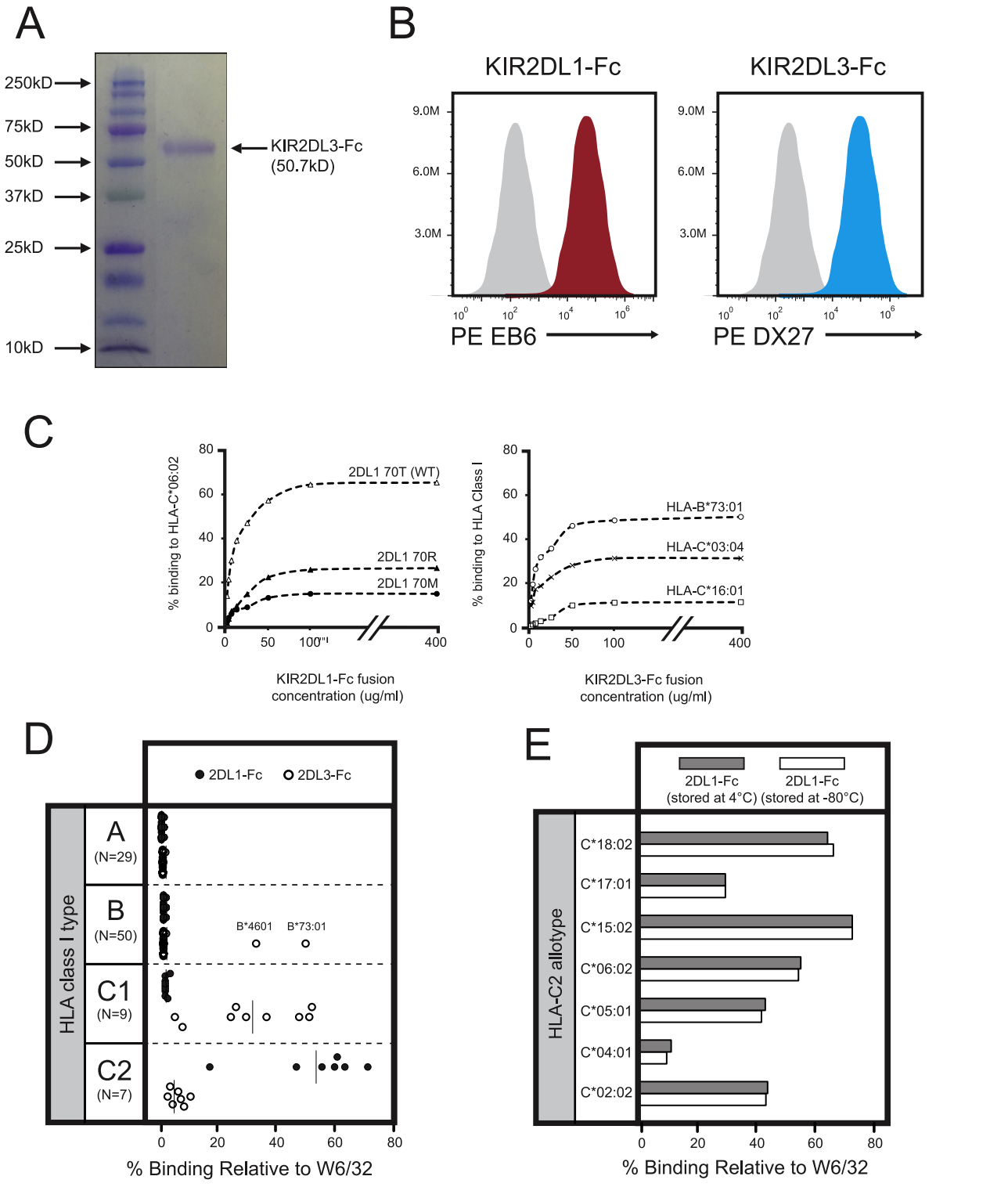

Fig. 3. (A) Shown is a reducing (SDS) gel stained with Coomasie Blue with a protein ladder in the left column (Precision plus Protein Kaleidoscope Standards, Bio-Rad, Cat # 1610375) and a band corresponding to KIR2DL3–Fc at 50.7 kDa in the right column. The gel was loaded with 10 μl of KIR2DL3–Fc protein (100 μg/ml). (B) KIR2D–Fc bound to IgG coated beads (Bangs Laboratories) are stained with KIR specific antibodies to assess their integrity. Representative flow cytometry plots showing staining of KIR2DL1 (left panel, red) and KIR2DL3–Fc (right panel, blue) fusion proteins with EB6 and DX27 antibodies respectively. (C) Titrations of the binding of KIR2D to beads coated with HLA class I molecules. Each of three KIR2DL1–Fc fusion proteins distinguished by substitutions at residue 70 bind to HLA-C*06:02 with different avidities. Both mutant and wild type KIR2DL1 show saturated binding at concentrations greater than 100 μg/ml. KIR2DL3–Fc binds to three HLA class I allotypes (HLA-B*73:01, HLA-C*03:04 and HLA-C*16:01) with different avidities. The binding of KIR2DL3–Fc to each allotype becomes saturated at concentrations above 100 μg/ml. (D) KIR2DL1–Fc binds to HLA-C2 bearing allotypes but not to HLA-C1, HLA-A or HLA-B allotypes. KIR2DL3–Fc binds to HLA-C1 allotypes and to HLA-C2 allotypes with lower avidity. KIR2DL3–Fc also binds to two HLA-B allotypes that encode the C1 epitope. (E) KIR–Fc fusion proteins are amenable to long-term storage at −80 °C. The binding of KIR2DL1–Fc stored at −80 °C for 12 months is compared to 2DL1–Fc stored at 4 °C.

Penicillin–Streptomycin) and/or anti-fungals (0.25 μg/ml Amphotericin B) to the culture medium. Cultures should be discarded immediately if there is evidence of microorganism contamination. A second reason for slow doubling is oxygen restriction. If the cell culture does not have sufficient surface area exposed to the air, cell growth will be retarded. This can be prevented by ensuring that flasks are filled no more than one-third (by volume) with culture medium. Ensuring that the flasks are shaken at between 120 and 150 rpm also ensures adequate oxygenation. Shaking at a higher rpm leads to cell damaging shearing stress and should be avoided. Further information on the culture of insect cells is available (Shrestha et al., 2008).

For the formation of intact baculovirus it is essential that transfer vector and linearized baculoviral DNA recombine during initial co-transfection of *Sf9* cells. We have obtained the best results with freshly isolated transfer vector and baculoviral DNA that has not been stored at 4 °C for more than two weeks. Additionally, freeze/thaw cycles of the transfer vector should be avoided where possible. Because the linearized baculovirus is a large DNA fragment (~130 kb), it is particularly susceptible to shear stress; over-zealous pipetting during transfection should therefore be avoided to minimize DNA and maximize transfection success.

The most common problems associated with the Luminex assay are high background and inter-assay variability. We have found that the following precautions minimize these problems. In this context we define high background readings as those in which the negative control bead binding is greater than 1% of the highest positive reading obtained. During the wash and incubation phases of the protocol, care should be taken to minimize any warming of the reagents. All wash reagents should be chilled to 4 °C and wash steps should be completed as quickly as possible to avoid unnecessary warming of the samples. This may mean reducing the number of KIR–Fc proteins under test in any one assay to expedite this phase.

Although not always the case, some KIR–Fc are not stable when stored at 4 °C and their use in the assay can lead to high background readings. To control for this issue, divide each batch of protein into 100 μl aliquots and store them at −80 °C. Similarly, HLA class I beads that have been thawed and stored at 4 °C are not typically stable for more than 3 months. The beads should also be divided into 10 μl aliquots and frozen at −80 °C if they are unlikely to be used within this time frame. Each of these precautions also helps to reduce both high background and inter-assay variability. Additionally, we include well characterized HLA-C1 and HLA-C2 receptors (e.g., KIR2DL3*001–Fc and KIR2DL1*003–Fc respectively) in every assay as positive controls. Changes in the avidity and specificity of the KIR–Fc under test can then be related not only to W6/32, but also to these KIR–Fc controls.

In addition to the failure of baculoviral amplification described above, a further limitation of this system is that we have, as yet, been unable to produce functional three domain KIR using the Fc fusion system. Although the KIR3D protein is expressed by insect cells, it does not fold into a tertiary structure that binds to KIR-specific antibody or to HLA class I. As such, the HLA class I reactivity of these receptors remains under investigation.

3. Results and discussion

The purpose of this protocol is to provide a simplified method with which to produce and test the reactivity of soluble two-domain KIR–Fc fusion proteins. We chose to use an insect cell expression system because most post-translational modifications are made correctly in insect cells and the system is scalable, allowing production of large quantities of soluble recombinant protein in a comparatively short time. We have sought to reduce variability in final protein yield by implementing a series of quality controls at points during the baculoviral amplification phase. These methodological improvements allow us to better track baculoviral amplification in *Sf9* cells and prevent the *Hi5* preparations having insufficient protein yield.

We have also designed a novel assay that tests the binding of KIR–Fc to HLA class I allotypes. This assay simultaneously detects the binding of KIR to 97 HLA class I allotypes. As a result it holds a clear advantage over previous cell-based binding assays that allowed examination of only a few KIR–HLA class I interactions at any one time. The assay is sensitive over a two-log range, permitting both strong and weak reactions to be interpreted with confidence and correlated with structural polymorphisms in both KIR and HLA class I (Frazier et al., 2013; Gendzekhadze et al., 2009; Graef et al., 2009; Hilton et al., 2012; Moesta et al., 2008).

The KIR–Fc HLA-bead binding assay has also been used to explore the binding characteristics of KIR in simian primates. The HLA class I specificity of primate KIR has been difficult to determine because of a comparative lack of cellular reagents. As such, the combination of methods described in this paper has led to a number of critical discoveries on the immunologic function and co-evolution of KIR and MHC class I. In Old World Monkeys, the lineage III *KIR* (precursor to the MHC-C receptors of higher primates) is represented by a single gene (Sambrook et al., 2005) while lineage II *KIR* genes have expanded and diversified. To identify their MHC epitope-specificity and avidity, a panel of rhesus macaque lineage II KIR–Fc was assayed using the methods present here (Older Aguilar et al., 2011). Although MHC-C is not present in macaques, their KIR recognize HLA-C epitopes more effectively than they recognize HLA-A and HLA-B, suggesting that MHC-C evolved to become a stronger ligand for KIR than HLA-A and -B. The emergence of *MHC-C* in the orangutan was accompanied by an expansion of lineage III KIR and their evolution as MHC-C receptors (Guethlein et al., 2007). All orangutan MHC-C allotypes have asparagine at position 80 and display the C1 epitope. Correspondingly, results from the KIR–Fc HLA bead binding assay showed that the orangutan has C1-specific KIR but no C2-specific KIR (Older Aguilar et al., 2010). In chimpanzees the *MHC-C* gene became fixed and the C2 epitope emerged. As a consequence, out of nine chimpanzee lineage III KIR genes (Abi-Rached et al., 2010), eight encode receptors with high avidity for HLA-C, comprising three C1-specific receptors and 5 C2-specific receptors (Moesta et al., 2009). Thus, results from the multiplex binding assay show that changes in the character of the *KIR* locus correlate with change in the *MHC* class I genes, suggesting co-evolution between these receptors and ligands and uncovering a progression in which the complexity of the *KIR* locus gets increasingly sophisticated across higher primate species.

3.1. Flow cytometry can be used to confirm baculoviral transfection

Surface glycoprotein GP64 is a baculovirus encoded glycoprotein that can be used as a marker for successful transfection and amplification of baculovirus in *Hi5* insect cells (Blissard and Rohrmann, 1989; Volkman and Goldsmith, 1988). Fig. 2 shows that GP64 expression is not detected on un-transfected *Hi5* cells but is expressed following transfection with high viral titre *Sf9* supernatant. *P0* viral stock was not sufficient to induce GP64 surface expression whereas surface expression was typically detected after transfection with *P1* viral stock and with each subsequent amplified viral stock (*P2* and *P3*) (Fig. 2). Surface expression of GP64 was sensitive to the baculoviral titre with *P2* transfected *Hi5* cells showing a 40% increase in surface expression of GP64 as compared to *Hi5* cells transfected with *P1* viral stocks. That *P3* stocks induced only marginally greater GP64 surface expression than *P2* viral stocks suggests that GP64 is either maximally up-regulated by a given viral titre or *Sf9* cells reach maximal viral amplification between the second and third amplification rounds.

3.2. Confirmation of KIR–Fc integrity by flow cytometry

Both EB6 antibody, which recognizes KIR2DL1, and DX27 antibody, which recognizes KIR2DL2/3, bound to KIR–Fc immobilized on anti-human IgG flow cytometry beads (Fig. 3B). This test provides a cost-effective way to test the integrity of both the KIR region and Fc region

of the final fusion protein, as both are required to have folded correctly to produce a positive result in the Luminex binding assay.

3.3. Titration of KIR2D–Fc fusion proteins against HLA class I shows that 100 μg/ml is an appropriate concentration to use in the binding assay

The binding of KIR–Fc fusion proteins to HLA class I increases with an increasing concentration of KIR–Fc fusion protein until binding becomes saturated at approximately 100 μg/ml. Use of KIR–Fc at greater concentrations (100–400 μg/ml) does not increase binding to HLA class I and avidity differences between individual allotypes are found to be consistent at this concentration. Additionally, this saturation point applies to between different HLA class I allotypes and for different naturally occurring and mutant KIR2D (Fig. 3C).

3.4. Multiplex Luminex assay comparing the binding of W6/32, KIR2DL1–Fc and KIR2DL3–Fc to HLA class I coated microbeads

KIR2DL1–Fc binds specifically and with high avidity to HLA-C2 but not HLA-C1 or any HLA-A or HLA-B allotypes (Fig. 3D). HLA-C2 allotypes display a range of avidity for KIR2DL1 with HLA-C*15:02 and HLA-C*04:01 having the highest and lowest avidities respectively (Fig. 3D). KIR2DL3–Fc binds specifically to HLA-C1 but does not bind to HLA-C2 or any HLA-A allotype. Unlike KIR2DL1, KIR2DL3 does bind to two unusual HLA-B allotypes (HLA-B*46:01 and HLA-B*73:01) that have the C1 epitope (Fig. 3D). HLA-C1 allotypes have a range of avidity for KIR2DL3 with HLA-C*03:04 and HLA-C*16:01 having the highest and lowest avidities, respectively. Both HLA-B*46:01 and HLA*73:01 bind with high avidity to KIR2DL3.

3.5. KIR–Fc fusion proteins remain functional following long-term storage at −80 °C

Each 1 l prep of *Hi5* cells yields between 2 and 4 mg of KIR–Fc protein. Given that the KIR–Fc are used at a dilution of 100 μg/ml in the multiplex binding assay, there is typically an excess of KIR–Fc reagent. KIR–Fc remain stable at 4 °C for 1–6 months, however, to allow repetition of a particular experiment over longer time periods and to provide stable positive controls, we investigated the storage of KIR–Fc aliquots at −80 °C (Fig. 3E). KIR–Fc show similar binding in the multiplex binding assay up to 12 months following initial freezing. Freezing the KIR–Fc is assumed to prevent the protein degradation, aggregation and misfolding that occurs at an unpredictable rate when stored at 4 °C.

4. Conclusions

We have described the production of KIR–Fc fusion proteins in an insect cell expression system and their interaction in a multiplex binding assay with a panel of 97 HLA class I allotypes. KIR–Fc production in insect cells is relatively simple, allowing production of large amounts of recombinant protein in around 20 days. The assay is sensitive enough to discriminate between single amino acid substitutions in the extracellular domains of the KIR molecule and has, as a result, greatly facilitated investigation of even closely related KIR allotypes. Furthermore, the results of this direct binding assay appear to correlate well with the results obtained in the limited cellular assays that were used to discover the KIR and first investigate their specificity for HLA class I.

References

Abi-Rached, L., et al., 2010. Human-specific evolution and adaptation led to major qualitative differences in the variable receptors of human and chimpanzee natural killer cells. PLoS Genet. 6 (11), e1001192.

Bjorkman, P.J., et al., 1987. The foreign antigen binding site and T cell recognition regions of class I histocompatibility antigens. Nature 329 (6139), 512.

Blissard, G.W., Rohrmann, G.F., 1989. Location, sequence, transcriptional mapping, and temporal expression of the gp64 envelope glycoprotein gene of the *Orgyia pseudotsugata* multicapsid nuclear polyhedrosis virus. Virology 170 (2), 537.

Colonna, M., Samaridis, J., 1995. Cloning of immunoglobulin-superfamily members associated with HLA-C and HLA-B recognition by human natural killer cells. Science 268 (5209), 405.

Colonna, M., et al., 1992. Alloantigen recognition by two human natural killer cell clones is associated with HLA-C or a closely linked gene. Proc. Natl. Acad. Sci. U. S. A. 89 (17), 7983.

Frazier, W.R., et al., 2013. Allelic variation in KIR2DL3 generates a KIR2DL2-like receptor with increased binding to its HLA-C ligand. J. Immunol. 190 (12), 6198.

Gendzekhadze, K., et al., 2009. Co-evolution of KIR2DL3 with HLA-C in a human population retaining minimal essential diversity of KIR and HLA class I ligands. Proc. Natl. Acad. Sci. U. S. A. 106 (44), 18692.

Graef, T., et al., 2009. KIR2DS4 is a product of gene conversion with KIR3DL2 that introduced specificity for HLA-A*11 while diminishing avidity for HLA-C. J. Exp. Med. 206 (11), 2557.

Guethlein, L.A., et al., 2007. Evolution of killer cell Ig-like receptor (KIR) genes: definition of an orangutan KIR haplotype reveals expansion of lineage III KIR associated with the emergence of MHC-C. J. Immunol. 179 (1), 491.

Hilton, H.G., Parham, P., 2013. Direct binding to antigen-coated beads refines the specificity and cross-reactivity of four monoclonal antibodies that recognize polymorphic epitopes of HLA class I molecules. Tissue Antigens 81 (4), 212.

Hilton, H.G., et al., 2012. Mutation at positively selected positions in the binding site for HLA-C shows that KIR2DL1 is a more refined but less adaptable NK cell receptor than KIR2DL3. J. Immunol. 189 (3), 1418.

Hitchman, R.B., Possee, R.D., King, L.A., 2009. Baculovirus expression systems for recombinant protein production in insect cells. Recent Pat. Biotechnol. 3 (1), 46.

Kost, T.A., Condreay, J.P., 1999. Recombinant baculoviruses as expression vectors for insect and mammalian cells. Curr. Opin. Biotechnol. 10 (5), 428.

Lanier, L.L., 1997. Natural killer cells: from no receptors to too many. Immunity 6 (4), 371.

Mandelboim, O., et al., 1996. Protection from lysis by natural killer cells of group 1 and 2 specificity is mediated by residue 80 in human histocompatibility leukocyte antigen C alleles and also occurs with empty major histocompatibility complex molecules. J. Exp. Med. 184 (3), 913.

Moesta, A.K., et al., 2008. Synergistic polymorphism at two positions distal to the ligand-binding site makes KIR2DL2 a stronger receptor for HLA-C than KIR2DL3. J. Immunol. 180 (6), 3969.

Moesta, A.K., et al., 2009. Chimpanzees use more varied receptors and ligands than humans for inhibitory killer cell Ig-like receptor recognition of the MHC-C1 and MHC-C2 epitopes. J. Immunol. 182 (6), 3628.

Moretta, A., et al., 1993. P58 molecules as putative receptors for major histocompatibility complex (MHC) class I molecules in human natural killer (NK) cells. Anti-p58 antibodies reconstitute lysis of MHC class I-protected cells in NK clones displaying different specificities. J. Exp. Med. 178 (2), 597.

Norman, P.J., et al., 2013. Co-evolution of human leukocyte antigen (HLA) class I ligands with killer-cell immunoglobulin-like receptors (KIR) in a genetically diverse population of sub-Saharan Africans. PLoS Genet. 9 (10), e1003938.

Older Aguilar, A.M., et al., 2010. Coevolution of killer cell Ig-like receptors with HLA-C to become the major variable regulators of human NK cells. J. Immunol. 185 (7), 4238.

Older Aguilar, A.M., et al., 2011. Rhesus macaque KIR bind human MHC class I with broad specificity and recognize HLA-C more effectively than HLA-A and HLA-B. Immunogenetics 63 (9), 577.

Parham, P., Moffett, A., 2013. Variable NK cell receptors and their MHC class I ligands in immunity, reproduction and human evolution. Nat. Rev. Immunol. 13 (2), 133.

Pei, R., et al., 1998. Simultaneous HLA Class I and Class II antibodies screening with flow cytometry. Hum. Immunol. 59 (5), 313.

Pei, R., et al., 2003. Single human leukocyte antigen flow cytometry beads for accurate identification of human leukocyte antigen antibody specificities. Transplantation 75 (1), 43.

Sambrook, J.G., et al., 2005. Single haplotype analysis demonstrates rapid evolution of the killer immunoglobulin-like receptor (KIR) loci in primates. Genome Res. 15 (1), 25.

Shrestha, B., Smee, C., Gileadi, O., 2008. Baculovirus expression vector system: an emerging host for high-throughput eukaryotic protein expression. Methods Mol. Biol. 439, 269.

Valiante, N.M., et al., 1997. Functionally and structurally distinct NK cell receptor repertoires in the peripheral blood of two human donors. Immunity 7 (6), 739.

Victor, M.E., et al., 2010. Insect cells are superior to *Escherichia coli* in producing malaria proteins inducing IgG targeting PfEMP1 on infected erythrocytes. Malar. J. 9, 325.

Volkman, L.E., Goldsmith, P.A., 1988. Resistance of the 64 K protein of budded *Autographa californica* nuclear polyhedrosis virus to functional inactivation by proteolysis. Virology 166 (1), 285.

Wilson, M.J., et al., 2000. Plasticity in the organization and sequences of human KIR/ILT gene families. Proc. Natl. Acad. Sci. U. S. A. 97 (9), 4778.

Winter, C.C., Long, E.O., 1997. A single amino acid in the p58 killer cell inhibitory receptor controls the ability of natural killer cells to discriminate between the two groups of HLA-C allotypes. J. Immunol. 158 (9), 4026.

Winter, C.C., Long, E.O., 2000. Binding of soluble KIR–Fc fusion proteins to HLA class I. Methods Mol. Biol. 121, 239.

Winter, C.C., et al., 1998. Direct binding and functional transfer of NK cell inhibitory receptors reveal novel patterns of HLA-C allotype recognition. J. Immunol. 161 (2), 571.

TISSUE ANTIGENS
IMMUNE RESPONSE GENETICS

Tissue Antigens ISSN 0001-2815

Direct binding to antigen-coated beads refines the specificity and cross-reactivity of four monoclonal antibodies that recognize polymorphic epitopes of HLA class I molecules

H. G. Hilton[1,2] & P. Parham[1,2]

1 Department of Structural Biology, Stanford University School of Medicine, Stanford, CA, USA
2 Department of Microbiology and Immunology, Stanford University School of Medicine, Stanford, CA, USA

Key words
epitope; human leukocyte antigen class I; monoclonal antibodies; polymorphism

Correspondence
Prof Peter Parham
Department of Structural Biology
Stanford University School of Medicine
Fairchild D-157
299 Campus Drive West
Stanford
CA 94305
USA
Tel: +1 6507237456
Fax: +1 6504248912
e-mail: peropa@stanford.edu

Received 15 January 2013; accepted 15 February 2013

doi: 10.1111/tan.12095

Abstract

Monoclonal antibodies with specificity for human leukocyte antigen (HLA) class I determinants of HLA were originally characterized using serological assays in which the targets were cells expressing three to six HLA class I variants. Because of this complexity, the specificities of the antibodies were defined indirectly by correlation. Here we use a direct binding assay, in which the targets are synthetic beads coated with 1 of 111 HLA class I variants, representing the full range of HLA-A, -B and -C variation. We studied one monoclonal antibody with monomorphic specificity (W6/32) and four with polymorphic specificity (MA2.1, PA2.1, BB7.2 and BB7.1) and compared the results with those obtained previously. W6/32 reacted with all HLA class I variants. MA2.1 not only exhibits high specificity for *HLA-A*02*, *-B*57* and *-B*58*, but also exhibited cross-reactivity with *HLA-A*11* and *-B*15:16*. At low concentration (1 µg/ml), PA2.1 and BB7.2 were both specific for *HLA-A*02* and *-A*69*, and at high concentration (50 µg/ml) exhibited significant cross-reactions with *HLA-A*68*, *-A*23* and *-A*24*. BB7.1 exhibits specificity for *HLA-B*07* and *-B*42*, as previously described, but reacts equally well with HLA-B*81, a rare allotype defined some 16 years after the description of BB7.1. The results obtained with cell-based and bead-based assays are consistent and, in combination with amino acid sequence comparison, increase understanding of the polymorphic epitopes recognized by the MA2.1, PA2.1, BB7.2 and BB7.1 antibodies. Comparison of two overlapping but distinctive bead sets from two sources gave similar results, but the overall levels of binding were significantly different. Several weaker reactions were observed with only one of the bead sets.

Introduction

Since first being reported in 1978 (1), monoclonal antibodies with specificity for human leukocyte antigen (HLA) class I molecules have been invaluable tools for both basic and clinical research in human immunology. These antibodies can be divided into two groups according to the types of epitope they recognize (2). Monomorphic antibodies, such as W6/32, the antibody described by Barnstable et al. (1), recognize monomorphic determinants that are common to all HLA class I variants, whereas polymorphic antibodies recognize determinants carried by a subset of such variants. Well-studied examples of polymorphic antibodies are PA2.1, BB7.1, BB7.2 and MA2.1. Originally, PA2.1 and BB7.2 were seen to be specific for HLA-A2 (2–4), but with more extensive characterization they were also shown to recognize and define *HLA-A*69*, a variant that is a recombinant of *HLA-A*02* and *HLA-A*68* (5). In a similar fashion, BB7.1 was originally seen to be specific for *HLA-B*07* (2) but was subsequently shown to recognize *HLA-B*42* (6), a recombinant of *HLA-B*07* and *HLA-B*08* (7) that is characteristic of African populations (8). MA2.1, which was originally described as recognizing HLA-A2 and HLA-B17 antigens (9), has been shown to react with both the *B*57* and *B*58* components of the HLA-B17 (10), but no additional reactivities have been reported.

In large part, the HLA class I specificity of monoclonal antibodies has been determined using panels of cells each of which minimally expresses one HLA-A, one HLA-B and one HLA-C allotype and more commonly express two allotypes for HLA-A, -B and -C. This complexity means that binding reactions cannot be directly attributed to particular HLA

class I variants but must be inferred through various types of correlation. As a consequence, there are limitations in the extent to which data can be interpreted and thus in the resolution and accuracy of the data. An initial approach to address these limitations was the use of mutant cell lines that lacked endogenous HLA class I expression and could be transfected to express a single HLA class I allotype of choice (11). A more recent approach has been to replace cells as the target antigen with synthetic beads each of which is coated with a single HLA class I allotype (12, 13). Elimination of cells from the assay facilitated the commercial development of panels of >90 different beads that provide a representation of the range of HLA-A, -B and -C diversity. By using such beads to determine the HLA class I specificities of Fc-fusion proteins made from killer-cell immunoglobulin-like receptors (KIRs), we have achieved results of higher resolution that are more reproducible and insightful than was possible with cell-based assays (14, 15). Here we have re-examined the HLA class I specificities of the MA2.1, PA2.1, BB7.2 and BB7.1 monoclonal antibodies using two panels of beads coated with HLA class I molecules.

Materials and methods

Binding of MA2.1, PA2.1, BB7.2 and BB7.1 antibodies to beads, each coated with a representative range of HLA-A, -B and -C allotypes was assessed in a multiplex assay on the Luminex platform (Luminex, Austin, TX). The bead panels tested were (a) LabScreen single-antigen beads (One Lambda, Canoga Park, CA) and (b) LifeCodes single-antigen beads (Gen-Probe, San Diego, CA). Antibodies (1 and 50 μg/ml) were incubated with each set of beads for 60 min at 4°C, washed four times and then labeled with anti-mouse Fc antibody conjugated with phycoerythrin and incubated for a further 60 min at 4°C. The fluorescent intensity and identification of individual labels of the beads were visualized on a Luminex 100 reader. In each experiment, data were collected from a minimum of 100 antigen-coated beads for each combination of bead and monoclonal antibody. The results presented are the mean fluorescence relative to the fluorescence intensity obtained with the W6/32 antibody obtained from three replicate experiments performed for each monoclonal antibody.

Results

Figure 1 provides a distillation of the results obtained from previous work using cell-based assays to study the HLA class I specificities of the MA2.1, PA2.1, BB7.2 and BB7.1 mouse monoclonal antibodies and the epitopes of HLA class I molecules that these antibodies recognize. In this study, these four antibodies were tested for binding to beads coated with single HLA-A, -B or -C allotypes. Two sets of commercially available beads (from One Lambda and Gen-Probe) were tested and compared. Together the two bead sets allowed us to test a total of 111 HLA class I allotypes (33 HLA-A, 66 HLA-B and 21 HLA-C allotypes). The HLA class I allotypes represented in each bead set are shown in Figure 2A.

The assay used to measure the binding of the monoclonal antibodies is essentially the same as the one that we designed and have used for measuring the binding of KIR-Fc fusion products to beads coated with HLA class I (14). In this assay, the binding of the antibodies recognizing polymorphic epitopes was normalized to that of the W6/32 monoclonal antibody that recognizes an epitope common to all HLA class I epitopes (1, 31). This normalization corrects for differences in the absolute amount of HLA class I on the various beads. As measured by the binding of W6/32, the amount of HLA class I on the beads varied with allotypes, but a more general property was that the One Lambda Labscreen beads consistently bound more W6/32 than the Gen-Probe LifeCodes beads (Figure 2B). Gen-Probe beads showed a mean reduction in W6/32 binding of 54% (range: 35%–69%), 52% (range: 20%–71%) and 50% (range: 23%–75%) for HLA-A, -B and -C allotypes, respectively as compared with One Lambda beads.

Specificity of the MA2.1 monoclonal antibody

The MA2.1 antibody bound strongly to the five *HLA-A*02* subtypes tested (*A*02:01, :02, :03, :05* and *:06*) and also to *HLA-B*57:01*, *B*57:03* and *B*58:01* (corresponding to the serological HLA-B17 antigen; Figure 3A). These results are consistent with the previously defined specificity of MA2.1 for the HLA-A2 and -B17 antigens (9). In addition, we observed a weak reactivity of MA2.1 with *HLA-B*15:16* and an even weaker one with *HLA-A*11*. These weak cross-reactions were detected only with the One Lambda beads.

Results from several groups of investigators are consistent with the GETR motif at residues 62–65 in the helix of the α_1 domains of *HLA-A*02*, *B*57* and *B*58* being critical for forming the epitope recognized by MA2.1 (Figure 1). Within this motif, glycine 62 is the only residue that is not found in any of the other 89 HLA-A, -B and -C allotypes tested. *HLA-B*15:16* and *HLA-A*11* differ only at position 62, having the RETR and QETR motifs, respectively, which correlates with them having some avidity for MA2.1. The replacement of glycine 62 with arginine in *B*15:16* is seen to be more favorable for binding MA2.1 than the glutamine residue at this position in *A*11* (Figure 3B). Other HLA class I allotypes having the QETR motif (e.g. *HLA-A*03*, *A*30* and *A*36*) are not recognized by MA2.1, suggesting that further residues, away from this motif in the α_1 domain also influence recognition of HLA class I by MA2.1.

In addition to the GETR motif at residues 62–65 in the α_1 domain, mutation at several positions in the α_2 domain (149, 152, 170, 174, 175 and 181) has been shown to influence MA2.1 binding (20, 22, 16, 24), as has the residue at position 8 in the peptide bound to HLA-A2 (20) (Figure 3C). These influences could involve direct contact with the antibody or be

	Result	Reference		
MA2.1 PA2.1 BB7.2	PA2.1 is specific for *HLA-A*02* and does not fix complement	1978	Parham and Bodmer	(3)
	BB7.2 has the same specificity as PA2.1 and does fix complement	1979	Brodsky *et al.*	(2)
	MA2.1 is specific for an epitope shared by *HLA-A*02* and B17 (*HLA-B*57* and *B*58*) and does not fix complement	1980	McMichael *et al.*	(9)
	BB7.2 and PA2.1 recognize *HLA-A*69* as well as *HLA-A*02*	1981	Parham and Brodsky	(4)
	The epitopes recognized by MA2.1 and PA2.1/BB7.2 overlap	1983	Ways and Parham	(10)
	Mutation at position 161 abrogates the epitope recognized by PA2.1 and BB7.2	1983	Taketani *et al.*	(16)
	MA2.1 binds *HLA-A*02:01, A*02:02, A*02:03, B*57:01* and *B*58:01* with similar affinity, which is 100-fold higher than the low affinities of PA2.1 and BB7.2	1983	Ways and Parham	(10)
	The *HLA-A*69:01* sequence combines the α_1 domain of *A*68:01* with the α_2 domain of *A*02* and locates the PA2.1/BB7.2 epitope to the α_2 domain	1985	Holmes and Parham	(5)
	The *HLA-B*58:01* sequence locates the MA2.1 epitope to residues 62-65 of the α_1 domain	1986	Ways *et al.*	(17)
	Substituting tryptophan at position 107 in *HLA-A*02:01* eliminates the epitope recognized by PA2.1 and BB7.2	1987	Salter *et al.*	(18)
	Substituting glycine for tryptophan at position 107 in *HLA-A*02:01* eliminates the PA2.1 & BB7.2 epitope, mutations at positions 62, 63, 65 & 66 eliminates the MA2.1 epitope	1988	Santos-Aguando *et al.*	(19)
	Mutations at positions 149 or 152 in *HLA-A*02:01* reduce MA2.1 binding	1989	Hogan *et al.*	(20)
	Correlation between the specifcities of mouse monoclonal antibodies and human alloantibodies reacting with *HLA-A*02*	1990	Fuller *et al.*	(21)
	Mutations at positions 170, 174, 175 & 181 of *HLA-A*02* reduce MA2.1 binding	1991	Lombardi *et al.*	(22)
	Mutation at position 62 of *HLA-A*02* eliminates the MA2.1 epitope, mutations at positions 107, 162 and 169 eliminates the PA2.1/BB7.2 epitope	1992	Hogan and Brown	(23)
	The peptides bound by *HLA-A*02* can alter its avidity for MA2.1 by ~30 fold. This enhanced avidity is sensitive to the residue at peptide position 8	1995	Barouch *et al.*	(24)
BB7.1	BB7.1 is specific for *HLA-B*07*	1979	Brodsky *et al.*	(2)
	The epitope recognized by BB7.1 does not overlap with the Bw6 epitope	1983	Parham	(25)
	Sequence comparison of Bw4+ HLA-A and -B allotypes locates the Bw6 and Bw4 epitopes to positions 79-83 in the α_1 domain	1986	Wan *et al.*	(26)
	BB7.1 also recognizes the characteristically African allotype *HLA-B*42*	1986	Parham *et al.*	(6)
	The *HLA-B*42:01* sequence combines the α_1 domain of *HLA-B*07* with the α_2 domain of *HLA-B*08* and locates the BB7.1 epitope to the α_1 domain	1988	Parham *et al.*	(7)
	Recombination mutants between B7 and B27 map the BB7.1 epitope to positions 63, 67 & 70 and the Bw6 epitope to positions 82 & 83	1988	Toubert *et al.*	(27)
	Correlation between the specificities of mouse monoclonal antibodies and human alloantibodies reacting with *HLA-B*07*	1990	Fuller *et al.*	(21)
	Replacing residues 65-80 of *HLA-A*02* with the the *HLA-B*07* counterparts does not introduce the BB7.1 epitope	1991	Domenech *et al.*	(28)
	Mutation at positions 166 and 169 in the α_2 domain of *HLA-B*07* eliminates the BB7.1 epitope	1992	McCutcheon and Lutz	(29)
	Natural and mutant recombinants show tyrosine 67 in *HLA-B*07* is critical in forming the BB7.1 epitope	1993	McCutcheon *et al.*	(30)

Figure 1 Summary of studies investigating the polymorphic antibodies MA2.1, PA2.1, BB7.2 (top panel) and BB7.1 (bottom panel). Listed is the main finding from each study, the study's first author and year of publication. The specific reference as listed in the current publication is noted to the right.

a consequence of indirect effects that alter the conformation of residues 62–65.

Specificity of the PA2.1 and BB7.2 monoclonal antibodies

When used at a concentration of 1 μg/ml, the PA2.1 and BB7.2 antibodies gave similarly strong reactions with five subtypes of *HLA-A*02* and with *HLA-A*69:01* (Figure 4A). For each of these reactions, the Gen-Probe beads gave weaker reactions than the One Lambda beads, the difference being greatest for *HLA-A*02:01*, as was also the case for MA2.1 (Figure 3A). These results are consistent with those obtained with the W6/32 antibody (Figure 2B).

When a much higher concentration of antibody was used (50 μg/ml), cross-reactions of the PA2.1 and BB7.2 antibodies were observed with *HLA-A*23:01*, *A*24:02*, *A*24:03*, *A*68:01*, *A*68:02* and *A*69:01* (Figure 4B). These

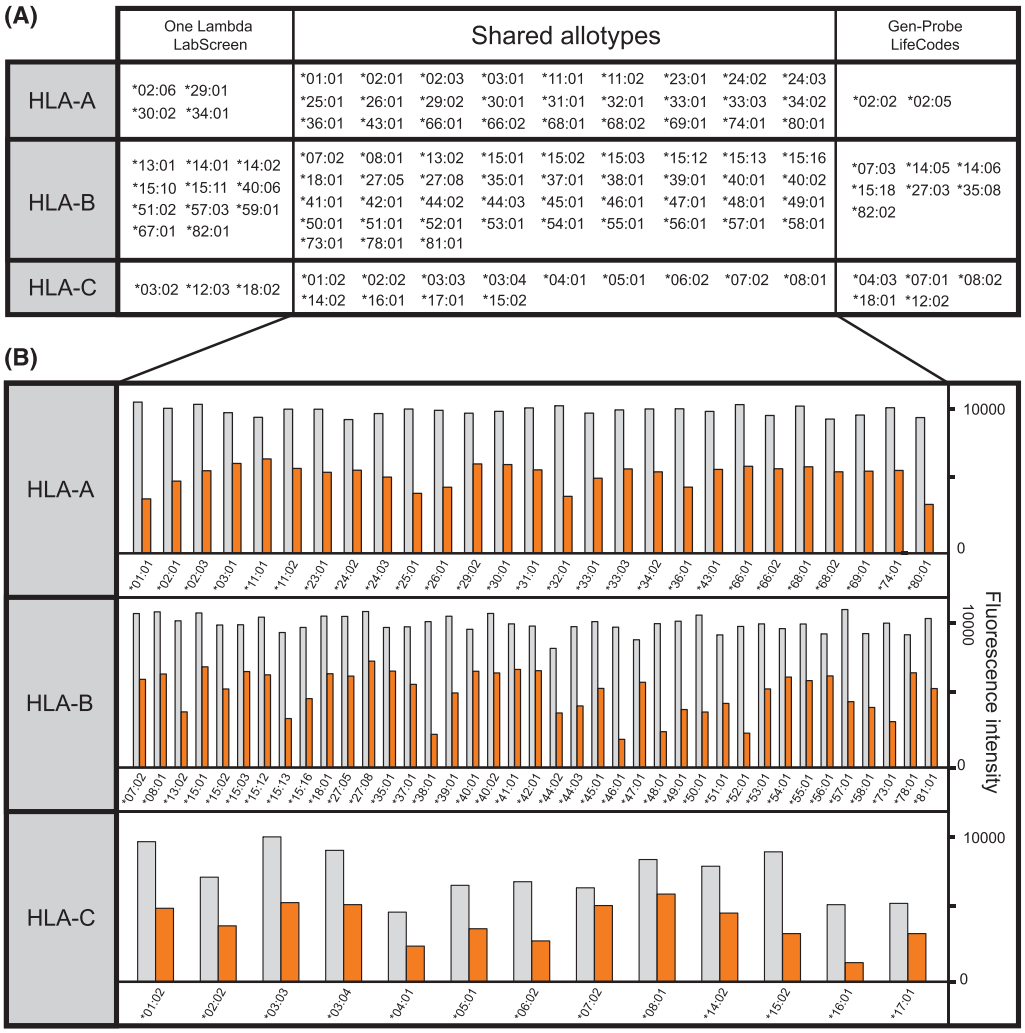

Figure 2 (A) Human leukocyte antigen (HLA) class I allotypes represented by the One Lambda LabScreen and Gen-Probe LifeCodes bead sets. (B) Binding of the monomorphic HLA class I antibody W6/32 to beads from One Lambda LabScreen (gray bars) and Gen-Probe LifeCodes (orange bars). The binding reactions shown are to the allotypes that are common to both bead sets.

cross-reactions correspond well with the cross-reactivity first described in the 1960s (32) between the serological A2, A28 (*A*68* and *A*69*) and A9 (*A*23* and *A*24*) antigens and more recently described for cell-binding assays with the I-145 monoclonal antibody (33). These cross-reactions were stronger for BB7.2 than PA2.1, a feature observed for both sets of HLA class I coated beads. The cross-reactivity was much stronger for *A*24:03* than either *A*24:02* or *A*23:01*. This must be due to the two substitutions that distinguish *A*24:03* from both *A*24:02* and *A*23:01* (34) and which are at positions 166 and 167 in the α_2 domain (Figure 3C). Consistent with the relative binding to PA2.1 and BB7.2, *HLA-A*24:03* shares the glutamate 166 and tryptophan 167 motif with *HLA-A*02*, whereas *HLA-A*24:02* and *A*23:01* share the aspartate 166 and glycine 167 motif with *HLA-A*01:01*, which binds neither PA2.1 nor BB7.2.

The combination of sequence comparisons (2, 4, 5, 10) and site-directed mutagenesis (18, 19, 23) has shown that tryptophan 107 in the α_2 domain is a critical factor in forming the epitope recognized by PA2.1 and BB7.2 (Figures 1 and 4B). In addition, mutations at positions 161, 163, 166, 167 and 169 can lead to loss of binding by PA2.1 and BB7.2, showing that these residues also contribute to forming the epitope (16, 23) (Figure 4C).

Specificity of the BB7.1 monoclonal antibody

As previously reported, we found that BB7.1 reacts with *HLA-B*07:02* and *HLA-B*42:01* (Figure 5A). In addition, we found that *HLA-B*81:01*, an African allotype (35, 36), also reacts strongly with BB7.1, which fits with both *HLA-B*81:01*, *B*42:01* and *B*07:01* having α_1 domains with identical sequence (Figure 5B) and residues 63–70 of the α_1

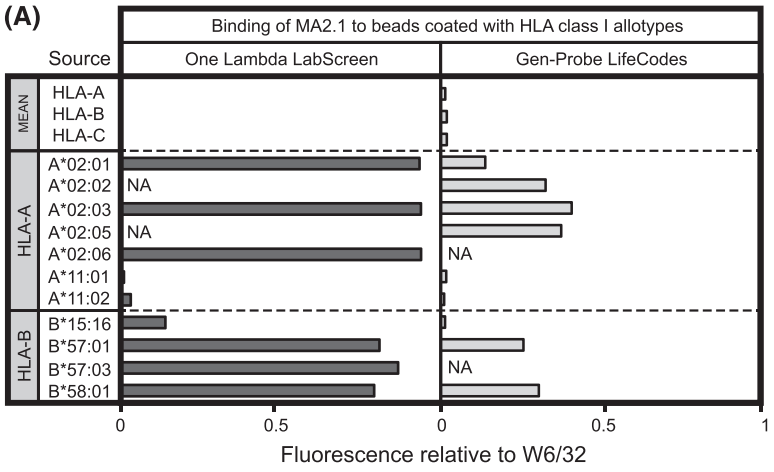

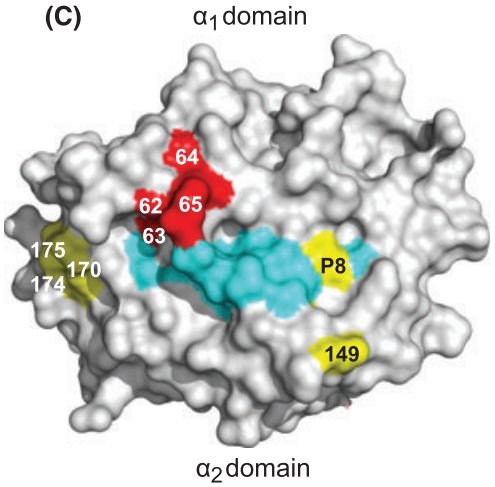

(B)

	Position	61	62	63	64	65	66	67	68	69	70	71	72	73	74	75	76	77	78	79	80	81	82	83	149	174	175
	Residue	D	G	E	T	R	K	V	K	A	H	S	Q	T	H	R	V	D	L	G	T	L	R	G	A	N	G
HLA-A	HLA-A*02:01	–	–	–	–	–	–	–	–	–	–	–	–	–	–	–	–	–	–	–	–	–	–	–	–	–	–
	HLA-A*02:02	–	–	–	–	–	–	–	–	–	–	–	–	–	–	–	–	–	–	–	–	–	–	–	–	–	–
	HLA-A*02:03	–	–	–	–	–	–	–	–	–	–	–	–	–	–	–	–	–	–	–	–	–	–	–	T	–	–
	HLA-A*02:05	–	–	–	–	–	–	–	–	–	–	–	–	–	–	–	–	–	–	–	–	–	–	–	–	–	–
	HLA-A*02:06	–	–	–	–	–	–	–	–	–	–	–	–	–	–	–	–	–	–	–	–	–	–	–	–	–	–
	HLA-A*11:01	–	Q	–	–	–	N	–	–	–	Q	–	–	–	D	–	–	–	–	–	–	–	–	–	–	–	–
	HLA-A*11:02	–	Q	–	–	–	N	–	–	–	Q	–	–	–	D	–	–	–	–	–	–	–	–	–	–	–	–
	HLA-A*23:01	–	E	–	–	G	–	–	–	–	–	–	–	–	–	–	E	N	–	R	I	A	L	R	–	–	–
	HLA-A*30:01	–	Q	–	–	–	N	–	–	–	Q	–	–	–	–	–	–	–	–	–	–	–	–	–	–	–	–
	HLA-A*69:01	–	R	N	–	–	N	–	–	–	Q	–	–	–	–	–	–	–	–	–	–	–	–	–	–	–	–
HLA-B	HLA-B*07:02	–	R	N	–	Q	I	Y	–	–	Q	A	–	–	D	–	E	S	–	R	N	–	–	–	–	–	–
	HLA-B*15:01	–	R	–	–	Q	I	S	–	T	N	T	–	–	Y	–	E	S	–	R	N	–	–	–	–	–	–
	HLA-B*15:16	–	R	–	–	–	N	M	–	–	S	A	–	–	Y	–	E	N	–	R	I	A	L	R	–	–	–
	HLA-B*57:01	–	–	–	–	–	N	M	–	–	S	A	–	–	Y	–	E	S	–	R	I	A	L	R	–	–	–
	HLA-B*57:03	–	–	–	–	–	N	M	–	–	S	A	–	–	Y	–	E	N	–	R	I	A	L	R	–	–	–
	HLA-B*58:01	–	–	–	–	–	N	M	–	–	S	A	–	–	Y	–	E	N	–	R	I	A	L	R	–	–	–

Figure 3 (A) Binding of MA2.1 (1 μg/ml) to beads coated with human leukocyte antigen (HLA) class I allotypes from the One Lambda LabScreen (left panel) and Gen-Probe LifeCodes (right panel) bead sets. (B) Alignment of HLA class I allotypes showing selected residues in the α_1 and α_2 domains. Residues from allotypes that form the epitope recognized by MA2.1 are shaded in gray. (C) Space-filling model of the binding surface of *HLA-A*02* (gray) with associated peptide (cyan). Residues highlighted in yellow fall within the footprint recognized by MA2.1. Residues 62–65 are critical for formation of the epitope recognized by MA2.1 and are highlighted in red.

domain being critical for the BB7.1 epitope (2, 6, 30, 28, 25, 27, 26, 21) (Figure 1). Comparably strong reactions for *HLA-B*07:02*, *B*42:01* and *B*81:01* were observed with the One Lambda beads, but the binding of BB7.1 to the Gen-Probe *B*42:01* bead was relatively weak. Even weaker was the binding to the *B*07:03* bead, which likely reflects an inherent difference between *B*07:02* and *B*07:03* in their avidities for BB7.1. That *B*07:03* differs from *B*07:02* by nonconservative substitutions at positions 69, 70 and 71 also provides evidence that favors this interpretation (37).

Both *HLA-B*56:01* and *B*82:01* have α_1 domains with identical sequence to that of *HLA-B*07:02*, *B*42:01* and *B*81:01* but these allotypes are not bound by BB7.1 suggesting that residues in the α_2 domain abrogate their recognition. *HLA-B*07:02*, *B*42:01* and *B*81:01* encode arginine at position 131 whereas *B*56:01* and *B*82:01* encode serine at this position. Similarly, both *B*56:01* and *B*82:01* encode leucine at position 163 whereas *HLA-B*07:02* and *B*81:01* both have glutamic acid. Interestingly, *HLA-B*42:01* has a threonine at position 131 which may explain its weaker recognition by BB7.1 as detected on both the One Lambda and Gen-Probe beads. That BB7.1 interacts with residues in the α_2 domain is further supported by the observation that mutation at positions 166 and 169 of *HLA-B*07* eliminates the BB7.1 epitope (29).

Therefore, whilst the α_1 domain residues between positions 63–71 likely form the dominant epitope for recognition by BB7.1, binding is influenced by polymorphism in the α_2 domain, suggesting that this antibody binds both the α_1 and α_2 regions of HLA class I. Given that this footprint would

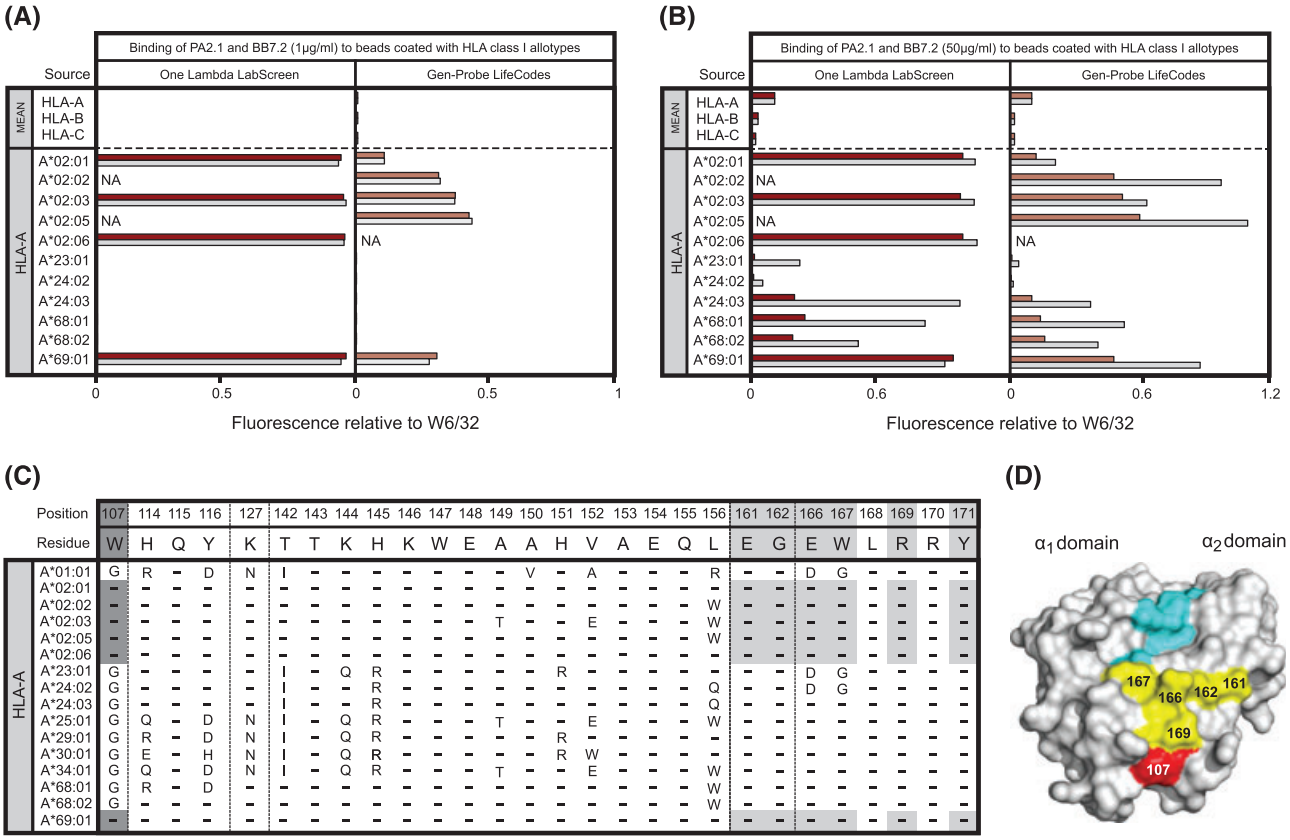

Figure 4 (A) Binding of PA2.1 (1 μg/ml) and BB7.2 (1 μg/ml) to beads coated with human leukocyte antigen (HLA) class I allotypes from the One Lambda LabScreen (left panel) and Gen-Probe LifeCodes (right panel) bead sets. (B) Binding of PA2.1 (50 μg/ml) and BB7.2 (50 μg/ml) to beads coated with HLA class I allotypes from the One Lambda LabScreen (left panel) and Gen-Probe LifeCodes (right panel) bead sets. (C) Alignment of HLA class I allotypes showing selected residues in the α_2 domain. Residues from allotypes that form the epitope recognized by PA2.1 and BB7.2 are shaded in gray. (D) Space-filling model of *HLA-A*02* (gray) with associated peptide (cyan). Residues highlighted in yellow fall within the footprint recognized by PA2.1 and BB7.2. Tryptophan at position 107 is considered critical for formation of the epitope recognized by PA2.1 and BB7.2 and is highlighted in red.

span the peptide-binding cleft, peptide variability is likely to influence BB7.1 recognition of HLA class I.

In summary, we find that the patterns of antibody reactivity observed here are entirely consistent with those obtained previously, and extend those results by being able to detect and distinguish reactions and cross-reactions in a quantitative manner. All the observed reactions are with HLA-A and -B variants, with no cross-reactivity for HLA-C, further emphasizing the distinctive properties of HLA-C (38).

Discussion

Consistent with previous studies we showed that MA2.1 bound to *HLA-A*02* subtypes and to *HLA-B*57* and *HLA-B*58* allotypes (9, 23). Experimental data and sequence analysis suggest that the α_1 residues GETR at positions 62–65 are critical in forming the epitope recognized by MA2.1 (23, 17). In this study, we showed weak interactions with MA2.1 are also formed when glycine at position 62 is substituted for arginine, as in *HLA-B*15:16* and glutamine as in *HLA-A*11:02*. This finding contrasts with results of a cellular assay in which substitution of glycine for arginine at position 62 abrogated recognition of *HLA-A*02* by MA2.1 (23). *HLA-B*15:16* has a high degree of sequence homology with *HLA-B*57*, which appears sufficient to confer reactivity with MA2.1 despite the introduction of a residue apparently less favorable for recognition by MA2.1 at position 62. That glutamine at position 62 results in weak binding to *HLA-A*11* and no detectable binding to other HLA-A allotypes with glutamine at this position (e.g. *HLA-A*03*, *A*30* and *A*36*) would suggest that this residue is less favorable for binding than both glycine and arginine. An alternative explanation is that a few of the peptides presented by either *HLA-B*15:16* and *HLA-A*11* form an epitope with a high affinity for MA2.1, sufficient to overcome the reduction in affinity incurred by the presence of either arginine or glutamine at position 62.

Several lines of evidence suggest that peptide variability influences recognition of HLA class I by MA2.1. Although

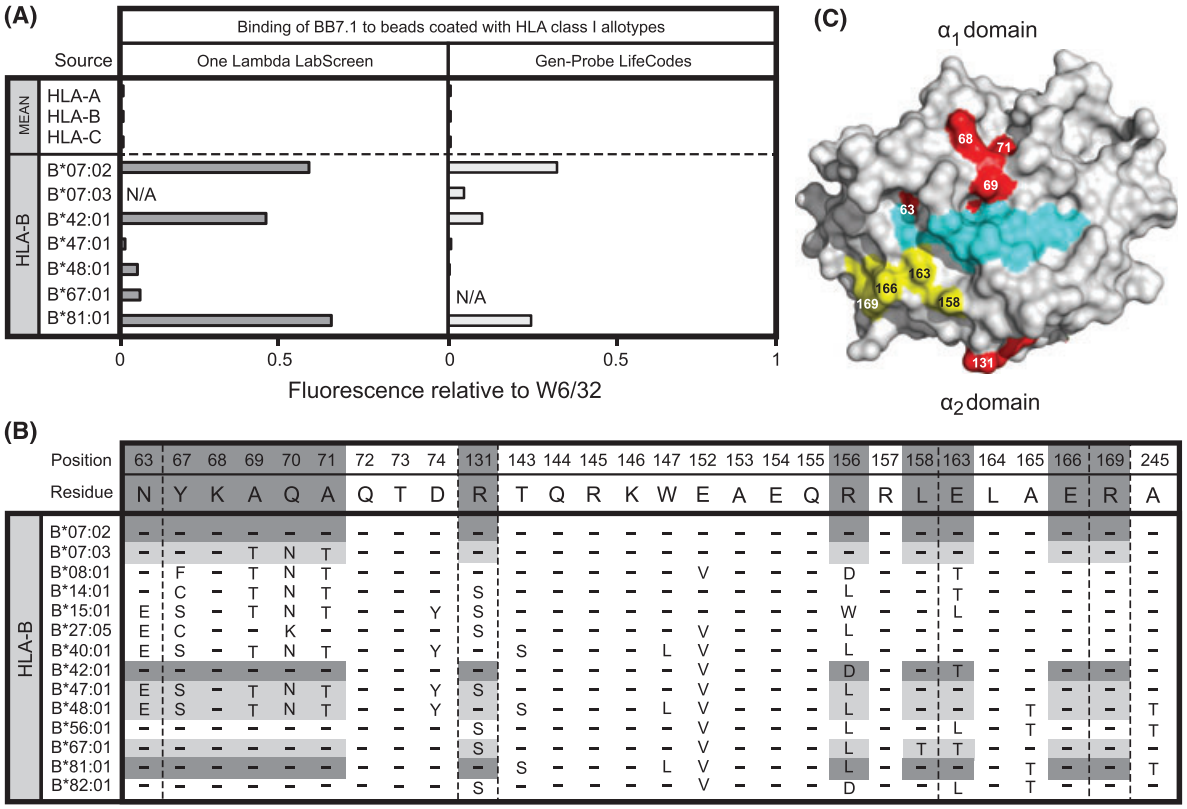

Figure 5 (A) Binding of BB7.1 (1 μg/ml) to beads coated with human leukocyte antigen (HLA) class I allotypes from the One Lambda LabScreen (left panel) and Gen-Probe LifeCodes (right panel) bead sets. (B) Alignment of HLA class I allotypes showing selected residues in the α_1 and α_2 domains. Residues from allotypes that form the epitope recognized by BB7.1 are shaded in gray. (C) Space-filling model of the binding surface of *HLA-B*07* (gray) with associated peptide (cyan). Residues highlighted in yellow fall within the footprint recognized by BB7.1. Residues 63–71 in the α_1 domain and position 131 in the α_2 domain are critical for formation of the epitope recognized by BB7.1 and are highlighted in red.

the residues critical for formation of the epitope recognized by MA2.1 are located in the α_1 domain, mutational experiments indicate that the binding footprint extends to residues in the α_2 domain of the HLA class I molecule (20, 22). This is supported by the finding that MA2.1 recognition of HLA-A2 is prevented in a competitive binding assay with PA2.1 (10), an antibody whose epitope is formed exclusively by residues in the α_2 domain. Together these studies suggest that MA2.1 binds to an area spanning the peptide-binding groove on the face of HLA class I molecule. Direct evidence of the effect of peptide variability is provided from the observation that MA2.1 recognizes HLA-A2 complexed with the HIV-1 p17 epitope (SLYNTVATL) at least 30 times more strongly than all other complexes studied, and this enhanced reactivity was sensitive to point mutation of threonine to alanine at position 8 in the peptide (24). Therefore there exist two possible explanations for the ability of the bound peptide to influence MA2.1 reactivity. Either MA2.1 is sensitive to peptide-induced conformational changes of the helices, or it directly contacts certain peptides in the groove of HLA class I. The identity of the bound peptides presented by HLA class I on beads manufactured by One Lambda and Gen-Probe is unknown, but we presume they are highly heterogeneous.

The weaker interactions between MA2.1 and *HLA-B*15:16* and *A*11:02* were evident only in the One Lambda LabScreen bead set. Similarly, weak interactions between BB7.1 and *HLA-B*48:01* and B*67:01 were identified with the One Lambda beads but these interactions were not observed in the Gen-Probe bead set. Our data and those of others suggests that the residues critical for formation of the epitope recognized by BB7.1 are found in the α_1 and α_2 domains suggesting that, like MA2.1, the identity of the peptide might play a role in the recognition of HLA class I by this antibody. Therefore, the weak interactions observed with BB7.1 might reflect the different peptide pools found in the One Lambda and Gen-Probe bead sets, with those from One Lambda collectively having higher binding affinity than those found in the Gen-Probe bead set. Such weak interactions were not evident for either PA2.1 or BB7.2, antibodies thought to recognize an epitope formed exclusively by residues found in the α_2 domain and as such they are unlikely to be subject to the same changes in peptide pool that we have hypothesized to influence recognition of MA2.1 and BB7.1.

An alternative explanation for the lower affinity of MA2.1 and BB7.1 for HLA class I allotypes presented on the Gen-Probe bead set is the lower antigen density present on these beads. We have shown that the antigen density present on the Gen-Probe bead set is approximately 50% of that present on the One Lambda bead set as evidenced by binding of the monomorphic HLA class I antibody W6/32. As a result the weak interactions noted on the One Lambda bead set might not reach the lower level of detection of the assay with the Gen-Probe bead set.

Acknowledgments

The authors thank Prof Rene Duquesnoy, University of Pittsburgh Medical Center for suggesting this study. The work was supported by National Institutes of Health Grant A122039 (to PP). HGH was supported by the March of Dimes Prematurity Center at Stanford University School of Medicine, Clinical and Translational Science Awards Grant UL1 RR025744 and a Stanford University School of Medicine Dean's Postdoctoral Fellowship.

Conflict of Interests

The authors have declared no conflicting interests.

References

1. Barnstable CJ, Bodmer WF, Brown G et al. Production of monoclonal antibodies to group A erythrocytes, HLA and other human cell surface antigens-new tools for genetic analysis. *Cell* 1978: **14**: 9–20.
2. Brodsky FM, Parham P, Barnstable CJ, Crumpton MJ, Bodmer WF. Monoclonal antibodies for analysis of the HLA system. *Immunol Rev* 1979: **47**: 3–61.
3. Parham P, Bodmer WF. Monoclonal antibody to a human histocompatibility alloantigen, HLA-A2. *Nature* 1978: **276**: 397–9.
4. Parham P, Brodsky FM. Partial purification and some properties of BB7.2. A cytotoxic monoclonal antibody with specificity for HLA-A2 and a variant of HLA-A28. *Hum Immunol* 1981: **3**: 277–99.
5. Holmes N, Parham P. Exon shuffling in vivo can generate novel HLA class I molecules. *EMBO J* 1985: **4**: 2849–54.
6. Parham P, Antonelli P, Herzenberg LA, Kipps TJ, Fuller A, Ward FE. Further studies on the epitopes of HLA-B7 defined by murine monoclonal antibodies. *Hum Immunol* 1986: **15**: 44–67.
7. Parham P, Lomen CE, Lawlor DA et al. Nature of polymorphism in HLA-A, -B, and -C molecules. *Proc Natl Acad Sci U S A* 1988: **85**: 4005–9.
8. Cao K, Hollenbach J, Shi X, Shi W, Chopek M, Fernandez-Vina MA. Analysis of the frequencies of HLA-A, B, and C alleles and haplotypes in the five major ethnic groups of the United States reveals high levels of diversity in these loci and contrasting distribution patterns in these populations. *Hum Immunol* 2001: **62**: 1009–30.
9. McMichael AJ, Parham P, Rust N, Brodsky F. A monoclonal antibody that recognizes an antigenic determinant shared by HLA A2 and B17. *Hum Immunol* 1980: **1**: 121–9.
10. Ways JP, Parham P. The binding of monoclonal antibodies to cell-surface molecules. A quantitative analysis with immunoglobulin G against two alloantigenic determinants of the human transplantation antigen HLA-A2. *Biochem J* 1983: **216**: 423–32.
11. Shimizu Y, Koller B, Geraghty D et al. Transfer of cloned human class I major histocompatibility complex genes into HLA mutant human lymphoblastoid cells. *Mol Cell Biol* 1986: **6**: 1074–87.
12. Pei R, Lee JH, Shih NJ, Chen M, Terasaki PI. Single human leukocyte antigen flow cytometry beads for accurate identification of human leukocyte antigen antibody specificities. *Transplantation* 2003: **75**: 43–9.
13. El-Awar N, Lee J, Terasaki PI. HLA antibody identification with single antigen beads compared to conventional methods. *Hum Immunol* 2005: **66**: 989–97.
14. Moesta AK, Norman PJ, Yawata M, Yawata N, Gleimer M, Parham P. Synergistic polymorphism at two positions distal to the ligand-binding site makes KIR2DL2 a stronger receptor for HLA-C than KIR2DL3. *J Immunol* 2008: **180**: 3969–79.
15. Hilton HG, Vago L, Older Aguilar AM et al. Mutation at positively selected positions in the binding site for HLA-C shows that KIR2DL1 is a more refined but less adaptable NK cell receptor than KIR2DL3. *J Immunol* 2012: **189**: 1418–30.
16. Taketani S, Krangel MS, Pious D, Strominger JL. Structural analysis of HLA-A2 antigen from immunoselected mutant 8.6.1: further definition of an HLA-A2-specific serological determinant. *J Immunol* 1983: **131**: 2935–8.
17. Ways JP, Rothbard JB, Parham P. Amino acid residues 56 to 69 of HLA-A2 specify an antigenic determinant shared by HLA-A2 and HLA-B17. *J Immunol* 1986: **137**: 217–22.
18. Salter RD, Clayberger C, Lomen CE, Krensky AM, Parham P. In vitro mutagenesis at a single residue introduces B and T cell epitopes into a class I HLA molecule. *J Exp Med* 1987: **166**: 283–8.
19. Santos-Aguado J, Barbosa JA, Biro PA, Strominger JL. Molecular characterization of serologic recognition sites in the human HLA-A2 molecule. *J Immunol* 1988: **141**: 2811–8.
20. Hogan KT, Clayberger C, Bernhard EJ et al. A panel of unique HLA-A2 mutant molecules define epitopes recognized by HLA-A2-specific antibodies and cytotoxic T lymphocytes. *J Immunol* 1989: **142**: 2097–104.
21. Fuller AA, Trevithick JE, Rodey GE, Parham P, Fuller TC. Topographic map of the HLA-A2 CREG epitopes using human alloantibody probes. *Hum Immunol* 1990: **28**: 284–305.
22. Lombardi G, Matsui M, Moots R et al. Limited regions of the alpha 2-domain alpha-helix control anti-A2 allorecognition: an analysis using a panel of A2 mutants. *Immunogenetics* 1991: **34**: 149–56.
23. Hogan KT, Brown SL. Localization and characterization of serologic epitopes on HLA-A2. *Hum Immunol* 1992: **33**: 185–92.
24. Barouch D, Davenport M, McMichael A, Reay P. A mAb against HLA-A2 can be influenced both positively and negatively by the associated peptide. *Int Immunol* 1995: **7**: 1599–605.

25. Parham P. Antigenic determinants of the HLA-B7 molecule; Bw6- and B7-specific determinants are spatially separate. *Immunogenetics* 1983: **18**: 1–16.
26. Wan AM, Ennis P, Parham P, Holmes N. The primary structure of HLA-A32 suggests a region involved in formation of the Bw4/Bw6 epitopes. *J Immunol* 1986: **137**: 3671–4.
27. Toubert A, Raffoux C, Boretto J et al. Epitope mapping of HLA-B27 and HLA-B7 antigens by using intradomain recombinants. *J Immunol* 1988: **141**: 2503–9.
28. Domenech N, Santos-Aguado J, Lopez de Castro JA. Antigenicity of HLA-A2 and HLA-B7. Loss and gain of serologic determinants induced by site-specific mutagenesis at residues 62 to 80. *Hum Immunol* 1991: **30**: 140–6.
29. McCutcheon JA, Lutz CT. Mutagenesis around residue 176 on HLA-B*0702 characterizes multiple distinct epitopes for anti-HLA antibodies. *Hum Immunol* 1992: **35**: 125–31.
30. McCutcheon JA, Smith KD, Valenzuela A, Aalbers K, Lutz CT. HLA-B*0702 antibody epitopes are affected indirectly by distant antigen residues. *Hum Immunol* 1993: **36**: 69–75.
31. Parham P, Barnstable CJ, Bodmer WF. Use of a monoclonal antibody (W6/32) in structural studies of HLA-A,B,C, antigens. *J Immunol* 1979: **123**: 342–9.
32. Svejgaard A, Kissmeyer-Nielsen F. Cross-reactive human HL-A isoantibodies. *Nature* 1968: **219**: 868–9.
33. Mizuno S, Yako F, Ohta H et al. A new murine lymphocytotoxic monoclonal antibody recognizing HLA-A2, -A28 and -A9. *Tissue Antigens* 1996: **48**: 224–7.
34. Little AM, Madrigal JA, Parham P. Molecular definition of an elusive third HLA-A9 molecule: HLA-A9.3. *Immunogenetics* 1992: **35**: 41–5.
35. Ellexson ME, Zhang G, Stewart D et al. Nucleotide sequence analysis of HLA-B*1523 and B*8101. Dominant alpha-helical motifs produce complex serologic recognition patterns for the HLA-B"DT" and HLA-B"NM5" antigens. *Hum Immunol* 1995: **44**: 103–10.
36. Vilches C, Sanz L, de Pablo R, Moreno ME, Puente S, Kreisler M. Molecular characterization of the new alleles HLA-B*8101 and B*4407. *Tissue Antigens* 1996: **47**: 139–42.
37. Bergmans AM, Tijssen H, Lardy N, Reekers P. Complete nucleotide sequence of HLA-B*0703, a B7 variant (BPOT). *Hum Immunol* 1993: **38**: 159–62.
38. Zemmour J, Parham P. Distinctive polymorphism at the HLA-C locus: implications for the expression of HLA-C. *J Exp Med* 1992: **176**: 937–50.

A Distinctive Cytoplasmic Tail Contributes to Low Surface Expression and Intracellular Retention of the Patr-AL MHC Class I Molecule

Ana Goyos,*[,†,‡] Lisbeth A. Guethlein,* Amir Horowitz,*[,†,‡] Hugo G. Hilton,* Michael Gleimer,*[,†,‡,1] Frances M. Brodsky,[§,¶,‖,2] and Peter Parham*[,†,‡]

Chimpanzees have orthologs of the six fixed, functional human *MHC class I* genes. But, in addition, the chimpanzee has a seventh functional gene, *Patr-AL*, which is not polymorphic but contributes substantially to population diversity by its presence on only 50% of *MHC* haplotypes. The ancestral *AL* gene emerged long before the separation of human and chimpanzee ancestors and then subsequently and specifically lost function during human evolution, but was maintained in chimpanzees. Patr-AL is an alloantigen that participates in negative and positive selection of the T cell repertoire. The three-dimensional structure and the peptide-binding repertoire of Patr-AL and HLA-A*02 are surprisingly similar. In contrast, the expression of these two molecules is very different, as shown using specific mAbs and polyclonal Abs made against Patr-AL. Peripheral blood cells and B cell lines express low levels of Patr-AL at the cell surface. Higher levels are seen for 221-cell transfectants expressing Patr-AL, but in these cells a large majority of Patr-AL molecules are retained in the early compartments of the secretory pathway: mainly the endoplasmic reticulum, but also *cis*-Golgi. Replacing the cytoplasmic tail of Patr-AL with that of HLA-A*02 increased the cell-surface expression of Patr-AL substantially. Four substitutions distinguish the Patr-AL and HLA-A*02 cytoplasmic tails. Systematic mutagenesis showed that each substitution contributes changes in cell-surface expression. The combination of residues present in Patr-AL appears unique, but each individual residue is present in other primate MHC class I molecules, notably MHC-E, the most ancient of the functional human MHC class I molecules. ***The Journal of Immunology*, 2015, 195: 3725–3736.**

The selective pressures imposed by diverse, fast-evolving pathogens cause the MHC class I genes of their mammalian hosts also to evolve rapidly (1). As a consequence, there is considerable species-specific character to *MHC class I* gene families. Characteristics shared by most mammalian species are highly polymorphic classical MHC class I molecules that engage highly variable types of lymphocyte receptors and conserved nonclassical MHC class I molecules that engage conserved types of lymphocyte receptors. Of the six human *MHC class I* genes that are functional, *HLA-A*, *-B*, and *-C* are highly polymorphic and provide ligands for the αβ TCRs of CD8 T cells and for the killer cell Ig-like receptors (KIR) of NK cells. In contrast, the *HLA-E*, *-F*, and *-G* genes exhibit little variation. HLA-E is the ligand for the CD94:NKG2A and CD94:NKG2C receptors of NK cells (2), which complement and collaborate with the KIR. By comparison, the function of HLA-F is poorly understood, but it could serve as a chaperone that transports unfolded HLA class I molecules back from the cell surface to the cell's interior (3). HLA-G is the most specialized, being expressed only by extravillous trophoblast during pregnancy (4) and monocytes (5). Cooperative interactions between HLA-G and the KIR2DL4 and LILRB1 receptors of uterine NK cells are necessary for the development of the placenta and the success of reproduction (6).

Counterparts to the *HLA class I* genes are restricted to simian primates, and the chimpanzee (*Pan troglodytes*) has orthologs of all six expressed *HLA class I* genes (7). For some 50% of chimpanzee *MHC* haplotypes, these genes (*Patr-A*, *-B*, *-C*, *-E*, *-F*, and *-G*) are the only expressed *MHC class I* genes, but the other 50% of haplotypes have a seventh expressed gene, *Patr-AL*, that is within an additional ∼125-kb block of genomic DNA that is next to the 80-kb block containing the *Patr-A* gene (8). More closely related to *Patr-A* than the other expressed genes, *Patr-AL* is one of a group of *A*-related genes (hence the name *A-like*) that includes the nonfunctional *MHC-H* and *MHC-J* genes (9). Although not yet proved, there is evidence for the existence of two forms of human *MHC* haplotype that correspond to the *Patr-AL*$^+$ and *Patr-AL*$^-$ chimpanzee haplotypes (8). Called *HLA*-Y, the human equivalent of *Patr-AL* is nonfunctional and contains a 5′ region of high sequence similarity with *Patr-AL* that is recombined with a 3′ region

*Department of Structural Biology, Stanford University School of Medicine, Stanford, CA 94305; †Department of Microbiology and Immunology, Stanford University School of Medicine, Stanford, CA 94305; ‡Stanford Immunology, Stanford University School of Medicine, Stanford, CA 94305; §Department of Bioengineering and Therapeutic Sciences, University of California San Francisco, San Francisco, CA 94143; ¶Department of Pharmaceutical Chemistry, University of California San Francisco, San Francisco, CA 94143; and ‖Department of Microbiology and Immunology, University of California San Francisco, San Francisco, CA 94143

[1]Current address: University of Michigan Medical School, University of Michigan, Ann Arbor, MI.

[2]Current address: Division of Biosciences, University College London, London, U.K.

ORCID: 0000-0002-6962-727X (A.G.).

Received for publication February 18, 2015. Accepted for publication August 7, 2015.

This work was supported by National Institutes of Health (NIH) Grants R01 AI031168 (to P.P.) and R01 GM038093 (to F.M.B.), NIH Ruth L. Kirschstein National Research Service Award Individual Postdoctoral Fellowship F32 AI089085 (to A.G.), NIH Training Grant T32 AI07290 (to A.G.), and Yerkes Base Grant ORIP/OD P51OD011132.

Address correspondence and reprint requests to Dr. Peter Parham, Department of Structural Biology, Stanford University, Fairchild D-159, 299 Campus Drive West, Stanford, CA 94305. E-mail address: peropa@stanford.edu

The online version of this article contains supplemental material.

Abbreviations used in this article: ALpoly, Patr-AL–specific rabbit polyclonal antiserum; BLCL, B lymphoblastoid cell line; ER, endoplasmic reticulum; HI-FBS, heat-inactivated FBS; IFB, intracellular FACS buffer; IP, immunoprecipitation; KIR, killer cell Ig-like receptor; β_2m, β_2-microglobulin; mfi, median fluorescence intensity; NIH, National Institutes of Health; NP-40, Nonidet P-40.

www.jimmunol.org/cgi/doi/10.4049/jimmunol.1500397

from another *A*-related gene (8). Neither *Patr-AL* nor *HLA-Y* exhibit significant polymorphism. Patr-AL originated long before the separation of human and chimpanzee ancestors (8, 9) and was specifically inactivated during human evolution. Such inactivation could have been driven by selection or by the demographic factors of population bottleneck and genetic drift. Study of Patr-AL will therefore define an immune system component that humans have lost.

Patr-AL forms a heterotrimeric complex with β_2-microglobulin (β_2m) and nonamer peptides to give a three-dimensional structure in which the Cα traces of the H chain and β_2m superimpose with their counterparts in other HLA class I structures (8). The peptide-binding specificity of Patr-AL is essentially the same as that of HLA-A*02, although the two molecules differ by >40 aa substitutions, of which 30 are in the α_1 and α_2 domains and 13 are predicted to contact peptide (8). These properties suggest that Patr-AL, like HLA-A and Patr-A, presents peptide Ags to αβ TCRs. Supporting this hypothesis, Patr-AL is an alloantigen recognized by the highly specific cytotoxic CD8 αβT cells that are present in chimpanzees lacking Patr-AL (8). This implies that Patr-AL is expressed in the thymus and mediates negative selection.

The major structural difference between Patr-AL and other human and chimpanzee MHC class I molecules is the upper face of the α helix of the α_2 domain, which is unusually electropositive and makes Patr-AL exceptional in having a basic isoelectric point (8). Previous preliminary analysis of mRNA levels indicated that the expression of Patr-AL was either very low or restricted to a minority of PBMCs (9). In the investigation reported in this article, we made Abs against Patr-AL and used them to study both endogenous Patr-AL protein expression and recombinant Patr-AL stably expressed in an MHC class I–deficient cell line and compared its expression with the well-characterized human HLA-A*02 protein.

Materials and Methods

Plasmids and mutagenesis

Expression vectors were constructed by using PCR to amplify exons 1–8 of Patr-AL*01:01:01 and HLA-A*02:07 from plasmids (8, 9) and cloning the amplicons into the HindIII and XbaI sites of the mammalian expression vector pcDNA3.1$^+$ (Invitrogen Life Technologies, Grand Island, NY), which drives expression via the CMV promoter. Patr-AL contains a methionine at the second position of the leader sequence peptide. A mutated construct was generated to express a threonine at that position (P2T). This mutation causes unstable binding of the leader peptide to HLA-E, resulting in poor cell-surface expression of HLA-E, preventing binding to CD94:NKG2A/C.

Vectors containing FLAG-tagged Patr-AL and HLA-A*02 were generated by inserting a modified 3xFLAG tag (DYKDHDGDYKDHDI-DYKDDDDK) between the signal sequence (encoded by exon 1) and the α_1 domain (encoded by exon 2) by a three-step PCR approach. All amplifications were with 0.2 μM of each primer, 0.2 mM total dNTPs, 1× enzyme buffer, 1.5 mM $MgCl_2$, 2.5 U HotStarTaq *Plus* DNA polymerase (Qiagen, Venlo, the Netherlands). An exon 1 and the first half of the 3xFLAG tag fragment (with 5′ HindIII site) was amplified from a cDNA clone by using primers HindIII-AL-L-KZ-F or HindIII-A0207-L-KZ-F and 3xFLAG-ALL-R (primers listed in Supplemental Fig. 1) with amplification conditions of 5 min at 95˚C, 35 cycles of 30 sec at 94˚C, 30 sec at 62˚C, and 40 sec at 72˚C followed by a final 10-min extension at 72˚C. A second fragment consisting of the second half of the 3xFLAG and exons 2–8 (with 3′ XbaI site) was amplified from a cDNA clone by using primers 3xFLAG-AL-F or 3xFLAG-A-F and XbaI_AL-A_Cyt_R with amplification conditions of 5 min at 95˚C, 35 cycles of 30 sec at 94˚C, 30 sec at 62˚C, and 1 min 10 sec at 72˚C followed by a final 10-min extension at 72˚C. The 3xFLAG primers were designed with a 22-bp overlap allowing them to join during the third PCR step. The two amplified fragments were purified by gel extraction (Qiagen). These two fragments were joined and amplified from 1 μl each of gel-purified PCR product by using primers HindIII-AL-L-KZ-F or HindIII-A0207-L-KZ-F and XbaI_AL-A_Cyt_R with amplification conditions of 5 min at 95˚C, 35 cycles of 30 sec at 94˚C, 1 min 25sec at 62˚C, and 40 sec at 72˚C followed by a final 10-min extension at 72˚C. Purified PCR products consisting of exon1-3xFLAG-exons2–8 were digested with HindIII and XbaI, cloned into pcDNA3.1$^+$, and the sequence determined (MCLAB, South San Francisco, CA).

To mutate specific residues in the transmembrane and cytoplasmic tails of 3xFLAG-tagged-Patr-AL or -HLA-A*02, we performed site-directed mutagenesis (QuikChange Lightning Multi Site-Directed Mutagenesis Kit; Agilent Technologies, Santa Clara, CA) following the manufacturer's protocol. Mutagenesis primers (Supplemental Fig. 2) were designed using Agilent Technologies QuikChange Primer Design Web site (http://www.genomics.agilent.com/primerDesignProgram.jsp) and synthesized by the Protein and Nucleic Acid Core Facility (Stanford University). All constructs were sequenced (MCLAB), using T7 forward and BGH reverse primers, to assess the accuracy of the insert.

Preparation of a mAb specific for native Patr-AL

Patr-AL–specific Abs were generated by immunizing 10 BALB/c mice with soluble complexes of recombinant Patr-AL extracellular domains, β_2m, and the ALDKATVLL peptide. Mice were primed at day 0 i.p. with 100 μg recombinant Patr-AL complexes in CFA (Sigma-Aldrich, St. Louis, MO) and boosted similarly with Ag in IFA (Sigma-Aldrich) on days 14, 28, and 56. Serum Ab titers were measured by ELISA using immobilized recombinant Patr-AL as Ag. The spleen from the mouse having the highest titer of Abs was harvested on day 62, and fusion of splenocytes with FOX-NY myeloma cells (ATCC, Manassas, VA) was performed for 5 min at a 5:1 ratio in PEG-3350 (Roche, Nutley, NJ). Hybridoma cells were cloned by limiting dilution or by single-cell sorting into 96-well plates on a FACSVantage Diva instrument (Becton-Dickinson, Santa Clara, CA) at the Stanford Core FACS facility. Clones were grown in the presence of BALB/c feeder splenocytes in Advanced DMEM (Invitrogen, Carlsbad, CA) supplemented with 20% FetalClone I HyClone (GE Healthcare, Logan, UT), pyruvate (Invitrogen), and L-glutamine (Invitrogen). Hybridoma clones were selected using the hypoxanthine/aminopterin/thymidine supplement (Invitrogen). Seven days after fusion, hybridoma supernatants were screened by ELISA using soluble recombinant Patr-AL–covered plates. The 96 hybridomas giving strongest binding to Patr-AL were chosen for expansion and screening by flow cytometry. In screening, the hybridoma supernatants were tested for binding to HLA class I–deficient 221 cells and to a panel of 221 cell transfectants, each expressing a single human or chimpanzee MHC-A allotype. These comprised human HLA-A*01:01, A*02:01, A*02:07, and A*03:01, and chimpanzee Patr-A*0:402, A*05:01, A*06:01, A*10:01, A*11:01, A*13:01, A*16:01, and A*20:01. mAb 10A5 was found to be the most specific and most sensitive, and was of the IgG1 H chain isotype and the κ L chain isotype. All experiments were approved by Stanford's Administrative Panel on Laboratory Animal Care.

The specificity of the 10A5 mAb was further assessed using the LabScreen Group 1 Luminex assay (One Lambda, Canoga Park, CA) as described previously (10). In this assay, 97 beads, each coated with a different HLA-A, -B, or -C allotype, were tested for binding to 10A5. This panel of HLA allotypes represents a broad range of HLA-A, -B, and -C variants. Although all the bead-coated HLA allotypes bound to W6/32, an Ab that reacts with all HLA class I molecules, none of the 97 HLA-A and -B allotypes bound to 10A5.

Preparation of a polyclonal Ab specific for unfolded Patr-AL

A Patr-AL–specific rabbit polyclonal antiserum (ALpoly) was raised (Anaspec, Fremont, CA) against the synthetic peptide QETQISK-VYAQNDRVN, corresponding to residues 86–101 of Patr-AL. This sequence has the highest divergence from both Patr-A and HLA-A sequences. A cysteine was added to the C terminus of the peptide, which enabled peptide conjugates to be made with keyhole limpet hemocyanin and BSA using hydroxysuccinimide. Antisera were raised in two rabbits according to approved company protocols. The antisera were assayed by ELISA using immobilized peptide as the Ag. The rabbit with higher serum titer was bled and Patr-AL–specific Abs affinity-purified from the serum using immobilized peptide. On Western blots, the resulting polyclonal Ab was shown to be highly specific for Patr-AL, failing to recognize Patr-A.

Cells, cell lines, and transfections

EBV-transformed chimpanzee B cell lines from both Patr-AL$^+$ and Patr-AL$^-$ individuals were generated in our laboratory as described previously (9). Blood samples were obtained from common chimpanzees housed at Yerkes Regional Primate Center (Atlanta, GA). PBMCs were isolated by Ficoll density gradient separation (Ficoll–Paque PLUS; GE Healthcare)

and cryopreserved in 90% heat-inactivated FBS (HI-FBS; Gemini Bio-Products) + 10% DMSO (EMD Millipore, Billerica, MA). Cryopreserved PBMCs were thawed and washed once in complete RPMI medium, resuspended at a concentration of 2×10^6 cells/μl, and allowed to recover overnight (15 h) at 37°C before performing any in vitro experiments.

Individual Patr-AL, HLA-A*02, and mutant cDNAs in the pcDNA3.1$^+$ vector were stably transfected into the MHC-A–, -B–, and -C–deficient cell line 721.221 (subsequently referred to as 221 cells). A total of 2×10^6 221 cells were transfected in 100 μl Cell Line Nucleofector Kit V (Lonza Group, Basel, Switzerland) using program A-024 in a Nucleofector 2b Device (Lonza Group) with 2 μg linearized DNA. Transfected 221 cells were mixed with 500 μl complete RPMI [RPMI 1640 (Gibco; Life Technologies, Grand Island, NY) + 10% HI-FBS, 2 mM L-glutamine, and antibiotics (penicillin 100 U/ml and streptomycin 100 μg/ml; Gibco; Life Technologies)] and 200 μl was plated into 3 wells of a 96-well round-bottom plate. Four weeks later, successfully transfected 221 were expanded and sorted for positive MHC cell-surface expression using the class I–specific Ab W6/32.

HeLa cells (ATCC Cell Lines) were plated in 24-well plates at 5×10^4 cells/well in 500 μl complete DMEM (Gibco; Life Technologies; + 10% HI-FBS, 2 mM L-glutamine, 100 U/ml penicillin, and 100 μg/ml streptomycin) for 24 h. Cells were then transfected with 1 μg of a pcDNA3.1$^+$ vector encoding FLAG-tagged Patr-AL, HLA-A, or mutant allotypes and 3 μl of the FuGENE 6 transfection reagent (Promega, Madison, WI) in 25 μl Opti-MEM (Gibco; Life Technologies) per well. Forty-eight hours after transfection, adherent cells were dissociated from the wells using 200 μl 0.05% trypsin EDTA solution (Gibco; Life Technologies) for staining using a 3xFLAG-specific, FITC-conjugated mAb (M2-FITC; Sigma-Aldrich) and analysis by flow cytometry.

Immunoprecipitation and endoglycosidase H treatment

Patr-AL was immunoprecipitated from stable 221-Patr-AL transfectants with the mAb 10A5, using the Dynabeads Co-Immunoprecipitation Kit (Invitrogen) and the manufacturer's protocol. In brief, 10 μg 10A5 was coupled overnight to 1 mg Dynabeads M-270 Epoxy. For each immunoprecipitation (IP) experiment, 1.5 mg Ab-coupled beads were used to immunoprecipitate Patr-AL from Nonidet P-40 (NP-40) cell lysates of 150 mg cells. Following the recommended washes, samples were subjected to Endoglycosidase H (New England Biolabs, Ipswich, MA) treatment. One thousand units of Endoglycosidase H in G5 buffer was used to digest 5 μl immunoprecipitate at 37°C for 1 h. For protein blotting, samples were heated at 95°C for 5 min, then separated by SDS-PAGE (Bio-Rad, Hercules, CA) and analyzed by Western blot using ALpoly at a concentration of 0.5 μg/ml.

Immunofluorescence and confocal microscopy

221-Patr-AL cells plated at 3.5×10^5 cells/well of a 24-well plate in 500 μl complete RPMI on a 12-mm Round No. 1 German Glass Poly-D-Lysine–coated glass coverslip (BD Biosciences, San Jose, CA) were allowed to attach for 1 h at 37°C. Cells were then fixed with a mixture of 70% methanol and 30% acetone for 10 min on ice followed by permeabilization for 1 min with cold acetone. After washing wells three times with DPBS (containing calcium chloride and magnesium chloride; Life Technologies), cells were blocked for 15 min with cold blocking buffer (DPBS containing 2% heat-inactivated goat serum, 1% BSA, 0.1% cold fish skin gelatin, 0.02% SDS, 0.1% NP-40, and 0.05% sodium azide, pH 7.2). Cells were then stained with 5 μg/ml primary Abs against Patr-AL (ALpoly), Invariant chain (PIN.1; Abcam, Cambridge, U.K.), *cis*-Golgi (GM130; BD Biosciences), or HLA-DR (L243; BD Biosciences) diluted in blocking buffer and incubated overnight at 4°C with gentle agitation. After washing with blocking buffer, cells were incubated with 4 μg/ml goat anti-rabbit IgG Alexa Fluor 488, goat anti-mouse IgG1 Alexa Fluor 555, or goat anti-mouse IgG2a Alexa Fluor 647 (Molecular Probes, Eugene, OR) secondary Abs in blocking buffer for 1 h at 4°C with gentle shaking. Cells were then washed in blocking buffer, followed by DPBS, and coverslips were mounted for microscopy in ProLong Gold antifade reagent (Life Technologies). Secondary Ab specificity was assessed by controls in which primary Ab was omitted.

Cells processed for immunofluorescence were analyzed by confocal laser-scanning microscopy using an upright system (DM6000, SP5; Leica) with an oil immersion objective (63×, 1.3NA; HCX Plan Apochromat; Leica, Solms, Germany) and argon (488) and HeNe (543 and 633) lasers. Images were acquired using LAS AF SP5 software (Leica) in sequential scan mode with a 400-Hz scan rate, line averages of 2, and a 512×512–pixel resolution. Z-stacks were collected at 0.3-μm intervals. The same settings were maintained for all samples within an experiment. Raw images were processed using Volocity (PerkinElmer, Waltham, MA) by applying a fine filter to improve image quality. Quantitative colocalization analysis was performed on processed images by calculating the Pearson's correlation coefficient using the staining intensity of voxels falling within the region of interest identified using the Lasso tool in Volocity. The automatically selected region of interest from individual channels was then overlaid and analyzed. A value of 0 represents no colocalization, whereas −1 represents negative colocalization, and 1 represents positive colocalization.

Flow cytometry

Patr-AL and HLA-A*02 were detected on the surface of stably transfected 221 cells by staining with mAbs 10A5 and BB7.2 (BD Biosciences), respectively, at 5 μg/ml in 50 μl FACS buffer (1 mM EDTA, 1% BSA, and 0.04% azide in PBS). W6/32 (purified in our laboratory) was used at 5 μg/ml as a pan-MHC class I Ab. After three washes with FACS buffer, a goat anti-mouse IgG Alexa Fluor 488 (Molecular Probes) secondary Ab, at a concentration of 4 μg/ml, was used to stain the cells. After three more washes with FACS buffer, cells were resuspended in FACS buffer containing 2 mM propidium iodide (BD Biosciences) and fluorescence measurements were acquired using an Accuri C6 cytometer (BD Biosciences).

To detect intracellular Patr-AL, we fixed 221 transfectants with a mixture of 70% methanol and 30% acetone for 10 min on ice, washed three times with intracellular FACS buffer (IFB: 1% BSA, 2% heat-inactivated goat serum, 0.1% cold fish skin gelatin, and 0.05% sodium azide in PBS at pH 7.2), after which one aliquot of cells was permeabilized for 10 min on ice using IFB supplemented with 0.02% SDS and 0.1% NP-40, and another aliquot was not permeabilized. From this point on, the permeabilized cells were washed with IFB containing NP-40 and SDS, whereas the unpermeabilized cells were washed with IFB only. Fixed and permeabilized cells were then stained with 100 μl 10A5 primary Ab at 5 μg/ml in IFB, washed three times, and subsequently stained with goat anti-mouse IgG Alexa Fluor 488 at 4 μg/ml. After three more washes with IFB, cells were resuspended in IFB containing 2 mM propidium iodide (BD Biosciences) and fluorescence measurements using an Accuri C6 cytometer.

We examined the cell-surface expression of 36 3xFLAG-tagged Patr-AL, HLA-A*02, and individual transmembrane and cytoplasmic tail mutants in HeLa cells (ATCC Cell Lines). Transiently transfected HeLa cells were detached from the wells using 200 μl 0.05% trypsin EDTA solution (Invitrogen), and the reaction was quenched with 1 ml complete RPMI. Detached cells were washed with blocking buffer and stained with 50 μl FITC-conjugated anti-FLAG mouse monoclonal IgG1, M2-FITC (Sigma-Aldrich) at a final concentration of 3 μg/ml in FACS buffer. After Ab staining, cells were washed three times with FB and finally resuspended in FB containing 2 mM propidium iodide and 2% paraformaldehyde. Cells expressing the FLAG-tagged mutants were detected by flow cytometry using an Accuri C6 cytometer (BD Biosciences). Expression levels of each mutant allotype were determined from the average median fluorescence intensity (mfi) of M2-FITC Ab-reactive cells. A minimum of three experiments was performed for each MHC allotype.

Results

Most Patr-AL molecules made by B lymphoblastoid cells do not reach the cell surface

Previously we showed that the Patr-AL protein can be detected in chimpanzee PBMCs and B lymphoblastoid cell lines (BLCL), but at a much lower level than classical MHC class I molecules (9). To facilitate further study of Patr-AL expression, we made mAbs from the B cells of mice immunized with soluble, recombinant Patr-AL. This Ag comprised the extracellular domains of Patr-AL, β_2m, and the nonamer Patr-AL binding peptide ALDKATVLL (8). Of many mAbs obtained, the 10A5 Ab was selected for use in this study because it binds strongly to Patr-AL and exhibits no detectable interaction with other MHC class I (Fig. 1). Thus, 10A5 binds to HLA-A–, -B–, and -C–deficient 221 cells transfected with Patr-AL, but not to untransfected 221 cells or to 221 cells transfected with either HLA-A or Patr-A (Fig. 1A).

The W6/32 Ab recognizes an epitope shared by all human and chimpanzee MHC class I molecules (11). It thus binds to the small amount of HLA-E expressed on the surface of 221 cells (12). Transfection of 221 cells with wild-type Patr-AL, Patr-AL expressing

a modified Leader peptide to prevent increased cell-surface HLA-E expression (P2T), Patr-A, or HLA-A causes cell-surface expression of these MHC class I molecules (Fig. 1B). Transfection of 221 cells with either version of Patr-AL induces an increase in W6/32 binding that is about a third of that seen for Patr-A or HLA-A (Fig. 1B). Binding of these same cell lines with an Ab specific to HLA-E (Fig. 1C) demonstrates that there is not a significant difference of cell-surface HLA-E expression between the two Patr-AL–expressing cell lines. This result shows that unlike HLA-A and Patr-A, the majority of Patr-AL molecules made by the transfected 221 cells do not reach the cell surface. This could arise from intracellular retention, intracellular degradation, or a combination of these factors.

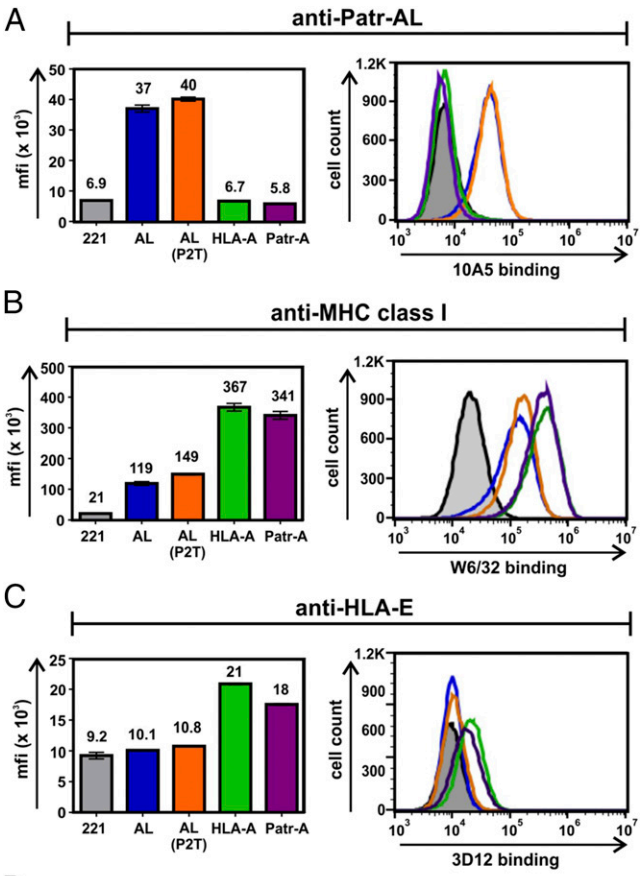

D

Comparison of 10A5 and W6/32 binding to HLA-A, -B and -C

HLA (# allotypes)	Antibody	Range		Mean
		Min	Max	
HLA-A (31)	10A5	10	46	23
	W6/32	22,960	23,612	23,225
HLA-B (50)	10A5	9	71	30
	W6/32	22,002	28,136	23,226
HLA-C (16)	10A5	34	77	49
	W6/32	17,715	23691	21,989

FIGURE 1. Cell-surface expression of Patr-AL is very low compared with HLA-A and Patr-A. (**A**–**C**) Surface staining, with anti–Patr-AL mAb 10A5 (A), anti–MHC class I mAb W6/32 (B), or anti–HLA-E mAb 3D12 (C), of 221 cells (221, shaded gray), and 221 cells transfected with Patr-AL expressing its native Leader peptide (AL, orange), Patr-AL expressing a mutated Leader that abrogates expression of HLA-E (AL [P2T], blue), HLA-A*02:07 (HLA-A, green), and Patr-A*04:02 (Patr-A, purple). Bar graph on the left shows the mfi values obtained for the histograms shown on the right. Error bars indicate SD between two replicates within an experiment. Histograms show staining intensity for intact, live cells. One representative experiment is shown from the three total performed. Not shown are data for 221 transfectants expressing other human (HLA-A*01:01, -A*02:01, -A*02:07, and -A*03:01) and chimpanzee (Patr-A*04:02, -A*05:01, -A*06:01, -A*10:01, -A*11:01, -A*13:01, -A*16:01, and -A*20:01) MHC-A allotypes that have expression levels comparable with the HLA-A*02:07 and Patr-A*24:02 transfectants. (**D**) Summary of the binding reactions of 10A5 and W6/32 Abs to microbeads, individually coated with 1 of 31 HLA-A, 50 HLA-B, and 16 HLA-C allotypes. Ab 10A5 bound to none of the HLA class I allotypes, whereas W6/32 bound to all of them and to similar extent (<15% variation between the beads). Data from at least 100 beads were obtained for each HLA class I allotype.

The exquisite specificity of the 10A5 Ab for Patr-AL is demonstrated by analysis to measure the binding of 10A5 to 97 HLA-A, -B, and -C variants and comparing the results with the binding achieved by W6/32. This analysis was performed by using a panel of Luminex beads, in which each bead is coated with a different HLA class I molecule (13). Whereas the binding of W6/32 to the 97 beads varied between a fluorescence intensity of 17,715 and 28,136, the binding of 10A5 varied between 9 and 77 (Fig. 1D). Thus, none of the 31 HLA-A, 50 HLA-B, and 16 HLA-C allotypes is bound significantly by the anti-Patr-AL mouse mAb 10A5.

Chimpanzee cells and cell lines differ in their expression of cell-surface Patr-AL

Because the *Patr-AL* gene is carried by ~50% of chimpanzee MHC haplotypes, individual chimpanzees can have 0, 1, or 2 copies of the *Patr-AL* gene. B cell lines made from the lymphocytes of four Patr-AL$^-$ chimpanzees and six Patr-AL$^+$ chimpanzees were analyzed by flow cytometry for their capacity to bind the 10A5 Ab (Fig. 2A). Cell lines from the Patr-AL$^-$ chimpanzees did not bind 10A5, whereas a variable but reproducible binding was observed for the cell lines from Patr-AL$^+$ chimpanzees (Fig. 2A). We measured the frequency of 10A5$^+$ cells because the fluorescence staining intensity of the bulk populations were similar. Only a minority of cells bound the 10A5 Ab, the number varying between 1 and 13% of cells. Both Miss Eve and Ericka have two copies of Patr-AL, Miss Eve being homozygous and Ericka being heterozygous (9). Because this information is not known for the other chimpanzee BLCL used in this study, we cannot exclude the possibility of a *Patr-AL* gene dosage effect in augmenting the expression of Patr-AL in Miss Eve and Ericka B cell lines.

Analogous results were obtained when PBMCs from 8 Patr-AL$^-$ chimpanzees and 16 Patr-AL$^+$ chimpanzees were similarly analyzed, but the fraction of cells from Patr-AL$^+$ chimpanzees that stain with 10A5 is <3% (Fig. 2C). In fact, most of the bulk PBMC populations we analyzed contained <1% of cells staining positive for 10A5, a value that is well within the background of the gating strategy used for this analysis. To test the possibility that Patr-AL was enriched in a particular subset of PBMCs, we performed immunophenotyping experiments where we identified T cells, B cells, NK cells, monocytes, and granulocytes, but did not observe such enrichment (data not shown). Chimpanzee PBMCs were also stimulated in vitro with the cytokine IFN-γ, a compound known to upregulate MHC class I expression, and with a potent polyclonal T cell stimulator, the superantigen staphylococcal enterotoxin A, to determine whether an upregulation of cell-surface Patr-AL could be detected. In vitro stimulation of chimpanzee PBMCs with IFN-γ or staphylococcal enterotoxin A at different concentrations for 48 h did not result in an increase in cell-surface Patr-AL (data not shown). Despite the reduced levels of cell-surface Patr-AL on chimpanzee BLCL and PBMCs, these cells do express a constitutive level of classical class I molecules on their cell surface (Fig. 2B, 2D), as expected. These results clearly show that Patr-AL, unlike classical MHC class I, is not constitutively expressed at cell surfaces.

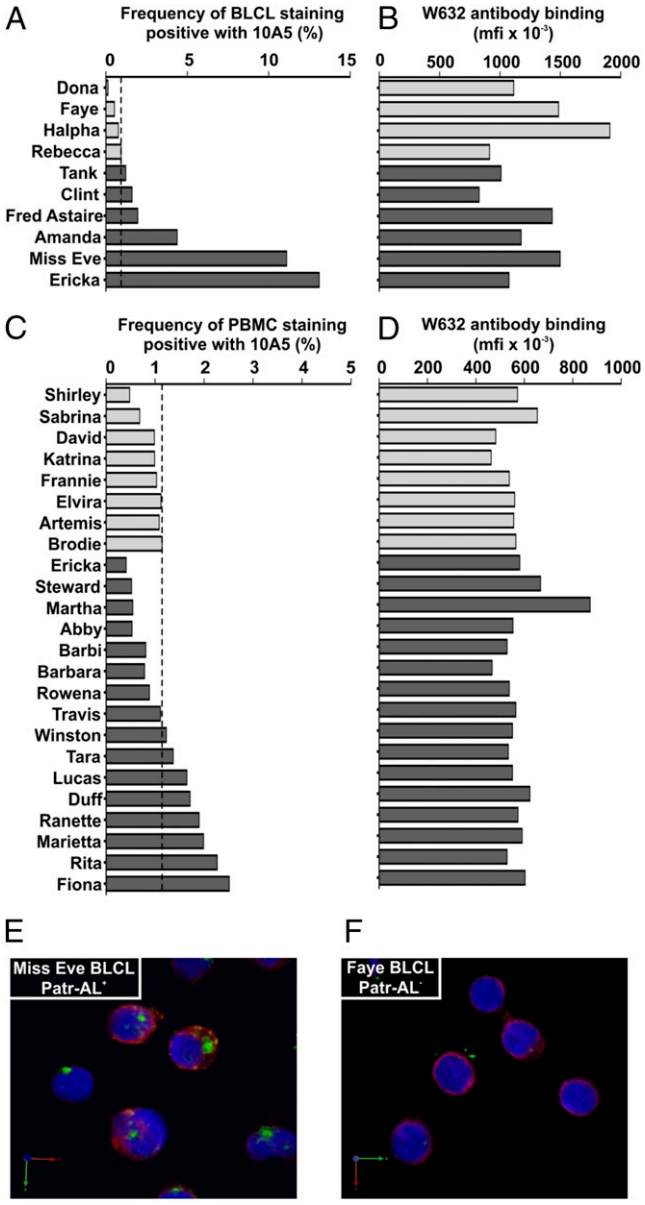

FIGURE 2. Patr-AL is not expressed constitutively on cell surfaces. (**A** and **B**) Cell-surface staining and flow-cytometric analysis of 10 BLCL derived from chimpanzee peripheral blood B cells. Cells were stained with Patr-AL–specific Ab 10A5 (A) and pan MHC class I–specific Ab W6/32 (B). For 10A5 staining (A), the bars show the frequency of Ab-binding intact, live cells. For W6/32 staining (B), the bars show mfi staining of the intact, live cells. Light gray shaded bars denote BLCL derived from chimpanzees that lack the *Patr-AL* gene; dark gray shaded bars denote BLCL derived from chimpanzees that carry the *Patr-AL* gene. (**C** and **D**) Shown are analyses comparable with those depicted in the upper panels but performed on samples of PBMCs obtained from 24 chimpanzees. (C) Frequency of cells staining for Patr-AL with the 10A5 Ab. (D) The mfi of staining for MHC class I as detected with the W6/32 Ab. (**E** and **F**) Multicolor immunofluorescence staining and confocal microscopy of chimpanzee BLCL derived from a Patr-AL$^+$ individual, Miss Eve (E) and a Patr-AL$^-$ individual, Faye (F) fixed with 70% methanol 30% acetone and stained with various Abs. Patr-AL was stained with ALpoly (green). The specificity of ALpoly was confirmed by the negative staining of 221 cells (data not shown) and BLCL derived from a Patr-AL$^-$ donor. Invariant chain was stained with the PIN.1 mAb, which identifies the ER and early ER-derived vesicles of the endolysosomal system (red). TOTO-3 (blue) is used as a nuclear counterstain. Original magnification ×63.

To determine whether endogenous Patr-AL could be detected intracellularly, we used immunofluorescence staining and high-resolution confocal microscopy to detect Patr-AL in chimpanzee BLCL derived from Miss Eve (Fig. 2E) or Faye (Fig. 2F). In these experiments, Patr-AL was detected using ALpoly. This Ab, which was raised against a synthetic peptide corresponding to residues 86–101 of the Patr-AL α_1 and α_2 domains, recognizes both native and denatured Patr-AL (see *Materials and Methods*). As a marker of the endoplasmic reticulum (ER), we used an Ab specific for the cytoplasmic tail of the MHC class II invariant chain. This Ab marks the ER and early secretory pathway, because the cytoplasmic tail becomes degraded when the invariant chain traffics from the secretory pathway to an endosomal compartment (14). A signal specific for Patr-AL is detected intracellularly in BLCL from a Patr-AL$^+$ donor, whereas no signal is detected in the BLCL derived from the Patr-AL$^-$. These results suggest that Patr-AL is intracellularly localized.

Patr-AL is synthesized and sequestered inside B lymphoblastoid cells

For Patr-AL and HLA-A*02, which have remarkably similar structures and peptide-binding specificities (8), we compared the distribution of molecules between the cell surface and intracellular compartments (Fig. 3). Transfected 221 cells expressing Patr-AL or HLA-A*02, under the control of the same promoter, were tested for binding 10A5 (Fig. 3A) and the HLA-A*02–specific Ab BB7.2 (Fig. 3B). Consistent with these specificities, the Patr-AL transfectant bound 10A5, but not BB7.2, whereas the HLA-A*02 transfectant bound BB7.2, but not Patr-AL. Furthermore, the cell-surface binding to Patr-AL by 10A5 (Fig. 3A) was only 6% that of HLA-A*02 to BB7.2 (Fig. 3B). Aliquots of transfected 221 cells were either fixed or first fixed and then permeabilized before staining with the 10A5 and BB7.2 Abs, to assess the relative amounts of intracellular Patr-AL and HLA-A*02. Permeabilization dramatically increased the specific binding of 10A5 to the Patr-AL–transfected cells (Fig. 3C), but did not similarly affect the binding of BB7.2 to HLA-A*02 (Fig. 3D). Thus, although similar amounts of Patr-AL and HLA-A*02 are made by the transfectants, because both are generated by expression under the control of the strong CMV promoter, >90% of HLA-A*02 is delivered to the cell surface, whereas >90% of Patr-AL is sequestered within the cell.

Patr-AL is retained within cells at an early stage in the secretory pathway

To identify the intracellular sites where Patr-AL is sequestered, we used immunofluorescence staining and high-resolution confocal microscopy to compare the intracellular distribution of Patr-AL with those of well-characterized intracellular markers. A significant colocalization of Patr-AL with the invariant chain was observed (Fig. 4A), showing a retention of Patr-AL in the ER and early secretory pathway. In contrast, there was little colocalization of Patr-AL with the mature MHC class II molecules detected by the L243 mAb (Fig. 4B), most of which are not associated with the invariant chain (Fig. 4C). Also observed was colocalization of Patr-AL with the Golgi matrix protein GM130, a *cis*-Golgi marker (Fig. 4D), but to lesser extent (~45%) than the colocalization of Patr-AL with invariant chain (Fig. 4A), suggesting that most of the intracellular Patr-AL is localized to the ER. Consistent with the results of flow cytometry (Fig. 1A), a small amount of Patr-AL was visualized on the cell surface in analysis of transient HeLa transfectants by microscopy (Supplemental Fig. 3). These results therefore show that, whereas small amounts of Patr-AL are observed on cell surfaces, most of the cellular Patr-AL is retained within the cell, mostly in the ER and to a lesser degree in the *cis*-Golgi.

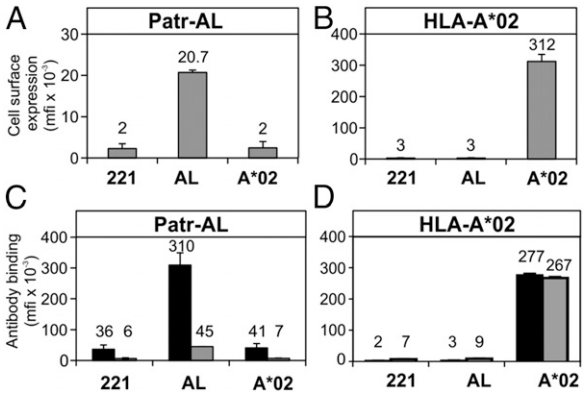

FIGURE 3. Transfected cells make comparable amounts of Patr-AL and HLA-A*02, but Patr-AL mainly stays inside the cell, whereas HLA-A*02 goes to the surface. Flow-cytometric analysis of 221 cells (221), 221 transfectants expressing Patr-AL (AL), and 221 transfectants expressing HLA-A*02:07 (A*02) after staining with anti–Patr-AL (10A5) and anti–HLA-A*02 (BB7.2) mAbs. (**A**) and (**B**) show cell-surface staining for Patr-AL (A) and HLA-A*02 (B). Bars give the mfi values of positively staining intact, live cells. Error bars represent SD between mfi shown for the data from three replicate experiments. (**C**) and (**D**) compare the amounts of Patr-AL (C) and HLA-A*02 (D) that are at intracellular and cell-surface locations. Because of the different physicochemical properties of the 10A5 and BB7.2 Abs, different protocols were used to detect their epitopes. For 10A5 staining (C), cells were fixed with 70% methanol 30% acetone, after which one aliquot of cells was permeabilized with cold acetone and the other was not. The cells were then stained with 10A5 and analyzed by flow cytometry. For BB7.2 staining (D), transfectants were fixed with 4% paraformaldehyde, after which one aliquot of cells was permeabilized with 0.04% saponin in FACS buffer and the other was not. The cells were then stained with the BB7.2 Ab and analyzed by flow cytometry. (C and D) Gray bars give the staining of nonpermeabilized cells, and black bars show the staining of the permeabilized cells. Error bars show the SD in mfi for data from three replicate experiments.

To confirm the results of the microscopy experiments, we examined the maturity of the oligosaccharide attached to N86 of Patr-AL, and hence whether Patr-AL has undergone posttranslational modification upon trafficking through the Golgi apparatus. IP of Patr-AL with the 10A5 Ab was performed on lysates prepared from 221 cells and 221 cells transfected with Patr-AL. The precipitates were treated with endoglycosidase H, which removes immature, but not mature, N-linked oligosaccharides and then subjected to SDS-PAGE and Western blotting using ALpoly. Analysis of the immunoprecipitates (Fig. 4E, *left panel*), as well as whole cell lysates (Fig. 4E, *right panel*), show that Patr-AL was detected, as expected, only in the Patr-AL–transfected cells. On treatment with endoglycosidase H, most, but not all, of the Patr-AL H chains were reduced in m.w. and were thus sensitive to the enzyme (Fig. 4E, *left panel*). This, in turn, shows that most, but not all, Patr-AL molecules carry an immature N-linked oligosaccharide. This result is consistent with intracellular Patr-AL molecules being sequestered principally in the ER and secondarily in the *cis*-Golgi.

To determine whether Patr-AL molecules travel to endolysosomal compartments, we examined lysosomes, late endosomes, and compartments containing mature MHC class II for the presence of Patr-AL. Patr-AL–transfected 221 cells were stained with ALpoly, monoclonal MHC class II–specific L243, and an mAb specific for Lamp-1, a marker of late endosomes and lysosomes (Fig. 4F). The extent of the colocalization among the three markers was quantified. A good correlation was observed between the presence of Lamp-1 and HLA-DR, but no correlation between the presence of Patr-AL and either Lamp-1 or HLA-DR (Fig. 4G). As is well established (15), we find that mature MHC class II molecules do travel to endolysosomal compartments. In contrast, we find no evidence for the movement of Patr-AL molecules from the ER to endolysosomal compartments during steady-state conditions. In conclusion, these experiments (Fig. 4) demonstrate that Patr-AL is actively retained at an early stage of the secretory pathway, which is predominantly in the ER but also includes the *cis*-Golgi.

In some circumstances, proteins that are retained in the ER can be brought to the cell surface by reducing the temperature to <37˚C (16, 17). To test this possibility for Patr-AL, we subjected 221 transfectants expressing Patr-AL or HLA-A*02 to overnight culture at temperatures ranging from 21 to 37˚C. The expression of Patr-AL and HLA-A*02 was then determined by flow cytometry using the 10A5 and BB7.2 Abs, respectively. Over this temperature range, there was no difference in the cell-surface expression of HLA-A*02. In contrast, for Patr-AL we observed a trend in which there was an increase by 31% of cell-surface expression as the temperature was lowered from 37 to 27˚C, which then reversed as the temperature was further lowered to 21˚C (Fig. 5).

The distinctive cytoplasmic tail of Patr-AL is a cause of intracellular retention

One mechanism used to retain transmembrane proteins inside cells involves sequence motifs in the cytoplasmic tail that are bound by tethering or adaptor proteins (18–20). In examining the sequence of the Patr-AL cytoplasmic tail, we found a modified tyrosine-based sorting signal, YFQA at positions 320–323, which would potentially affect endocytosis or *trans*-Golgi network sorting, but no dileucine-based endocytic protein sorting motifs, none of which would be relevant to the localization of Patr-AL in the early secretory pathway. Comparing the cytoplasmic tail sequences of MHC class I molecules from different species identified four residues (F321, N326, S329, and E333) that appear unique to Patr-AL (Fig. 6A, Supplemental Fig. 4). Moreover, these are the only four residues that distinguish the cytoplasmic tails of Patr-AL and HLA-A*02. Remarkably, this combination of residues found in Patr-AL's cytoplasmic tail is unique to Patr-AL and not found in cytoplasmic tail sequences of the known Patr-AL orthologs (8), HLA-Y, Gogo-OKO, and Popy-A, nor in any other characterized MHC class I molecule (Supplemental Fig. 4). We therefore hypothesized that one or more of these four residues contribute to the intracellular retention and low cell-surface expression of Patr-AL.

To test this hypothesis, we made Patr-AL and HLA-A*02 mutants in which their cytoplasmic tails were swapped, the prediction being that mutant Patr-AL with the HLA-A*02 tail would have higher cell-surface expression, whereas mutant HLA-A*02 with the Patr-AL tail would have lower cell-surface expression. Stable 221 transfectants expressing the two recombinant mutants and the two parental molecules were tested for their capacity to bind Patr-AL–specific 10A5 and HLA-A*02–specific BB7.2. Expression of the Patr-AL mutant with the HLA-A*02 tail was 5.0-fold higher than that of Patr-AL (Fig. 6B). Similarly, the cell-surface expression of HLA-A*02 was 4.5-fold that of the HLA-A*02 mutant with the Patr-AL tail (Fig. 6C). These results were recapitulated by high-resolution confocal microscopy analysis of transient HeLa transfectants (Supplemental Fig. 3). These results demonstrate that one or more of the four substitutions that distinguish the cytoplasmic tails of Patr-AL and HLA-A*02 contribute to the differential cell-surface expression of these two MHC class I molecules. However, these differences can account for only approximately one third of the 13.4-fold difference in the expression of HLA-A*02 and Patr-AL in 221 transfectants

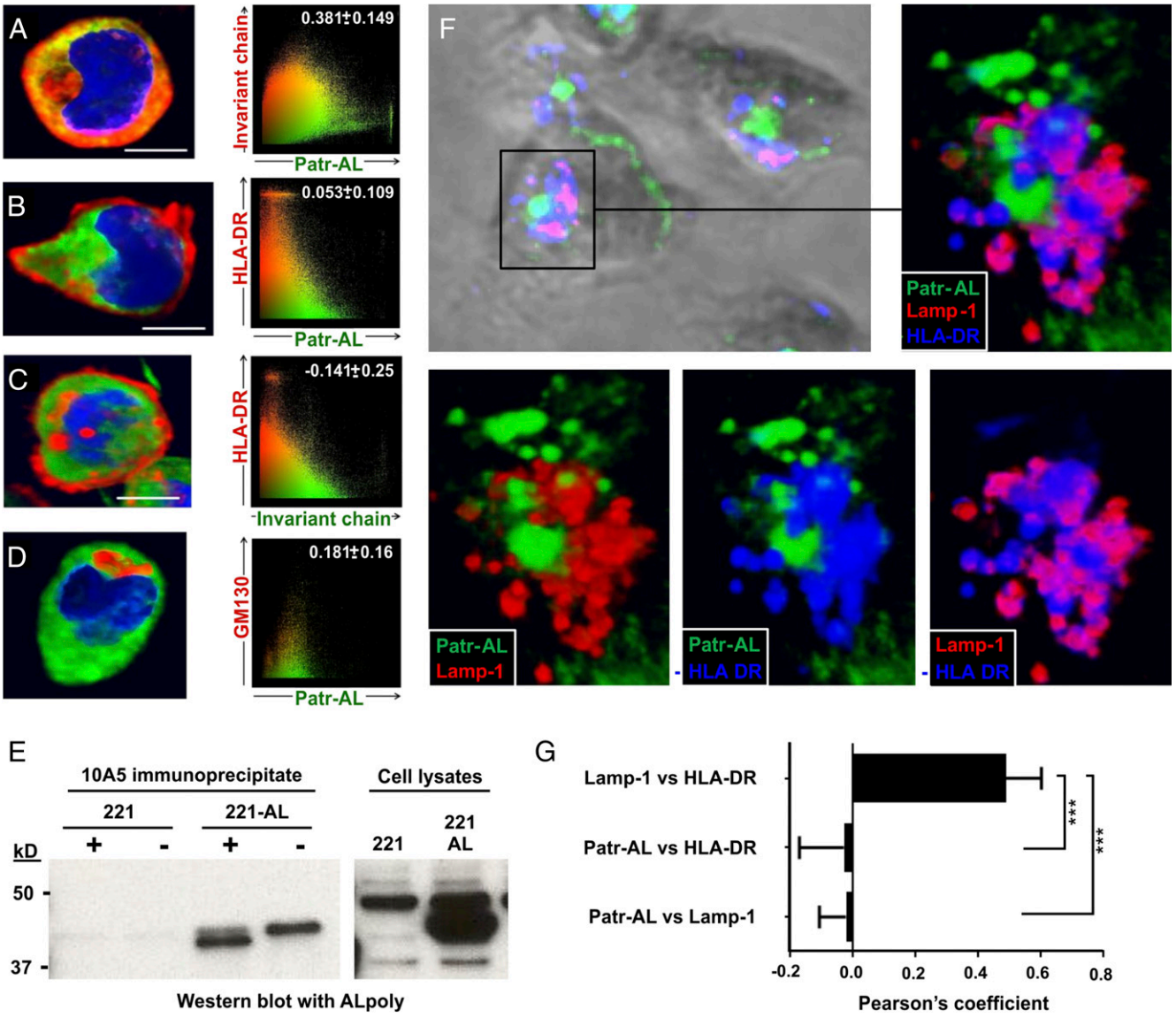

FIGURE 4. Patr-AL concentrates in the ER and the *cis*-Golgi. (**A**–**D**) Multicolor immunofluorescence staining and confocal microscopy of 221-Patr-AL transfectants (*left panels*) fixed with 70% methanol 30% acetone and stained with various Abs. Patr-AL was stained with ALpoly. The specificity of ALpoly was confirmed by the negative staining of 221 cells (data not shown). HLA-DR is stained with the L243 mAb, which recognizes mature class II molecules that lack the invariant chain. Invariant chain is stained with the PIN.1 mAb. Golgi matrix protein of 130 kDa is stained with the GM130 mAb. The *right panels* are scattergrams showing the quantitative colocalization analysis of pairs of markers. Numbers in the scattergram are Pearson's correlation coefficient values for the indicated channels (1 = perfect colocalization, 0 = no colocalization, −1 = negative colocalization) as averaged from analysis of 50 cells. Scale bar, 5 μm. For (A)–(D), blue represents DNA. (**E**) Patr-AL was immunoprecipitated from Patr-AL–transfected 221 cells (221-AL) using the 10A5 Ab and the Dynabeads Co-Immunoprecipitation Kit (Invitrogen). 221 cells served as the negative control. Immunoprecipitates were treated with Endoglycosidase H (1000U) (+) or not (−), and analyzed by SDS-PAGE on a 4–15% gradient gel. Western blotting was performed using ALpoly to detect Patr-AL (*left panel*). For comparison, total lysates of 221 and 221-AL cells were similarly analyzed by SDS-PAGE and Western blotting (*right panels*). (**F**) Multicolor immunofluorescence staining and confocal microscopy of 221 cells transfected with Patr-AL. Cells were fixed (as described earlier) and simultaneously stained with ALpoly (green), anti-lysosomal and anti-late endosomal marker, Lamp-1 (red), and HLA-DR (blue). The Lamp-1$^+$ and HLA-DR$^+$ compartments within each cell were analyzed by quantitative colocalization analysis of pairwise comparisons for each of the three channels imaged. Pink color shows overlap of red and blue staining. (**G**) From the data illustrated in (F), mean values for Pearson's correlation coefficient were calculated from pairwise comparisons of fluorescence intensity measurements, of 20 cells, from each of the 3 channels imaged. Error bars represent SD between average Pearson's correlation coefficient values for the 20 cells sampled. ***$p < 0.0001$.

(Fig. 1C). Thus, substitutions in other domains of the Patr-AL and HLA-A*02 proteins are also implicated in altering cell-surface expression.

The four residues that distinguish the cytoplasmic tail of Patr-AL all act to reduce cell-surface expression

To determine the effects of the four substitutions that distinguish the cytoplasmic tails of Patr-AL and HLA-A*02, we made sets of 16 Patr-AL and 16 HLA-A*02 mutants that represent all possible combinations of the dimorphisms at positions 321, 326, 329, and 333. To facilitate comparison of the cell-surface expression of these mutants, we included 3xFLAG epitopes at the N terminus of each mutant and parental allotype. These constructs were transiently transfected into HeLa cells and their cell-surface expression assessed by flow cytometry using the M2 mAb that recognizes the 3xFLAG epitope (Fig. 7).

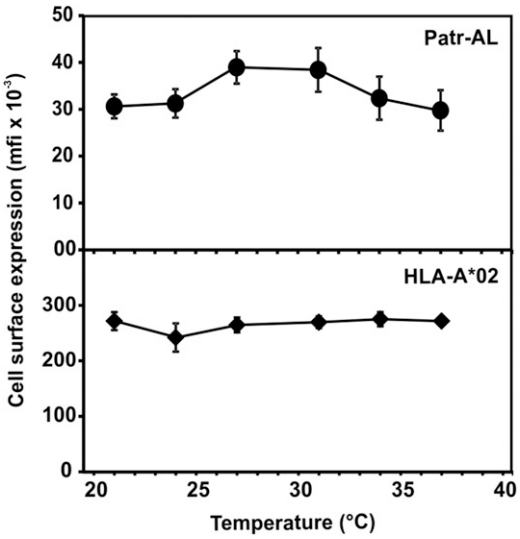

FIGURE 5. Cell-surface expression of Patr-AL, but not HLA-A*02, is temperature sensitive. 221 cells transfected with Patr-AL (*upper panel*) and HLA-A*02 (*lower panel*) were cultured in complete RPMI medium and incubated for 16 h at various temperatures from 21 to 37°C. Cell-surface expression of Patr-AL (10A5) and HLA-A*02 (BB7.2) were subsequently assayed by Ab staining and flow cytometry. The average mfi values for positively staining, live cells are plotted. Error bars represent SD between mfi shown for the data from three replicate experiments.

The cytoplasmic tail of Patr-AL is distinguished by F321, N326, S329, and E333. We compared the expression levels of Patr-AL cytoplasmic tail mutants upon stepwise mutagenesis from an HLA-A*02 (*right* of each panel in Fig. 7) with a Patr-AL cytoplasmic tail (*middle* of each panel in Fig. 7). The results from the subset of Patr-AL mutants shown in Fig. 7A allow us to assess how each individual residue influences the cell-surface expression of Patr-AL. F321 has the strongest impact, accounting for ~50% of the effect in reduced surface expression of the Patr-AL tail. The other 50% is due to lesser contributions from the residues at positions 326, 329, and 333. Among the six combinations of two-residue mutants, F321 and E333 give the greatest effect (Fig. 7B), whereas among the four possible mutants combining three of the residues, it is the combination of F321, S329, and E333 that is most effective (Fig. 7C). However, none of these mutants is as effective as the combination of all four residues present in the cytoplasmic tail of Patr-AL. Thus, for Patr-AL, although phenylalanine at position 321 plays a dominant role in the decrease of Patr-AL surface expression, each of the four Patr-AL cytoplasmic tail–specific residues have all made contributions in reducing the cell-surface expression of Patr-AL.

In similar analysis of the four substitutions that distinguish the HLA-A*02 cytoplasmic tail from that of Patr-AL, the presence of either S321, A329, or D333 is sufficient to restore cell-surface expression to a level that is greater or equal to that of HLA-A*02. Also, the presence of S326 achieves 92% of wild-type HLA-A*02 expression (Fig. 7C). Although individually the four residues have positive effects, in combinations they have more varied effects. Thus, the combination of S321, S326, and D333 causes little increase of HLA-A*02 cell-surface expression over that seen with the full Patr-AL cytoplasmic tail mutant of HLA-A*02 (Fig. 7A), and the combinations of either S326 or A329 with D333 also have small effects (Fig. 7B). In contrast, several combinations of residues raise the level of cell-surface expression much more than that of HLA-A*02 (Fig. 7A). Thus, there are antagonistic and synergistic effects between the residues at positions 321, 326, 329, and 333 in HLA-A*02. These results suggest that for both Patr-AL and HLA-A, whereas polymorphisms in cytoplasmic tail residues contribute to differences in cell-surface expression, other factors simultaneously regulate their surface expression.

Natural sequence variation in the transmembrane domain influences cell-surface expression

Because multiple factors are implicated in reducing cell-surface expression of Patr-AL, we investigated the effect of the single amino acid difference that distinguishes the transmembrane domains

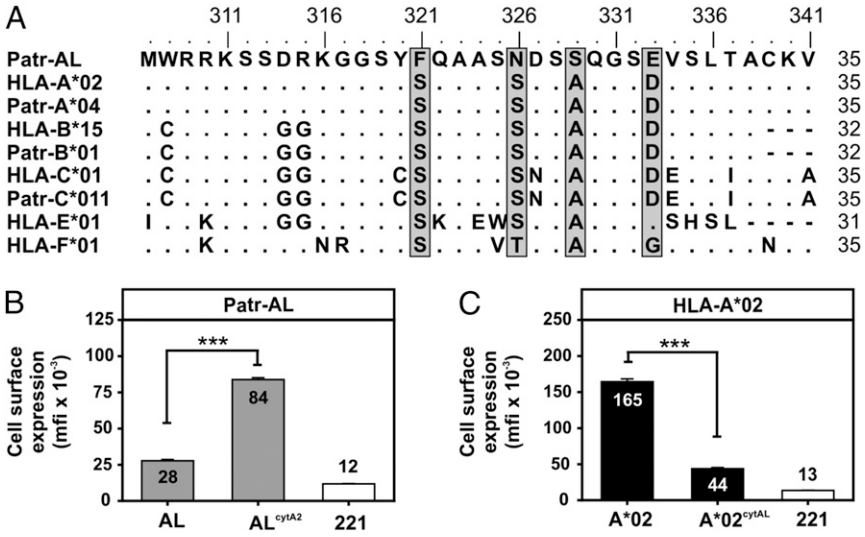

FIGURE 6. Unique features in the cytoplasmic tail contribute to the intracellular retention of Patr-AL. (**A**) Amino acid sequence alignment of the cytoplasmic tails from Patr-AL and other human and chimpanzee MHC class I molecules. Shaded gray are positions 321, 326, 329, and 333 where Patr-AL has a unique combination of amino acid residues. (**B**) 221 cells transfected with either Patr-AL (AL) or a mutant of Patr-AL (AL^{cytA2}) having the cytoplasmic tail of HLA-A*02 were stained with anti–Patr-AL Ab (10A5) and analyzed by flow cytometry. (**C**) 221 cells transfected with HLA-A*02 (A*02) or a mutant of HLA-A*02 (A*02^{cytAL}) having the cytoplasmic tail of Patr-AL were stained with anti–HLA-A*02 Ab (BB7.2) and analyzed by flow cytometry. For 10A5 binding (B) and BB7.2 binding (C) the average mfi value of cells is plotted. Error bars represent the SD between mfi for the data from three replicate experiments. ***$p \leq 0.0005$.

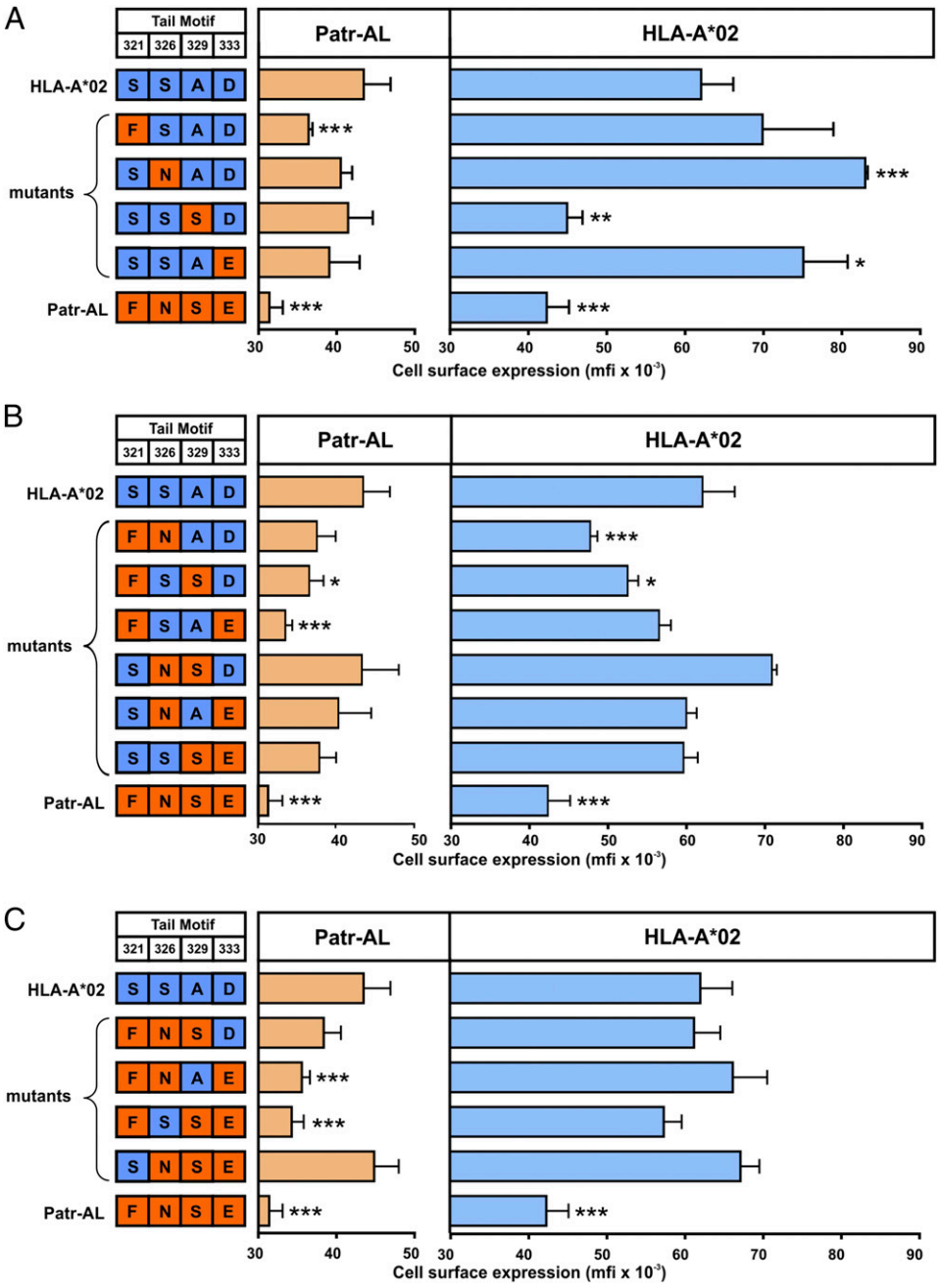

FIGURE 7. The four residues that distinguish the cytoplasmic tail of Patr-AL all contribute to the intracellular retention of Patr-AL. Patr-AL, HLA-A*02:07, and mutants of them that represent all 16 combinations of the natural polymorphisms at positions 321, 326, 329, and 333 were transiently transfected into HeLa cells. Each wild-type and mutant contained 3xFLAG epitopes at the N terminus that enabled their surface expression to be compared using the anti-3xFLAG Ab and flow-cytometric analysis. Within each panel, a subgroup of the mutants are compared with the Patr-AL full tail mutant (*middle panels*) and wild-type HLA-A*02 (*right panels*). Shown in the *left panels* are the sequence motifs at positions 321, 326, 329, and 333 shared by the Patr-AL and HLA-A*02 paired in each row. Orange boxes denote residues naturally occurring in Patr-AL; blue boxes denote residues naturally occurring in HLA-A*02. (**A**) Mutants have one residue shared with Patr-AL and three with HLA-A*02. (**B**) Mutants have two residues shared with Patr-AL and two with HLA-A*02. (**C**) Mutants have three residues shared with Patr-AL and one with HLA-A*02. In each panel, the horizontal bars give the levels of cell-surface expression as mfi. At least three replicates were analyzed for each mutant. Values that are statistically different from the HLA-A*02 cytoplasmic tail are: $***p < 0.0001$, $**p < 0.0005$, $*p < 0.005$. These values were calculated by one-way ANOVA for each pairwise comparison.

of Patr-AL and HLA-A. At position 295, Patr-AL has valine and HLA-A*02 has glycine. Mutants were made, in which these residues were swapped and analyzed using the same methods applied to the cytoplasmic tail mutants (Fig. 8).

The substitution of valine for glycine at position 295 in Patr-AL has no significant effect on cell-surface expression. Neither did polymorphism at position 295 affect cell-surface expression of the Patr-AL mutant that has the cytoplasmic tail of HLA-A*02 (Fig. 8). In contrast, mutating residue 295 from glycine to valine in HLA-A*02 increases the surface expression by 30%. This effect is not seen in the HLA-A*02 mutant that has both the transmembrane domain and the cytoplasmic tail of Patr-AL, and that gives identical cell-surface expression to HLA-A*02. However, the HLA-A*02 mutant with just the Patr-AL cytoplasmic tail has expression reduced by 32% (Fig. 8). These results demonstrate that in contrast with Patr-AL, in HLA-A, both the transmembrane and cytoplasmic tail residues play a role in surface expression. This suggests that the cell-surface expression of Patr-AL and HLA-A*02 is regulated by two different mechanisms and further establishes how natural substitutions in the transmembrane domain and cytoplasmic tail can antagonize or synergize in determining the level of cell-surface expression of MHC class I molecules (Fig. 9).

Discussion

To study the expression of Patr-AL, we made a specific mAb that binds to Patr-AL with high specificity but does not react with other human or chimpanzee MHC class I molecules. This Ab binds at a low level to small numbers of PBMCs. Greater surface expression of Patr-AL occurs when human class I–deficient 221 cells are transfected with *Patr-AL* expressed under control of the CMV promoter. For this reason, we used 221 transfectants to examine the cell-surface expression and intracellular distribution of Patr-AL. A minority of Patr-AL molecules are detected at the cell

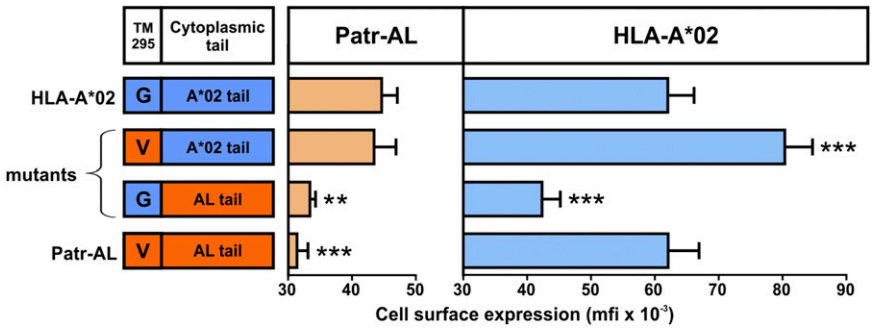

FIGURE 8. Natural variation at position 295 of the transmembrane region affects expression of HLA-A*02, but not Patr-AL. Patr-AL and HLA-A*02:07 differ at position 295 in the transmembrane region, as well as at four positions in the cytoplasmic domain. For both Patr-AL and HLA-A*02, mutants were made to give all combinations of the transmembrane region and cytoplasmic domain. Mutant construction, analysis of cell-surface expression, and calculation of significance values were as described in the legend for Fig. 7. At least three replicates were analyzed for each mutant. ***$p < 0.0001$, **$p < 0.0005$.

surface (~10%), the majority being retained inside the cell within the ER and the *cis*-Golgi. This behavior contrasts with HLA-A*02, which is predominantly expressed at the cell surface. That a substantial majority of Patr-AL molecules are located within cells could explain, at least in part, the small amounts of Patr-AL detected on the surface of PBMCs. In addition, the Patr-AL promoter could limit the extent of transcription in the cells in which Patr-AL is transcribed, but this has yet to be investigated.

The retention of Patr-AL in early compartments of the secretory pathway is likely to be an active process and one that could be critical to its immunological function. Precedents for the intracellular retention of MHC class I molecules are provided by human MR1 and mouse Qa-1 (21–23). MR1 binds to the vitamin B metabolites released by bacteria and yeast-infecting mucosal tissue (24). On binding such Ags, MR1 moves to the cell surface where it is recognized by mucosal-associated T cells. Qa-1 monitors Ag processing in the ER by being sensitive to a self-peptide

MHC class I molecule	Length of cytoplasmic tail	Location of motif in cytoplasmic tail	Type of motif
MICA*001	45	E E L V Q V L D Q H P V G D D L G F Q P D	Dihydrophobic basolateral sorting motif [28]
CD1d	14	T F K R S Y Q G V L	Threonine-based cell surface targeting motif [38]
		T F K R S Y Q G V L	Tyrosine-based endosomal targeting motif [39]
CD1c	14	V F K K S Y Q D I L	Tyrosine-based endosomal targeting motif [39]
CD1b	14	A Y M R S Y Q N I P	Tyrosine-based endosomal targeting motif [39]
CD1a	10	A F R K F C	-
HLA-G	8	L K K S	Dilysine ER retrieval motif [42]
HLA-F	35	M K K S R N R G S Y S Q A T A G V S L T V	RxR motif forward transport motif [40]
		M K K S R N R G S Y S Q A T A G V S L T V	Tyrosine-based endosomal targeting motif [41]
		M K K S R N R G S Y S Q A T A G V S L T V	C-terminal valine ER export motif [40]
HLA-E	31	I K K S G K G G S Y S K A S A E S H S L	Tyrosine-based endosomal targeting motif [41]
HLA-C*01	35	M R K S G K G G S C S Q A S A D E S L I A	Dihydrophobic internalization motif [27]
		M R K S G K G G S C S Q A S A D E S L I A	Lysosomal targeting motif [27]
HLA-A*02	35	M R K S R K G G S Y S Q A S A D V S L T V	Tyrosine-based endosomal targeting motif [41]
Patr-AL	35	M R K S R K G G S Y F Q A N S E V S L T V	Tyrosine-based endosomal targeting motif [41]
	35	M R K S R K G G S Y F Q A N S E V S L T V	Patr-AL-specific motif

310 315 321 326 329 333 335 340

Position numbers refer to the Patr-AL sequence

FIGURE 9. The cytoplasmic tails of MHC class I molecules contain sorting motifs that contribute to their patterns of intracellular trafficking. The cytoplasmic tail sequence and motif contents are compared among Patr-AL and human MHC class I molecules. Cytoplasmic tails of MHC class I molecules differ in length and in their contents of intracellular sorting motifs. All sorting motifs are shaded gray, with the exception of the Patr-AL–specific motif, which is shaded light orange. Functionally important residues within each motif are colored red. One motif is highlighted per tail sequence. Numbers on the scale represent the position within the cytoplasmic tail of Patr-AL. References for each motif described are also noted (27, 28, 38–42).

called FL9 that accumulates only when the ER-resident aminopeptidase malfunctions (23). On binding to FL9, Qa-1 is released from the ER and translocates to the cell surface where it is recognized by cytotoxic T cells that kill the defective cell (23). Both the examples of MR1 and Qa-1 retention rely on the unavailability of their ligands. Although peptides that can be presented by Patr-AL are similar to those presented by HLA-A*02 (7), and are therefore readily available, it is still possible that Patr-AL may preferentially bind some type of modified peptide. To this end, the unusually electropositive patch on the α_2 domain of Patr-AL is notable (7). We speculate that Patr-AL binds an electronegative macromolecule that is normally not available in the ER.

Underlying the intracellular retention of Patr-AL are four amino acid substitutions that distinguish the cytoplasmic tails of Patr-AL and HLA-A*02. This was first appreciated by swapping the cytoplasmic tails of Patr-AL and HLA-A*02, and further dissected by mutagenesis at the four positions (321, 326, 329, and 333) that distinguish the two tails. In Patr-AL, each of the four residues acts to decrease cell-surface expression, suggesting a stepwise evolution that was driven by a continued process of selection for intracellular retention. The FNSE motif of Patr-AL is not shared with any other known MHC class I molecule. In hominoid MHC class I, N326 and E333 both occur, but not together. In Old World Monkey MHC class I molecules (Supplemental Fig. 4), all four residues occur, but no more than two in any particular MHC class I variant. Residues F321, N326, and E333 occur in Old World Monkey MHC-B, and S329 is present in MHC-E (Supplemental Fig. 4). In fact, all four residues of the Patr-AL motif are distributed among the MHC-E molecules of the simian primates (Supplemental Fig. 4). This observation and knowledge that HLA-E is probably the oldest of the expressed MHC class I genes in simian primates (25, 26) raise the possibility that the FNSE motif first evolved at the MHC-E locus and was subsequently introduced into Patr-AL by recombination or gene conversion.

A variety of motifs that determine the intracellular movements and localization of MHC class I molecules have been identified (18) (Fig. 9). For example, the cytoplasmic tail sequence of the classical MHC class I HLA-C contains a dihydrophobic internalization and lysosomal targeting signal (27) that contributes to its low cell-surface expression, when compared with HLA-A and HLA-B. Cytoplasmic tails can also contain motifs essential for the protein's function and localization, such as the dihydrophobic motif in the cytoplasmic tail of MIC-A that determines its basolateral sorting (19, 28). The FNSE motif of Patr-AL involves different residues and is nonoverlapping with other motifs (Fig. 9). Thus, the cytoplasmic tail of Patr-AL is seen to contain a unique sequence motif that is implicated in limiting cell-surface expression. It is also notable that a single amino acid difference in the transmembrane domain has some contribution to the limitation of Patr-AL expression, and that lowering the temperature of cells can partially induce Patr-AL expression. Thus, in addition to the strong retention motif defined, other features, such as interaction with accessory molecules and/or peptide binding, could contribute to Patr-AL expression.

The cytoplasmic tails of HLA class I molecules are targets for viral proteins that subvert HLA class I function, and thus prevent elimination of virus-infected cells by cytotoxic CD8 T cells (29). For example, the BILF1 protein of EBV prevents Ag-presenting HLA class I molecules from reaching the cell surface by directing them to lysosomes for degradation (30). Resistance to BILF1-mediated downregulation is conferred by defined residues, C320, N327, and/or E334, in the cytoplasmic tail of HLA class I (31). N326 and E333 in the FNSE motif of Patr-AL are predicted to prevent recognition by BILF1. Furthermore, F321 and N326 in Patr-AL's FNSE motif are predicted to prevent recognition by the Nef proteins of human HIV and chimpanzee SIVcpz (32–35). These Nef proteins bind to the cytoplasmic tail of MHC-A allotypes, including HLA-A*02, and deliver them to lysosomes for degradation (36). Being resistant to the subversive actions of viral proteins would allow Patr-AL to potentially function as an Ag-presenting molecule from where it localizes in the early secretory pathway. For example, there are intracellular pathogens that exploit this part of the secretory pathway for replication, such as *Legionella pneumophila* and related species (37), which infect a wide variety of hosts, suggesting that Patr-AL may be well placed to stimulate a cytotoxic T cell response against such organisms.

Acknowledgments

We thank the Yerkes Regional Primate Center for the samples of chimpanzee peripheral blood and the Stanford Microscopy Facility for use of their Leica SP5 upright confocal microscope. We also thank Bich Tien N. Rouse for expertise in generating the 10A5 mAb specific for Patr-AL.

Disclosures

The authors have no financial conflicts of interest.

References

1. Parham, P. 2005. MHC class I molecules and KIRs in human history, health and survival. *Nat. Rev. Immunol.* 5: 201–214.
2. Lee, N., M. Llano, M. Carretero, A. Ishitani, F. Navarro, M. López-Botet, and D. E. Geraghty. 1998. HLA-E is a major ligand for the natural killer inhibitory receptor CD94/NKG2A. *Proc. Natl. Acad. Sci. USA* 95: 5199–5204.
3. Goodridge, J. P., A. Burian, N. Lee, and D. E. Geraghty. 2010. HLA-F complex without peptide binds to MHC class I protein in the open conformer form. *J. Immunol.* 184: 6199–6208.
4. Kovats, S., E. K. Main, C. Librach, M. Stubblebine, S. J. Fisher, and R. DeMars. 1990. A class I antigen, HLA-G, expressed in human trophoblasts. *Science* 248: 220–223.
5. Yang, Y., W. Chu, D. E. Geraghty, and J. S. Hunt. 1996. Expression of HLA-G in human mononuclear phagocytes and selective induction by IFN-gamma. *J. Immunol.* 156: 4224–4231.
6. Rouas-Freiss, N., R. M. Gonçalves, C. Menier, J. Dausset, and E. D. Carosella. 1997. Direct evidence to support the role of HLA-G in protecting the fetus from maternal uterine natural killer cytolysis. *Proc. Natl. Acad. Sci. USA* 94: 11520–11525.
7. Adams, E. J., and P. Parham. 2001. Species-specific evolution of MHC class I genes in the higher primates. *Immunol. Rev.* 183: 41–64.
8. Gleimer, M., A. R. Wahl, H. D. Hickman, L. Abi-Rached, P. J. Norman, L. A. Guethlein, J. A. Hammond, M. Draghi, E. J. Adams, S. Juo, et al. 2011. Although divergent in residues of the peptide binding site, conserved chimpanzee Patr-AL and polymorphic human HLA-A*02 have overlapping peptide-binding repertoires. *J. Immunol.* 186: 1575–1588.
9. Adams, E. J., S. Cooper, and P. Parham. 2001. A novel, nonclassical MHC class I molecule specific to the common chimpanzee. *J. Immunol.* 167: 3858–3869.
10. Hilton, H. G., and P. Parham. 2013. Direct binding to antigen-coated beads refines the specificity and cross-reactivity of four monoclonal antibodies that recognize polymorphic epitopes of HLA class I molecules. *Tissue Antigens* 81: 212–220.
11. Brodsky, F. M., and P. Parham. 1982. Evolution of HLA antigenic determinants: species cross-reactions of monoclonal antibodies. *Immunogenetics* 15: 151–166.
12. Lo Monaco, E., L. Sibilio, E. Melucci, E. Tremante, M. Suchànek, V. Horejsi, A. Martayan, and P. Giacomini. 2008. HLA-E: strong association with beta2-microglobulin and surface expression in the absence of HLA class I signal sequence-derived peptides. *J. Immunol.* 181: 5442–5450.
13. Moesta, A. K., P. J. Norman, M. Yawata, N. Yawata, M. Gleimer, and P. Parham. 2008. Synergistic polymorphism at two positions distal to the ligand-binding site makes KIR2DL2 a stronger receptor for HLA-C than KIR2DL3. *J. Immunol.* 180: 3969–3979.
14. Ferrari, G., A. M. Knight, C. Watts, and J. Pieters. 1997. Distinct intracellular compartments involved in invariant chain degradation and antigenic peptide loading of major histocompatibility complex (MHC) class II molecules. *J. Cell Biol.* 139: 1433–1446.
15. Neefjes, J., M. L. Jongsma, P. Paul, and O. Bakke. 2011. Towards a systems understanding of MHC class I and MHC class II antigen presentation. *Nat. Rev. Immunol.* 11: 823–836.
16. Ljunggren, H. G., N. J. Stam, C. Ohlén, J. J. Neefjes, P. Höglund, M. T. Heemels, J. Bastin, T. N. Schumacher, A. Townsend, K. Kärre, et al. 1990. Empty MHC class I molecules come out in the cold. *Nature* 346: 476–480.
17. Taner, S. B., M. J. Pando, A. Roberts, J. Schellekens, S. G. Marsh, K. J. Malmberg, P. Parham, and F. M. Brodsky. 2011. Interactions of NK cell

receptor KIR3DL1*004 with chaperones and conformation-specific antibody reveal a functional folded state as well as predominant intracellular retention. *J. Immunol.* 186: 62–72.
18. Lizée, G., G. Basha, and W. A. Jefferies. 2005. Tails of wonder: endocytic-sorting motifs key for exogenous antigen presentation. *Trends Immunol.* 26: 141–149.
19. Kozik, P., R. W. Francis, M. N. Seaman, and M. S. Robinson. 2010. A screen for endocytic motifs. *Traffic* 11: 843–855.
20. Hsu, K. C., S. Chida, D. E. Geraghty, and B. Dupont. 2002. The killer cell immunoglobulin-like receptor (KIR) genomic region: gene-order, haplotypes and allelic polymorphism. *Immunol. Rev.* 190: 40–52.
21. Miley, M. J., S. M. Truscott, Y. Y. Yu, S. Gilfillan, D. H. Fremont, T. H. Hansen, and L. Lybarger. 2003. Biochemical features of the MHC-related protein 1 consistent with an immunological function. *J. Immunol.* 170: 6090–6098.
22. Chua, W. J., S. Kim, N. Myers, S. Huang, L. Yu, D. H. Fremont, M. S. Diamond, and T. H. Hansen. 2011. Endogenous MHC-related protein 1 is transiently expressed on the plasma membrane in a conformation that activates mucosal-associated invariant T cells. *J. Immunol.* 186: 4744–4750.
23. Nagarajan, N. A., F. Gonzalez, and N. Shastri. 2012. Nonclassical MHC class Ib-restricted cytotoxic T cells monitor antigen processing in the endoplasmic reticulum. *Nat. Immunol.* 13: 579–586.
24. Kjer-Nielsen, L., O. Patel, A. J. Corbett, J. Le Nours, B. Meehan, L. Liu, M. Bhati, Z. Chen, L. Kostenko, R. Reantragoon, et al. 2012. MR1 presents microbial vitamin B metabolites to MAIT cells. *Nature* 491: 717–723.
25. Averdam, A., B. Petersen, C. Rosner, J. Neff, C. Roos, M. Eberle, F. Aujard, C. Münch, W. Schempp, M. Carrington, et al. 2009. A novel system of polymorphic and diverse NK cell receptors in primates. *PLoS Genet.* 5: e1000688.
26. Flügge, P., E. Zimmermann, A. L. Hughes, E. Günther, and L. Walter. 2002. Characterization and phylogenetic relationship of prosimian MHC class I genes. *J. Mol. Evol.* 55: 768–775.
27. Schaefer, M. R., M. Williams, D. A. Kulpa, P. K. Blakely, A. Q. Yaffee, and K. L. Collins. 2008. A novel trafficking signal within the HLA-C cytoplasmic tail allows regulated expression upon differentiation of macrophages. *J. Immunol.* 180: 7804–7817.
28. Suemizu, H., M. Radosavljevic, M. Kimura, S. Sadahiro, S. Yoshimura, S. Bahram, and H. Inoko. 2002. A basolateral sorting motif in the MICA cytoplasmic tail. *Proc. Natl. Acad. Sci. USA* 99: 2971–2976.
29. Hansen, T. H., and M. Bouvier. 2009. MHC class I antigen presentation: learning from viral evasion strategies. *Nat. Rev. Immunol.* 9: 503–513.
30. Zuo, J., L. L. Quinn, J. Tamblyn, W. A. Thomas, R. Feederle, H. J. Delecluse, A. D. Hislop, and M. Rowe. 2011. The Epstein-Barr virus-encoded BILF1 protein modulates immune recognition of endogenously processed antigen by targeting major histocompatibility complex class I molecules trafficking on both the exocytic and endocytic pathways. *J. Virol.* 85: 1604–1614.
31. Griffin, B. D., A. M. Gram, A. Mulder, D. Van Leeuwen, F. H. Claas, F. Wang, M. E. Ressing, and E. Wiertz. 2013. EBV BILF1 evolved to downregulate cell surface display of a wide range of HLA class I molecules through their cytoplasmic tail. *J. Immunol.* 190: 1672–1684.
32. Cohen, G. B., R. T. Gandhi, D. M. Davis, O. Mandelboim, B. K. Chen, J. L. Strominger, and D. Baltimore. 1999. The selective downregulation of class I major histocompatibility complex proteins by HIV-1 protects HIV-infected cells from NK cells. *Immunity* 10: 661–671.
33. Kasper, M. R., J. F. Roeth, M. Williams, T. M. Filzen, R. I. Fleis, and K. L. Collins. 2005. HIV-1 Nef disrupts antigen presentation early in the secretory pathway. *J. Biol. Chem.* 280: 12840–12848.
34. Williams, M., J. F. Roeth, M. R. Kasper, R. I. Fleis, C. G. Przybycin, and K. L. Collins. 2002. Direct binding of human immunodeficiency virus type 1 Nef to the major histocompatibility complex class I (MHC-I) cytoplasmic tail disrupts MHC-I trafficking. *J. Virol.* 76: 12173–12184.
35. Specht, A., M. Q. DeGottardi, M. Schindler, B. Hahn, D. T. Evans, and F. Kirchhoff. 2008. Selective downmodulation of HLA-A and -B by Nef alleles from different groups of primate lentiviruses. *Virology* 373: 229–237.
36. Roeth, J. F., M. Williams, M. R. Kasper, T. M. Filzen, and K. L. Collins. 2004. HIV-1 Nef disrupts MHC-I trafficking by recruiting AP-1 to the MHC-I cytoplasmic tail. *J. Cell Biol.* 167: 903–913.
37. Hubber, A., and C. R. Roy. 2010. Modulation of host cell function by *Legionella pneumophila* type IV effectors. *Annu. Rev. Cell Dev. Biol.* 26: 261–283.
38. Liu, J., D. Shaji, S. Cho, W. Du, J. Gervay-Hague, and R. R. Brutkiewicz. 2010. A threonine-based targeting signal in the human CD1d cytoplasmic tail controls its functional expression. *J. Immunol.* 184: 4973–4981.
39. Moody, D. B., and S. A. Porcelli. 2003. Intracellular pathways of CD1 antigen presentation. *Nat. Rev. Immunol.* 3: 11–22.
40. Boyle, L. H., A. K. Gillingham, S. Munro, and J. Trowsdale. 2006. Selective export of HLA-F by its cytoplasmic tail. *J. Immunol.* 176: 6464–6472.
41. Lizée, G., G. Basha, J. Tiong, J. P. Julien, M. Tian, K. E. Biron, and W. A. Jefferies. 2003. Control of dendritic cell cross-presentation by the major histocompatibility complex class I cytoplasmic domain. *Nat. Immunol.* 4: 1065–1073.
42. Park, B., S. Lee, E. Kim, S. Chang, M. Jin, and K. Ahn. 2001. The truncated cytoplasmic tail of HLA-G serves a quality-control function in post-ER compartments. *Immunity* 15: 213–224.